Los Alamos Environmental Restoration Records Processing Facility

ER Record I.D.# 70334

LOS ALAMOS NATIONAL LABORATORY
ENVIRONMENTAL RESTORATION
Records Processing Facility
ER Records Index Form

ER ID NO. 70334 ***Date Received:*** 3/8/01 ***Processor:*** YCA ***Page Count:*** 106

Privileged: (Y/N) N ***Record Category:*** P

FileFolder: N/A

Correction: (Y/N) N ***Corrected No.*** 0 ***Corrected By Number:*** 0

Administrative Record: (Y/N) Y

Refilmed: (Y/N) N ***Old ER ID Number:*** 0 ***New ER ID Number:*** 0

Miscellaneous Comments:

ER CATALOG #ER2000-0738

THIS FORM IS SUBJECT TO CHANGE. CONTACT THE RPF FOR LATEST VERSION. (JUNE 1997)

30850

156

70334

Los Alamos National Laboratory

UNIVERSITY OF CALIFORNIA

Environmental Science and Waste Technology (E)
Environmental Restoration, MS M992
Los Alamos, New Mexico 87545
505-667-0808/FAX 505-665-4747

Date: December 21, 2000
Refer to: ER2000-0738

Mr. Carl Will
NMED – Hazardous Waste Bureau
2044 A Galisteo
Santa Fe, NM 87502

SUBJECT: PILOT VAPOR EXTRACT TEST AT TA-54, MDA L, October 1997, LA-UR-00-6024

Dear Mr. Will:

Per your telephone request of 12/14/2000 we have enclosed one copy of the following report: Pilot Vapor Extract Test at TA-54, MDA L, October 1997, LA-UR-00-6024.

In order to save trees, if any of the CC'd would like a copy of this report, please call John Hopkins at (505) 667-9551.

Sincerely,

John Hopkins
Environmental Restoration Project

JH/vn

Enclosure: Pilot Vapor Extract Test at TA-54, MDA L, October 1997, LA-UR-00-6024

Cy (w/enc.):
E/ER File, MS M992
RPF, MS M707

Cy (w/o enc.):
J. Canepa, E/ER, MS M992
J. Bearzi, NMED-HWB

MAR 0 8 2001

LA-UR-00-6024

Pilot Vapor Extract Test at TA-54, MDA L

October 1997

by

ERM/Golder Los Alamos Project Team

for

Field Unit 5
Environmental Restoration Project
Los Alamos National Laboratory

EXECUTIVE SUMMARY

This report analyzes and discusses in detail the results of the Active Pilot Vapor Extraction Test (PVET) first described in the Pilot Extraction Study Plan (PESP) for the organic plume at MDA L (LANL 1992, 0788) and performed over a 34 day period from September 19, 1995 to October 23, 1995. Section 1 of this report also summarizes the regulatory status and gives a brief history of previous tests performed on the plume. Section 2 provides a detailed description of the stratigraphy of the mesa where the organic vapor plume is located and summarizes the known hydrogeologic properties of the different formations.

The test was designed using a three dimensional air flow model. The design of the PVET is in Appendix B of this report. Section 3 briefly discusses the design and describes the implementation. Section 4 describes the effect of the test on the movement of vapor phase compounds. Section 5 presents analyses of test results using both numerical and analytical methods. Analytical calculations are used to confirm near-field permeability measurements from packer tests. Numerical and analytical results are compared with each other and with field measurements of pore gas pressure and plume velocity taken during the test. Section 6 presents conclusions and recommendations based on the results presented in this report.

The two analysis methods yielded similar answers leading to the conclusion that air flow in the radius of influence of the test can be adequately predicted using standard porous media modeling techniques based on in-situ permeability measurements from packer tests. The test further indicated that organic vapors in the tuffs beneath MDA L move readily toward an extraction well with little or no sorption. Plume control using extraction techniques was therefore shown to be feasible at MDA L and plume movement in response to extraction can be adequately predicted within areas where a permeability and stratigraphic database similar to that developed for the test zone is available. These results provide a foundation for determining the feasibility of both active extraction and passive extraction techniques at MDA L and support a change in focus at this time from active to passive extraction techniques using natural subsurface air flow induced by changes in atmospheric pressure.

CONTENTS

1.0 INTRODUCTION 1-1
1.1 Purpose of the PVET 1-1
1.2 Regulatory Overview 1-4
1.3 History 1-4
1.3.1 Disposal at MDA L, TA-54 1-5
1.3.2 Monitoring Well Network 1-5
1.3.3 Vapor-phase contamination 1-10
1.3.4 Previous Investigations 1-12
1.3.4.1 Early Geohydrologic Tests (1980s) 1-12
1.3.4.2 Pilot tests in borehole 54-1003 1-14
1.3.4.2.1 Pilot Test 1 (18 October 1994) 1-14
1.3.4.2.2 Pilot Test 2 (7-11 November 1994) 1-15
1.3.4.2.3 Test 3 (23-28 November 1994) 1-16
1.3.4.3 MDA L RFI 1-16
1.3.4.3.1 MDA L RFI PVET Boreholes 1-16
1.3.4.3.2 MDA L RFI Sample Results 1-17

2.0 ENVIRONMENTAL SETTING 2-1
2.1 Climate 2-1
2.2 Geologic Setting 2-1
2.2.1 Stratigraphy 2-2
2.2.1.1 Bandelier Tuff 2-5
2.2.1.1.1 Otowi Member 2-5
2.2.1.1.1.1 Guaje Pumice Bed 2-5
2.2.1.1.1.1.1 Lithology 2-5
2.2.1.1.1.1.2 Distribution and Thickness 2-6
2.2.1.1.1.2 Otowi Member Tuff 2-6
2.2.1.1.1.2.1 Lithology 2-6
2.2.1.1.1.2.2 Distribution and Thickness 2-6
2.2.1.1.2 Cerro Toledo interval 2-7
2.2.1.1.2.1 Lithology 2-7
2.2.1.1.2.2 Distribution and Thickness 2-7
2.2.1.1.3 Tshirege Member 2-7
2.2.1.1.3.1 Tsankawi Pumice Bed 2-8
2.2.1.1.3.1.1 Lithology 2-8
2.2.1.1.3.1.2 Distribution and Thickness 2-8

2.2.1.2 Unit 1g 2-8
2.2.1.2.1 Lithology 2-8
2.2.1.2.2 Distribution and Thickness 2-9
2.2.1.3 Unit 1v 2-9
2.2.1.3.1 Lithology 2-9
2.2.1.3.2 Distribution and Thickness 2-11
2.2.1.4 Unit 2 2-11
2.2.1.4.1 Lithology 2-11
2.2.1.4.2 Distribution and Thickness 2-12
2.2.2 Hydrology 2-12
2.2.2.1 Surface Water 2-12
2.2.2.2 Ground Water 2-13
2.2.2.2.1 Alluvial Water 2-13
2.2.2.2.2 Perched Water 2-13
2.2.2.2.3 Main Aquifer 2-14

2.2.3 Geohydrologic Characteristics of Bandelier Tuff Subunits at MDA L 2-14
2.2.3.1 Bulk Density 2-15
2.2.3.2 Porosity 2-16
2.2.3.3 Volumetric Moisture Content 2-17
2.2.3.4 Gravimetric Moisture Content 2-17
2.2.3.5 Saturation 2-18
2.2.3.6 Saturated Hydraulic Conductivity 2-18
2.2.3.7 Induration and Welding 2-18
2.2.3.8 Conceptual Role of Fractures and Rock Matrix in Air Flow 2-19

3.0 TEST DESCRIPTION 3-1
3.1 PVET Design and Instrumentation 3-1
3.1.1 Extraction System 3-1
3.1.2 Monitoring Systems 3-2
3.2 PVET Implementation 3-7
3.3 PVET Results 3-7

4.0 PVET EFFECT ON VAPOR PHASE COMPOUNDS 4-1
4.1 TCA Response and Recovery 4-3
4.1.1 Downgradient from the extraction well 4-3
4.1.2 Upgradient from the extraction well 4-4
4.2 TCA behavior and stratigraphy 4-4
4.3 Response of Other Vapor Phase Compounds Monitored During PVET 4-9
4.3.1 Carbon Dioxide 4-9

4.3.3 Water Vapor 4-9

5.0 NUMERICAL AND ANALYTICAL MODELING OF ACTIVE PILOT VAPOR EXTRACTION TEST 5-1
5.1 Numerical Modeling of Active Pilot Vapor Extraction Test 5-1
5.2 Analytical Modeling of Active PVET 5-3
5.2.1 Determination of Steady State 5-6
5.2.2 Estimation of the Radius of Influence (R_i) and Near Field Permeability 5-7
5.2.3 Calculation of Vapor Velocity 5-8
5.2.4 Calculation of Contaminant Plume Velocity 5-11
5.3 Discussion of Modeling Results 5-11

6.0 CONCLUSIONS AND RECOMMENDATIONS 6-1

7.0 REFERENCES 7-1

8.0 CONTRIBUTORS 8-1

APPENDIX A, Pilot Study Extraction Plan (PESP) for Organic Vapor Plume MDA L
APPENDIX B, Pilot Scale Vapor Extraction System Design for OU 1148

LIST OF FIGURES

Figure 1-1 Location of Los Alamos National Laboratory 1-2
Figure 1-2. Location of TA-54 within the Laboratory 1-3
Figure 1-3. Locations of MDAs in TA-54 1-6
Figure 1-4. Locations of Inactive Subsurface Disposal Units at MDA L and Vapor Monitoring Wells at MDA L and the Formerly Proposed MDA G Expansion Area, TA-54 1-7
Figure 1-5. Locations of the Pilot Extraction Wells and PVET monitoring wells east of MDA L in the Formerly Proposed MDA G Expansion Area, TA-54. 1-13
Figure 2-1. Detailed stratigraphic column in the vicinity of MDA L, TA-54. 2-3
Figure 2-2. Cross section of Mesita del Buey at MDA L and location of MDA L on Mesita del Buey. 2-4
Figure 2-3. Cross-section A-A parallel to Mesita del Buey through the extraction well, 54-1017. 2-20
Figure 2-4. Cross section B-B oblique to Mesita del Buey through the extraction well, 54-1017. 2-21
Figure 3-1. PVET vacuum extraction system schematic 3-1
Figure 3-2. PVET site layout 3-2

the extraction well, 54-1017.
Figure 3-1. PVET vacuum extraction system schematic....3-1
Figure 3-2. PVET site layout....3-2
Figure 3-3. Automated precision soil gas pressure monitoring system. 3-4
Figure 3-4. Automated soil gas sampling and analysis system. 3-5
Figure 3-5. Extraction system process measurements....3-9
Figure 3-6. Expanded 4-day plot of extraction processes. 3-10
Figure 3-7. Soil gas pressure response for monitoring ports in 3-11
borehole 54-1018 during the extraction test.
Figure 3-8. Soil gas pressure response for monitoring ports in 3-12
borehole 54-1004 during the extraction test.
Figure 3-9. Soil gas pressure response for monitoring ports in 3-13
borehole 54-2025 during the extraction test.
Figure 3-10. Soil gas pressure response for monitoring ports in 3-13
borehole 54-1003 during the extraction test.
Figure 3.11. Soil gas pressure response for monitoring ports in....3-14
borehole 54-1005 during the extraction test.
Figure 3-12. Soil gas pressure response for monitoring ports I 3-14
borehole 54-2002 during the extraction test.
Figure 3-13. Soil gas response for monitoring ports in borehole 3-15
54-1006 during the extraction test.
Figure 3-14. Expanded time plot for 54-1004 pressure data. 3-16
Figure 3-15. Expanded time plot for 54-1018 pressure data. 3-17
Figure 4-1. Locations of PVET monitoring wells east of MDA L....4-2
Figure 4-2. TCA Concentrations at Well 54-1018 (20 ft downgradient....4-5
from extraction well)
Figure 4-3. TCA Concentrations at Well 54-2024 (51 ft downgradient....4-6
from extraction well)
Figure 4-4. TCA Concentrations at Well 54-1003 (96 ft downgradient....4-7
from extraction well)
Figure 4-5. TCA Concentrations at Well 54-1004 4-8
(30 ft upgradient from extraction well)
Figure 4-6 CO_2 at Well 54-1018 4-10
Figure 4-7 CO_2 at Well 54-2024 4-11
Figure 4-8 CO_2 at Well 54-1003 4-12
Figure 4-9 CO_2 at Well 54-1004 4-13
Figure 4-10 O_2 at Well 54-1018 4-14
Figure 4-11 O_2 at Well 54-2024 4-15
Figure 4-12 O_2 at Well 54-1003 4-16
Figure 4-13 O_2 at Well 54-1004 4-17
Figure 4-14 H_2O at Well 54-1018....4-18

Figure 4-15 H_2O at Well 54-2024 4-19
Figure 4-16 H_2O at Well 54-1003 4-20
Figure 4-17 H_2O at Well 54-1004 4-21
Figure 5-1. In-situ measured air permeability in borehole 54-1018, extraction well configuration, and permeability distribution used in AIR3D model. 5-4
Figure 5-2. Modeled and measured vacuum pressure profiles at steady state conditions during the vapor extraction test. 5-5
Figure 5-3. Modeled radial (positive toward the well) soil gas velocity profile at steady state conditions during the extraction measurement. 5-5
Figure 5-4. AIR3D modeled pressure distribution about the extraction zone. Contours are in 500 Pa increments. Ground surface is at 6785 ft. elevation. 5-6
Figure 5-5. Method for Determining Radius of Influence 5-9
Figure 5-6. Method for Determining Steady-State Test Period 5-10
Figure 5-7. TCA Concentration Contours on Julian Day 270 and 290 5-13

LIST OF TABLES

Table 1-1. Summary of existing EM-8 monitoring wells at MDA-L 1-8
Table 1-2. Summary of ER monitoring wells at MDA-L 1-9
Table 1-3. Maximum Vapor Phase VOCs at MDA L, 1 QCY '96 1-11
Table 1-4. Monitoring wells and ports detecting pilot test 2 vacuum 1-15
Table 1-5. VOCs detected in the 67 ft core sample in borehole 54-1003 1-18
Table 2-1. Summary of Geohydrologic Properties 2-16
Table 3-1. Soil gas sampling and pressure measurement port locations 3-3
Table 3-2. PVET Monitoring System Specifications 3-6
Table 4-1. Summary of PVET monitoring wells, ports, and compounds 4-1
Table 5-1. Comparison of modeled and measured extraction flow conditions 5-2

1.0 INTRODUCTION

This report presents the results of the active Pilot Vapor Extraction Test (PVET) on subsurface vapor-phase volatile organic compounds (VOCs) at material disposal area (MDA) L, technical area (TA) -54 at Los Alamos National Laboratory (Laboratory) (Fig. 1-1 and Fig. 1-2). This test was planned and described in the Pilot Extraction Study Plan (PESP) for the organic vapor plume at MDA L (Appendix A, RFI Work Plan for OU 1148 (LANL 1992-0788)).

1.1 PURPOSE OF THE PVET

The PVET is one of several pilot tests using a mechanically induced negative vapor pressure (hereinafter termed "active extraction") to pull subsurface air containing VOCs through an extraction well to the ground surface. The purpose of the PVET was to

- Study the effect of the PVET on subsurface vapor-phase VOCs as monitored by a selected set of monitoring wells; and
- Evaluate the performance of the PVET using instrumentation to monitor changes in subsurface vapor pressure and air flow.

The purpose of this report is to

- Summarize the regulatory status, history and previous work on the vapor-phase VOCs;
- Summarize the geohydrological characteristics of the rocks hosting the vapor-phase VOCs;
- Describe the response of the vapor-phase VOC concentrations during the PVET, and the change (recovery) of the vapor-phase VOC concentrations after the PVET;
- Describe the performance of the PVET as a remediation system monitored by changes in subsurface vapor pressure and air flow;
- Interpret the results of the PVET in regards to the geohydrological properties of the host rocks; and
- Provide a foundation for modifying the Pilot Extraction Study Plan (PESP) for the Organic Vapor Plume at MDA L, Appendix A, "RCRA Facilities Investigation (RFI) Work Plan for Operable Unit 1148" (LANL, 1992, 0788) from active extraction to pilot studies using natural subsurface air flow which is not artificially induced (hereinafter termed "passive extraction").

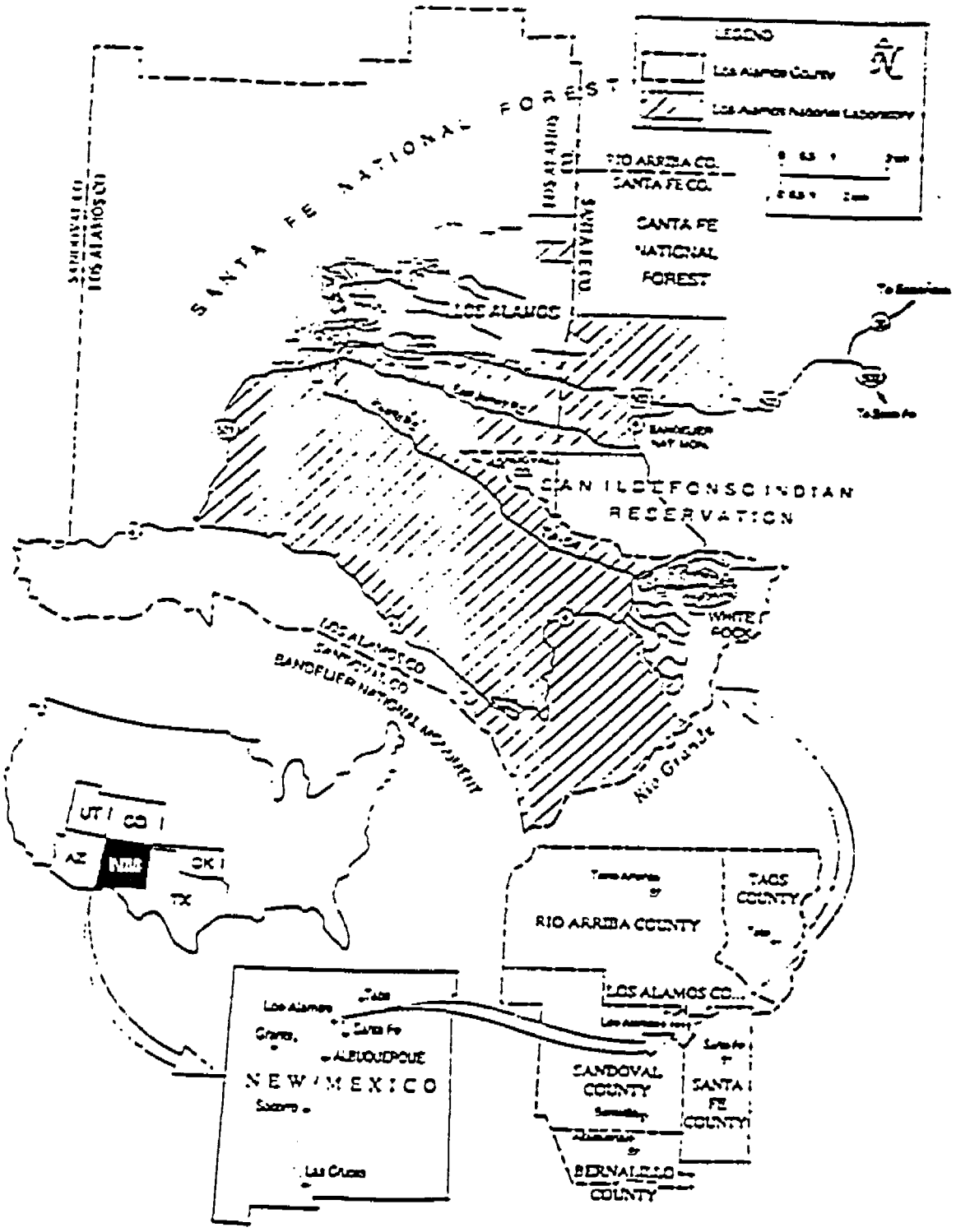

Figure 1-1 Location of Los Alamos National Laboratory

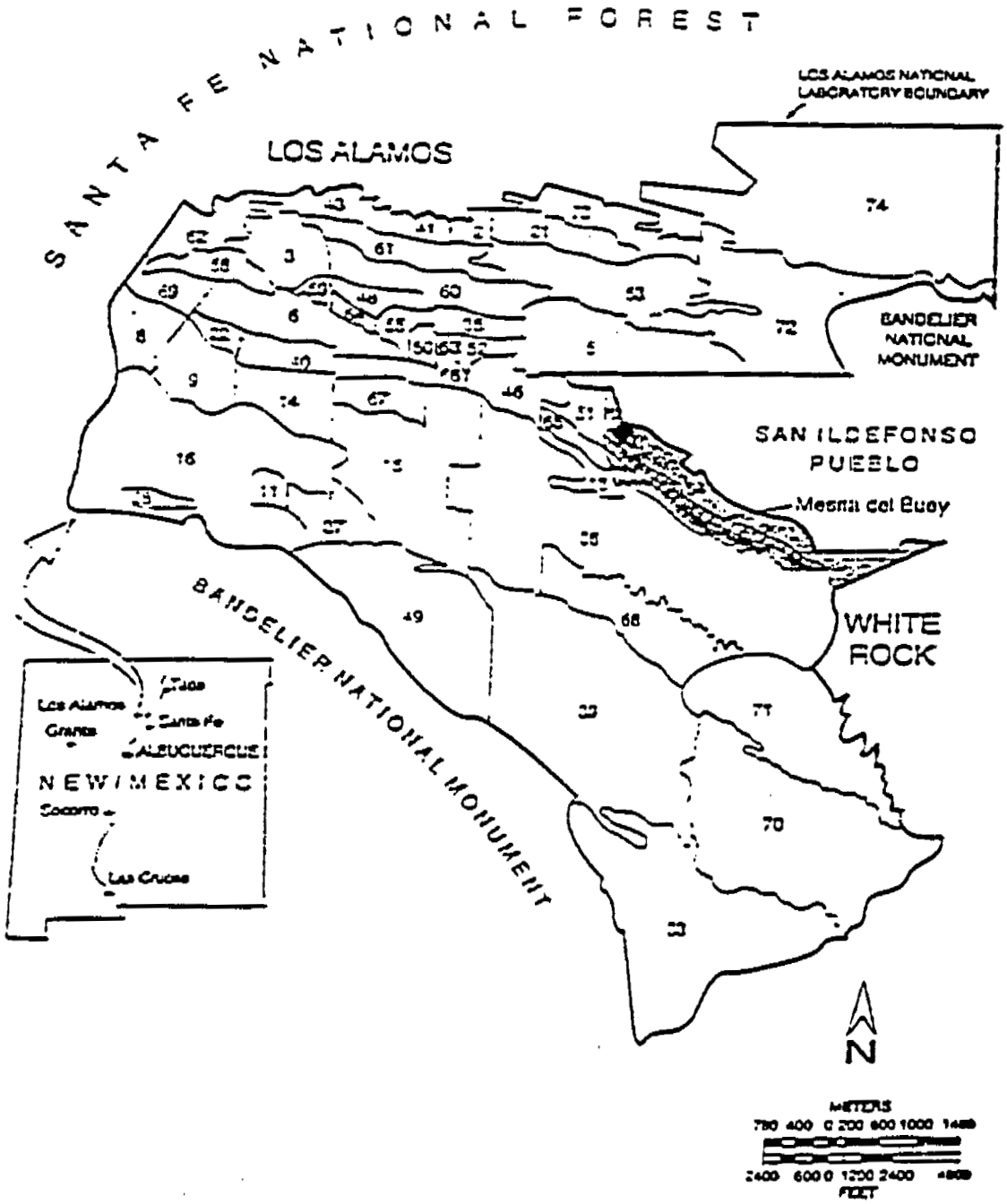

Figure 1-2. Location of TA-54 within the Laboratory.

1.2 REGULATORY OVERVIEW

The PVET was proposed in the PESP as an addendum to the Environmental Restoration (ER) Project's OU-1148 RFI. In 1994, OU-1148 became part of Field Unit (FU) -5 during a reorganization of the ER Project. The OU-1148 RFI includes MDA L, which is also identified as potential release site (PRS) 54-006.

An RFI status report on potential subsurface contaminant pathways at MDA L was drafted in 1996 and as of autumn-1997 is in final review (Environmental Restoration Project, in progress. "RFI Report for Potential Release Site 54-006, MDA L (located in former Operable Unit 1148), Field Unit 5," Los Alamos National Laboratory report LA-UR-97-xxxx, Los Alamos, New Mexico. (Environmental Restoration Project, in progress)).

The purpose of the RFI investigation of PRS 54-006 is to

- Satisfy the regulatory requirements of the Hazardous and Solid Waste Amendment (HSWA) Module, Module VIII of the Laboratory's RCRA Part B operating permit;
- Through a staged approach, characterize the nature and extent of contamination emanating from MDA L and identify potential transport pathways; and
- Provide the basis for implementing subsequent processes through corrective action ultimately leading to no further action (NFA) status for PRS 54-006 and its removal from the Laboratory's RCRA Part B operating permit.

According to the PESP the purpose of the pilot extraction study is to investigate

- retraction of the horizontal boundary of the [vapor-phase VOC] plume to the vicinity of the security fence at MDA L;
- retraction of the bottom of the [vapor-phase VOC] plume to the depth of the basalt layer (if indeed the plume has spread to lower depths); and
- a means for preventing any future regeneration of the [vapor-phase VOC] plume away from the subsurface sources. Pilot Extraction Study Plan (PESP) for the Organic Vapor Plume at MDA L, Appendix A, RCRA Facilities Investigation (RFI) Work Plan for Operable Unit 1148 (LANL, 1992, 07SS).

1.3 HISTORY

During the late 1950s, MDA L and other MDAs at TA-54 (MDAs G, H, and J) were opened for disposal of Laboratory-derived waste. This activity was authorized by the U.S. Atomic Energy Commission based on reviews by the

Laboratory and the U.S. Geological Survey. The nature of materials disposed at MDA L is documented in Operable Unit 1148 Data Report (IT Corporation 1992, 08-0015).

1.3.1 Disposal at MDA L, TA-54

MDA L is a 2.58 acre site within TA-54 (Fig. 1-3). From the late 1950s to 1985, MDA L was used as a land disposal site for hazardous chemicals. Former land disposal units include one inactive covered chemical waste disposal pit designated as Pit A, 34 inactive covered disposal shafts, two lead stringer shafts, and three inactive covered chemical waste disposal impoundments designated as Impoundments B, C, and D (Fig. 1-4). Table 5.3-2 of the "RFI Work Plan for Operable Unit 1148 (LANL 1992, 0788) lists the capacity of the pit, impoundments, and shafts and the months they were used. A summary of disposed materials is provided in the OU-1148 RFI Work Plan and in the MDA L RFI Report (in progress).

Historical records of the land disposal at MDA L indicate that solvents were disposed in Pit A and in the 34 disposal shafts. This resulted in a subsurface VOC plume that currently extends beyond the facility boundary (MDA L Phase 1 RFI Report, in progress). The subsurface vapor-phase VOCs were detected during the mid-1980s after the land disposal operations ceased. Pursuant to the Laboratory's interest in controlling and ultimately remediating the vapor-phase VOCs, the plume is monitored on a quarterly schedule and pilot studies were initiated to characterize extraction. Those activities are in accordance with the Laboratory's HSWA Module, Module VIII, RCRA Part B operating permit.

MDA L is currently used for RCRA-permitted chemical waste storage and treatment, and for mixed waste storage under interim status authority. The former land disposal units are covered by asphalt and/or chemical waste storage structures.

1.3.2 Monitoring Well Network

From 1985 to 1988, the Laboratory's Environmental Management (EM) -8 installed a series of monitoring wells in boreholes drilled in and around MDA L (Kearl, et. al., 1986, 0135). The purpose of the wells was to characterize the vapor-phase VOCs emanating from former subsurface disposal units at MDA L. Some of these wells are now unuseable and abandoned. The remaining wells are now labeled as 54-2000 series monitoring wells (Table 1, Fig. 1-4).

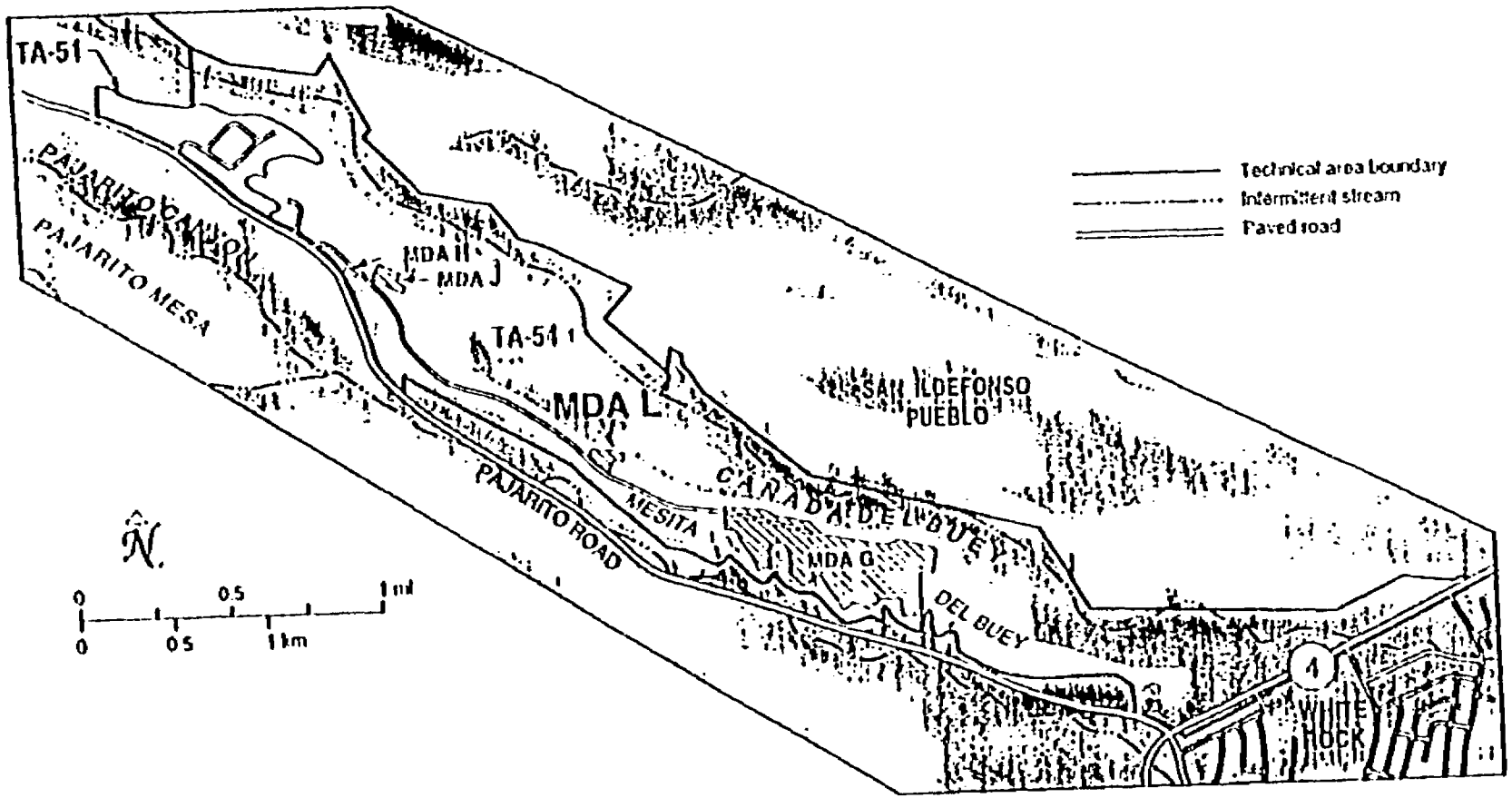

Figure 1-3. Locations of MDAs in TA-51.

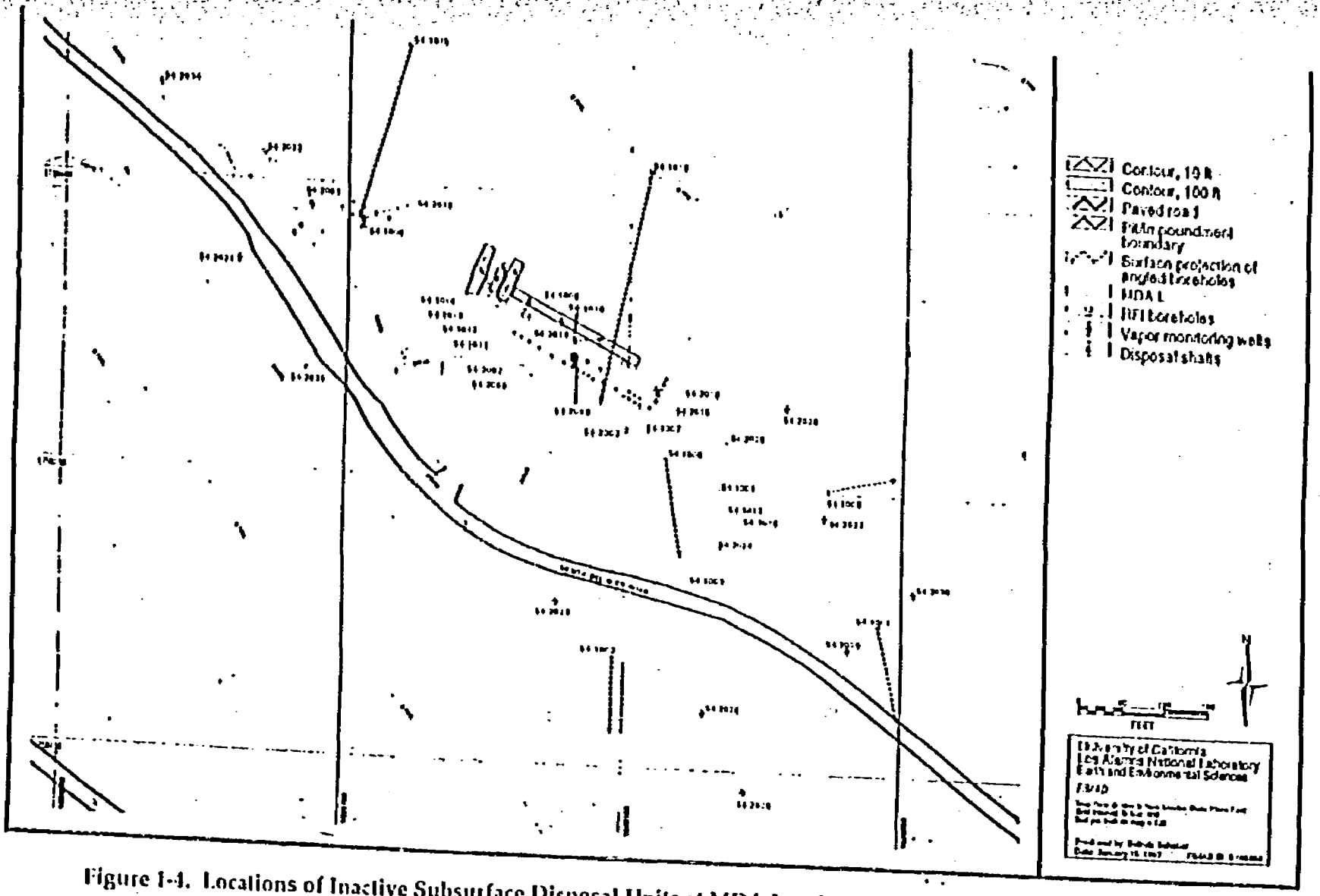

Figure 1-4. Locations of Inactive Subsurface Disposal Units at MDA L and Vapor Monitoring Wells at MDA L and the Formerly Proposed MDA G Expansion Area, TA-54.

Table 1-1. Summary of existing EM-8 monitoring wells at MDA-L

Location Identity	Depth (ft.)	Borehole Attitude	Date Drilled	Easting[1] "X"	Northing[1] "Y"	Elevation[2] "Z"
54-2002	200	Vertical	1986	1,640,097.00	1,759,324.00	6,792.0
54-2015	82	Vertical	1985	1,640,139.00	1,759,379.00	6,789.3
54-2016	102	Vertical	1986	1,640,094.00	1,759,413.00	6,788.9
54-2020	200	Vertical	1986	1,640,329.00	7,759,362.00	6,776.2
54-2023	200	Vertical	1986	1,640,006.00	1,759,083.00	6,790.2
54-2024	200	Vertical	1986	1,640,233.00	1,759,170.00	6,790.0
54-2025	190	Vertical	1988	1,640,247.00	1,759,313.00	6,785.5
54-2026	250	Vertical	1988	1,640,422.00	1,759,028.00	6,786.1
54-2027	250	Vertical	1988	1,640,387.00	1,759,217.00	6,781.8
54-2028	250	Vertical	1988	1,640,214.00	1,758,930.00	6,793.4
54-2029	288	Vertical	1988	1,640,276.00	1,758,823.00	6,790.5
54-2030	243	Vertical	1988	1,640,517.00	1,759,116.00	6,779.4

[1] NAD 83 (north American datum, 1983).
[2] Feet above mean sea level.

The 54-2000 series wells are vertical boreholes containing either galvanized steel pipe or individual sampling tubes extending from sampling ports located every 20 feet from the ground surface to the bottom. The annulus of each well at the individual sampling ports was filled with a graded sand pack to facilitate pore-gas sampling. In most of the 54-2000 series wells, bentonite seals were placed above and below the sand packs. The intervals between the sand packs and bentonite seals is filled with either crushed tuff, a bentonite/gravel mixture, or clean sand.

In 1993, the ER Project's OU-1148, as part of the MDA L RFI, installed additional vapor monitoring wells in RFI boreholes drilled east of MDA L. These wells are designated as 54-1000 series wells on Fig. 1-4. The purpose of the additional wells was to study the vapor-phase VOCs beneath MDA L and the adjacent vicinity at TA-54 (Appendix A, Pilot Extraction Study Plan for the Organic Vapor Plume at MDA L, OU-1148 RFI Work Plan).

In the winter of 1994 and 1995, monitoring wells 54-1015 and 54-1016 were installed in two deep boreholes drilled from the adjacent canyon northeast of MDA L. The purpose of these wells was to test for the presence of vapor and liquid phased VOCs at depth below MDA L. The boreholes angled to approximately 550 feet and 600 feet deep, respectively, below former disposal units at MDA L (Fig. 1-4).

In March of 1995, two additional wells, designated as 54-1017 and 54-1018, were installed in the midst of the monitoring well network east of MDA L (Fig. 1-4). Well 54-1017 was designed as an extraction well for subsequent pilot tests on the vapor-phase VOCs. An additional monitoring well, designated as 54-1018, was installed 20 feet from the extraction well to monitor the

performance of pilot tests in the extraction well. Table 1-2 lists the 54-1000 series boreholes in which monitoring wells were installed to perform studies on the vapor-phase VOCs.

Table 1-2. Summary of ER monitoring wells at MDA-L

Location Identity	Depth (feet)	Borehole Attitude	Date Drilled	Easting[1] "X"	Northing[1] "Y"	Elevation[1] "Z"
54-1001	318	Angle	9/9/93 to 9/16/93	1,640,646.68	1,759,056.84	6,781.7
54-1002	310	Angle	9/20/93 to 9/23/93	1,640,084.82	1,759,006.00	6,789.3
54-1003	299	Vertical	10/3/93 to 10/4/93	1,640,249.27	1,759,123.17	6,791.7
54-1004	340	Vertical	10/8/93 to 10/18/93	1,640,235.60	1,759,248.14	6,788.2
54-1005	291	Angle	12/1/93 to 12/3/93	1,640,389.79	1,759,254.01	6,778.5
54-1006	323	Angle	9/24/93 to 10/1/93	1,640,156.05	1,759,289.42	6,790.3
54-1015[3]	530	Angle	11/17/94 to 1/9/95	1,639,785.98	1,759,842.72	6,708.2
54-1016[3]	607	Angle	2/1/95 to 3/17/95	1,640,128.89	1,759,686.03	6,700.4
54-1017[4]	159	Vertical	4/19/95 to 4/20/95	1,640,245.71	1,759,219.49	6,788.3
54-1018	328	Vertical	4/21/95 to 5/8/95	1,640,263.68	1,759,208.89	6,787.8

[1] NAD 83 (north American datum, 1983).
[2] Feet above mean sea level.
[3] Monitoring wells 54-1015 and 54-1016 can sample perched water at selected depths.
[4] Borehole 54-1017 is the pilot extraction study well.

Wells 54-1002 through 54-1006 were outfitted with vapor monitoring systems using Seamist™ borehole liners. A Seamist™ liner is a flexible polymer membrane deployed and inflated in place by a small over pressure of air. Monitoring ports are located at selected depths in the liners constructed for these wells. Teflon tubing extends from each subsurface port to the well head, where instruments may be attached to collect vapor samples, or to monitor subsurface vapor pressure or other physical parameters. Seamist™ liners may be withdrawn and reused; in a few cases they have been used to install additional sensors for temperature and humidity.

Multiport Solinst™ monitoring wells were installed in boreholes 54-1015 and 54-1016. Each Solinst™ well was constructed using a 2-inch diameter schedule 80 polyvinyl chloride (PVC) pipe with either vapor and/or moisture monitoring ports positioned at depths corresponding to hydrogeologic horizons of interest. Teflon™ tubing extends from each monitoring port to the well head for collecting samples, or for monitoring subsurface vapor pressure or other physical parameters. In wells 54-1015 and 54-1016, sampling ports capable of delivering both vapor and water samples were installed at depths where higher moisture content was observed. To date, no perched water has been sampled due to insufficient accumulation. Following the Solinst™ monitoring well installations, well completion operations involved backfilling with graded sand packs around the ports, bentonite seals below and above the ports, and a fine-grained sand/bentonite/rock-flour

mixture between the ports. Each well was completed with a steel access box mounted atop 10-inch diameter steel surface casing extending though a four foot by four foot cement pad.

1.3.3 Vapor-phase contamination

The MDA L Phase 1 RFI Report in progress presents a detailed discussion of the vapor-phase contamination beneath MDA L. Since the implementation of quarterly vapor sampling in 1988, several sampling and analysis techniques have been used to optimize the quality of the VOC data collected. A summary of pre-1992 vapor phase VOC composition and extent was presented in Appendix A of the OU-114S Work Plan. Vapor phase VOC concentrations are greatest below the former disposal units and taper off to nondetected values within several hundred feet from the source(s). "The principal vapor phase organic compounds, listed in descending order of concentration were 1,1,1-trichloroethane (TCA), trichloroethene (TCE), carbon tetrachloride, chloroform, tetrachloroethene (PCE), toluene, and benzene. Other contaminants that have been detected, but at much lower concentrations, include chlorobenzene, xylenes, and 1,2,4-trimethylbenzene. TCA is the vapor phase contaminant with the highest concentration. The measured concentrations of TCA are almost an order of magnitude greater than the values measured for TCE, the contaminant of second highest concentration (Pilot Extractio n Study Plan for the Organic Vapor Plume at MDA L, Appendix A, RCRA Facilities Investigation (RFI) Work Plan for Operable Unit 114S (LANL, 1992, 0788).

The MDA L Phase 1 RFI Report updated the results of the vapor phase VOC sampling to include the first quarterly sampling results in 1996. Complete results (1 QCY '96) were included as Attachment 6 of the RFI Report. Table 1-3 presents maximum vapor phase VOC concentrations in 1 QCY '96 samples compared to respective Subpart S Action Levels for air and soil.

Table 1-3. Maximum Vapor Phase VOCs at MDA L, 1 QCY '96

Well Number, Sample Depth Volatile Organic Compound	CAS#	Maximum Concentration (ppmv)	Subpart S Action Level (air) (mg/m³)[1]	Subpart S Action Level (soil) (mg/kg)[2]
Well 2015, 82 feet[3]				
1,1,1-Trichloroethene (TCA)	71-55-6	523	1,000	7,000
Trichloroethene (TCE)	79-01-6	139	NL	60
Methylene chloride	75-09-2	45	0.3	90
1,2,-Dichloropropane	78-87-5	43		
Toluene	108-88-3	24	7,000	20,000
Tetrachloroethene (PCE)	127-18-4	17	1	10
Trichloroflouromethane (F11)	75-69-4	12		
M+P-Xylene	108-38-3	6	1,000[4]	200,000[4]
1,1,2-Trichloroethane	79-00-5	1		
Ethylbenzene	100-41-4	1	NL	8,000
Well 54-2002, 100 feet				
Trichloroflouroethane (F113)	76-13-1	87		
O-Xylene	95-47-6	8	1,000[4]	200,000[4]
Well 54-2002, 180 feet				
1,1,-Dichloroethene	75-35-4	35	0.03	10
Chloroform	67-66-3	28	0.04	100
Acetone	67-64-1	21		
1,1-Dichloroethane	75-34-3	13	0.04	8
Benzene	71-43-2	6	NL	NL
Well 2001, 100 feet				
1,2,-Dichloroethane	107-06-2	27	NL	NL
Dichloroflouromethane (F12)	75-71-8	3		
Chlorodibromomethane	124-48-1	2		
Well 2025, 100 feet				
Chlorobenzene	108-90-7	3	20	2,000

[1] Reference
[2] Reference
[3] Maximum depth of well
[4] Total for mixed xylenes

The conclusions reached by the MDA L RFI regarding the VOC plume are the following:

- No new VOCs are being detected although the list of vapor phase VOCs analyzed is growing;
- The list of vapor-phase VOC analytes has grown with improvements in sampling and analysis; and
- Based on a statistical analysis of samples from 1994 to 1996, the vapor phase VOC plume is laterally static.

Following the administrative suspension of quarterly vapor phase VOC sampling in mid-1996, sampling resumed in February 1997. Samples were collected primarily from perimeter monitoring wells.

1.3.4 Previous Investigations

Previous investigations on the vapor phase VOCs includes the following:

- Initial detection and characterization by International Technology (IT) Corporation in the mid 1980s;
- RCRA Facilities Investigation (RFI) Work Plan for Operable Unit 1148 (LANL, 1992, 0788);
- Quarterly pore-gas sampling;
- Appendix A, Voluntary Correction Plan, addendum to theRCRA Facilities Investigation (RFI) Work Plan for Operable Unit 1148 (LANL, 1992, 0788);
- Appendix A revised, Pilot Extraction Study Plan (PESP) for the Organic Vapor Plume at MDA L, Appendix A, RCRA Facilities Investigation (RFI) Work Plan for Operable Unit 1148 (LANL, 1992, 0788);
- Pilot tests in borehole 54-1003, Test 1 (18 October 1994), Test 2 (7-11 November 1994), and Test 3 (23-28 November 1994); and
- MDA L Phase 1 RFI report (in progress)

For the following discussions refer to the detailed site map of the extraction area (Fig. 1-5)

1.3.4.1 Early Geohydrologic Tests (1980s)

The following discussion was presented in Appendix A (Pilot Extraction Study Plan for the Organic Vapor Plume at MDA L) in the RFI Work Plan for Operable Unit 1148 (LANL, 1992, 0788).

"In 1985 and 1986, a variety of [geohydrological] tests were conducted to evaluate physical characteristics of the unsaturated volcanic tuff beneath MDA L. The tests included instrumentation of boreholes with thermocouple psychrometers, thermistors, and pressure gauges (transducers); air injection

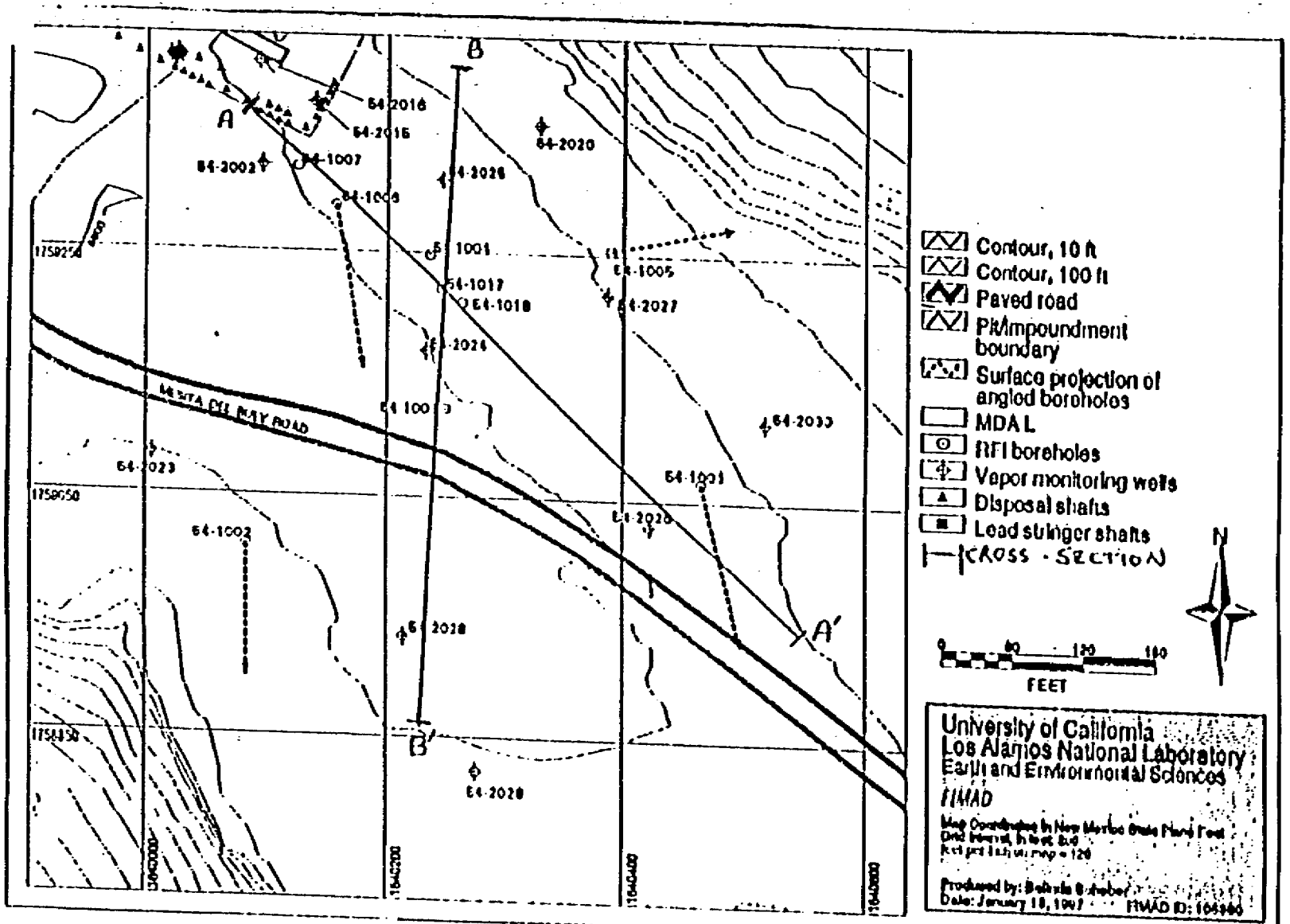

Figure 1-5. Locations of the Pilot Extraction Wells and PVET monitoring wells east of MDA L in the Formerly Proposed MDA G Expansion Area, TA-51.

and vacuum tests in boreholes using packers to isolate test intervals; and laboratory tests on core samples. Complete [geohydrological] test results can be found in the IT Corporation report (1987, 0327) and the Kearl, et. at., Report (Citation of Bendix GJ44 1986, 0135). A summary of the [geohydrological] test results was presented in Appendix A (Pilot Extraction Study Plan for the Organic Vapor Plume at MDA L) in the RFI Work Plan for Operable Unit 1148 (LANL, 1992, 0788). That summary of the [geohydrological] test results is repeated here:

- Porosity of the volcanic tuff is high with average values near 50%.
- Air permeability: varies between 10^{-9} and 10^{-7} cm^2 with the highest values measured in fracture zones.

  Intrinsic permeability (Klinkenberg tests on core samples) varies between 1.5×10^{-9} and 2.5×10^{-9} cm^2.
- Water potential varies from -1 bar near the surface to as low as -15 bars below 30 foot depth.
- Water content (gravimetric measurement) is usually in the range of 2%-4% (by volume), except at some fractures, or within the more highly welded portion of Unit 1b [1v(c)], or at some contact surfaces, where the content may reach 10% or 20%.
- Temperature is in the range 9-10°C, and is nearly independent of depth, below 30 ft depth.

1.3.4.2 Pilot tests in borehole 54-1003

As preparation for the larger-scale PVET, small scale pilot tests were performed by applying an active negative pressure at well 54-1003 (Fig. 1-3).

1.3.4.2.1 Pilot Test 1 (18 October 1994)

On 18 October 1994, a small scale pilot test applied a few psi of negative pressure at the surface of well 54-1003 (299 ft deep) for a duration of 4.33 hours. The negative pressure was applied using a hand-held electric pump. The effects of this small scale pilot test were measured by pressure transducers in Seamist™ monitored ports located in well 54-1004, 125 ft from well 54-1003. Prior to the test, monitoring ports had been positioned in well 54-1004 at depths of 37.5 ft, 48.9 ft, 70.3 ft, 113.2 ft, 124.3 ft, 140 ft, 179.8 ft, 223 ft, 254.5 ft, 310 ft, and 335 ft below the ground surface.

The results of this small scale pilot test indicated that the pressure transducers at 37.5 ft, 48.9 ft, 70.3 ft, 254.5 ft, and 310 ft in well 54-1004 detected the vacuum applied at well 54-1003. Of these monitoring locations, the port at 254.5 ft

indicated the fastest response to the vacuum. In addition, this port showed the closest behavior to atmospheric pressure as monitored by a pressure transducer located at the ground surface at well 54-1003.

1.3.4.2.2 Pilot Test 2 (7-11 November 1994)

From 7 November to 11 November 1994, a second small scale pilot test applied a few psi of negative pressure at the surface of well 54-1003. The negative pressure was applied using a hand-held electric pump. The effects of this small scale pilot test were measured by pressure transducers in Seamist™ monitored ports located in vertical wells 54-2024, 54-1004, and 54-2023 and in angle wells 54-1006, 54-1005 , and 54-1002 (Fig. 1-5). Table 1-4 is a list of wells and monitoring ports detecting the pilot test 2 vacuum based upon pressure vs. time plots.

Table 1-4. Monitoring wells and ports detecting pilot test 2 vacuum

Well Number, Declination Port Designation	Angle depth (ft)	Vertical Depth (ft)	Horizontal Distance from well 54-1003 (ft)
Well 54-2024, vertical			
Port I	NA [1]	200	50
Well 54-1006, 65° [2]			
Port H	188.2	169.1	118.5
Port J	249.8	224.5	97.5
Port K	283.8	255.0	87
Port L	314.5	282.7	78
Well 1004, vertical			
Port I	NA	222.3	125
Port J	NA	253.7	125
Port K	NA	313.0	125
Port L	NA	338.0	125
Well 54-1005, 69° [2]			
Port J	241.7	225.6	270
PortL	284.0	265.1	283.5
Well 54-1002, 69° [2]			
Port L	304.3	282.1	291

[1] NA indicates not applicable
[2] Declination is angle in degrees from horizontal

During pilot test 2, concentrations of 1,1,1-trichloroethane (TCA), trichloroethene (TCE), tetrachloroethene (PCE), vinyl chloride, and carbon dioxide (CO_2) were measured by a Bruel and Kjaer (B&K) Multi-gas Monitor Type 1302 at the well head for well 54-1003.

The B&K is an accurate, reliable and stable quantitative gas analyzer which is microprocessor controlled. Its measurement principle is based on the photoacoustic infra-red detection principle. In effect this means that the 1302 can be used to measure almost any gas which absorbs infra-red light. The B & K is capable of providing quantitative analysis of up to 5 compounds and water vapor in gas mixtures, with preselection and calibration for the specific compounds of interest.

During extraction, the concentrations of all analytes exhausted at well 54-1003 declined steadily (Fig. 1-6).

1.3.4.2.3 Test 3 (23-28 November 1994)

From 23 November to 28 November 1994, a third small scale pilot test applied a few psi of negative pressure at the surface of well 54-1003. The negative pressure was applied using a hand-held electric pump. The instrumentation used for the second small scale pilot test remained in place and was used to monitor the effects on pressure and contaminant concentrations between the second and third pilot tests. Figure 1-6 is a plot showing that contaminant concentrations declined in the open extraction well (54-1003) between the end of the second pilot test on 11 November 1994 (Julian Day 314 of 1994) and the start of the third pilot test on 23 November 1994 (Julian Day 327 of 1994).

This behavior indicated that once the pore volume was swept of air containing VOCs, the evacuated volume was apparently not replenished rabidly with air containing additional VOCs.

1.3.4.3 MDA L RFI

The primary objective of the MDA L Phase 1 RFI was to determine the nature and extent of contamination emanating from beneath MDA L. As the Laboratory's interest in controlling the vapor phase VOCs developed with the design of the PESP, it became apparent to integrate the objectives of the RFI and the PESP where-ever possible to maximize cost efficiency. Therefore, the RFI boreholes drilled near MDA L (boreholes 54-1001 through 54-1006 and 54-1015 through 54-1018) were designed to accept monitor wells and air-flow instrumentation. Pursuant to the RFI Work Plan, core samples were collected from the boreholes and analyzed for RFI chemical constituents, where-ever practical.

1.3.4.3.1 MDA L RFI PVET Boreholes

Boreholes 54-1001 through 54-1006 were drilled to depths ranging from 299 feet to 340 feet using an eight-inch diameter hollow stem auger and continuous coring technique. In each borehole, eight-inch diameter steel

surface casing was installed to a depth of 30 feet below the ground surface (bgs). Core samples were collected from boreholes 54-1001 through 54-1006 and analyzed for VOCs.

Boreholes 54-1015 and 54-1016 were drilled to depths of 530 feet and 607 feet, respectively, using air rotary installation of eight inch diameter ODEX™ casing to the bottom of each borehole. The boreholes were selectively cored for approximately 10 feet within every 40-foot interval below 260 feet. Core samples were collected and analyzed for VOCs and tritium. Following the installation of a Solinst™ multiport monitoring well in each borehole, the ODEX™ casing was withdrawn while annular well completion materials were installed.

Borehole 54-1017 was drilled to a depth of 159 feet using an eight-inch diameter hollow stem auger and reamed to 10 inches. Borehole 54-1017 contains 75 feet of 10-inch diameter steel casing and is open below the casing to a depth of 150 feet. Borehole 54-1018 was drilled to a depth of 328 feet using an eight-inch diameter hollow stem auger and continuous coring technique. No samples were collected for chemical analysis from either borehole. Samples were collected from 54-1018 for moisture content and possible future geotechnical analyses. Borehole 54-1018 contains 30 feet of eight-inch diameter steel casing. Boreholes 54-1001 through 54-1006 and 54-1018 were left open below the steel casing to become Seamist™ monitoring wells.

1.3.4.3.2 MDA L RFI Sample Results

PESP boreholes 54-1001, 54-1002, 54-1004, 54-1005, 54-1006 were drilled within the area of the vapor-phase VOC plume, as determined by the 54-2000 series wells (Pilot Extraction Study Plan (PESP) for the Organic Vapor Plume at MDA L, Appendix A, "RCRA Facilities Investigation (RFI) Work Plan for Operable Unit 114S" (LANL, 1992, 0788). No VOCs were detected in any of the core samples collected from these PESP boreholes. In addition, no VOCs were detected in core samples collected from boreholes 54-1015, and 54-1016 (Table 5.1.6-1, MDA L Phase I RFI report, in progress). However, in PESP borehole 54-1003, five VOCs were detected in one core sample at concentrations only slightly greater than the analytical detection limits (Table 3). This core sample was collected at a depth of 66.5 feet to 67.5 feet. No VOCs were detected in any other samples collected from borehole 54-1003.

Table 1-5. VOCs detected in the 67 ft core sample in borehole 54-1003.

VOC	Concentration (mg/Kg)	Detection Limit (mg/Kg)	SAL* (mg/Kg)
Bromobenzene	0.0075	0.005	not available
Dibromomethane	0.0073	0.005	650
Dichlorobenzene (1,2) [0-]	0.013	0.005	2300
Dichloropropane [1,3-]	0.0068	0.005	not available
Isopropyltoluene [4-]	0.0052	0.005	not available

* Screening Action Level (SAL)

Screening Action Levels (SALs) are defined for only two of the five VOCs detected in the 67 foot core sample from borehole 54-1003. A SAL is a concentration of the respective compound at which risk to human health from the compound is present if exposure occurs. The SALs for dibromomethane and dichlorobenzene (1,2) [0-] are approximately five orders of magnitude greater than the detected concentrations (Table 3). Therefore, these two VOCs were eliminated as compounds of potential concern (COPCs) by the screening assessment in the MDA L RFI Phase 1 Report (in progress). The remaining VOCs with no SALs (bromobenzene, dichloropropane [1,3-], and isopropyltoluene [4-]) were also eliminated as COPCs because they were detected at concentrations only slightly greater than detection limits (Table 3) and at a depth where exposure is not likely to occur (Environmental Restoration Project, in progress. "RFI Report for Potential Release Site 54-006, MDA L (located in former Operable Unit 114S), Field Unit 5," Los Alamos National Laboratory report LA-UR-97-xxxx, Los Alamos, New Mexico. (Environmental Restoration Project, in progress, project number)).

Analyses of core samples retrieved from boreholes located within the volatile plume indicate that there is no sorption of organic vapors on the matrix of the rhyolitic tuff nor are there liquids present. However, samples of pore gases withdrawn from the same boreholes indicate that vapors are distributed within the pore volumes (MDA L Phase I RFI, in progress).

2.0 ENVIRONMENTAL SETTING

The Laboratory is located on the Pajarito Plateau which forms an apron on the eastern flank of the Jemez Mountains in north central New Mexico. This plateau is eight to 16 miles wide and 30 to 40 miles long and gently slopes from the Sierra de los Valles on the west to the Rio Grande rift on the east. The plateau is dissected by east- southeast-trending canyons and mesas. The Laboratory's facilities are distributed across this terrain on Department of Energy (DOE) land.

TA-54 and MDA L are located on Mesita del Buey in the southeastern portion of the DOE land. At MDA L, the surface of Mesita del Buey is relatively flat and approximately 500 feet wide. The average altitude at MDA L is approximately 6,900 feet above mean sea level. In the vicinity of TA-54, Mesita del Buey is 100 ft to 140 ft higher than Pajarito Canyon on the southwest and a tributary to Cañada del Buey on the northeast.

2.1 CLIMATE

Los Alamos County has a semiarid, temperate, mountain climate. Summers are generally sunny with warm to hot days and cool nights. Summer temperatures typically range from 50°F at night to 95°F during the day. Winter temperatures typically range from 0°F at night to 32°F during the day. Surface winds average approximately 7 mph, but can vary significantly with time of day, location and height above the ground surface because of the dissected canyon and mesa terrain. The combination of high altitude and arid climate produce significant evaporation potential on the Pajarito Plateau. Evaporation of free-standing water is much greater than the amount of annual precipitation. The annual mean evaporation of shallow free-standing water is approximately 74 inches at TA-54. The average annual precipitation is estimated to be approximately 14 inches at TA-54 (Los Alamos Climatology, LA-11735-MS, 1990).

Approximately 40% of the precipitation on the Pajarito Plateau is produced by brief, intense thunderstorms from July through September. The remainder of the annual precipitation is predominantly winter snowfall which can vary significantly from year to year. Spring showers provide a relatively small component of the annual precipitation.

2.2 GEOLOGIC SETTING

Mesita del Buey is formed by stratigraphic cooling units of the Tshirege Member of the Bandelier Tuff. Moderately indurated volcanic tuff forms the mesa caprock and hosts the former disposal units at MDA L. Less indurated

(softer) tuff forms the mesa slopes. Older stratigraphic units are not exposed in the vicinity of MDA L (Figure 2-1). The lower mesa slopes and the adjacent canyon bottoms are covered with colluvium and alluvium that eroded from soils and *ex situ* tuff on the mesa top and upper slopes.

Soil on the mesa top is a sandy mixture of dissaggregated tuff. The soil is approximately one foot thick where present. *In situ* tuff locally crops out. On the upper mesa slopes, large blocks of indurated tuff have sloughed from the mesa caprock. The mesa soil and tuff support a piñon-juniper woodland with a variety of grasses, shrubs, and cactus. The larger piñon trees have extended roots to a depth of 42 feet along fractures (Report on activities for the pilot program for root distribution studies for FY93, internal LANL memorandum, Martens to Neeper, September 1993).

2.2.1 Stratigraphy

The stratigraphic rock units studied at MDA L during the Phase 1 RFI consist of, from oldest to youngest, the Cerros del Rio Basalt, the Puye Formation, the Otowi Member of the Bandelier Tuff, the Cerro Toledo interval, and the Tshirege Member of the Bandelier Tuff (Figure 2-2). Detailed descriptions of the stratigraphic units studied during the MDA L RFI drilling can be found as Attachment 1 of the MDA L RFI Report; borehole logs of 54-1000 series boreholes are in Attachment 2 and graphic profiles of each 54-1000 series borehole showing RCRA sample locations are in Attachment 3 (Environmental Restoration Project, in progress. "RFI Report for Potential Release Site 54-006, MDA L (located in former Operable Unit 1148), Field Unit 5," Los Alamos National Laboratory report LA-UR-97-xxxx, Los Alamos, New Mexico. (Environmental Restoration Project, in progress)).

The stratigraphic rock units hosting vapor phase VOCs beneath MDA L, and in the area of influence of the PVET, are limited to cooling units in the Tshirege Member of the Bandelier Tuff. The Tshirege Member is a multiple-flow ash-flow sheet, and a compound cooling unit, consisting of (from oldest to youngest) the basal Tsankawi Pumice Bed and a sequence of cooling units designated as units 1g, 1v, and 2 (Broxton and Reneau, 1995). Physical properties of the separate cooling units vary both vertically and laterally and result in zonal patterns of welding (compaction), induration (hardness), and crystallization (devitrification).

In outcrop, the more indurated portions of the cooling units are cliff-forming horizons. These rocks typically contain steeply dipping fractures and cooling joints that vary in size and abundance. Purtyman and Kennedy (1971) and Reneau and Vaniman (in preparation) summarize cooling joints in the Los

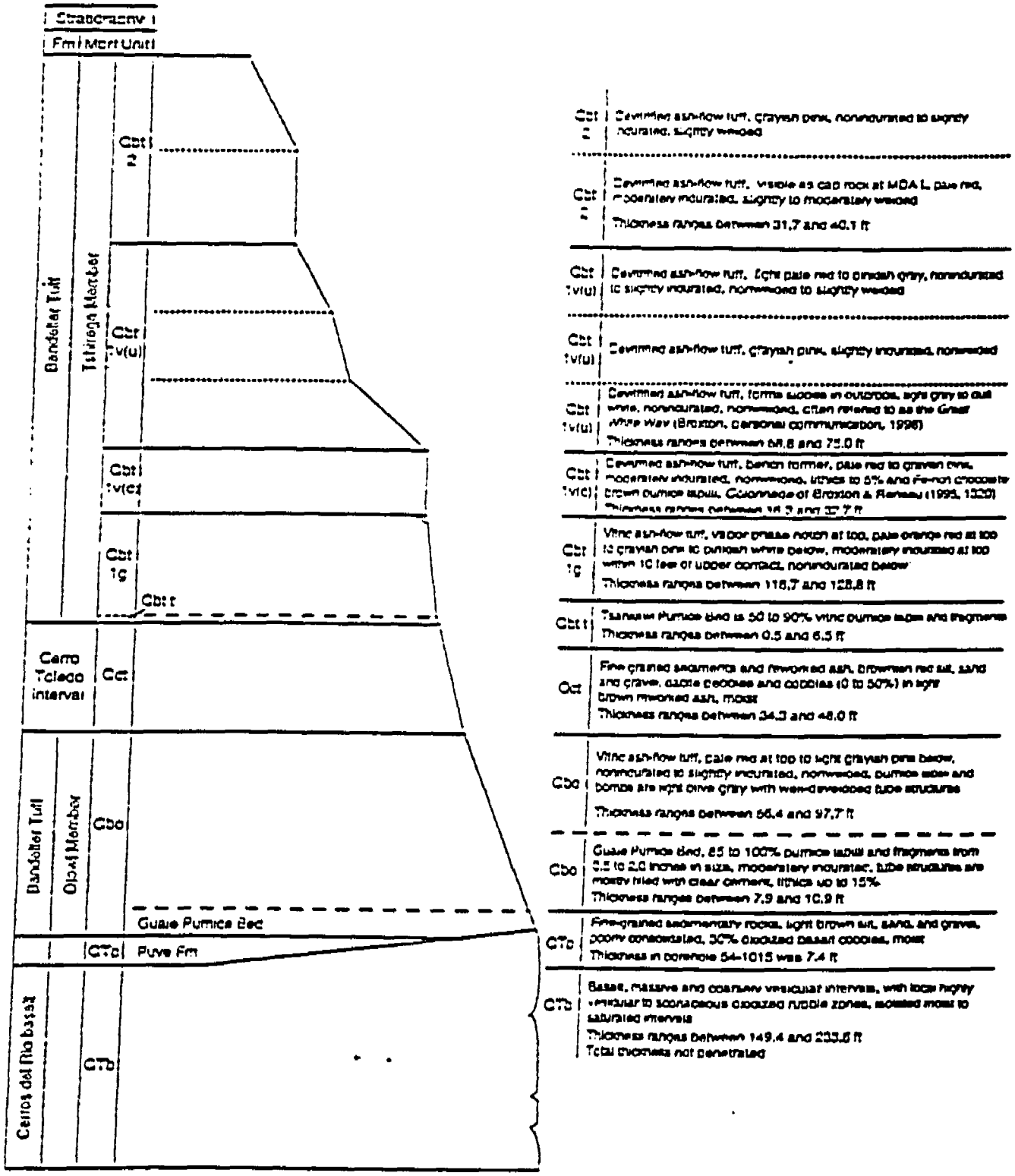

Figure 2-1. Detailed stratigraphic column in the vicinity of MDA L, TA-54.

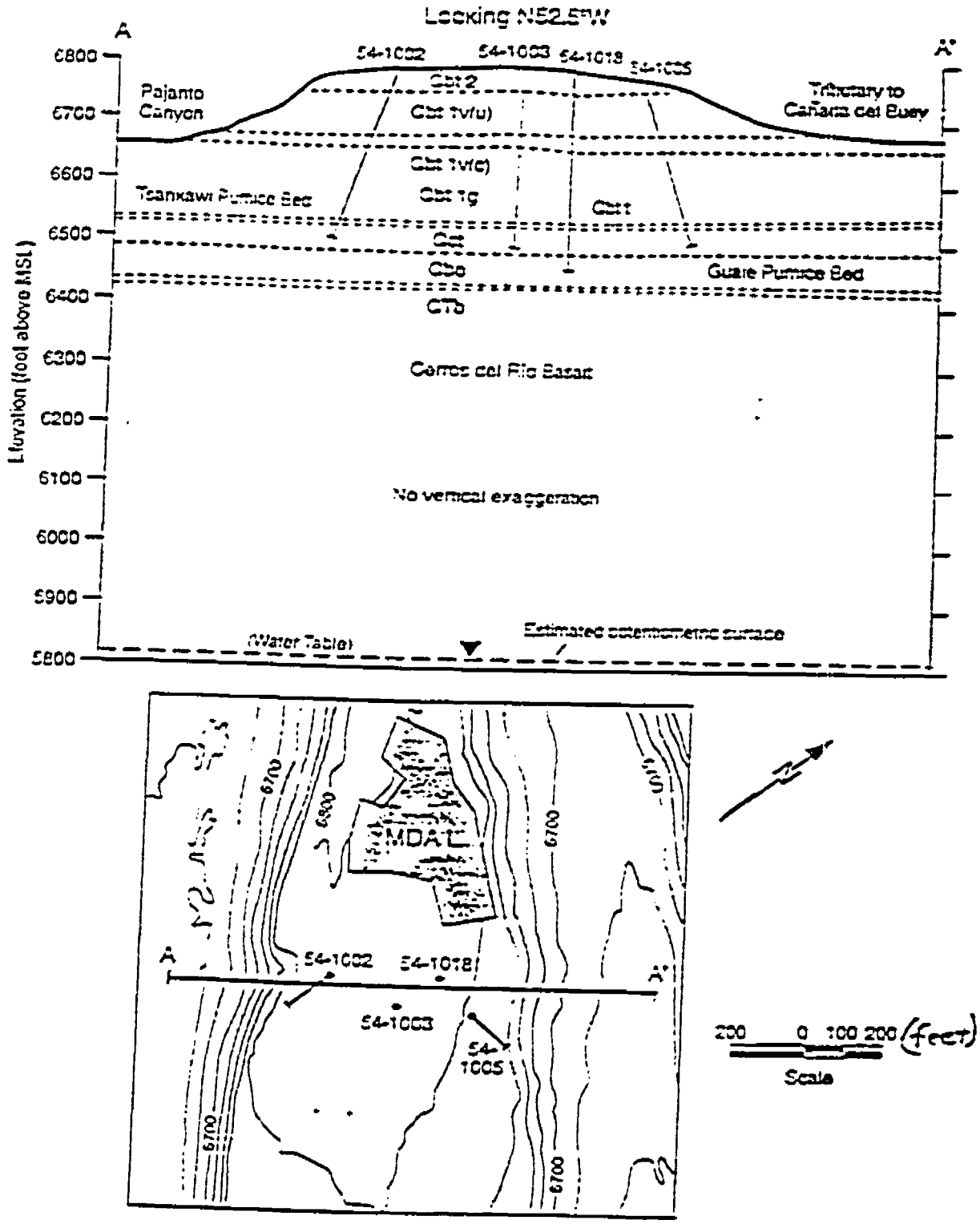

Figure 2-2. Cross section of Mesita del Buey at MDA L and location of MDA L on Mesita del Buey.

Alamos area. The less indurated (softer) portions of the cooling units form slopes at the ground surface. In the subsurface, these rocks are probably too soft to support the continuation of fractures or joints from adjacent more indurated tuff (MDA G Performance Assessment, in progress). A disruption, or fracture of the less indurated tuff matrix is physically absorbed and not perpetuated by the softer rock matrix. Drilling itself likely disrupts the delicate three-dimensional matrix of the nonindurated tuff by transmitting kinetic energy during the coring operation. Nonindurated tuff is typically recoverered as soft powder. The coring operation will destroy any evidence of fractures in the nonindurated tuff, if present.

Figures 2-3 and 2-4 are cross-sections showing the stratigraphy of the Bandelier Tuff in the area of the PVET. The locations of the cross-sections are shown on Figure 1-5.

2.2.1.1 Bandelier Tuff

The Bandelier Tuff is a series of pyroclastic ash flows derived from explosive eruptions in the Valles caldera located in the Jemez Mountains west of the Laboratory. The Bandelier Tuff consists of two members: the Otowi Member and the Tshirege Member (Smith, et al., 1970). The Otowi and Tshirege Members of the Bandelier Tuff are separated by an erosional/depositional interval informally designated the Cerro Toledo interval that is not considered part of the Bandelier Tuff (Smith, et al., 1970).

2.2.1.1.1 Otowi Member

The Otowi Member of the Bandelier Tuff is dated at 1.613 ± 0.011 million years before present (Ma) by Ma, Izett and Obradovich (1994).

2.2.1.1.1.1 Guaje Pumice Bed

The Guaje Pumice Bed is the basal pumice fall deposit of the Otowi Member of the Bandelier Tuff.

2.2.1.1.1.1.1 Lithology

The Guaje Pumice Bed beneath MDA L is a very light gray to light olive gray to pale yellowish brown hard aggregate consisting of vitric pumice lapilli and pumice fragments from 0.5 to 2.0 inches in size. Pumice lapilli typically exhibit olive to light yellow oxidation and may contain up to 10 percent mafic inclusions. The pumice lapilli interiors are very glassy and tube structures are mostly to partially destroyed. The remnant tube structures are filled with a clear silica-like cement that causes the lapilli to clump together and gives a moderate to strong induration to the pumice bed (MDA L RFI Report, in progress).

Lithics are dark gray to black, partially oxidized, 0.05 to 0.5 inch basalt pebbles and fragments up to 15 percent and averaging five percent. Lithic fragments are also incorporated into the cemented pumice aggregate.

2.2.1.1.1.1.2 Distribution and Thickness

Both boreholes 54-1015 and 54-1016 drilled through the Guaje Pumice Bed beneath MDA L. In borehole 54-1015, the Guaje Pumice Bed is 10.9 vertical feet thick and overlies moist fine-grained ash arbitrarily assigned to the Puye Formation. In borehole 54-1016, the Guaje Pumice is 7.9 vertical feet thick and overlies a 1.5 ft thick clay soil horizon atop basalt.

2.2.1.1.1.2 Otowi Member Tuff

2.2.1.1.1.2.1 Lithology

With the exception of the basal Guaje Pumice Bed, the Otowi Member of the Bandelier Tuff is a massive, nonwelded, pumice rich vitric ash flow tuff. The pumice lapilli are fully inflated and tube structures are intact. Pumice lapilli make up 20 percent by volume of the tuff and range in size from 0.2 to 3.0 inches. Their color is light gray to light yellow or olive brown. The pumice glass is unaltered. The pumice lapilli are supported by a pale red ash matrix at the top of the member to light grayish pink ash below. The ash consists of minute glass shards, phenocrysts, perlite clasts and broken pumice fragments (Caporusio, F. A., Description of rock units in drill core at TA-54, Los Alamos National Lab, 1994).

Phenocrysts are predominantly quartz and sanidine (potassium-feldspar) from 0.05 to 0.15 inches in size. Clinopyroxene and amphibole are accessory phenocryst minerals. In total, phenocrysts make up approximately 10 percent by volume of the tuff. Lithic fragments are typically less than 0.3 inch in size and consist primarily of aphanitic intermediate composition lavas. Lithics comprise less than two percent by volume of the tuff. Pumice swarms occur sporadically in which pumice lapilli may represent up to 30 percent of the volume of the tuff (Caporusio, F. A., Description of rock units in drill core at TA-54, Los Alamos National Lab, 1994).

2.2.1.1.1.2.2 Distribution and Thickness

The Otowi Member is not exposed at the surface in the vicinity of MDA L. Of the 18 boreholes in the MDA L Phase 1 RFI drilling program, four boreholes were deep enough to encounter the Otowi Member. Of these four boreholes, two boreholes ended in the Otowi Member. Where completely penetrated in boreholes 54-1015 and 54-1016, the Otowi Member including the basal Guaje Pumice Bed ranges in vertical thickness from 64.3 ft (54-1016) to 108.6 ft (54-

1015). This difference in thickness between 54-1015 and 54-1016, over a lateral distance of approximately 380 ft, suggests the thinning of the Otowi Member caused by the presence of a basalt high to the east of MDA L (Broxton and Reneau, 1996).

2.2.1.1.2 Cerro Toledo interval

2.2.1.1.2.1 Lithology

Broxton, et al., (1993) describe the Cerro Toledo interval as the following: "This interval included epiclastic tuffaceous sandstones, siltstones, and ash and pumice falls. In addition, the Cerro Toledo interval contains intercalated gravel, cobbles, and boulder deposits made up of material derived from erosion of dacitic lavas from the Tchicoma Formation."

Beneath MDA L, the Cerro Toledo interval consists predominantly of moist brownish red silt, sand, gravel and from 10 to 50 percent subrounded dacite pebbles and cobbles. The finer grained matrix consists predominantly of reworked ash and up to 40 percent sand to gravel sized quartz and sanidine reworked phenocrysts. The pebbles and cobbles are predominantly intermediate composition lavas with accessory granite, arkose, feldspar-rich obsidian, and flow banded rhyolites (Caporusio, F. A., Description of rock units in drill core at TA-54, Los Alamos National Lab, 1994). Pebbles and cobbles typically range in size from 0.5 to 2.0 inches but may be as large as 4.0 inches in diameter.

2.2.1.1.2.2 Distribution and Thickness

The Cerro Toledo interval is not exposed at the surface in the vicinity of MDA L but does crop out in the bottom of Cañada del Buey near MDA G approximately 0.5 mile east-southeast of MDA L. Of the 18 boreholes in the MDA L Phase 1 RFI drilling program, nine boreholes were deep enough to encounter the Cerro Toledo interval. Of these nine boreholes, five boreholes ended in and four boreholes penetrated the Cerro Toledo interval. Where completely penetrated, the Cerro Toledo interval ranges in vertical thickness from a minimum of 34.3 ft in borehole 54-1015 to a maximum of 48.0 ft in borehole 54-1016. The average thickness of the Cerro Toledo interval beneath MDA L is 40.2 ft.

2.2.1.1.3 Tshirege Member

The Tshirege Member of the Bandelier Tuff is dated at 1.223 ± 0.018 Ma by Ma, Izett and Obradovich (1994).

2.2.1.1.3.1 Tsankawi Pumice Bed

The Tsankawi Pumice Bed is the basal pumice fall deposit of the Tshirege Member of the Bandelier Tuff. It overlies the volcaniclastic deposits of the Cerro Toledo Interval.

2.2.1.1.3.1.1 Lithology

The Tsankawi Pumice Bed consists of 70 to 90 percent, 0.3 to 4.0 inch diameter, white, vitric, phenocryst poor pumice lapilli in one to three discrete 0.5 to 2.0 foot thick beds. Where more than one pumice bed exists, they are typically separated by intervals of ash flow tuff over a vertical thickness of 2.0 to 6.0 feet. The upper contact of the Tsankawi Pumice Bed is arbitrarily established at the bottom of a thick pumice-rich ash flow tuff.

2.2.1.1.3.1.2 Distribution and Thickness

The Tsankawi Pumice Bed is not exposed in the vicinity of MDA L but does crop in the bottom of Cañada del Buey near MDA G approximately 0.8 mile east-southeast of MDA L. Of the 18 boreholes in the MDA L Phase 1 RFI drilling program, nine boreholes penetrated the Tsankawi Pumice Bed. The Tsankawi Pumice Bed ranges in vertical thickness from a minimum of 0.5 ft in borehole 54-1004 to a maximum of 6.5 ft in borehole 54-1005. The average thickness of the Tsankawi Pumice Bed beneath MDA L is 2.4 ft.

2.2.1.2 Unit 1g

2.2.1.2.1 Lithology

Unit 1g is a massive, nonwelded, mostly nonindurated, vitric (glassy) ash flow tuff. The unit is predominantly grayish pink to pinkish white. On average, the upper nine feet of the unit is pale orange red and is the only indurated tuff in the unit. Fractures occur in the indurated tuff but are probably absent in the nonindurated majority of the unit. Pumice lapilli are gray to white in a pinkish white ash matrix in 60 percent of the unit and olive gray in the iron-rich upper part. The lapilli exhibit a silky vitreous luster and the tube structures are well preserved and fully inflated. On average, the lapilli make up 20 percent by volume of the tuff and range in size from 0.3 to 1.5 inch in diameter. Pumice swarms occur locally. Pumice lapilli range in volume from 20 to 40 percent with an average pumice size of 1.5 inches in diameter. The lapilli are also phenocryst rich, containing up to 35 percent phenocrysts locally. Phenocrysts are predominantly quartz (up to 0.1 inch) and sanidine (up to 0.05 inch) which typically do not exhibit schiller iridescence. Accessory minerals consist of rare minute ferromagnesian minerals that are probably amphiboles. In the tuff matrix, phenocrysts make up 20 percent by volume of the tuff and are identical to phenocrysts in the pumice lapilli. Dacite lithics from 0.1 to 2.0 inches is size are from zero to

three percent of the nonindurated majority of the unit. However, dacite lithics locally comprise up to 10 percent of the indurated iron-rich upper portion of the unit.

The lower contact of unit 1g is the pumice fall deposit(s) of the Tsankawai Pumice bed. The upper contact of unit 1g is the vapor-phase notch of Crowe et al. (1978). This contact is at the top of an interval of devitrification which is the transition from the glassy (vitric) tuff in unit 1g to the overlying crystallized (devitrified) tuff in younger stratigraphic units (Broxton and Reneau, 1995). The upper contact of unit 1g is established at the first appearance of glassy pumice going down section. The vapor-phase notch is laterally extensive throughout the Pajarito Plateau and creates a good marker horizon in boreholes.

2.2.1.2.2 Distribution and Thickness

Unit 1g is not exposed at the surface in the vicinity of MDA L but does crop out in the bottom of Cañada del Buey near MDA G approximately 0.8 mile east-southeast of MDA L. Of the 18 boreholes in the MDA L Phase 1 RFI drilling program, 13 boreholes were deep enough to encounter unit 1g. Of these 13 boreholes, five boreholes ended in unit 1g. Where completely penetrated, unit 1g ranges in vertical thickness from a minimum of 116.7 ft in borehole 54-1005 to a maximum of 128.8 ft in borehole 54-1006. The average thickness of unit 1g beneath MDA L is 125.5 ft.

Within unit 1g , the interval of devitrification ranges in thickness from a minimum of zero to a maximum of 5.6 ft in borehole 54-1016. The average thickness of the interval of devitrification beneath MDA L is 3.5 ft.

The interval of devitrification is contained within the indurated iron-rich upper portion of unit 1g. The thickness of the indurated iron-rich upper portion of unit 1g varies significantly over lateral distances of several hundred feet. This subunit ranges in thickness from a minimum of 4.0 in borehole 54-1004 to a maximum of 18.8 feet in borehole 54-1001. The average thickness of the indurated upper portion of unit 1g at MDA L is 8.9 feet.

2.2.1.3 Unit 1v

2.2.1.3.1 Lithology

Unit 1v is a sequence of devitrified tuffs which are nonwelded to slightly welded, nonindurated to moderately indurated, poorly sorted, vapor-phase altered, pumice-rich ash flows. It consists of crystal-rich brown to gray pumice lapilli set in a dull white, grayish pink, or light pale red matrix of minutely crystallized ash shards and larger subhedral phenocrysts. Pumice lapilli range from eight to 15 percent of the tuff by volume with an average at 12 percent. The pumice lapilli range from 0.2 to 2.5 inches in diameter and are equant to

elongate in shape. The lapilli typically exhibit a megascopically visible sugary texture caused by the nucleation and growth of euhedral tridymite or cristobalite and sanidine crystals along the relict tube structures during devitrification. With the exception of the lowest subunit, the matrix of unit 1v is also surgery from the presence of up to 60 percent minute vapor phase deposited tridymite crystals (Warren, personal communication, 1997) Discrete pumice accumulations (swarms) occur within this unit and range in volume from 20 to 40 percent with an average pumice size of 1.5 inches in diameter. Phenocrysts in unit 1v range in volume from 20 to 30 percent and average near 25 percent. They consist predominantly of sanidine and quartz with an average size of 0.15 inch. Lithic fragments are predominantly dacitic in composition and are typically less that one percent of the total volume, except in the basal subunit described below (Caporusio, F. A., Description of rock units in drill core at TA-54, Los Alamos National Lab, 1994).

Unit 1v consists of subunits based on slightly differing physical characteristics. The subunits form a combination of step-like benches and slopes in outcrop (Broxton and Reneau, 1995) and are traceable between boreholes drilled at MDA L. The basal subunit of unit 1v is a resistant orange-brown tuff that creates a bench above unit 1g and is designated 1v(c) due to its "colonnade" appearance in outcrop (Broxton and Reneau, 1995). In core, subunit 1v(c) exhibits distinct characteristics that distinguish it from adjacent subunits.

The lower contact of subunit 1v(c) corresponds to the top of the interval of devitrification described previously. This contact is the first appearance of vitric pumice going down section. Subunit 1v(c) is moderately indurated, which distinguishes it from the overlying nonindurated subunit of unit 1v (Fig. 2-1). Subunit 1v(c) typically contains from 2 to 10 percent dacite lithics (increasing down section) that range from 0.2 to 2.0 inches in diameter. Subunit 1v(c) typically hosts coarsely devitrified, dark chocolate brown, iron-rich, pumice lapilli. In contrast to the overlying subunits of unit 1v, the tuff matrix in subunit 1v(c) is typically devoid of the surgary fine-grained vapor phase silica devitrification product. Subunit 1v(c) contains cristobalite as the SiO_2 devitrification product as opposed to tridymite in the overlying portions of unit 1v (Broxton, et al, 1993). Cristobalite is the higher temperature polymorph of quartz (SiO_2) suggesting that a higher temperature regime existed in subunit 1v(c) during devitrification than in younger stratigraphic units. In addition, subunit 1v(c) typically exhibits a moisture spike at the vapor phase notch and a moisture increase in contrast to the overlying subunits (Broxton, et al., 1993, Stimac, et al., 1995). In borehole 54-1001, minute magnetite crystals were observed within the matrix of subunit 1v(c) at clay-filled fractures. The magnetite crystals are typically surrounded by diffuse limonite halos disseminated in the tuff matrix.

Subunit 1v(u) overlying 1v(c) is a sequence of ash flow tuffs which are nonindurated and light gray to dull white at the base, slightly indurated and grayish pink in the middle, and nonindurated to slightly indurated light pale red to pinkish gray at the top. The variations of induration in subunit 1v(u) create step-like slopes between the cliff-forming caprock on the mesa and the bench-forming subunit 1v(c) at the canyon floors (Fig. 2-1). In the subsurface, the basal portion of subunit 1v(u) is distinctly light gray to dull white and nonindurated in contrast to subunit 1v(c). In the field, the nonindurated basal portion of subunit 1v(u) is informally referred to as the "Great White Way" (Broxton, personal communication, 1996). The middle portion is slightly more indurated, grayish pink, and nonwelded. Pumice lapilli at this level in subunit 1v(u) have light gray cores, light pinkish white spherulitic clay deposits along relict tube structures, and much less accumulation of dark brown iron which occurs typically at the lapilli perimeters. In the upper portion of subunit 1v(u), the ash is pale red to pinkish gray, non- to slightly-indurated, and non- to slightly- welded (Fig. 2-1). The pumice lapilli are light gray to brown and iron-poor compared to lapilli lower in the subunit.

2.2.1.3.2 Distribution and Thickness

In the vicinity of MDA L, subunit 1v(c) is covered by alluvium on the lower slopes of Mesita del Buey (Fig. 2-1). Near MDA G approximately 1/2 mile east-southeast of MDA L, subunit 1v(c) forms a bench immediately above the lower alluvium slopes. Of the 18 boreholes in the MDA L Phase 1 RFI drilling program, 13 boreholes penetrated subunit 1v(c). Of these 13 boreholes, subunit 1v(c) was indistinguishable from subunit 1v(u) in five boreholes. Where distinguishable, subunit 1v(c) ranges in thickness from a minimum of 16.3 ft in borehole 54-1002 to a maximum of 26.0 ft in boreholes 54-1017 and 54-1018. The average thickness of subunit 1v(c) at MDA L is 20.6 ft.

Subunit 1v(u) forms the slopes above the bench where subunit 1v(c) is exposed through the alluvium and extends to the base of the surface caprock of the mesa (Fig. 2-1). Of the 18 boreholes in the MDA L Phase 1 RFI drilling program, 11 boreholes penetrated subunit 1v(u). Subunit 1v(u) ranges in thickness from a minimum of 65.0 ft in boreholes 54-1017 and 54-1018 to a maximum of 75.0 ft in borehole 54-1009. The average thickness of subunit 1v(u) at MDA L is 70.6 ft.

2.2.1.4 Unit 2

2.2.1.4.1 Lithology

Unit 2 is a massive, slightly indurated to strongly indurated, moderately welded, vapor phased altered ash-flow tuff. All pumice lapilli or bombs in this unit show slight but discernible flattening. Unit 2 consists of 5 to 10 percent dark gray to light brown crystal-rich pumice lapilli set in a pale red ash matrix containing 35 to 40 percent phenocrysts. Pumice lapilli range in

size from 0.4 to 3.0 inches, averaging 1.0 inch throughout the unit. Pumice swarms occur locally, with pumice bombs up to 6.0 inches in length and 15 to 20 percent by volume. With increasing depth, the pumice lapilli change in color to moderate dark brown with gray cores. The elongated pumice lapilli typically exhibit a linear sugary texture similar to that displayed in the devitrified tuffs of unit 1v. The compaction (welding) of unit 2 has mostly eliminated the surgery matrix of unit 1v(u), however, less indurated portions of unit 2 also contain very minute vapor phase tridymite in the tuff matrix.

Phenocrysts in unit 2 consist predominantly of bipyramidal quartz and rhombohedral sanidine typically showing blue schiller iridescence. Phenocryst abundance in unit 2 is up to 40 percent by volume and nearly double the phenocryst abundance in unit 1v. Hornblende-bearing pumice lapilli are rare but notable. Where observed, they are typically less than one percent of the tuff and are light gray in color due to minute mafic crystals (up to 20 percent) in the lapilli. Lithics are rare (less than one percent by volume) and are predominantly intermediate in composition. The lithics range in size from 0.1 to 2.0 inches and average 1.0 inch (Caporusio, F. A., Description of rock units in drill core at TA-54, Los Alamos National Lab, 1994).

Fractures, or cooling joints are common in unit 2 at MDA L. Most fractures are vertical to steeply dipping. Tree roots are seen in fractures within 60 feet of the ground surface. Fractures are typically surrounded by oxidized tuff. The fracture walls may locally be coated with calcite and amorphous red-brown clay, or opal-like material. Reneau and Vaniman (1994) report that average joint spacing at MDA G approximately 1/2 mile east-southeast of MDA L varies from 3.2 to 4.2 feet. The maximum joint openings are 2 inches but most are less than 0.25 inch.

2.2.1.4.2 Distribution and Thickness

In the vicinity of MDA L, unit 2 forms the surface of Mesita del Buey and is the youngest stratigraphic unit exposed (Fig. 2-1). Unit 2 is locally separated from the underlying unit 1v by a base surge deposit consisting of 60 percent quartz and sanidine crystals (Caporusio, F. A., Description of rock units in drill core at TA-54, Los Alamos National Lab, 1994). Of the 18 boreholes in the MDA L Phase 1 RFI drilling program, 16 boreholes were started in unit 2. Although not completely penetrated in the vicinity MDA L, unit 2 ranges in thickness from a minimum of 30.8 ft in borehole 54-1005 to a maximum of 40.5 ft in borehole 54-1014. The average thickness of unit 2 at MDA L is 36.9 ft.

2.2.2 Hydrology

2.2.2.1 Surface Water

Los Alamos area surface water consists primarily of intermittent streams. Springs on the flanks of the Jemez Mountains supply water into the upper reaches of some canyons. Precipitation is periodic and of variable volume.

In most areas of the plateau, the amount of runoff and spring water is insufficient to maintain surface flow before it is depleted by evaporation, transpiration, and infiltration. Only a few larger streams fed by multiple springs or surface water discharge flow continuously.

Adjacent to MDA L, Pajarito Canyon and the tributary to Canada del Buey contain intermittent streams. The flow derives predominantly from summer thunderstorms and spring snow melt. Runoff from summer storms reaches a maximum discharge in less than 2 hours and typically dissipates in less than 24 hours. Spring snow melt takes place over a period of several weeks to several months at low discharge rates.

2.2.2.2 Ground Water

Ground water exists in three modes in the Los Alamos area: (1) water in shallow alluvium in canyons, (2) perched water occasionally found in deeper bed rock strata beneath canyon floors, and (3) the much deeper main aquifer of the Los Alamos area (Hydrogeologic Work Plan, draft, 1996).

2.2.2.2.1 Alluvial Water

Water in shallow alluvium in the canyon bottoms is likely to be irregularly distributed. It derives predominantly from infiltration of surface water runoff near drainages or saturation of alluvium near widely scattered springs. The presence and flow of ground water in the alluvium is a function of intermittent surface water supply, proximity to springs, and abrupt changes in the nature of the alluvium (e.g., dams created by large blocks of volcanic tuff or basalt, preferential pathways along zones of higher permeability, or retardation by clay, mineralization, or organic debris in fractures).

2.2.2.2.2 Perched Water

Extensive shallow drilling, particularly the geological characterization drilling in the mid-1980s (Kearl et al. 1986, 0135) and the RFI drilling in the 1990s, encountered no laterally continuous perched aquifers within the Tshirege Member of the Bandelier Tuff. However, boreholes 54-1015 and 54-1016 encountered water in older stratigraphic units several hundreds of feet above the main aquifer. The sedimentary Cerro Toledo interval and fine-grained material arbitrarily assigned to the Puye Formation were moist to saturated. The Cerros del Rio Basalt was locally moist to saturated in approximately 50 percent of the core retrieved. A two-foot thick oxidized clay soil horizon overlying the basalt in boreholes 54-1016 was saturated (gravimetric moisture content was 24 percent). In borehole 54-1015 at depths of 490 feet, 510 feet, and 521 feet, and in borehole 54-1016 at depths of 592 feet and 595.5 feet, from one quart to one gallon of water was emitted from the cased borehole by the drilling air circulation system required for ODEX™ casing installation. Repeated attempts to sample the water in borehole 54-1015 were unsuccessful because of the lack of available water volume. On 26 April 1996, water

sampling was unsuccessful in both deep monitoring wells; insufficient water volume had accumulated at the water monitoring ports. Thus these wet zones are not considered to be perched aquifers.

Recent isotopic study of perched water collected at the Laboratory suggest that the perched water is relatively old and likely not derived from surface infiltration (Brent Newman, LANL TA-51, personal communication, 1997). It has been speculated that bodies of perched water may be isolated remnants of a higher main aquifer beneath the Pajarito Plateau during a less arid climate (Gilkeson, personal communication, 1997). The unsaturated zone beneath the Pajarito Plateau is in effect "drying out" (c.f., the difference between annual precipitation at 14 inches per year and surface evaporation at 74 inches per year described in Section 2.1). This theory is supported by the presence of an iron-oxide (limonite) water mark on basalt core at a depth of 381.5 in borehole 54-1015. This water mark is at an elevation of 6373 feet which is approximately 550 feet higher than the estimated current elevation of the main aquifer.

2.2.2.2.3 Main Aquifer

Depths to the main aquifer beneath the Laboratory have been compiled by Purtyman (1984, 0196). At Mesita del Buey, the depth ranges from about 1040 feet in well PM-2 in the vicinity of MDA H approximately 0.8 mile west-northwest of MDA L to 900 feet beneath the eastern portion of MDA G, approximately one mile east-southeast of MDA L. Well PM-2 is the main aquifer water level measurement point nearest MDA L. Based on the surrounding data, the main aquifer beneath MDA L is estimated to be at an elevation of 5,820 above sea level and at a depth of 970 feet below the mesa (Fig. 2-2). To date, there has been no drilling to the main aquifer in the vicinity of MDA L. However, a borehole was proposed in the OU-1148 RFI Work Plan to be drilled to the main aquifer between MDA L and MDA G. The drilling of this borehole is suspended at present. Host rocks for the aquifer beneath MDA L are probably sedimentary fanglomerates, conglomerates, and sandstones of the Santa Fe Group beneath and interlayered with thick basalt flows.

2.2.3 Geohydrologic Characteristics of Bandelier Tuff Subunits at MDA L

The PVET is concerned with extracting air and contained vapor phase VOCs through various cooling units and subunits of the Tshirege Member of the Bandelier Tuff. Therefore, in regard to the performance of the PVET, specific hydraulic properties and geohydrological characteristics of these rocks are important to understand the "environmental medium" through which the VOCs will move.

The MDA G Performance Assessment (in progress), compiled a summary of hydraulic properties of Bandelier Tuff units from boreholes at TA-54, including boreholes 54-1001 through 54-1006 located adjacent to MDA L. Hydraulic properties summarized include bulk density, volumetric moisture content, porosity, saturation, saturated hydraulic conductivity, and matrix tension. In addition to these quantitative analytical measurements, qualitative observations of geohydrologic properties compiled from geologic logging, such as induration (hardness), the presence or preservation of fractures, and matrix properties (grain size and presence of alteration clay and minute silica), are discussed in the following sections.

2.2.3.1 Bulk Density

Bulk density measurements ranged from a minimum of 1.05 g/cm^3 in the combined Tsankawi Pumice Bed and Cerro Toledo Interval to a maximum of 1.46 g/cm^3 in Unit 2. Average values for isolated stratigraphic units are compiled in Table 2.1. Average bulk density values demonstrate a gradual but consistent decline going downsection (Table 2.1).

Table 2-1. Summary of Geohydrologic Properties[1]

Stratigraphic Units/Subunits		Hydraulic Properties[2]					Geohydrologic Characteristics[3]		
Strat. Unit[4]	Strat. Sub-unit[5]	Bulk Density (g/cm³)	Porosity (%)	Vol. Moist. Cont.[6] (%)	Satur-ation (%)	Sat. Hydr. Cond.[7] (cm/s)	Grav. Moist. Cont.[8] (%)	Indur-ation[9]	Fract-ures[10]
2	2(u) ..... 2(l)	1.37	45.7	2.57	5.7	4.37 X 10^{-4}	2.12 ..... 1.24	mod ..... strng	many ..... many
1v(u)	1v(u₂) ..... 1v(u₁)	1.24	48.7	1.89	3.7	1.48 X 10^{-4}	1.03 ..... 1.79	slight ..... non	mod ..... none
1v(c)	1v(c)	1.18	49.3	10.88	21.3	1.67 X 10^{-4}	5.11	mod	mod
1g	1g(u)[11] 1g	1.15	46.2	8.94	16.9	1.88 X 10^{-4}	5.77 ..... 5.83	mod ..... non	mod ..... none
Tsank-awi/ Cerro Toledo	Tsank-awi/ Cerro Toledo	1.12	47.3	14.0	30.3	8.65 X 10^{-4}	10.80 ..... 8.49	mod ..... slight	rare ..... rare

(1) Averaged by stratigraphic unit
(2) From Table 3, MDA G Performance Assessment (LAUR-95-2696)
(3) From MDA L and MDA G RFI boreholes.
(4) Stratigraphic nomenclature follows Broxton and Reneau, 1995. See Fig. 2-2.
(5) Stratigraphic subunits from MDA L and MDA G RFI borehole logging.
(6) Volumetric Moisture Content
(7) Saturated Hydraulic Conductivity
(8) Gravimetric Moisture Content
(9) Qualitative induration (hardness) scale is non=nonindurated, slight=slightly indurated, mod=moderately indurated, strg=strongly indurated
(10) Qualitative fracture scale is none=not present, rare=few present, mod=some present, many=fractures abundant
(11) Subunit 1g(u) includes the upper indurated and iron-rich portion (average

2.2.3.2 Porosity

Porosity measurements ranged from a minimum of 39.3 percent in unit 1g to a maximum of 73.6 percent in Unit 2. Porosity measurements within individual stratigraphic units, or subunits, vary significantly (Fig. 2-5). This is a function of either lateral and vertical heterogeny within each unit, measurement location at secondary features such as fractures, or laboratory analytical error.

Rogers and Gallaher (LA-1296S-MS, 1995) published the results of porosity tests on geotechnical core samples obtained from boreholes 54-1001, 54-1002, 54-1003, and 54-1006 located east of MDA L (Daniel B. Stephens & Associates, Inc. "Laboratory Analysis of Soil Hydraulic Properties of Boreholes 54-1001, 54-1002, 54-1003, and 54-1006").

Although the data are limited to only five samples from each borehole, the following general observations are suggested (Fig. 2-5):

- Porosity ranges from a minimum value of 39.3% to a maximum value of 52.6%.
- Although both the minimum and maximum porosity values came from samples of Unit 1g, they came from different boreholes. This suggests that the porosity of Unit 1g is variable over lateral distances of several hundred feet;
- The indurated upper portion of Unit 1g (Unit 1g(u)) demonstrates a consistency of porosity values at 46 to 49%.
- Unit 1v(c) (Colonnade) exhibits a variable porosity at the top of the subunit near the contact with Unit 1v(u).
- Unit 1v(u) (upper) shows a range of porosity values from a minimum of 41.4% to a maximum of 51%, indicating a lateral variability of porosity in Unit 1v(u). However, the porosity values in this unit exhibit a trend toward higher values downsection in Unit 1v(u) toward Unit 1v(c).

Average values for isolated stratigraphic units are compiled in Table 2-1. Average porosity values show a slight maximum in unit 1v(c).

2.2.3.3 Volumetric Moisture Content

Volumetric moisture content measurements ranged from a minimum of 0.7 percent in Unit 2 to a maximum of 27 percent in Unit 1g. By stratigraphic unit, units 2 and 1v(u) average less than three percent, units 1v(c) and 1g average 10.9 and 8.9 percent, respectively, and the combined Tsankawi Pumice Bed and Cerro Toledo Interval average 14 percent (Table 2-1) MDA L and MDA G RFI borehole logging typically noted moisture in core or cuttings collected from the volcanoclastic Cerro Toledo Interval.

2.2.3.4 Gravimetric Moisture Content

The MDA G Performance Assessment states "Around disturbed settings caused by disposal activities, near surface moisture content dramatically increases above the natural background state because of a loss of plant evapotranspiration and suppression of atmospheric venting by installation of asphalt surfaces. There is evidence that the increased moisture content may occur to depths of 50 ft beneath disturbed areas." Because of the location of the PVET east of MDA L and removed from the asphalt-covered former

disposal units, the gravimetric moisture content measurements done on five-foot samples collected from boreholes 54-1001 through 54-1006 and 54-1018 represent natural moisture conditions in the subsurface rocks in the vicinity of MDA L.

Gravimetric moisture content measurements from these boreholes, averaged by stratigraphic unit, or subunit, mimic the volumetric moisture content compiled from the much larger borehole database utilized in the MDA G Performance Assessment (Table 2-1).

In boreholes 54-1001 through 54-1006 plus 54-1018, average gravimetric moisture content measurements ranged from a minimum of 1.03 percent in Unit 1v(u) to a maximum of 10.8 percent in the Tsankawi Pumice Bed. The subunits of units 2 and 1v(u) average less than three percent, units 1v(c), 1g(u), and 1g average 5.1, 5.7. and 5.8 percent, respectively, the Tsankawi Pumice Bed averaged 10.8 percent, and Cerro Toledo interval average 8.5 percent (Table 2-1) MDA L and MDA G RFI borehole logging typically noted moisture in core or cuttings collected from the volcaniclastic Cerro Toledo interval.

2.2.3.5 Saturation

Saturation measurements ranged from a minimum of 1.3 percent in units 2 and 1v(u) to a maximum of 50.3 percent in the combined Tsankawi Pumice Bed and Cerro Toledo interval. The compilation of average saturation values by stratigraphic unit yields a distribution similar to average volumetric and gravimetric moisture contents (Table 2-1). The highest average is in the combined Tsankawi Pumice Bed and Cerro Toledo interval and a second peak is demonstrated in unit 1v(c).

2.2.3.6 Saturated Hydraulic Conductivity

Saturated Hydraulic Conductivity is a measure of how readily a single fluid moves through a porous medium at saturation. Conductivity values for the stratigraphic units presented in Table 2-1 are taken from Stephans and Associates (1994a, 1992) and Kearl et al. (1986a, b).

2.2.3.7 Induration and Welding

Induration is synonomous with lithification (Glossary of Geology, American Geological Institute, 1980, p. 316) and is defined as "the hardening of a rock or rock material by heat, pressure, or the introduction of cementing material". Welding also denotes consolidation but implies deformation or earth movement (Glossary of Geology, American Geological Institute, 1980, p. 698). As a geohydrological characteristic of different units, or subunits, beneath MDA L, induration as hardness is not the same as welding. Although welding contributes to lithification and is also variable between and probably within units, or subunits, in pyoclastic terrain, welding is indicated primarily

by elongate pumice lapilli and bombs. In pumice-rich welded tuff, a distinct linear fabric is formed by the regular alignment of the ellipsoidal pumice lapili suggesting post-depositional compaction.

In the units and the subunits of the Tshirege Member beneath MDA L, units 2, 1v(c), and 1g(u) are moderately to strongly indurated. In addition, unit 2 is typically slightly to moderately welded. Because of their relative hardness, these rocks form benches or cliffs where exposed at the ground surface. In contrast, units 1v and 1g are non- to slightly-indurated, or much softer. Also, rocks beneath unit 2 are typically non- to only slightly welded underlying the welded tuff in unit 2. Where exposed, these units form slopes (c.f, Fig. 2-1). The relative induration of different units or subunits of the Tshirege Member is listed in Table 2-1.

The importance of induration as a geohydrological characteristic of the various units and subunits of the Tshirege Member is indirect. Induration is a rock feature which will effect the presence or absence of fractures, or cooling joints, in a particular unit. In addition, induration will correlate with characteristics of the rock matrix. In turn, these physical characteristics will influence the efficiency of air movement in different strata with differing relative values.

2.2.3.8 Conceptual Role of Fractures and Rock Matrix in Air Flow

The MDA G Performance Assessment presents a review of fracture presence in Tshirege Member units at TA-54. Fracture mapping was done at open disposal pits at MDAs G and J and the north wall of Pajarito Canyon (Purtyman and Kennedy 1971, Purtyman et al. 1978, Reneau and Vaniman 1994, and Reneau et al, 1995). These exposure are in unit 2. In addition, fractures have been logged, where preserved, during subsurface drilling investigations (MDA L RFI Report, in progress).

The presence of fractures is influenced by the induration and welding of the tuff units. Kearl et al. (1986 a,b) report an increase in the number of fractures in the more indurated units (units 2,1v(c), and 1g(u)), and less frequent to probably nonexistent in softer units (units 1v(u) and 1g). Broxton and Reneau (1995) describe the basal part of unit 1v (1v(c)) as 'a resistant, orange-brown tuff with a "colonnade" appearance because of abundant vertical fractures'. Table 2-1 indicates a direct correlation between induration and presence of fractures. Unit 1v(c) was straddled by the open interval of the extraction well-54-1017 (Fig. 2-3 and 2-4).

Figure 2-3 Cross-section A-A' parallel to Mesita del Buey through the extraction well, 54-1017

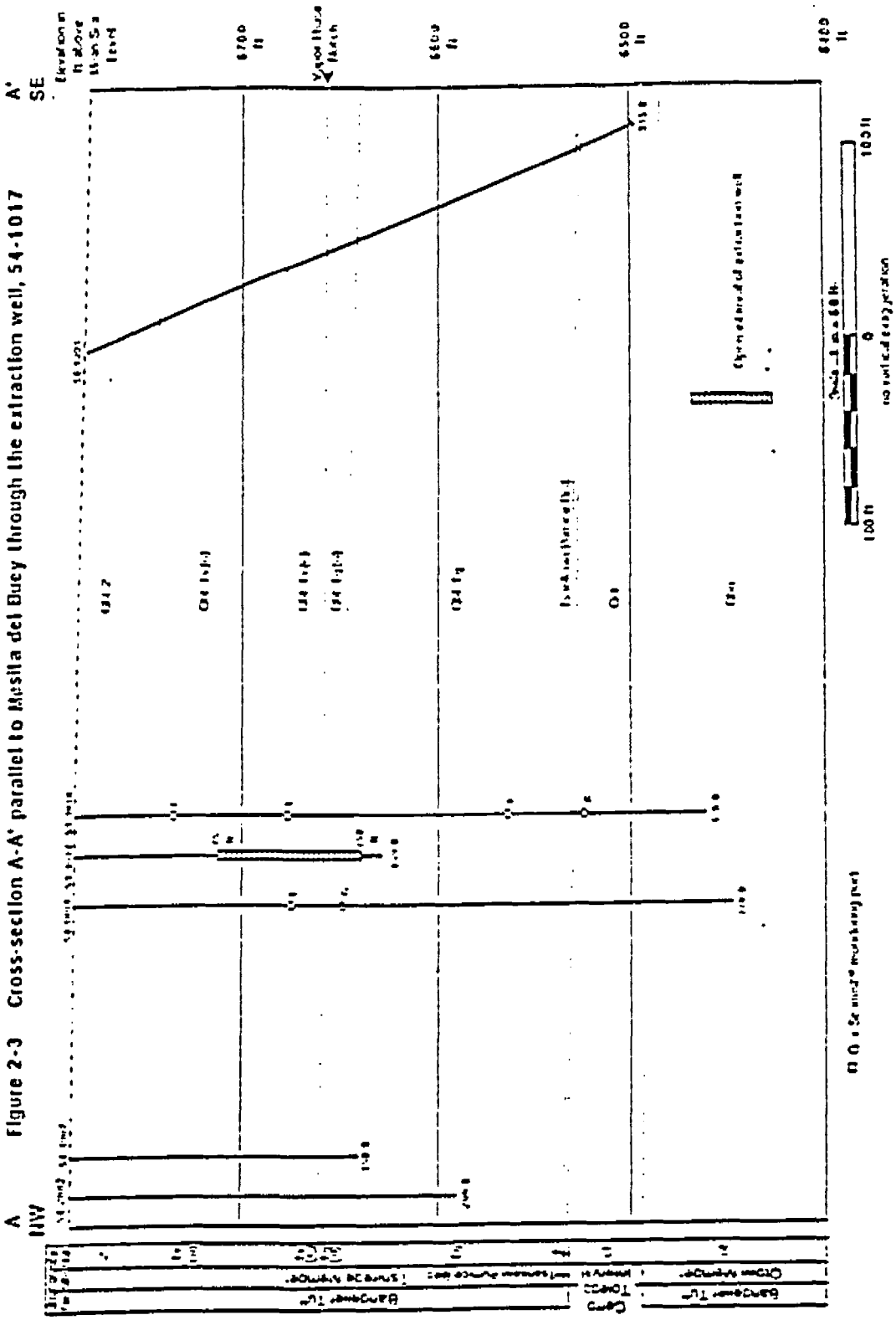

Figure 2-4 Cross-section B-B' oblique to Mesita del Buey through the extraction well, 54-1017

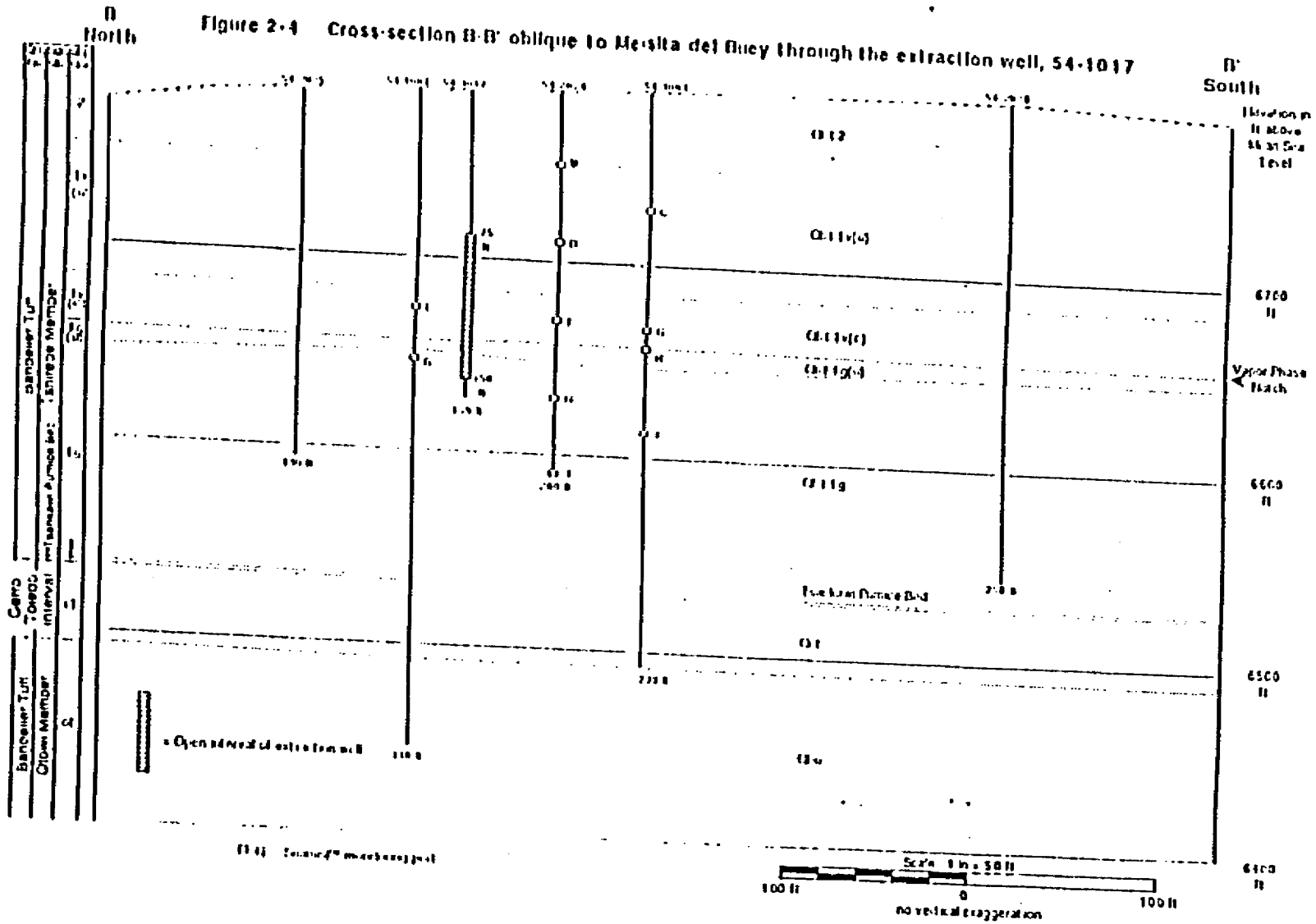

In Pit 39 at MDA G, hosted by unit 2 tuff, fractures are typically filled with smectite clays to a depth of 9.8 to 13.1 ft, and with opal and calcite locally associated with tree roots observed to a depth of 66 ft. 'The presence of tree roots suggests the availability of water, however, associated mineral precipitation may work to occlude transport pathways' (MDA G Performance Assessment). Calcium carbonate was detected in fractures in the study at MDA J (Davenport, 1993), which also indicates the presence of water in a fracture in unit 2 tuff. Recent ER drilling at the TA-73 landfill (airport site) found elevated moisture associated with fractures at depths to 135 ft below the ground surface.

Little is known about fracture presence, frequency, aperture, continuity, and coatings or fillings below Unit 2a. Definitive characterization of fracture fillings and coatings is missing for all units. The available information is insufficient to determine whether fractures may be a critical flow path in the system. Characterization of this site would benefit from study of fracture coatings and fills and their material properties to augment existing data on population, aperture, and orientation. This information is most accessible from existing and future disposal pit walls (LAUR-85-2696).

3.0 TEST DESCRIPTION

3.1 PVET DESIGN AND INSTRUMENTATION

The preliminary design of the PVET is included in Appendix B, where numerical design simulations are presented that define the general layout of the test and monitoring design. Appendix B also includes the preliminary extraction hardware and instrumentation design. The following sections describe the as-built test configuration.

3.1.1 Extraction System

Borehole 54-1017 was completed as the extraction well for the pilot test. Steel surface casing (8 in. diameter) extended to a total depth of 75 ft., and the open hole (9 in. diameter) extended downward to a total depth of 150 ft.

The vapor extraction system consists of a regenerative blower, air filter, vacuum breaker valve, and manual flow control valve to adjust the vacuum flow rate if necessary. The regenerative blower is a Gast 5 hp, 208 volt unit capable of up to 203 cubic feet per minute (5740 l/m) and a maximum vacuum of 88 inches of water column (21.9 kPa). The extraction system schematic is depicted in Figure 3-1.

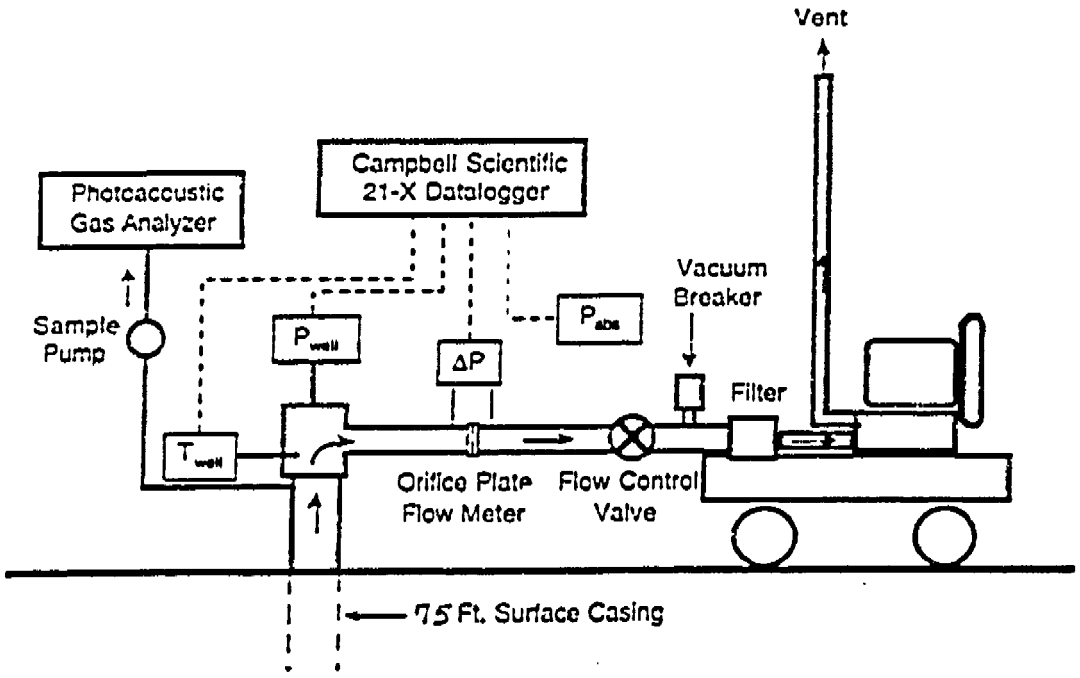

Figure 3-1. PVET vacuum extraction system schematic.

3.1.2 Monitoring Systems

Three types of monitoring systems were used to quantify the processes during the field test: extraction system process monitoring, soil gas pressure monitoring, and soil gas contaminant concentration monitoring. The extraction system was monitored by instruments and a datalogger located in an instrument trailer at the extraction well. Three standalone soil gas pressure monitoring units were located in insulated enclosures near their respective wells. The soil gas analyzer unit was located in the instrument trailer at the extraction well. Sampling port assignments for the soil gas pressure and gas analysis units are depicted in Table 3-1. The site layout is depicted in Figure 3-2.

The extraction monitoring system consisted of extraction air flow, well vacuum, temperature measurements, and a Bruel and Kjaer Model 1302 photoacoustic analyzer (Figure 3-1). Air flow was measured by an Oripac™ orifice plate flow meter, consisting of a 2.43-inch diameter orifice in a 4-inch ID pipe. Pressure drop across the orifice plate was measured with a sensitive differential pressure transducer. Air temperature was measured with a Type K thermocouple inserted in the air stream, and well vacuum measured with a differential pressure transducer ported into the wellhead assembly. The mass flow out of the well was calculated and stored in real time by the datalogger. A small capacity vacuum pump continuously extracted soil gas from the flow stream and provided it to the photoacoustic analyzer for online analysis.

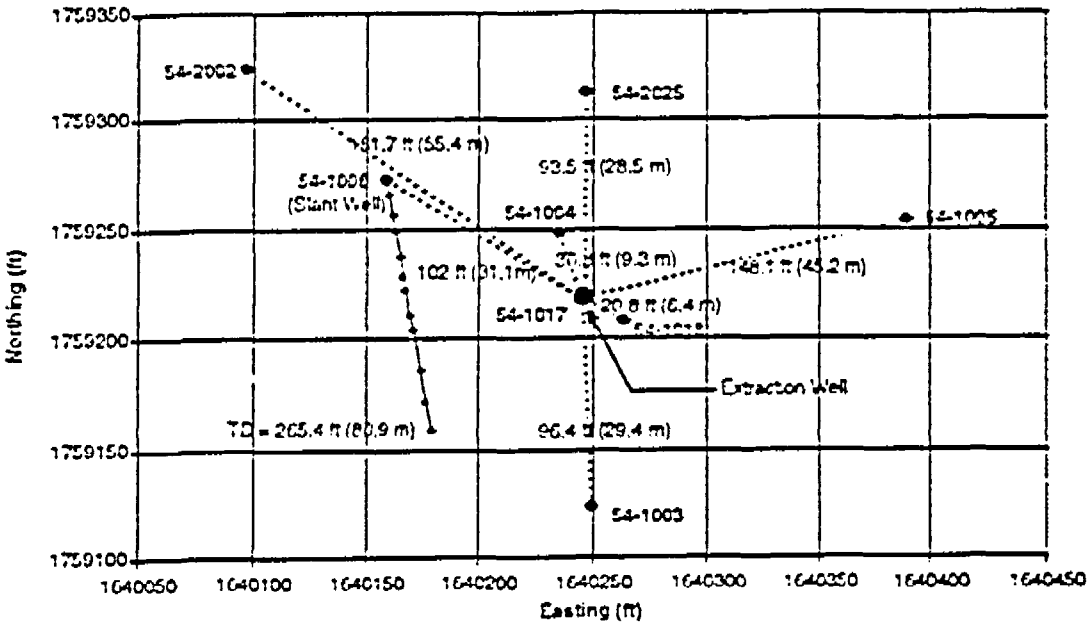

Figure 3-2. PVET site layout.

Table 3-1. Soil gas sampling and pressure measurement port locations

Gas Sampling and Analysis Ports			Pressure Monitoring Ports		
Borehole	Type	Port Depth (Vert. Depth) Ft., (m)	Borehole	Type	Port Depth (Vert. Depth) Ft., (m)
54-2024	Piezometer*	40	54-2002	Piezometer	80
		80			140
		120			200
		160	54-2025	Piezometer	100
		200			160
54-1003	SEAMIST**	62.4	54-1004	SEAMIST	37.5
		124.0			48.9
		136.0			70.3
		173.8			80.3
					124.3
54-1004	SEAMIST	113.2			179.8
		140.0			222.3
					253.7
54-1018	SEAMIST	50.6			313.0
		111.2			338.0
		223.5			
		263.3	54-1005	SEAMIST	120.2
					165.0
					284.0
			54-1006	SEAMIST	39.1
					57.3
					79.3
					98.4
					124.3
					145.0
					159.0
					188.2
					205.0
					249.8
					283.8
					314.5

* Piezometer wells were constructed by lowering metal sample tubes to depth and backfilling with granular materials.
** SEAMIST™ wells used removable pneumatic membranes with integral sampling lines.

Soil gas pressure was measured with three similar data units (Figure 3-3). Each of these scanning systems consisted of a 16-port solenoid valve manifold that sequentially connected the individual downhole sampling lines to a precision barometric pressure transducer. The manifold was controlled by a Campbell Scientific CR-7 datalogger, that also collected and archived the pressure data. During the first 24 hours of the extraction test these systems

scanned pressures every 15 minutes in order to acquire the initial transient response of the test, after which the sampling interval was changed to 45 minutes for the duration of the test. The temperature of the pressure transducer was controlled to +/-2 C to minimize temperature effects on the pressure transducer response. These scanning units were housed in insulated enclosures or trailers and powered by photovoltaic panel/battery units.

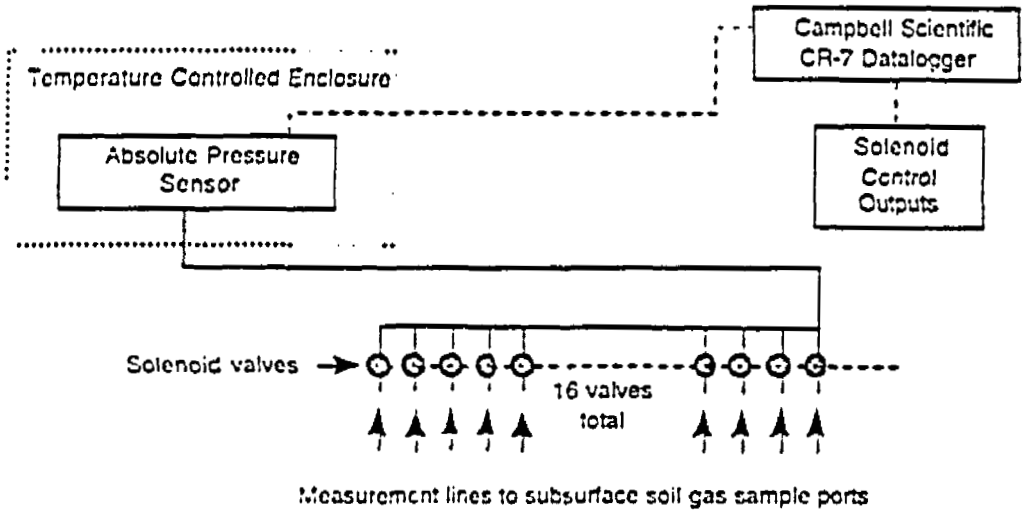

Figure 3-3. Automated precision soil gas pressure monitoring system.

Soil gas composition was measured by an automated 16-port sampling and analysis system (Figure 3-4). In this system a solenoid valve manifold connected the downhole sampling tubes to a sample pump, which transferred the soil gas to an intermediate Tedlar sample bag. A Bruel and Kjaer Model 1302 photoacoustic analyzer sampled from the Tedlar bag and reported the composition of five compounds in the soil gas. The system automatically purged the sample lines and the Tedlar holding bag to minimize cross contamination of the samples. Atmospheric samples were also analyzed. This system gathered and analyzed soil gas samples every 3 hours for the duration of the test.

The specifications of the primary measuring components in each of these monitoring systems are listed in Table 3-2.

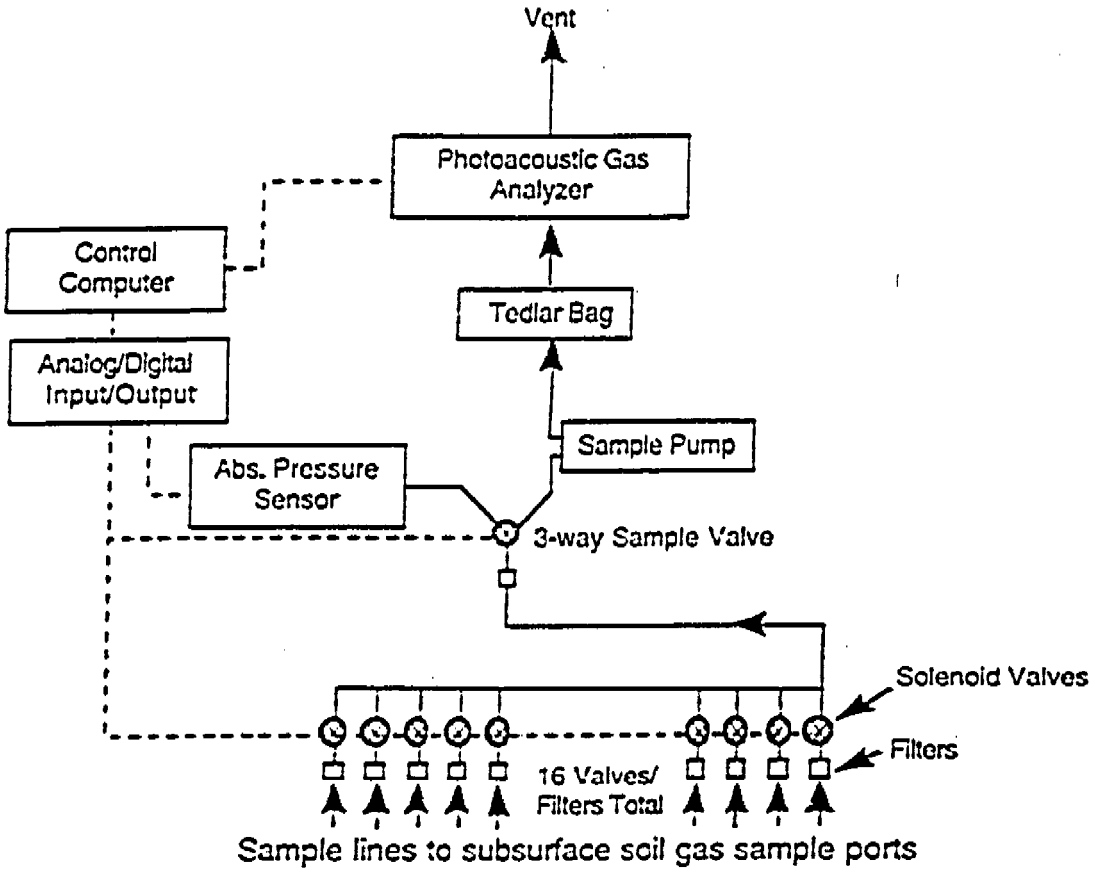

Figure 3-4. Automated soil gas sampling and analysis system.

Table 3-2. PVET Monitoring System Specifications

System	Measured Process	Sensor	Range	Accuracy
1. Extraction System Monitor (data collected on Campbell Scientific 21X datalogger)	Flow orifice plate differential pressure	Setra #239 pressure transducer	0-5" W.C. (0-1246 Pa)	+/- 0.007" W.C. (1.74 Pa)
	Extraction air temperature	Type K thermocouple		+/- 1° C
	Well vacuum	Innovex diff. pressure transducer	0-5 psi (0-34.47 kPa)	+/- 0.05 psi (+/- 344.7 Pa)
	Atmospheric pressure	Setra #270 absolute pressure transducer	60,000-110,000 Pa	+/- 50 Pa
2. Soil gas pressure monitors (data collected on Campbell Scientific CR-7 datalogger)	Soil gas pressure	Setra #270 absolute pressure transducer	60,000-110,000 Pa	+/- 50 Pa
3. Soil gas analysis system (controlled and recorded by a portable PC)	Soil gas contaminant concentration	Bruel & Kjaer Model 1302 Photoacoustic Analyzer Calibrated for: 1,1,1 - trichloroethane (TCA) Trichloroethene (TCE) Trichlorofluoromethane (Freon 11) Trichlorotrifluoroethane (Freon 113) Carbon dioxide Water vapor		

3.2 PVET IMPLEMENTATION

The preparations for the pilot extraction test required extensive evaluation of soil gas pressure and composition data from all of the downhole sample ports. Pressure response from the downhole ports was compared to barometric pressure to identify and repair leaks in the measurement tubing, which in some cases extended over 100 ft. from the monitoring units to the wellheads. The data from the soil gas analysis system was compared to samples gathered manually at the wellhead to ensure sample integrity. The extraction system was operated (without drawing air from the extraction well) to ensure its readiness.

The soil gas sampling and analysis system started collecting background data eight days prior to operation of the extraction blower. Soil gas pressure data was acquired for 24 hours prior to starting the extraction test. The vacuum blower was energized just before noon on September 19, 1995 (Julian day 262). After 24 hours the sampling frequency of the pressure measuring systems was slowed from 15-minute to 45-minute intervals. The extraction system operated for 34 days, until the blower was turned off on October 23, 1995 (Julian day 296). The test was terminated after evaluation of the soil gas contaminant data determined that the process had achieved steady state and further changes in the measured parameters were expected to be minimal.

3.3 PVET RESULTS

The measurements discussed in this section are the extraction system process measurements (flow, temperature, vacuum), barometric pressure, and the response of the soil gas pressure at the downhole locations. Analysis of the pressure data is discussed in Section 5.1 of this report. The gas composition results are discussed in Section 4.

Extraction system process measurements are shown for the total test in Figure 3-5, and expanded for the first four days of operation in Figure 3-6. As indicated in Figure 3-6, the well vacuum and flow reached steady conditions within two days. At this flow rate the orifice plate flowmeter is accurate to within +/- 5% of the indicated flow (nominally 25 standard cubic feet per minute, or 0.85 kg/min). The well vacuum achieved a steady value of approximately 18.6 kPa (72 inch water column). Perturbations to the flow and vacuum data in the first day are due to the vacuum breaker valve in the extraction system opening and allowing additional air into the flowing stream to the vacuum blower (a protective feature to protect the blower from overheating). The nature of the valve hysteresis caused it to open and relieve the well vacuum, then close in an unsteady oscillatory nature. After discussions with the blower manufacturer the setting on the breaker valve was adjusted to prevent opening under these conditions and the balance of

the flow data is relatively steady. The extracted air flow temperature achieves a relatively constant 12 C value for the duration of the test. The diurnal perturbations observed in the data are suspected to be due to temperature gradients in the datalogger, which influence its thermocouple reference junction correction and induce a 1 to 2 degree artificial oscillation (this effect was observed in previous testing of the datalogger while evaluating the response of thermocouple psychrometers to datalogger enclosure conditions).

The pressure response of the downhole sampling locations listed in Table 3-1 is plotted in Figures 3-7 through 3-13 for the duration of the test. While it is difficult in some cases to differentiate the downhole pressure response from barometric effects, for the wells near to the extraction well (particularly 54-1018 and 54-1004) the effects can be readily distinguished. If the vacuum extraction system were not operating, the plotted pressures would all maintain equal average values over a time span of several days. The pressure response of measurement ports at depth is attenuated (in magnitude of the pressure fluctuation) and shifted in time (delayed) from the barometric pressure due to the permeability of the tuff and port depth. The vacuum extraction system tends to shift downward the pressure response of affected ports. For well 54-1004, for example, ports in the depth range of the extraction interval (75 - 150 ft.) show average values noticeably below barometric, whereas ports below 200 ft. indicate very little deviation from average barometric pressure.

Downhole pressures are plotted for the first day of the extraction system operation for well 54-1004 and 54-1018 in Figures 3-14 and 3-15, respectively (these were the most affected wells due to their proximity to the extraction well). The pressure response of ports near the extraction depth is almost immediate (within 15 to 30 minutes) in these wells, while several hours are required for more distant ports to respond.

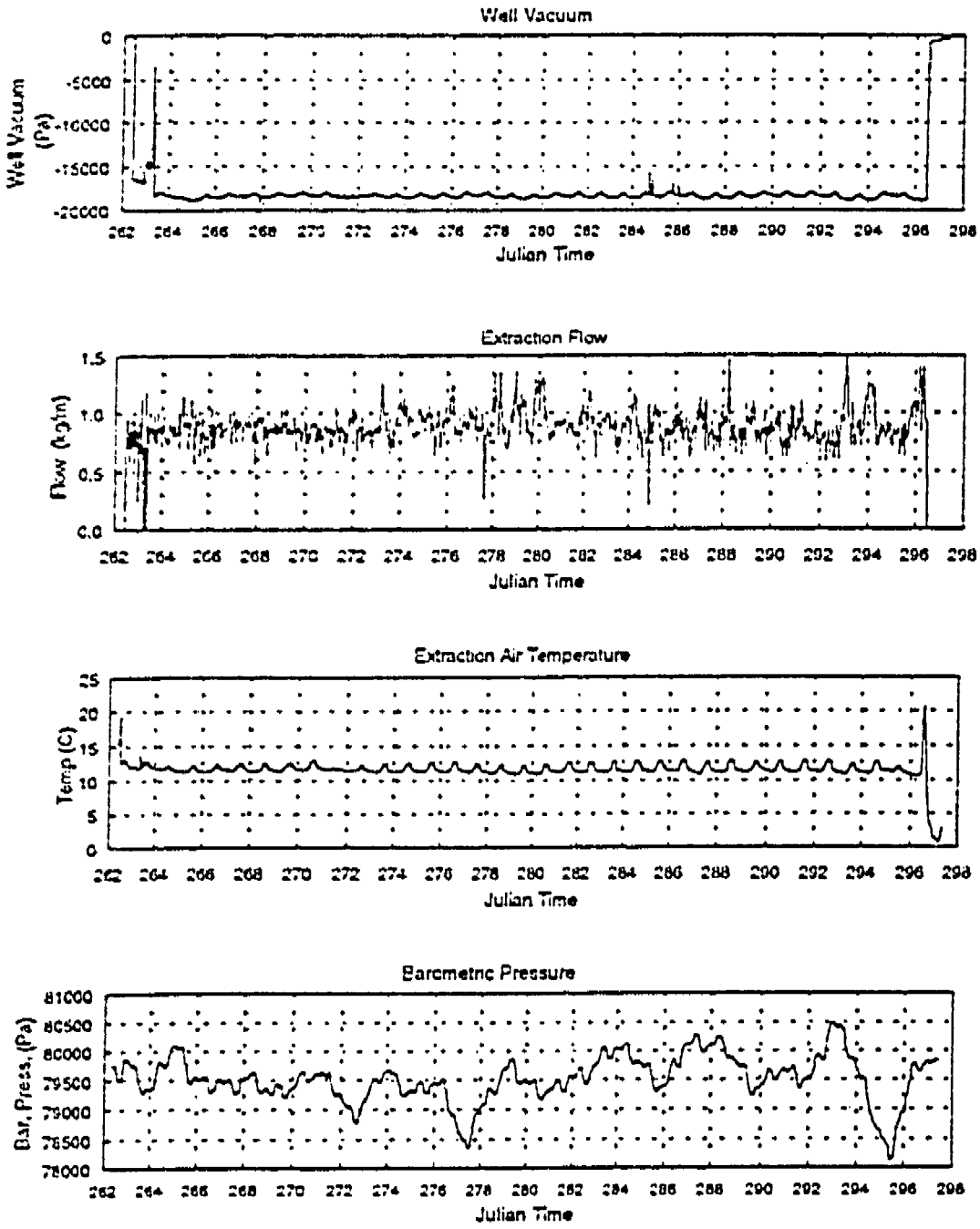

Figure 3-5. Extraction system process measurements.

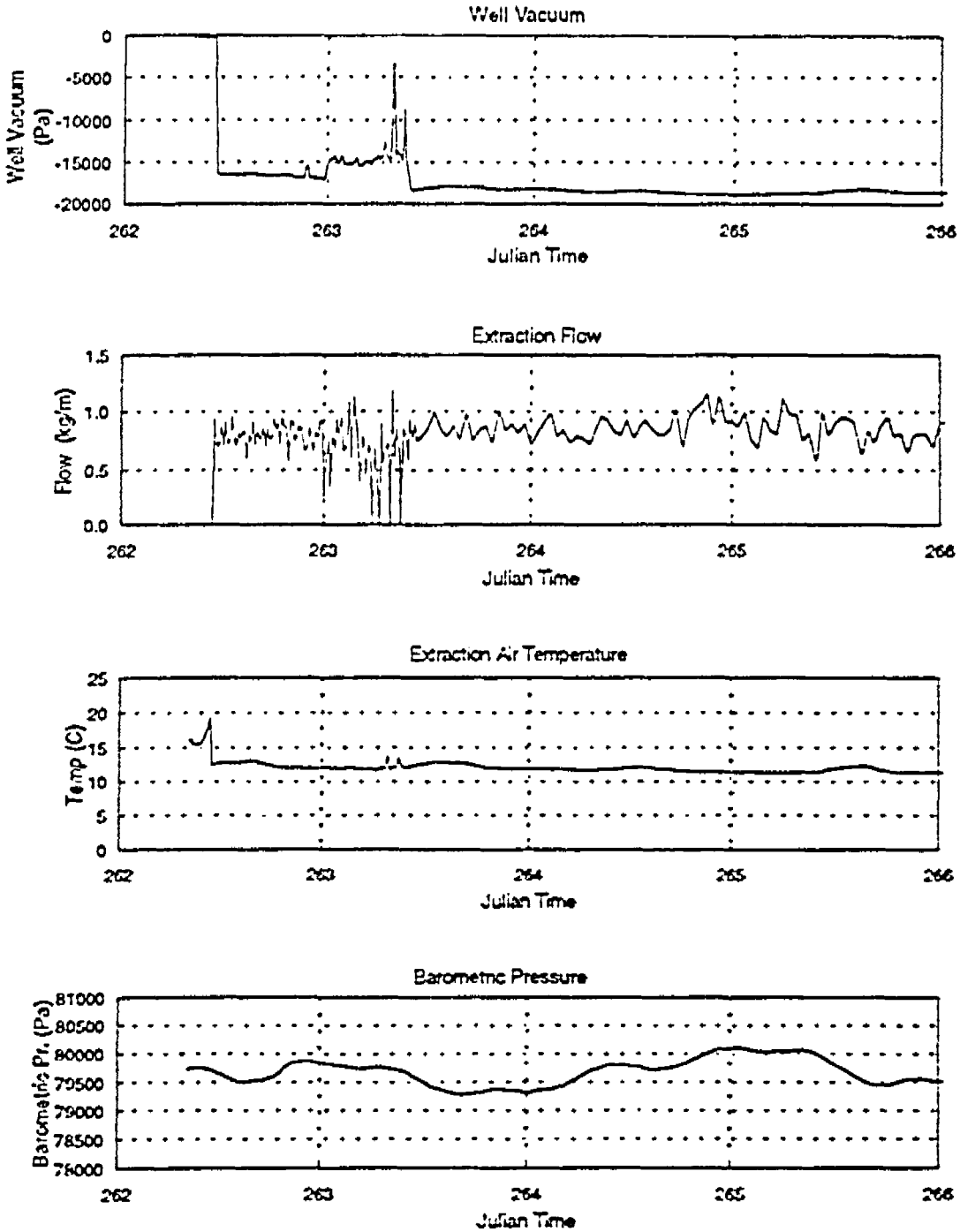

Figure 3-6. Expanded 4-day plot of extraction processes.

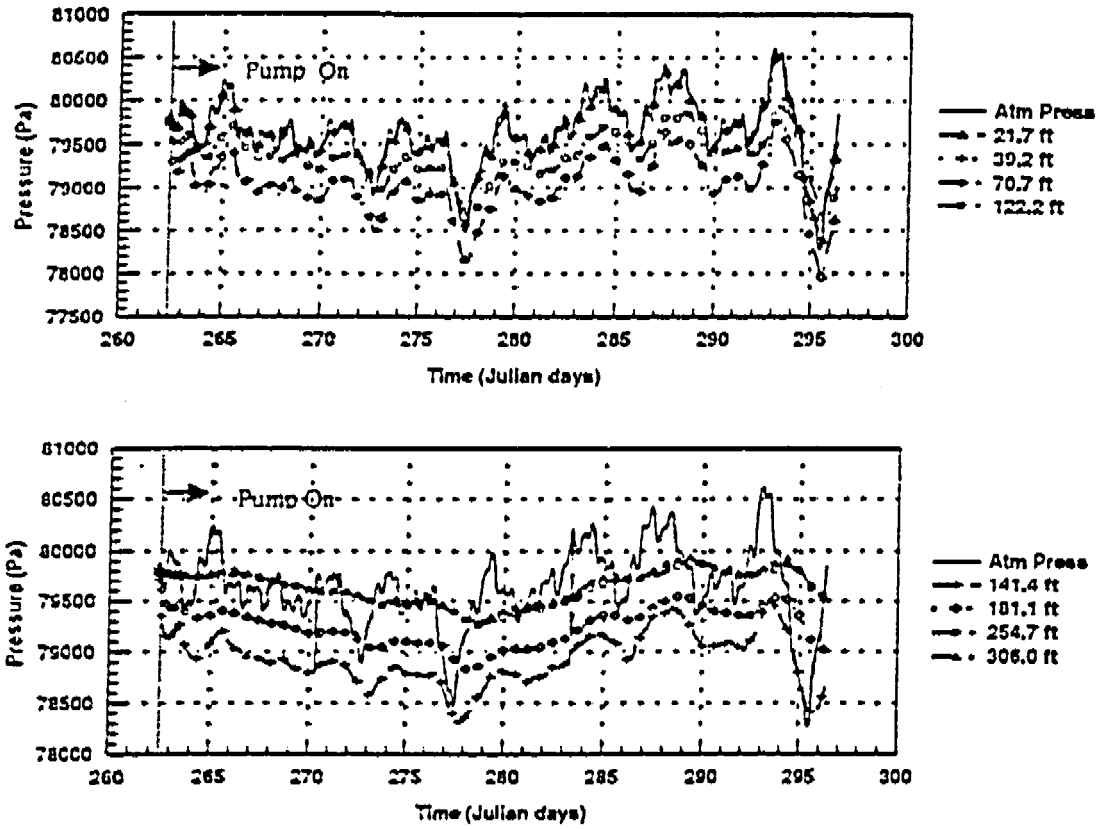

Figure 3-7. Soil gas pressure response for monitoring ports in borehole S4-1018 during the extraction test.

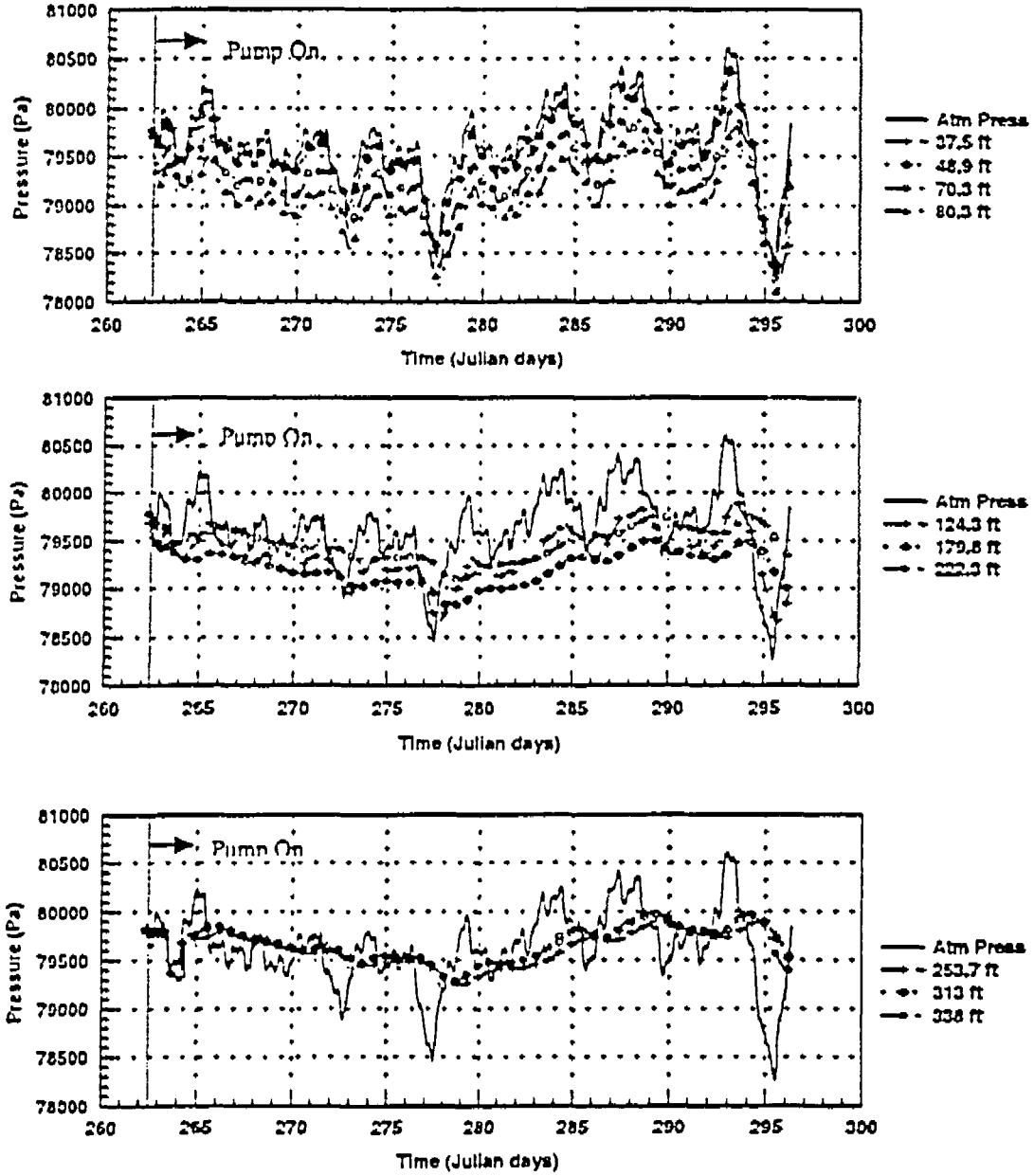

Figure 3-8. Soil gas pressure response for monitoring ports in borehole 54-1004 during the extraction test.

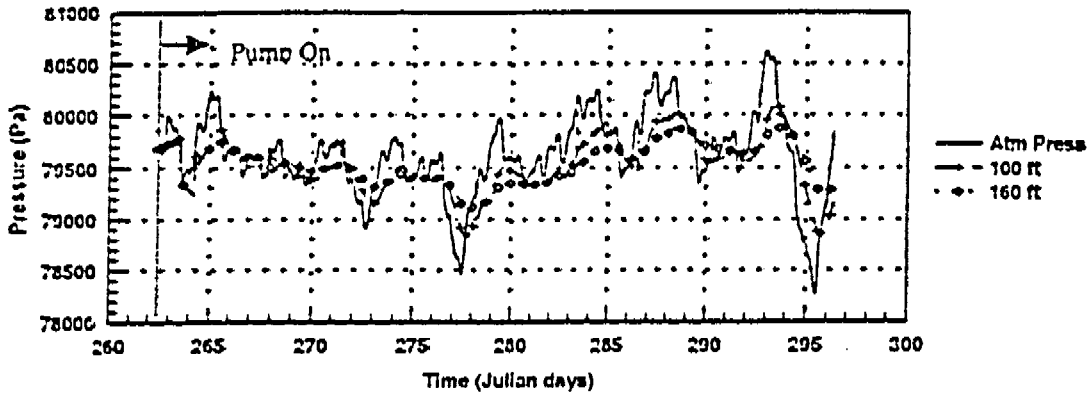

Figure 3-9. Soil gas pressure response for monitoring ports in borehole 54-2025 during the extraction test.

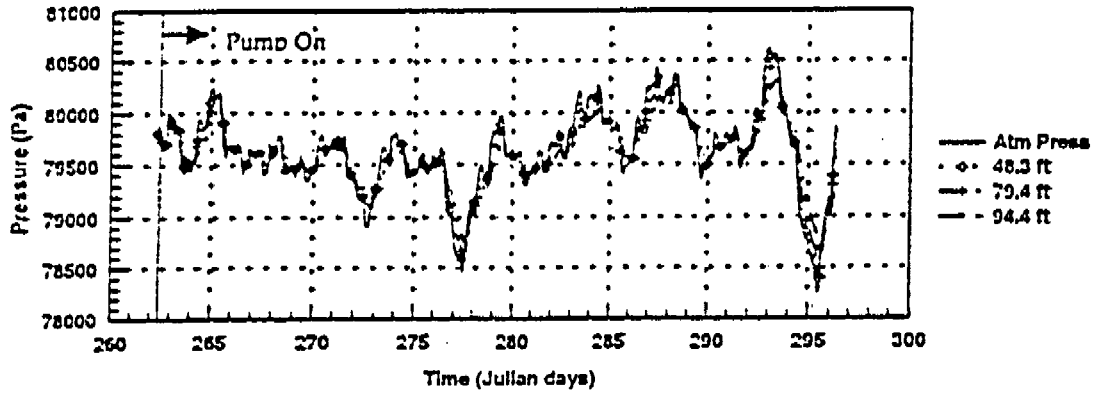

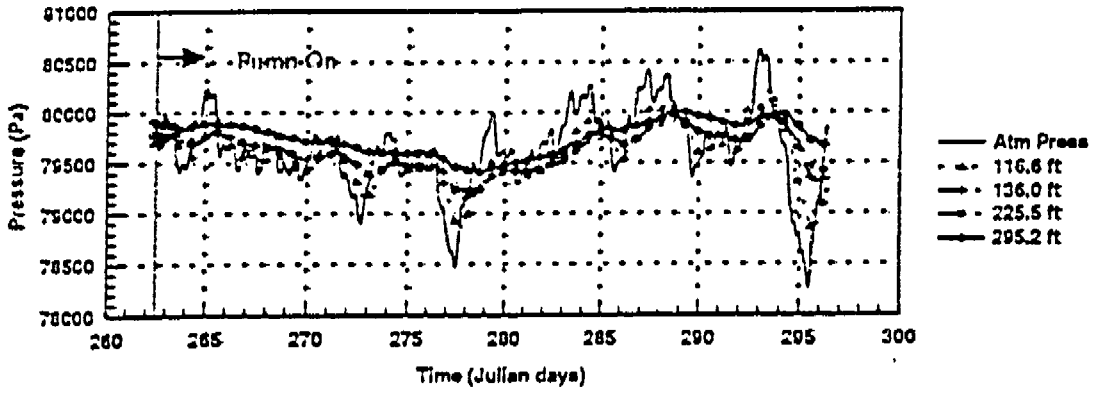

Figure 3-10. Soil gas pressure response for monitoring ports in borehole 54-1003 during the extraction test.

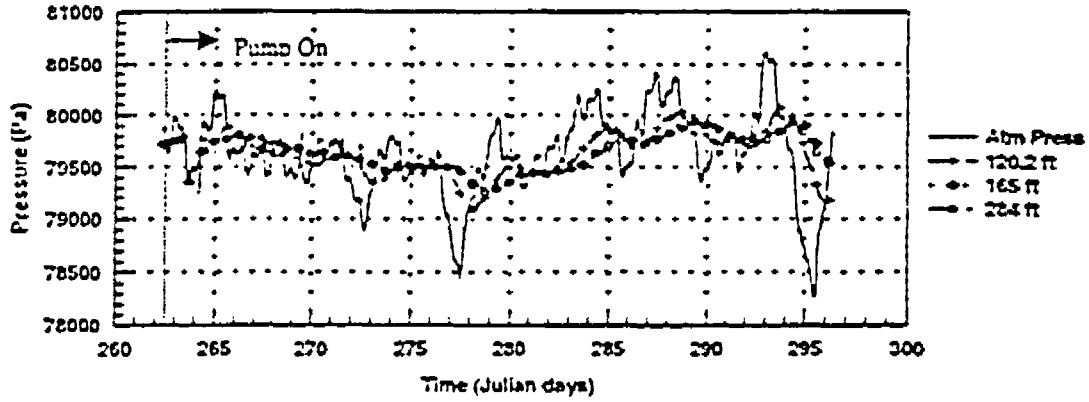

Figure 3-11. Soil gas pressure response for monitoring ports in borehole 54-1005 during the extraction test.

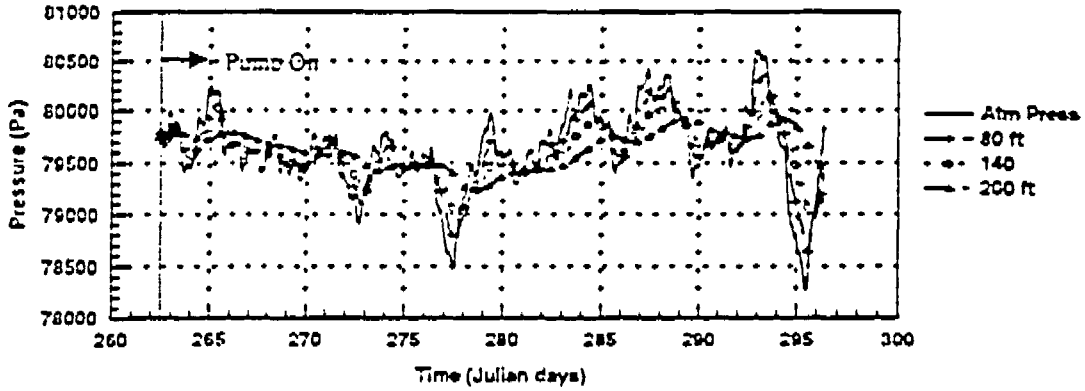

Figure 3-12. Soil gas pressure response for monitoring ports in borehole 54-2002 during the extraction test.

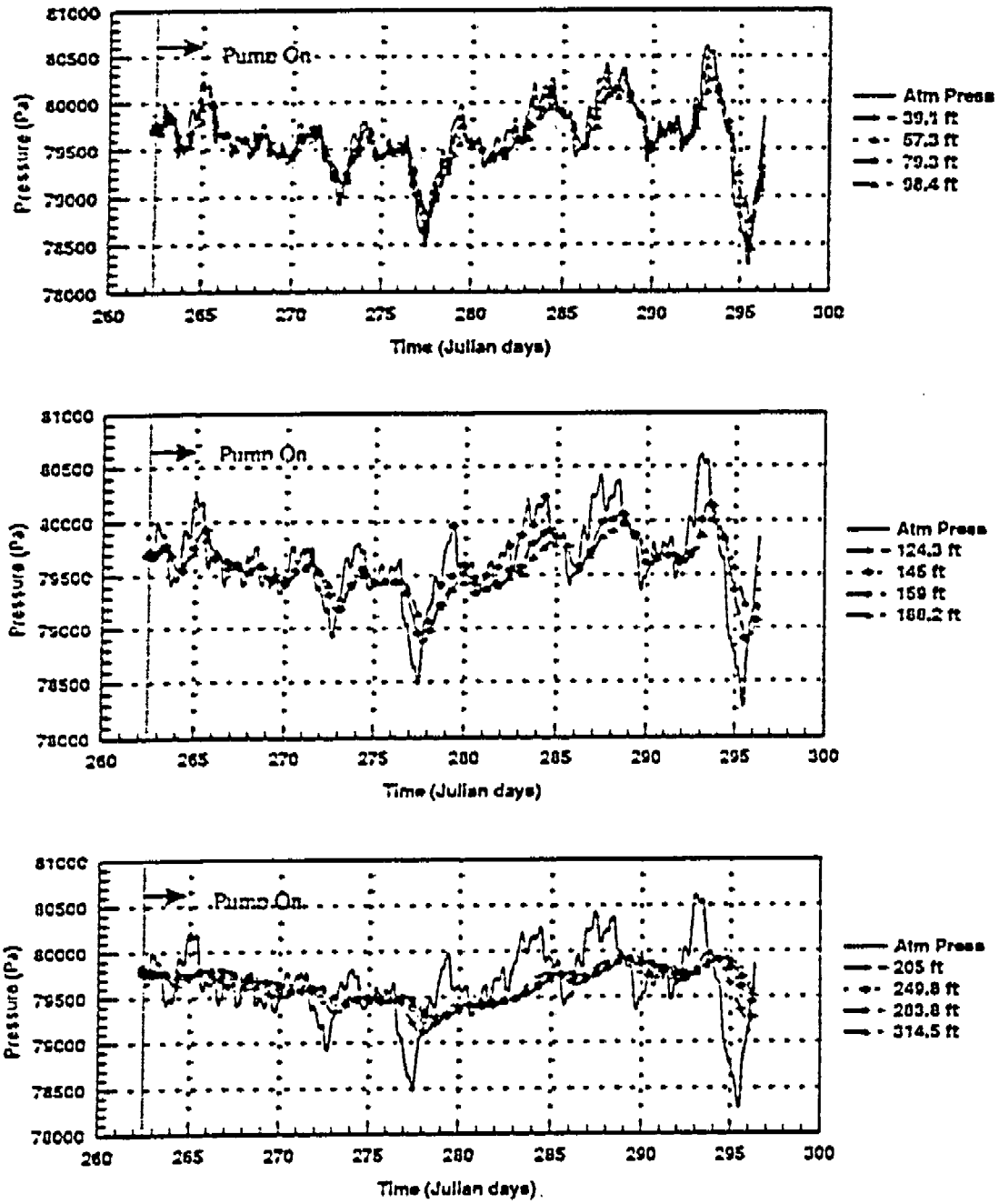

Figure 3-13. Soil gas response for monitoring ports in borehole 54-1006 during the extraction test.

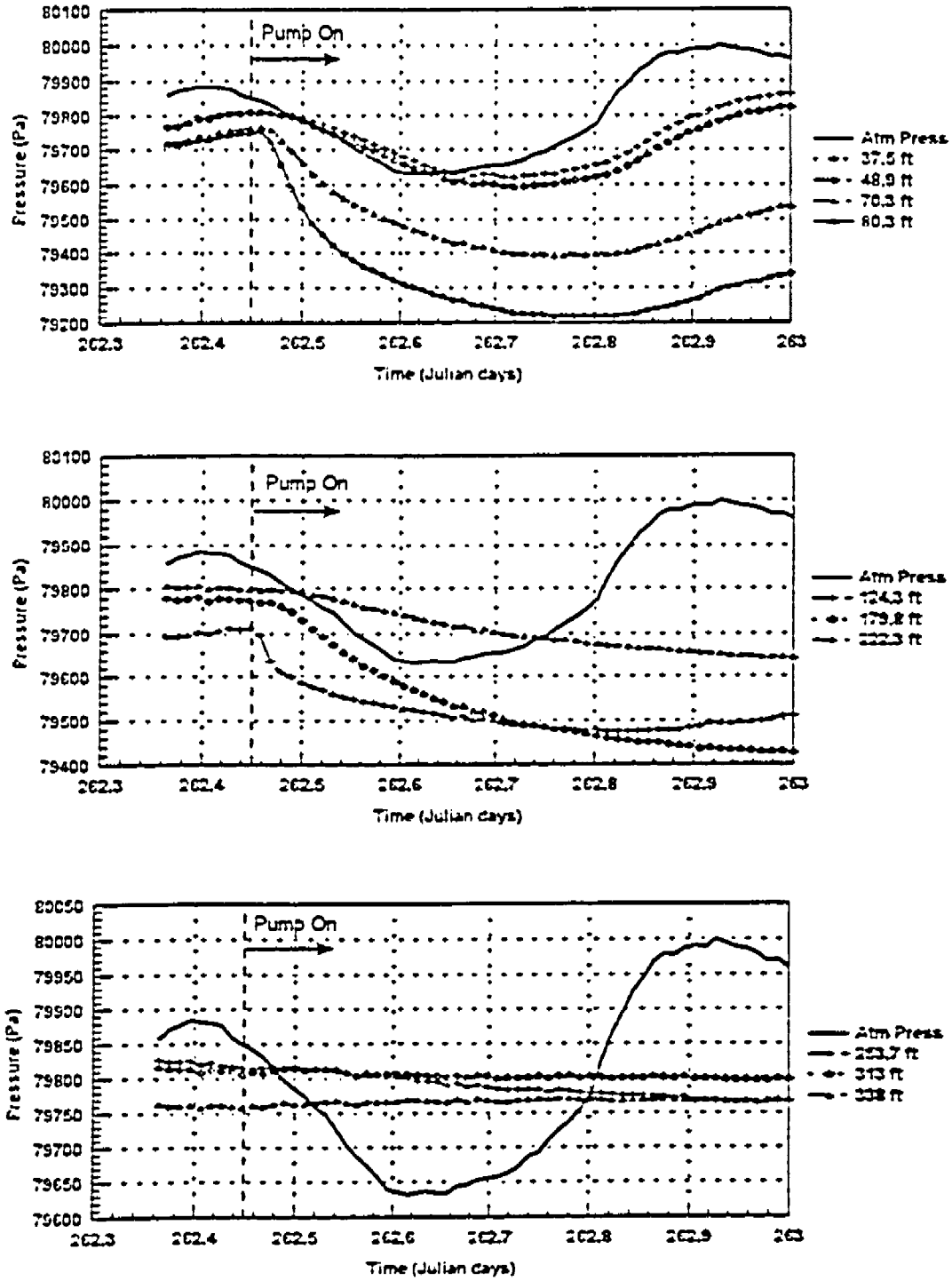

Figure 14. Expanded time plot for 54-1004 pressure data.

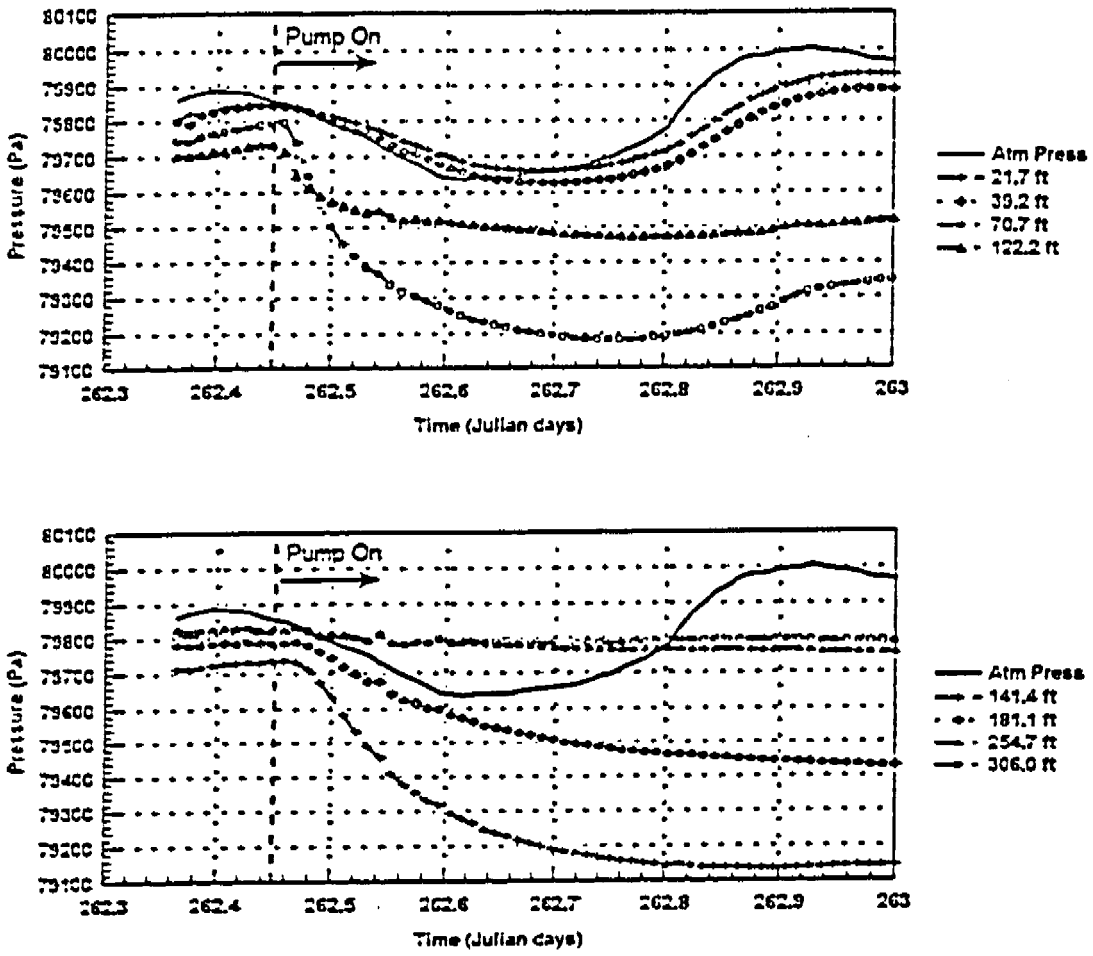

Figure 3-15. Expanded time plot for S4-101S pressure data.

4.0 PVET EFFECT ON VAPOR PHASE COMPOUNDS

The PVET was expected to have a radius of influence of approximately 120 feet surrounding the pilot extraction well (54-1017) (Final Report: Pilot Scale Vapor Extraction System Design for OU-114S (SEA-TR-94-039/revised) 14 March 1995 (see Appendix B). Monitoring wells 54-1003, 54-1004, 54-1006, 54-101S, 54-2024 and 54-2025 are located within this radius (Fig. 4-1). Of these wells, 54-1003, 54-1004, 54-101S, and 54-2024 were instrumented to detect changes in target VOC and other inorganic compound concentrations at selected monitoring port depths (Table 4-1). Concentrations of 1,1,1-trichloroethane (TCA), trichloroethene (TCE), trichloroflouromethane (Freon 11), trichloro-triflouroethane (Freon 113), water vapor (H_2O), carbon dioxide (CO_2), and oxygen (O_2) were measured on a three-hour schedule by a Bruel and Kjaer (B&K) nondispersive infared analyzer before, during, and after the operation of the extraction blower from the selected monitoring ports.

Table 4-1. Summary of PVET monitoring wells, ports, and compounds

Monitoring Port Data				Volatile Organic Compounds				Inorganic Compounds		
Well ID	Port ID	Port Depth (feet)[1]	Strat. Unit/ (Subunit)[2]	TCA[3]	TCE[4]	Freon 11[5]	Freon 113[6]	H_2O	CO_2	O_2
54-1003	C	62.4	Qbt 1v(u_2)	x	x	x	x	x	x	x
	G	124.0	Qbt 1v(c)	x	x	x	x	x	x	x
	H	136.0	Qbt 1g(u)	x	x	x	x	x	x	x
	J	173.8	Qbt 1g	x	x	x	x	x	x	x
54-1004	E	113.2	Qbt 1v(c)	x	x	x	x	x	x	x
	G	140.0	Qbt 1g	x	x	x	x	x	x	x
54-101S	C	50.6	Qbt 1v(u_2)	x	x	x	x	x	x	x
	E	111.2	Qbt 1v(c)	x	x	x	x	x	x	x
	I	223.5	Qbt 1g	x	x	x	x	x	x	x
	K	263.3	Qct	x	x	x	x	x	x	x
54-2024	B	40.0	Qbt 2	x	x	x	x	x	x	x
	D	80.0	Qbt 1v(u_2)	x	x	x	x	x	x	x
	F	120.0	Qbt 1v(c)	x	x	x	x	x	x	x
	H	160.0	Qbt 1g	x	x	x	x	x	x	x
	J	200.0	Qbt 1g	x	x	x	x	x	x	x

(1) Depths are vertical feet below ground surface
(2) Stratigraphic nomenclature follows Broxton and Reneau, 1995. See Fig. 2-1.
(3) 1,1,1-Trichloroethane
(4) Trichloroethene
(5) Trichloroflouromethane
(6) Trichlorotriflouroethane

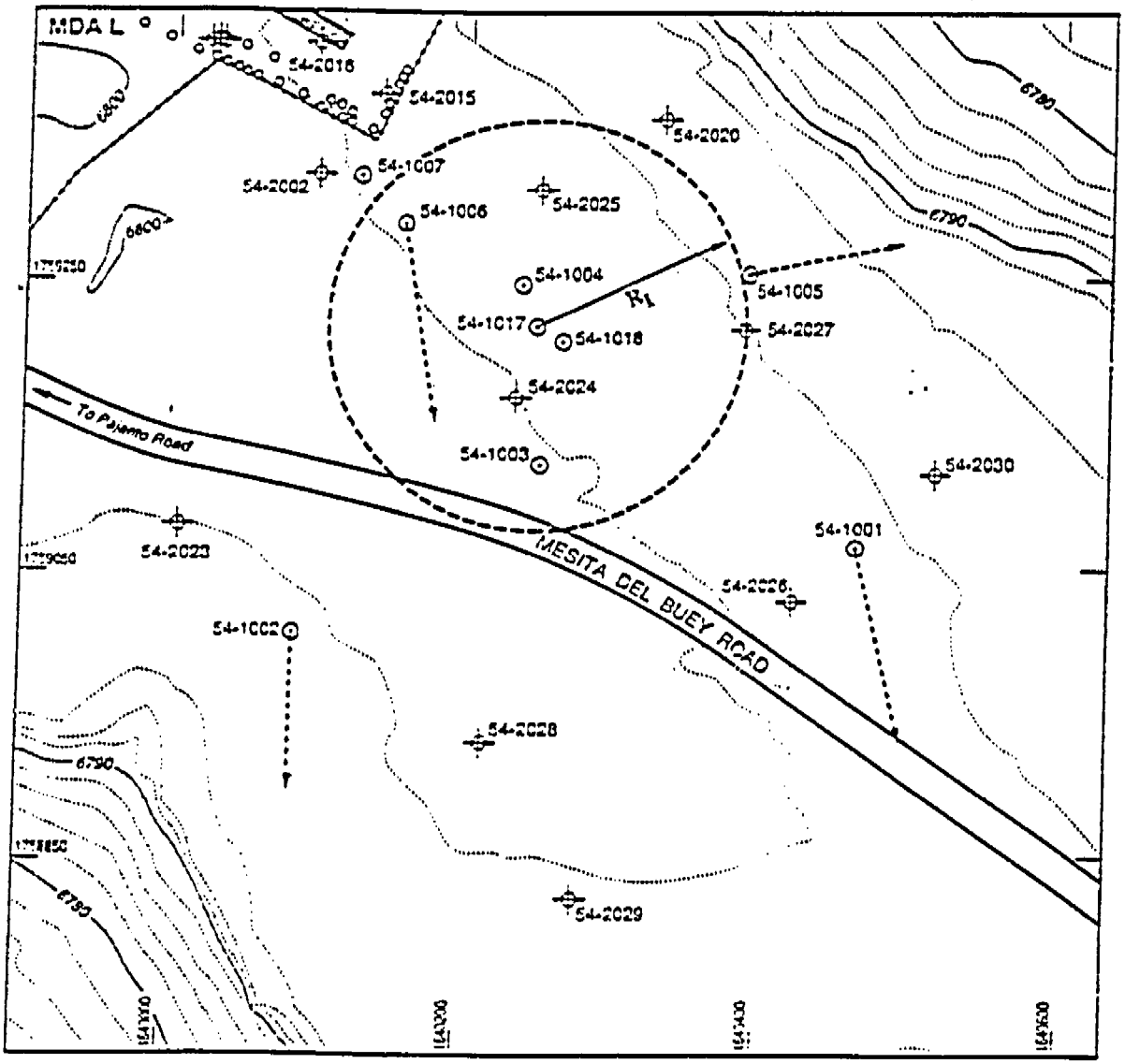

Figure 4-1. Locations of PVET monitoring wells east of MDA L and the interpolated "radius of influence" taken from subsurface pressure measurements.

Of the VOCs monitored, TCA concentration profiles were found to be representative of TCE, Freon 11, and Freon 113. Also, TCA concentrations are higher than any other VOC. Therefore, the PVET influence on vapor phase TCA concentrations is presented in detail in the following sections. Oxygen, water vapor, and carbon dioxide all showed erratic behavior probably due to condensation effects which are descibed in Section 4.3.

4.1 TCA RESPONSE AND RECOVERY

The affect of the active extraction test on vapor phase TCA concentrations in different locations is influenced by the monitoring port location relative to the extraction well and the closest source of the vapor phase VOCs below the eastern corner of MDA L (Fig. 1-3). Relative to the vapor phase VOC source, monitoring wells 54-1018, 54-2024, and 54-1003 are located at increasing distances downgradient from the extraction well (Fig. 4-1). In contrast, monitoring well 54-1004 is located upgradient from the extraction well towards the VOC source.

4.1.1 Downgradient from the extraction well

Monitoring well 54-1018 is located 20 feet southeast of the extraction well (Fig. 4-1). TCA concentrations as a function of time at well 54-1018 are shown graphically in Fig. 4-2. The data are smoothed and zeroed using a rolling 48-hour average to subtract false TCA concentrations apparently detected at the ground surface that are probably B&K instrument noise (Fig. 4-2). Prior to PVET startup (JD 260.5), TCA subsurface concentrations ranged from a minimum of 30.4 ppm at port K to a maximum of 91.5 ppm at port E. During the operatrion of the extraction blower, TCA concentrations at ports C and E exhibit significant reduction in TCA concentrations while ports I and K showed little relative response (Fig. 4-2). Following the extraction blower shutdown on JD 296.5, TCA concentrations at ports C and E demonstrated a steady increase (Fig. 4-2). During both the extraction blower operation and following shutdown, port E at 111.2 ft showed a greater relative change in TCA concentrations than port C at 50.6 ft (Fig. 4-2). This is expected as port E is located within the open interval of the extraction well (75 ft to 150 ft) (Fig. 4-3).

Monitoring well 54-2024 is located 51 feet southeast of the extraction well (Fig. 4-1). TCA concentrations measured as a function of time at well 54-2024 are shown graphically in Fig. 4-3. TCA concentrations in port F in well 54-2024 behaved similar to TCA concentrations in port E in well 54-1018 (Figs. 4-2 and 4-3). Port F in well 54-2024 is also located at a depth within the open interval

of the extraction well (Fig. 2-4). However, in well 54-2024, port F demonstrated even more of a decrease in TCA concentration during the active extraction, and more of an initial rebound following extraction blower shutdown, than port E in well 54-1018 (Figs. 4-2 and 4-3).

Monitoring well 54-1003 is located 96 feet south of the extraction well (Fig. 4-1). TCA concentrations measured as a function of time at well 54-1003 are shown graphically in Fig. 4-4. During the operation of the extraction blower, TCA concentrations measured in port G in well 54-1003 demonstrate a similar behavior with less TCA than in port E in well 54-1018 and port F in well 54-2024 (c.f., Figs. 4-4, 4-3, and 4-2). Following extraction blower shutdown, TCA concentrations in port G in well 54-1003 showed a slight increase (rebound) similar to but less than TCA concentrations in port E in well 54-1018 and port F in well 54-2024 (c.f., Figs. 4-4, 4-3, and 4-2).

4.1.2 Upgradient from the extraction well

Monitoring well 54-1004 is located 30 feet northwest of the extraction well towards the VOC source beneath the southeastern portion of MDA L (Fig. 4-1). TCA concentrations as a function of time at well 54-1004 are shown graphically in Fig. 4-5. Due to the location of well 54-1004 between the extraction well and the VOC source, TCA concentrations in well 54-1004 are much higher than in wells downgradient from the extraction well. Note that the vertical scale in Fig. 4-5 is condensed to accommodate the relatively higher TCA concentrations closer to the VOC source.

During the operation of the extraction blower, TCA concentrations measured in ports E and G in well 54-1004 demonstrate an increase in TCA concentrations in contrast to comparable ports C and E in well 54-1018 located on the downgradient side of the extraction well (c.f., Figs. 4-2 and 4-5). This indicates that the negative pressure applied at well 54-1017 during the operation of the extraction blower actually pulled air containing higher TCA concentrations from closer to the VOC source towards the extraction well.

4.2 TCA BEHAVIOR AND STRATIGRAPHY

The response and recovery of vapor phase TCA concentrations is influenced by the geohydrologic characteristics of the various stratigraphic subunits of the Bandelier Tuff through which they moved. Table 4-1 lists the stratigraphic unit or subunit in which each monitoring port is located (c.f., Table 4-1, Figs. 4-3 and 4-4).

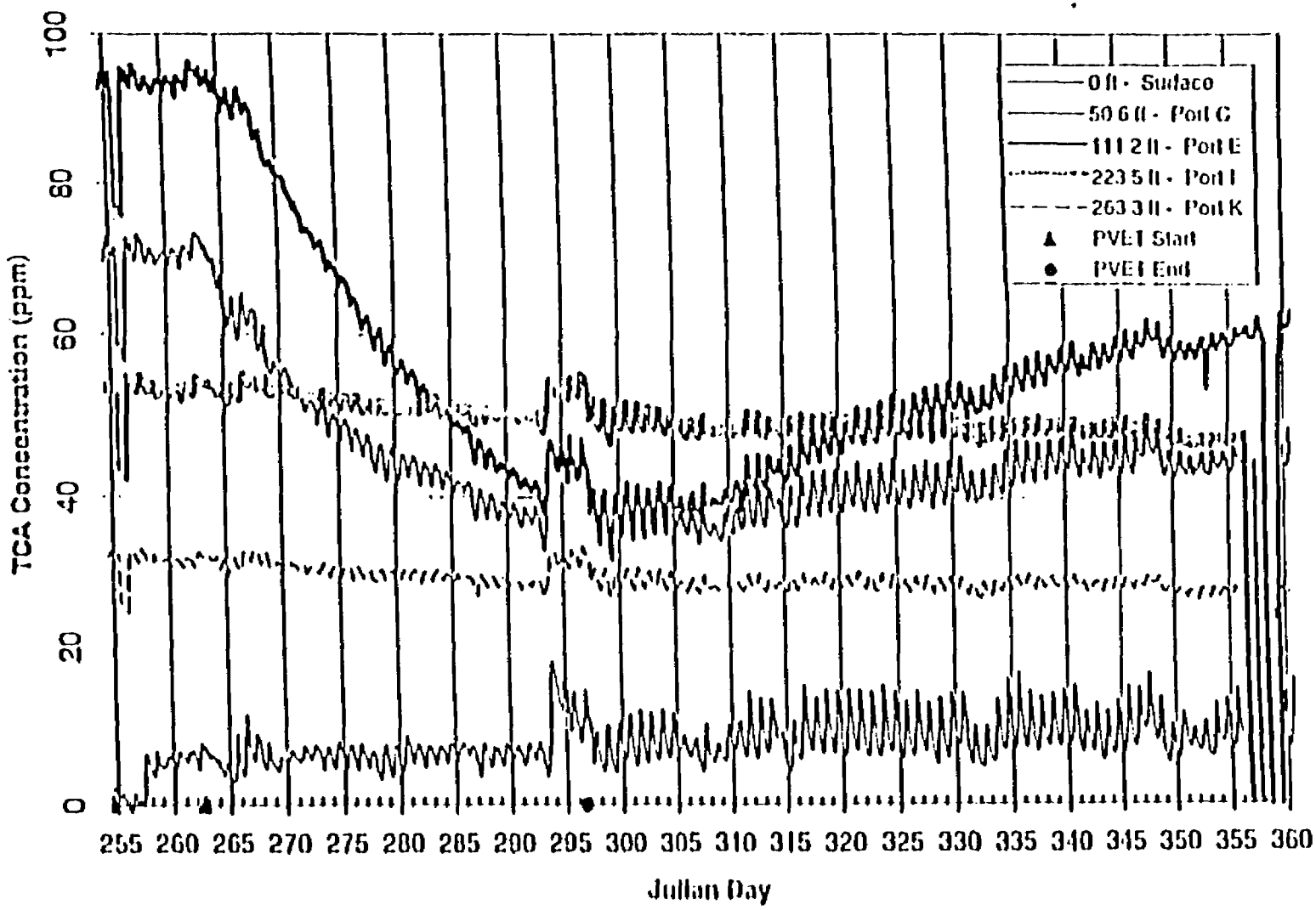

Figure 4-2. TCA Concentrations at Well 51-1018
(20 ft downgradient from extraction well)

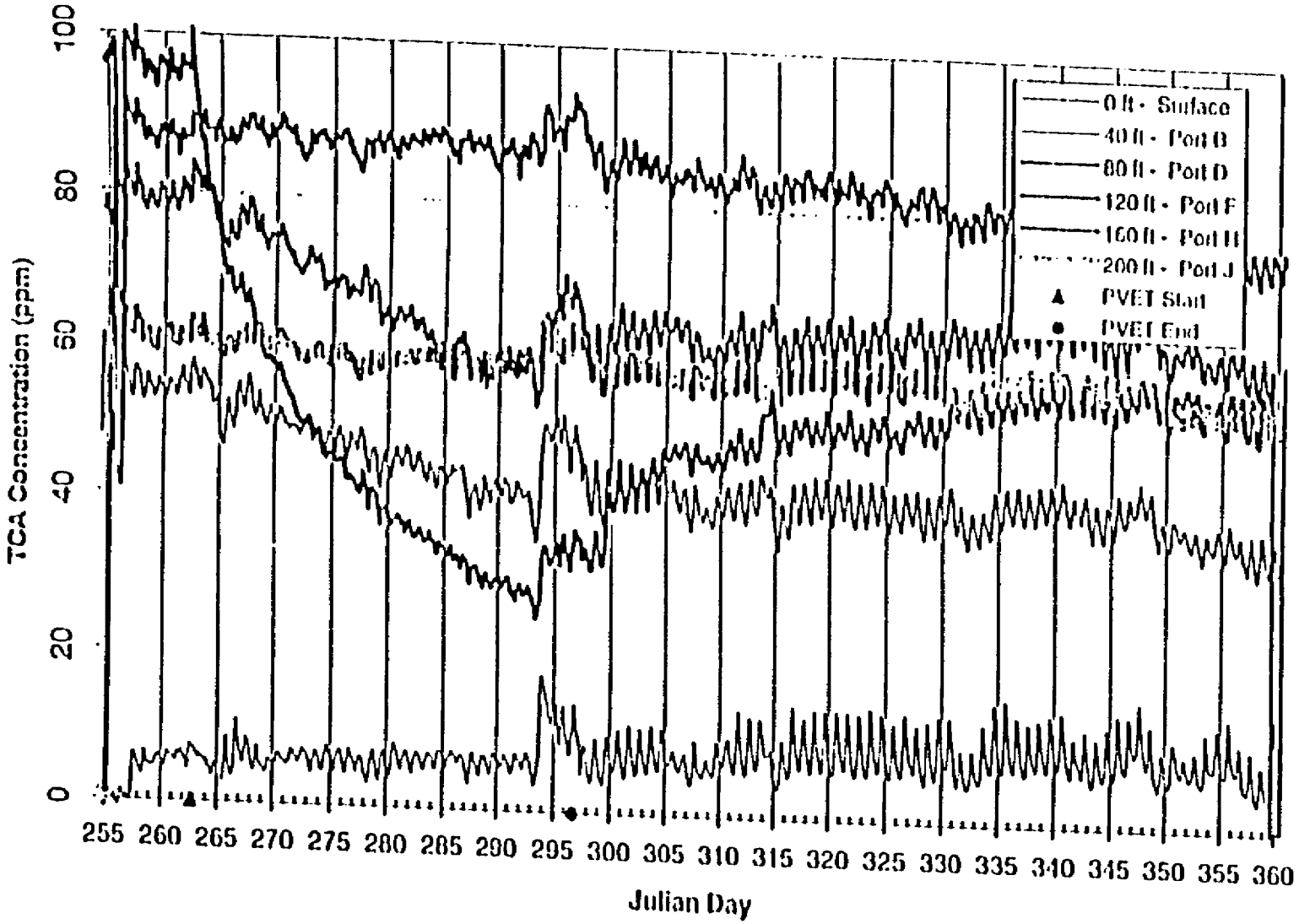

Figure 4-3. TCA Concentrations at Well 51-2024 (51 ft downgradient from extraction well)

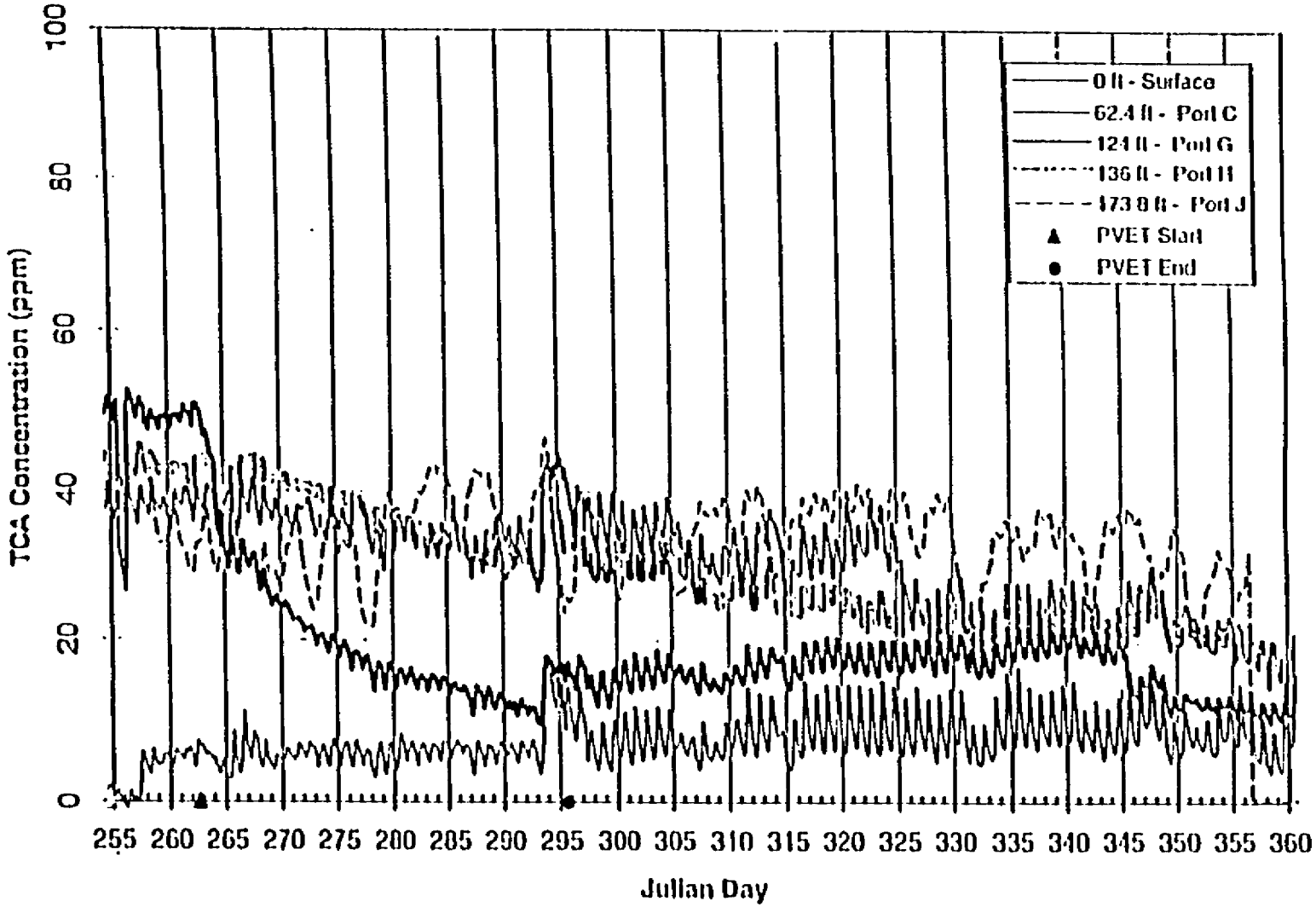

Figure 4-4. TCA Concentrations at Well 51-1003 (96 ft downgradient from extraction well)

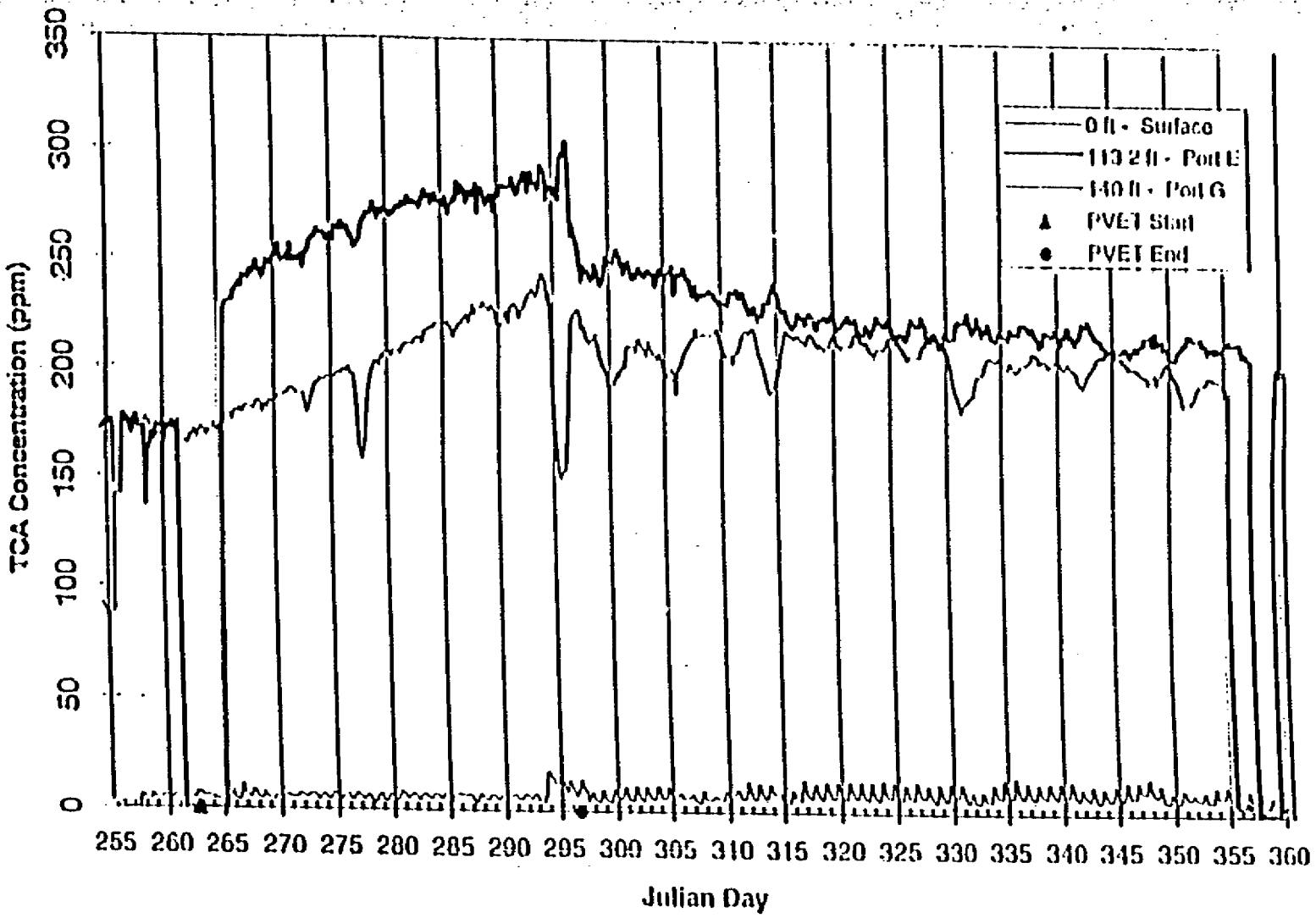

Figure 4-5. TCA Concentrations at Well 51-1001
(30 ft upgradient from extraction well)

4.3 RESPONSE OF OTHER VAPOR PHASE COMPOUNDS MONITORED DURING PVET

In addition to TCA, oxygen, carbon dioxide, and water vapor concentrations were also logged periodically during the PVET. The following sections describe the response of these compounds as measured during the test and graphically present the data collected.

4.3.1 Carbon Dioxide

Figures 4-6 and 4-7 show the concentrations of carbon dioxide as measured over time in well 1018 and 2024 at four different depths and surface. In the shallower depths a slight increase in carbon dioxide concentration occurred during the time period of the test, while Fig. 4-2 and 4-3 indicates a marked decrease in contaminant at these depths. This may indicate that carbon dioxide is present due to natural processes in the shallower depths.

Figure 4-8 shows carbon dioxide concentrations as plotted over time in well 1003. Little response in the carbon dioxide concentration is noted at this radial distance for the time period of the test. Figures 4-5 and 4-9 show almost an exact correlation in the response of carbon dioxide and TCA during the PVET. This indicates that the higher concentrations of TCA toward the source provide a suitable substrate for microbial respiration.

4.3.2 Oxygen

The oxygen data collected and presented in Figs. 4-10 - 4-13 show little response and remain static throughout the PVET.

4.3.3 Water Vapor

The water vapor data collected and presented in Figs. 4-14 - 4-17 show a noisy fluctuation over time and little can be inferred from the resulting figures.

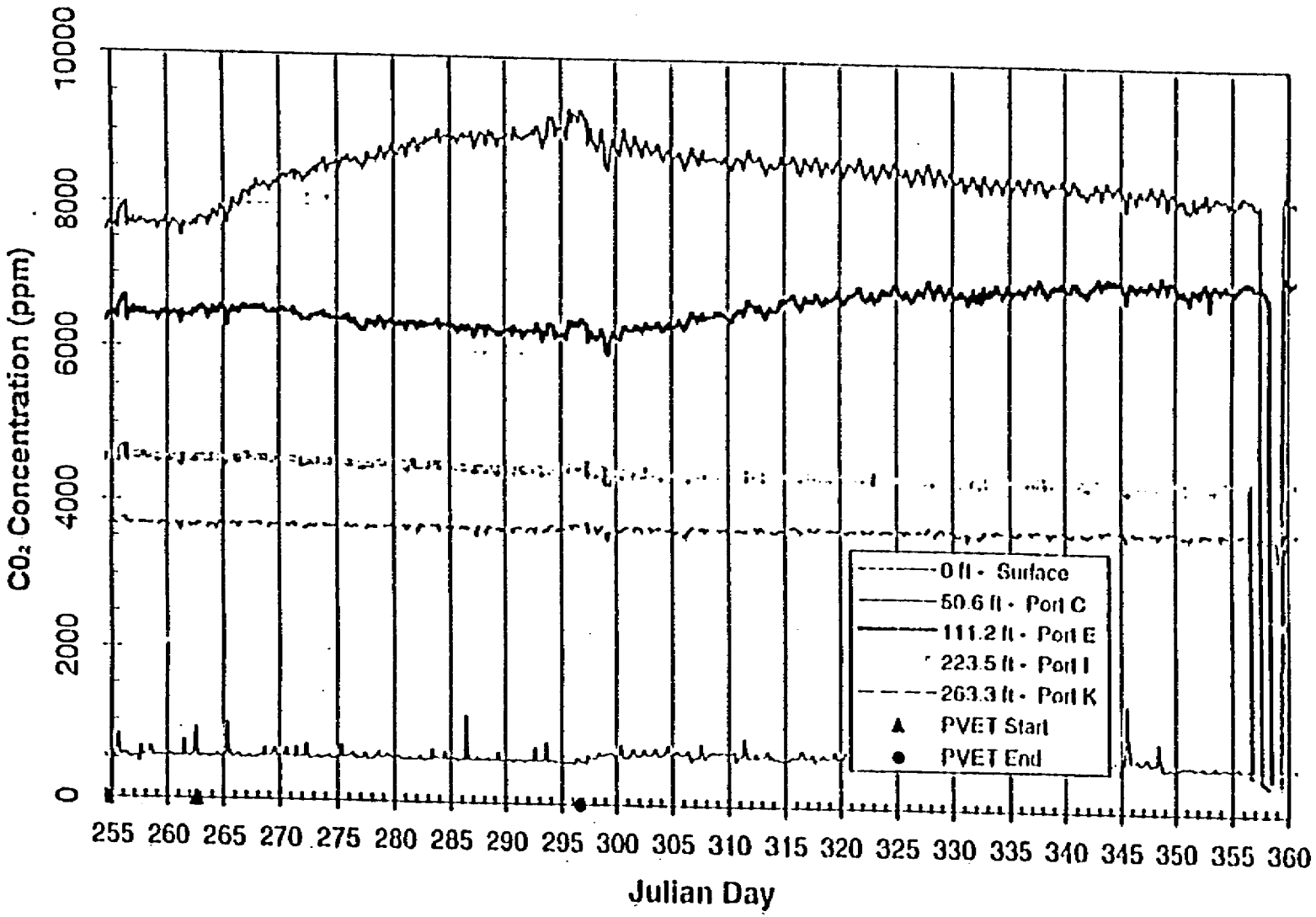

Figure 4-6. CO_2 at Well 54-1018

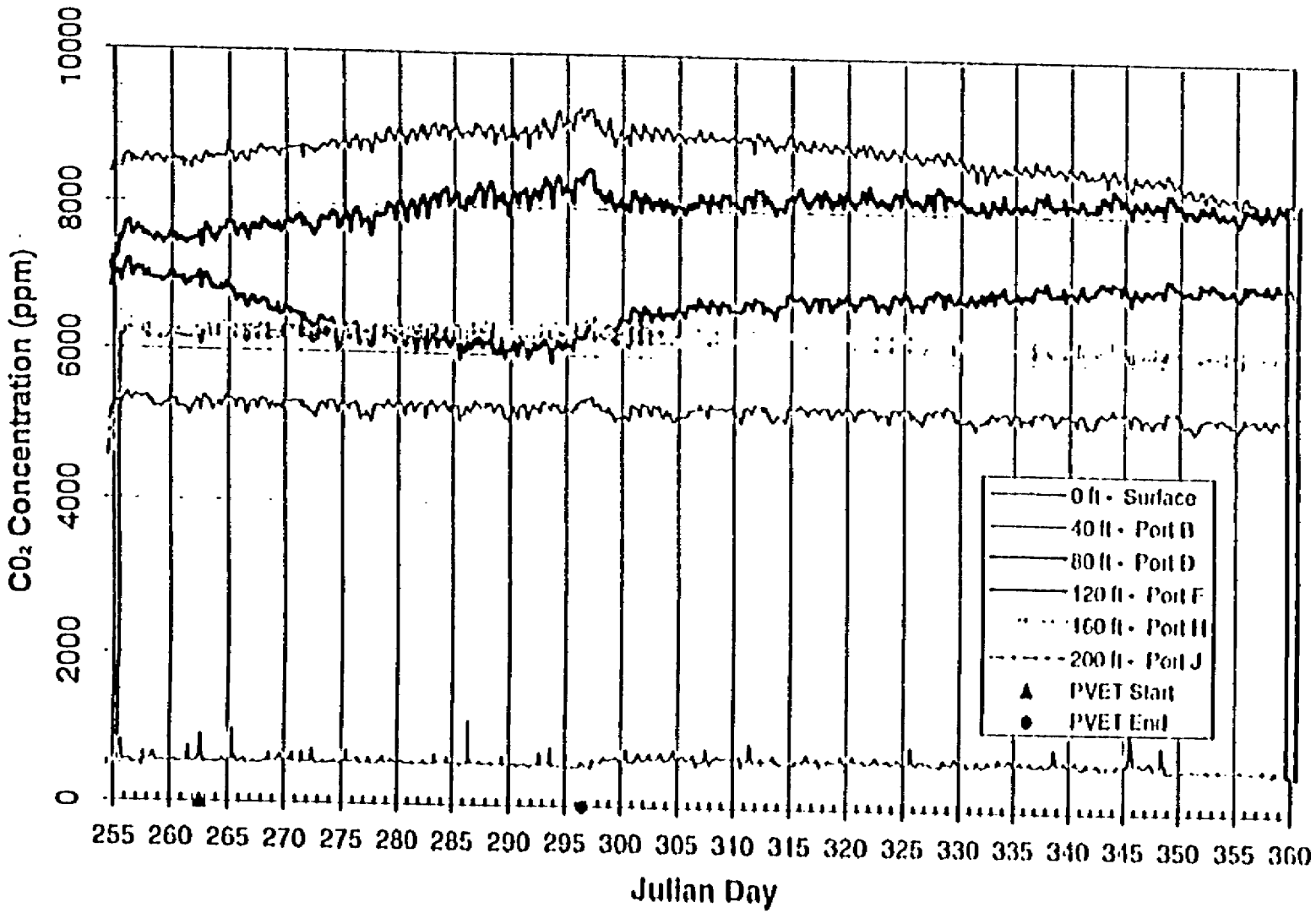

Figure 4-7. CO_2 at Well 54-2024

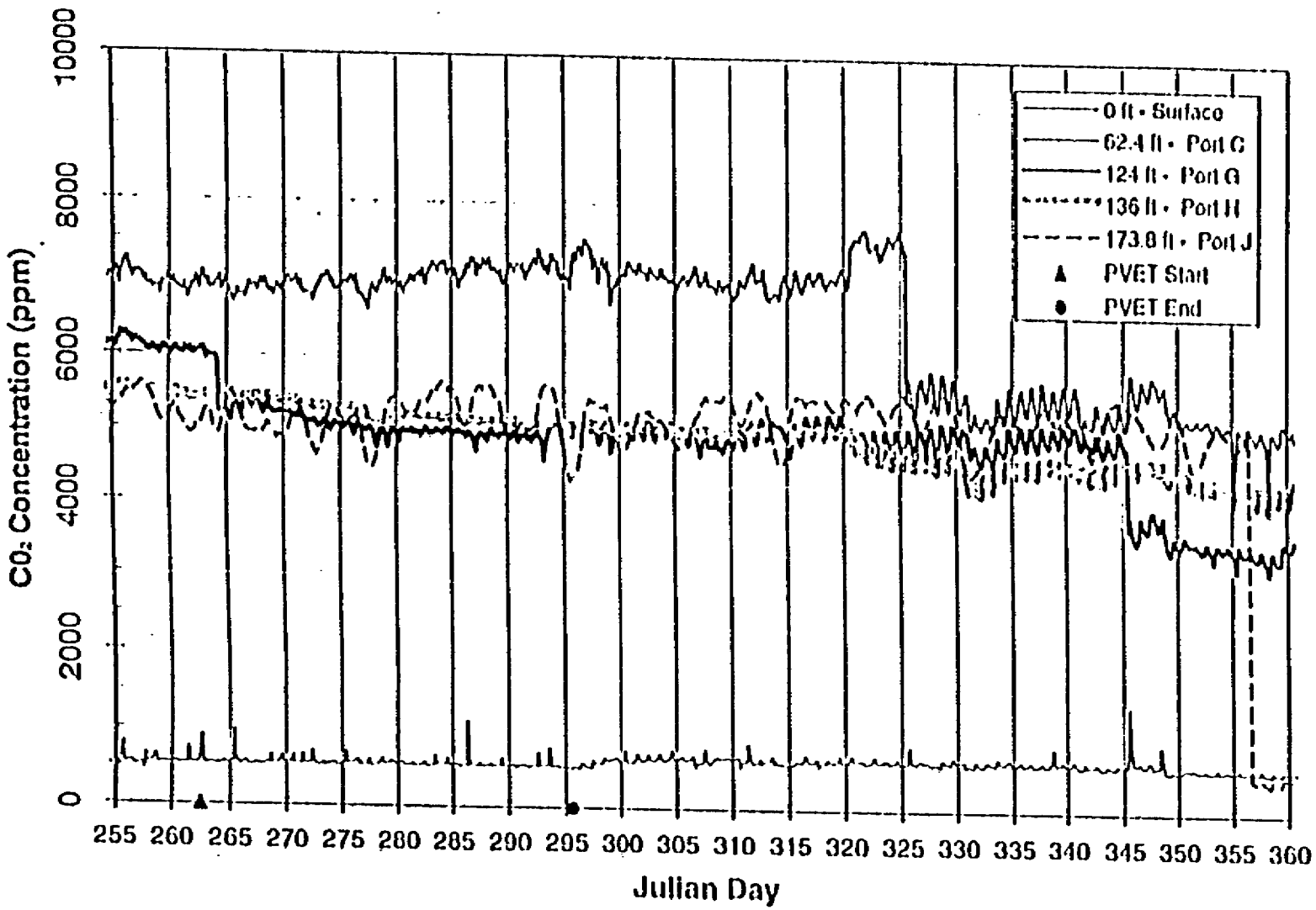

Figure 4-8. CO_2 at Well 54-1003

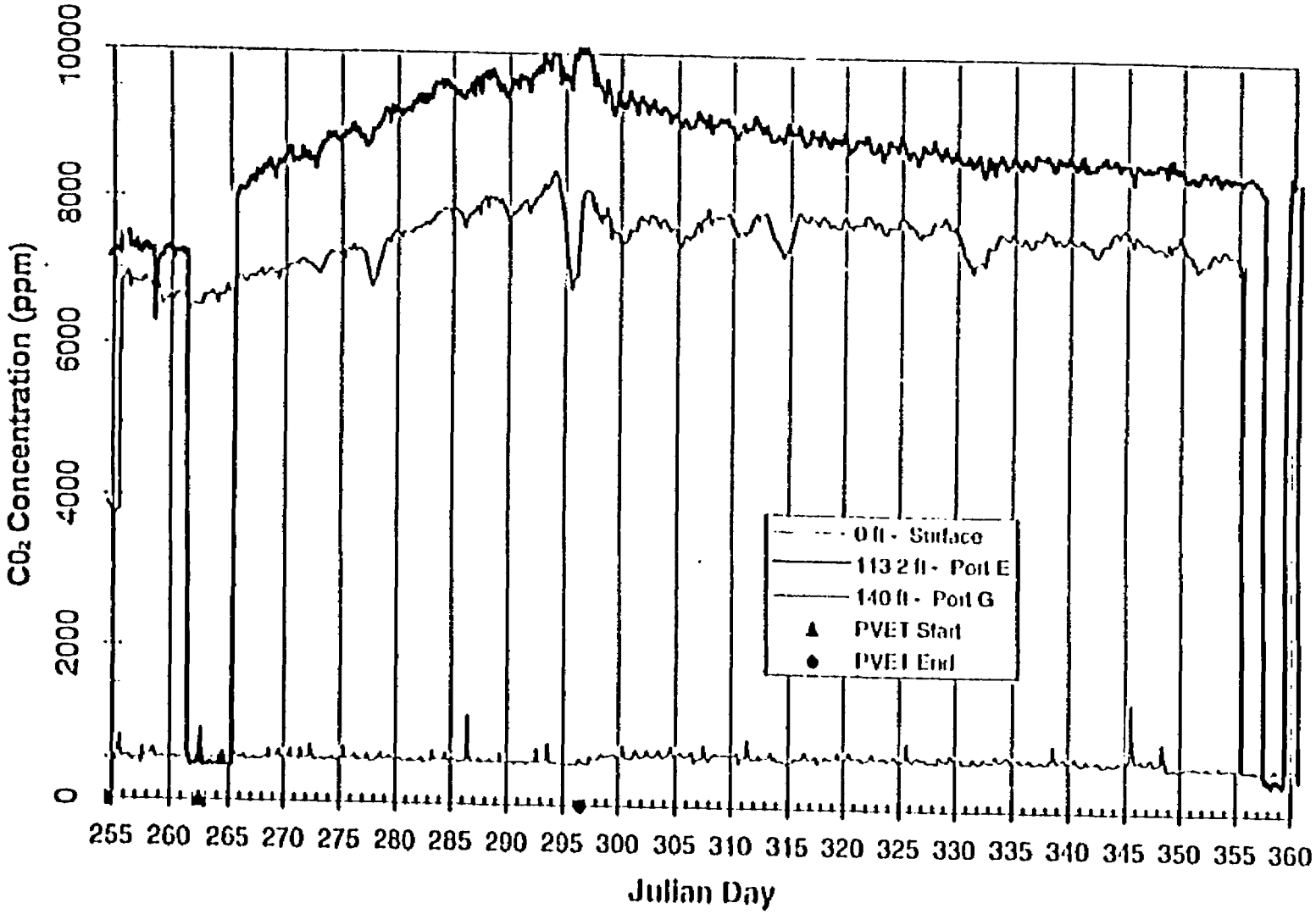

Figure 4-9. CO_2 at Well 54-1004

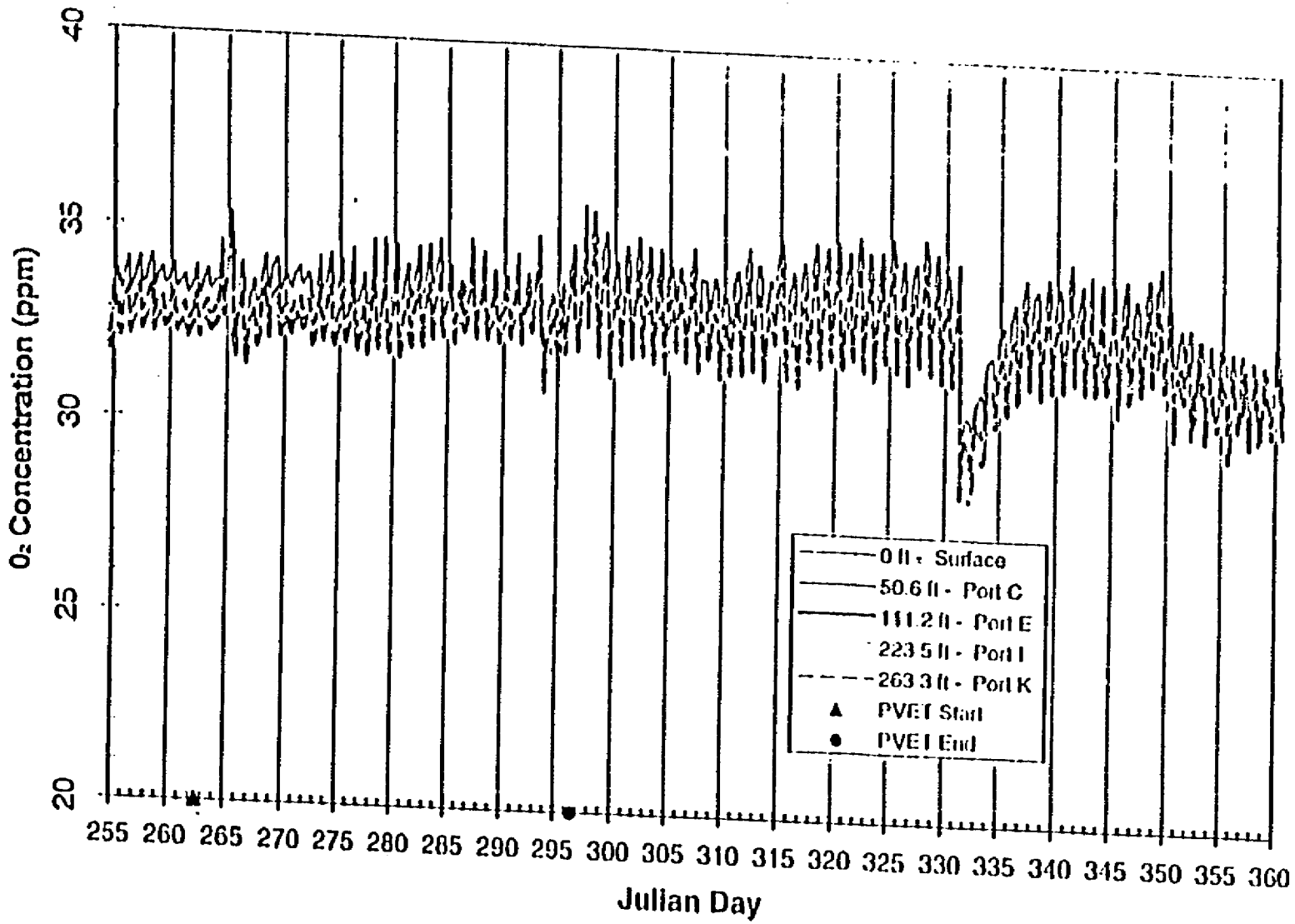

Figure 4-10. O_2 at Well 54-1018

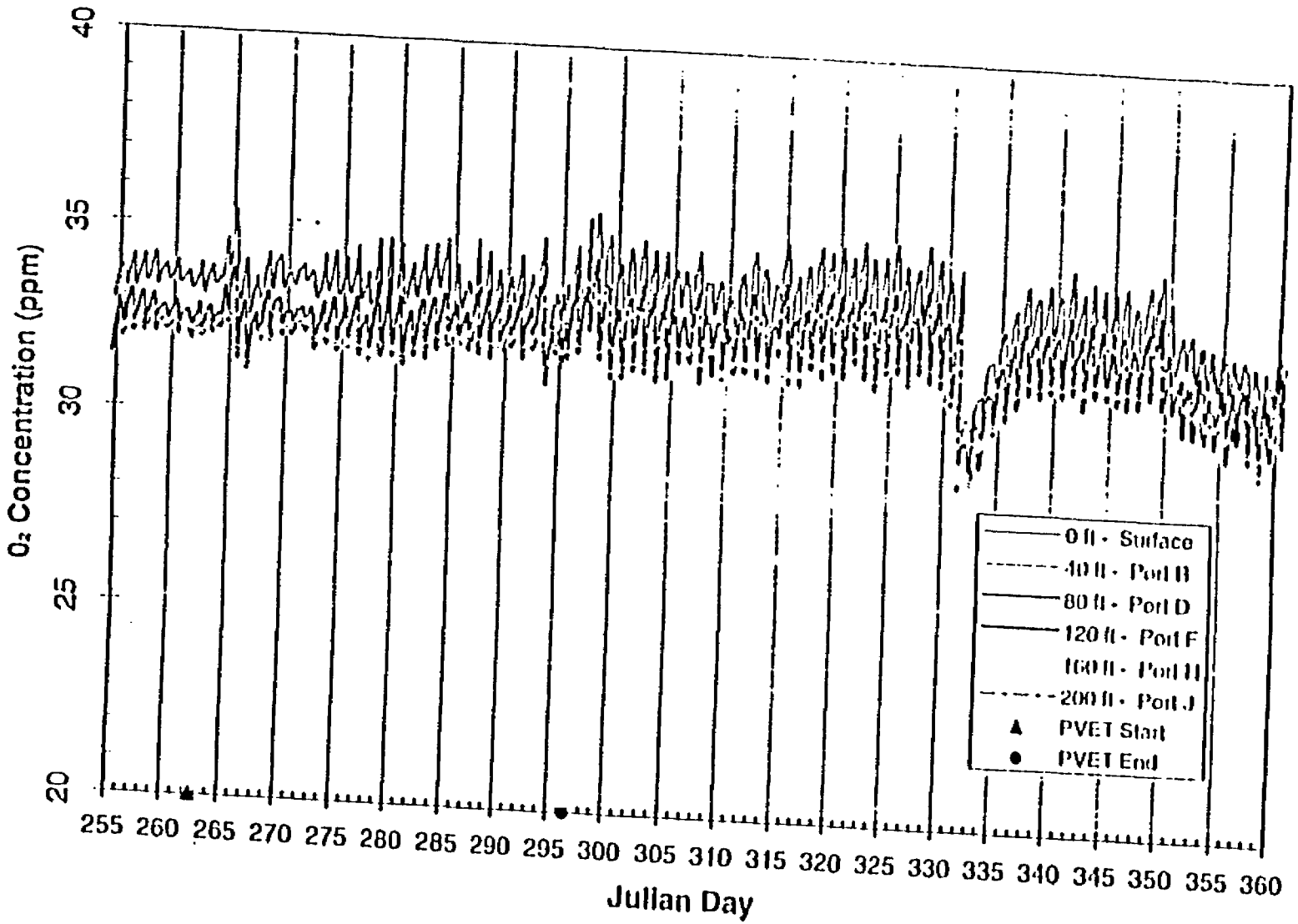

Figure 4-11. O_2 at Well 54-2024

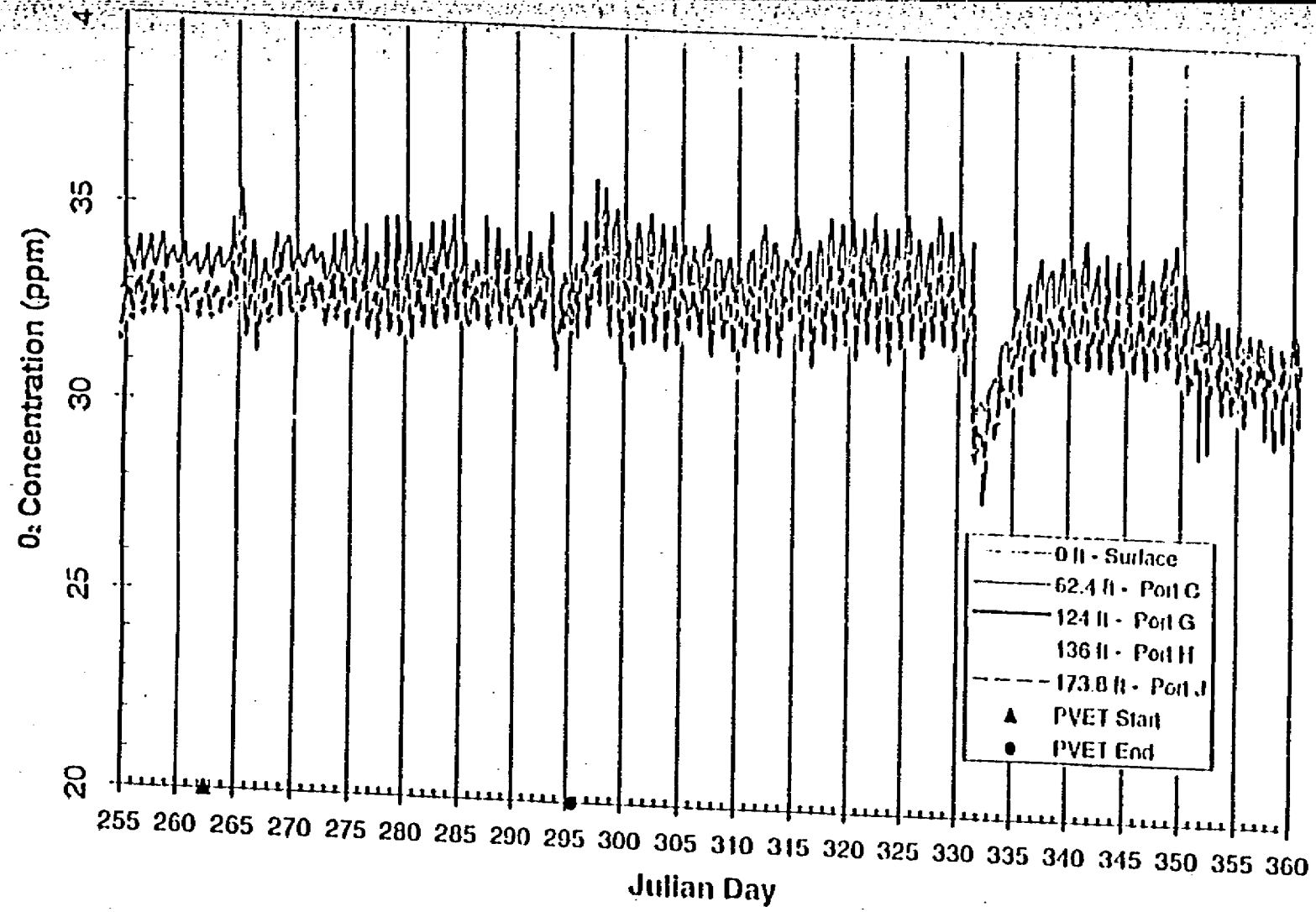

Figure 4-12. O_2 at Well 54-1003

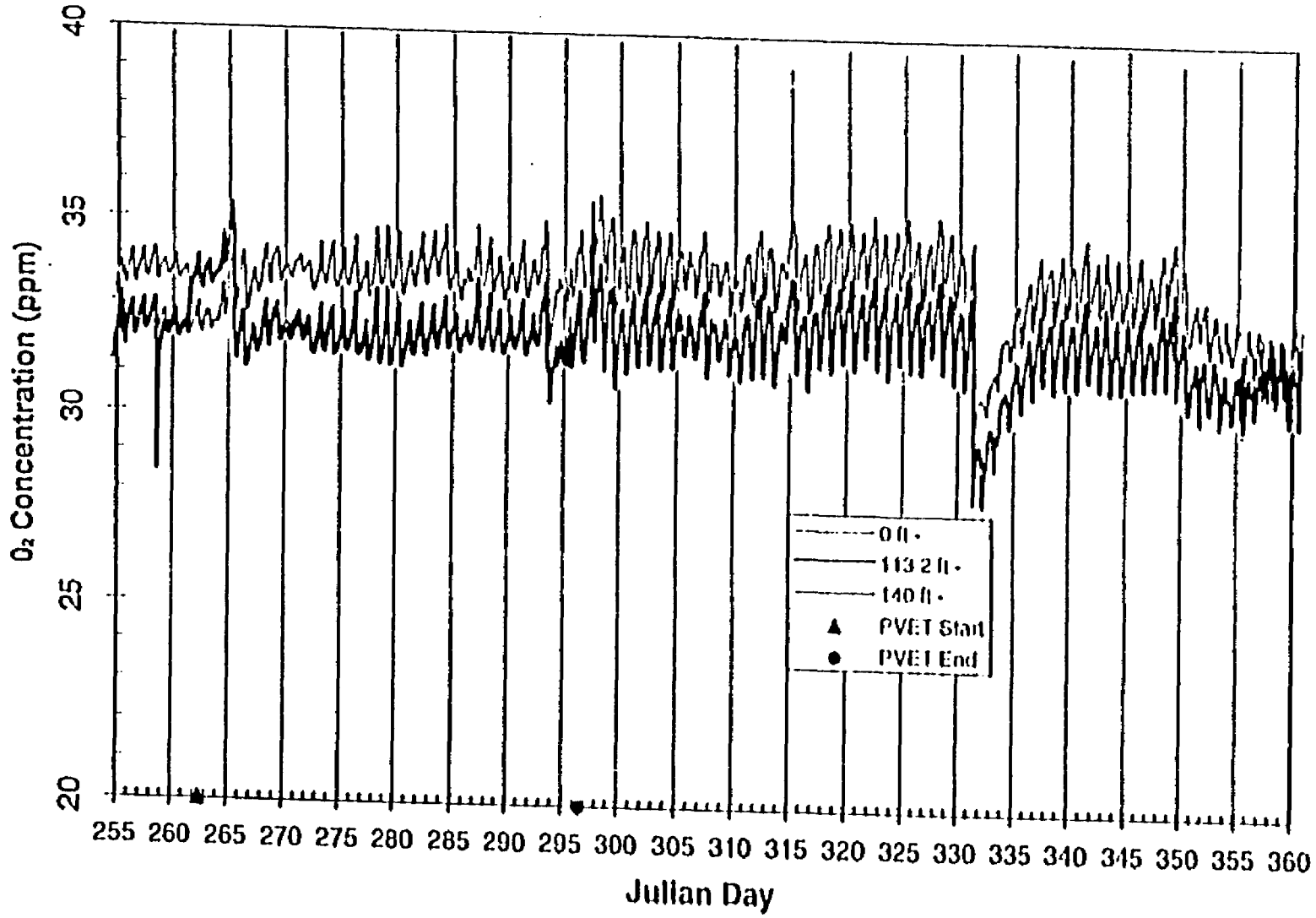

Figure 4-13. O_2 at Well 54-1004

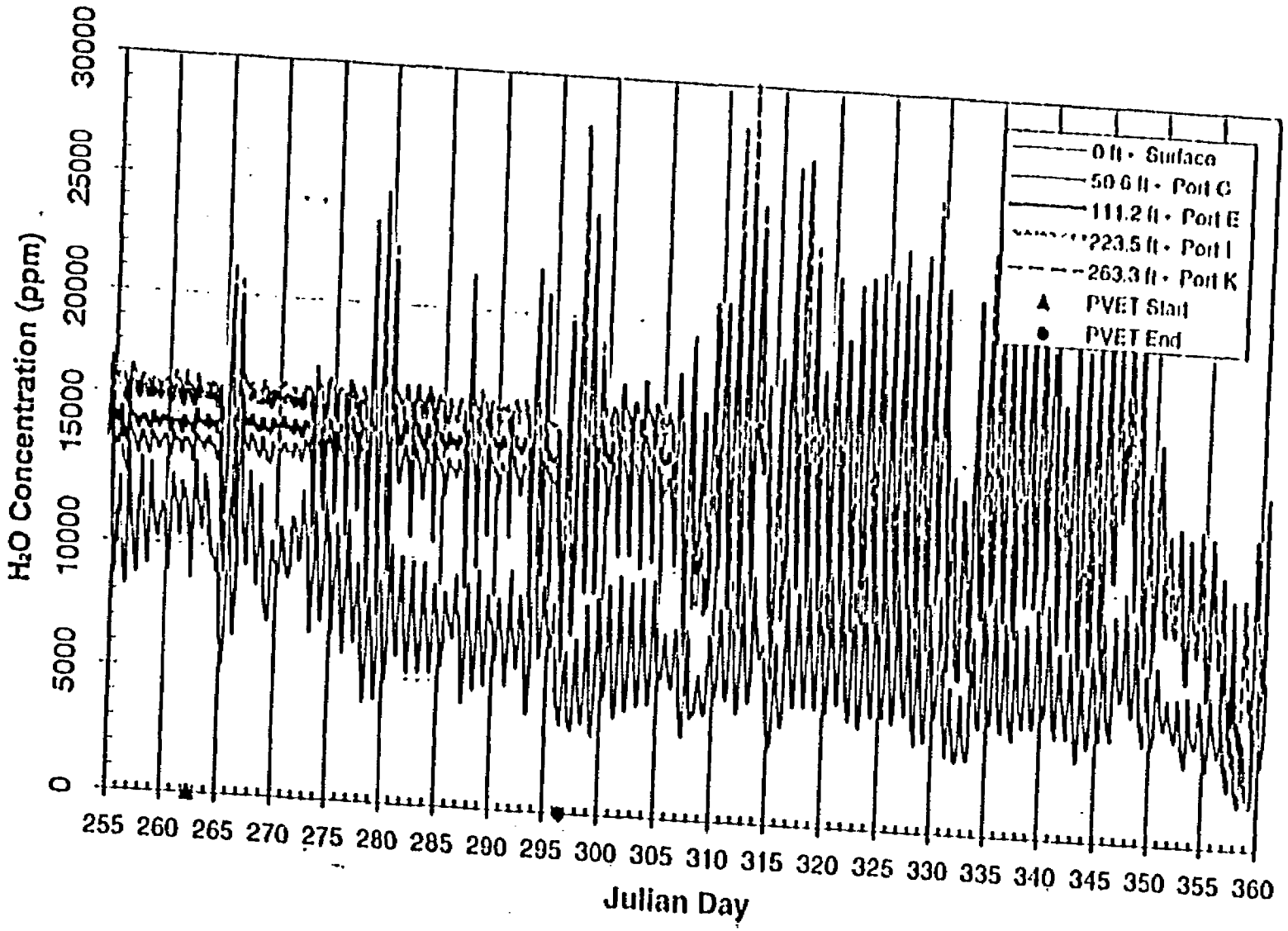

Figure 4-14. H_2O at Well 54-1018

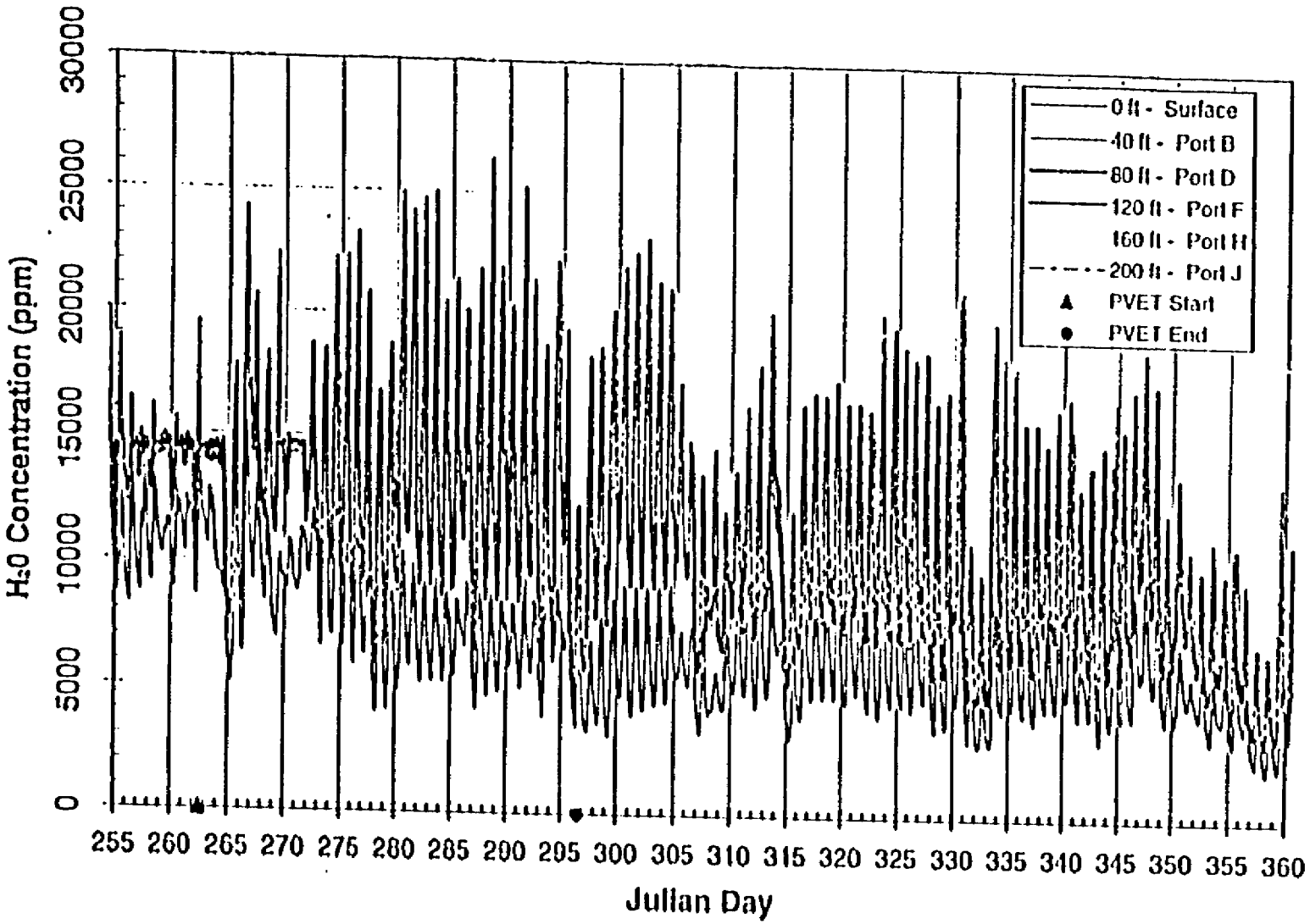

Figure 4-15. H_2O at Well 54-2024

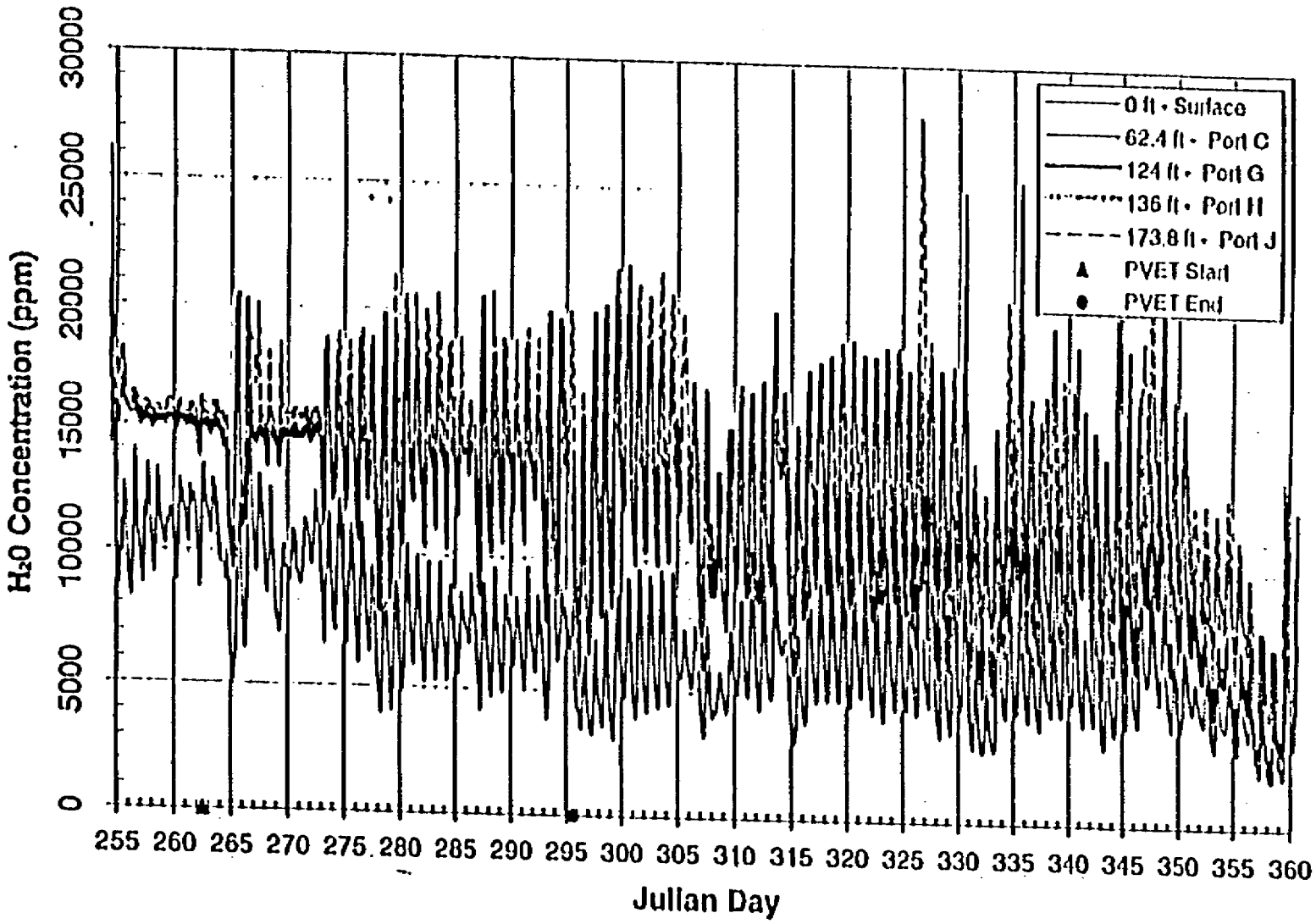

Figure 4-16. H_2O at Well 54-1003

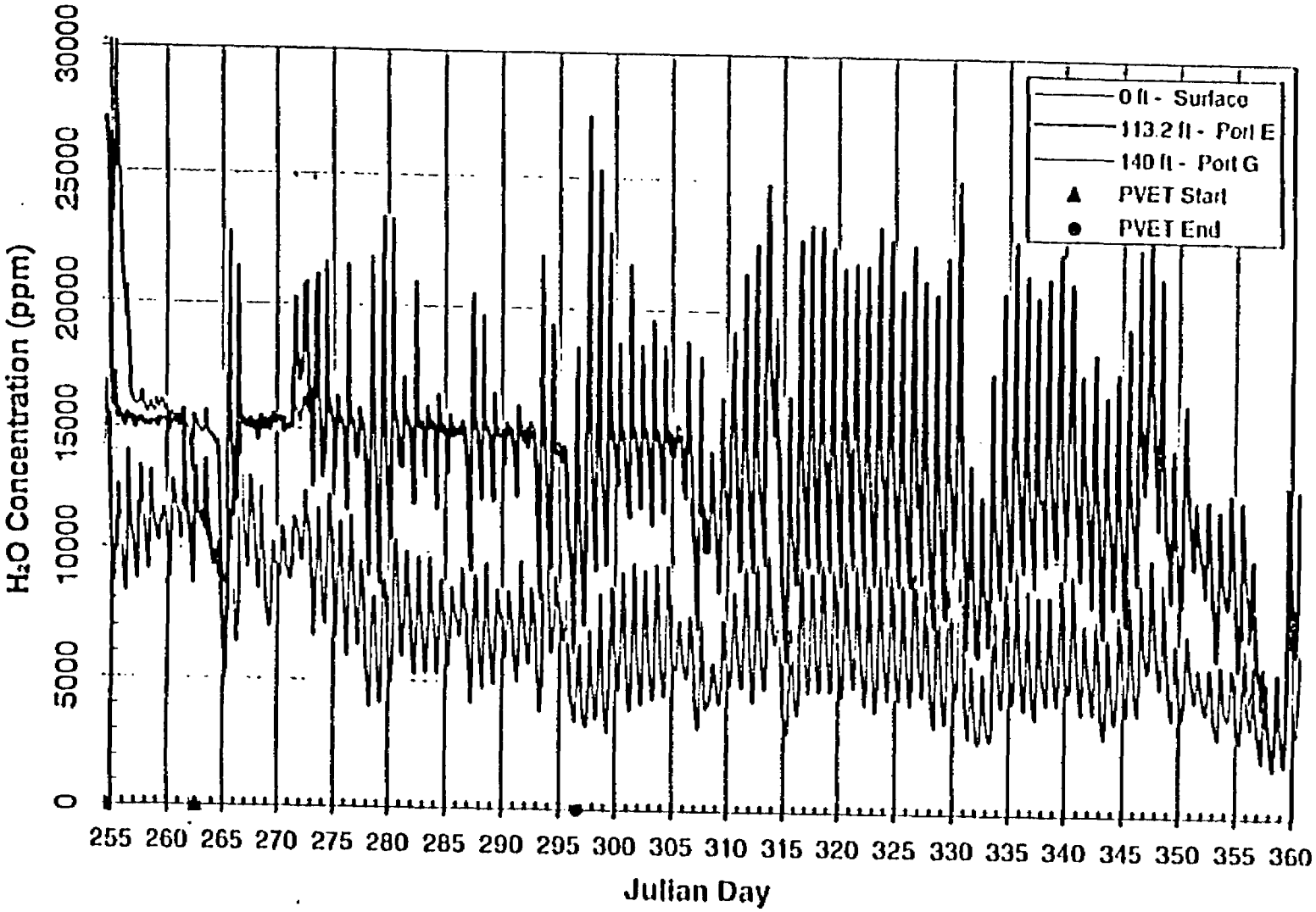

Figure 4-17. H_2O at Well 54-1004

5.0 NUMERICAL AND ANALYTICAL MODELING OF ACTIVE PILOT VAPOR EXTRACTION TEST

In situ soil vapor extraction has become a widely used method for the remediation of volatile compounds from permeable soils. In practice, vapor extraction system designs are based on a parameter known as the "radius of influence" R_I (m), which is assumed to be some measure of the volume of soil expected to be remediated by a single well (Johnson, et al, 1992). The approach used in this instance was to determine R_I from the steady-state vapor-phase pressure distribution data. Section 5.1 describes the preliminary numerical modeling and briefly compares these results to the analytical modeling and the actual results of the test presented in Section 5.2.

The open interval of the extraction well (54-1017) extended 75 ft to 150 ft below ground surface (bgs). In general, the permeability is somewhat larger in Unit 1v-c (colonnade) of the Bandelier Tuff, which is also the region of maximum VOC concentration. Consequently, the open interval of the active extraction borehole was centered on this depth.

5.1 NUMERICAL MODELING OF ACTIVE PILOT VAPOR EXTRACTION TEST

Initial design calculations were performed to determine the monitoring well layout and extraction system requirements. Three dimensional simulations were conducted with the AIR3D code (Joss, et al.), which models air flow but not contaminant transport through geologic media. The permeability distribution was based on earlier measurements in boreholes 54-1003 and 54-1004. This effort, and the AIR3D code, is discussed in detail in Appendix B.

After the extraction test, the model developed for test design was modified and used for test analysis. The original permeability values were replaced with the measured permeability distribution in boreholes 54-1017 and 54-1018, which were drilled and characterized with straddle packer measurements after the initial AIR3D modeling was completed. The procedures and results of the straddle packer measurements in boreholes 54-1017 and 54-1018 are discussed in detail in a separate report (SEA-175). The new measurements indicated lower permeability in the region of the extraction zone than was used in the original modeling, where a bulk medium permeability of 1.5 Darcies was applied. The revised simulations incorporated permeabilities of 0.2 and 0.6 Darcies in the extraction zone. The in-situ measurements from well 54-1018 and values used in the new model are depicted in Figure 5-1. The permeability varied as indicated by depth, but was modeled as uniform in the horizontal direction (within a horizontal layer the permeability was assumed to be homogeneous and

isotropic). Geometric layering was adjusted in the simulation to match the as-built configuration of the extraction well. Model boundary conditions remained the same as in the design model.

The modeled and measured extraction flows and pressures are compared in Table 5-1. The extraction vacuum is specified in the model, and the code calculates the resultant flow into the well. Note that the modeled extraction flow and measured average flow vary by 24% (the modeled flow being lower than the measured). These values agree favorably given that the model did not consider deviations from homogeneous and isotropic conditions. The in-situ permeability measurements which produced the data in Figure 5-1 assumed homogeneous and isotropic conditions locally at the measurement point.

Table 5-1. Comparison of modeled and measured extraction flow conditions.

Parameter	Modeled Value	Steady State Test Value
Atmospheric Pressure	80.0 kPa	79.5 kPa
Extraction Well Vacuum	-18.6 kPa	-18.4 kPa
Extraction Mass Flow	0.66 kg/min	0.87 kg/m

The predicted steady state model vacuum pressures at a depth of 35.1 m (115 ft) and the actual vacuum pressures at approximately the same depth are plotted as a function of radial distance from the extraction well in Figure 5-2. In general, the model vacuum pressures were an order of magnitude greater than the average measured vacuum pressures. This difference is thought to result from an increasing far-field permeability that forced the majority of the pressure loss to occur in the near-field of the extraction well where permeabilities were lower. Steady state pressure contours are shown in Figure 5-3.

The predicted model soil gas velocity at a depth of 35.1 m (115 ft) was plotted as a function of radial distance from the extraction well in Figure 5-4. The soil gas velocity was calculated using modeled flows and Equation 5.1.

$$v = (k / \mu\phi) * (dP / dx) \qquad \text{(Eq. 5.1)}$$

v = soil gas velocity
k = model layer permeability at a depth of 35.1 m (115 ft) = 0.6 darcy (0.6×10^{-12} m^2)
μ = viscosity of air at 10 degrees C (283.15 K) = 1.76e-5 Pa * s
ϕ = assumed model soil porosity = 0.3
dP = change in pressure over the distance dx
dx = radial distance

At a radial distance of 15 m (49 ft) the soil gas velocity was calculated to be 0.5 m/day (5.79×10^{-6} m/s). In Section 5.2.4 the velocity of the soil gas between

radial distances of 6 to 26 m (20 to 85 ft) (average of 16m (52.5 ft) was estimated to be 0.5 m/day (5.79×10^{-6} m/s) based on the rate of movement of the contaminant plume itself. The soil gas velocity calculated from the modeled pressures agreed with the estimated values for soil gas velocity. A good comparison of soil gas velocity values is thought to have been obtained despite the heterogeneity in the permeability field because the higher pressure gradient in the model was compensated by a lower modeled permeability. This result indicates that gross system behavior can be adequately predicted by the assumption of homogeneity provided that the differences in material property values are not large. The modeled soil gas velocity is shown in Figure 5-3.

5.2 ANALYTICAL MODELING OF ACTIVE PVET

The following sections describe the analytical calculations performed to predict vapor and plume movement during the active PVET. The extraction test was modeled using an analytical expression relating the steady state one-dimensional compressible radial flow of gas to a vertical extraction well (Johnson et al., 1990) using the steady state parameters for R_I, atmospheric pressure, and applied well-head vacuum (Section 5.2). These results were compared against average field measurements over the time period of the test to verify that the assumptions are valid and the airflow through the subsurface when a vacuum is induced can be accurately predicted.

The first step was to infer when steady state conditions were reached from the pressure data plotted over time when steady state was reached (sec. 5.2.1), and to calculate the steady state parameters for use in the steady state radial gas flow equation (Equation 5-2). The next step was to determine R_I from the steady-state vapor-phase pressure distribution data within the extraction interval and to estimate the near field permeability (Sec. 5.2.2) using Equation 5-2. The third step was to use the steady state parameters developed in Section 5.2.1 in Darcy's law equation for the estimation of linear velocity of a compressible gas in porous media (Equation 5-3) to produce a conservative prediction of vapor velocity within the extraction interval (Sec 5.2.3). This value was compared with actual plume velocity (change in concentration over time), in the colonnade, to verify the understanding of vacuum pressure distribution and the induced vapor-phase velocity within the extraction interval (Sec. 5.2.4).

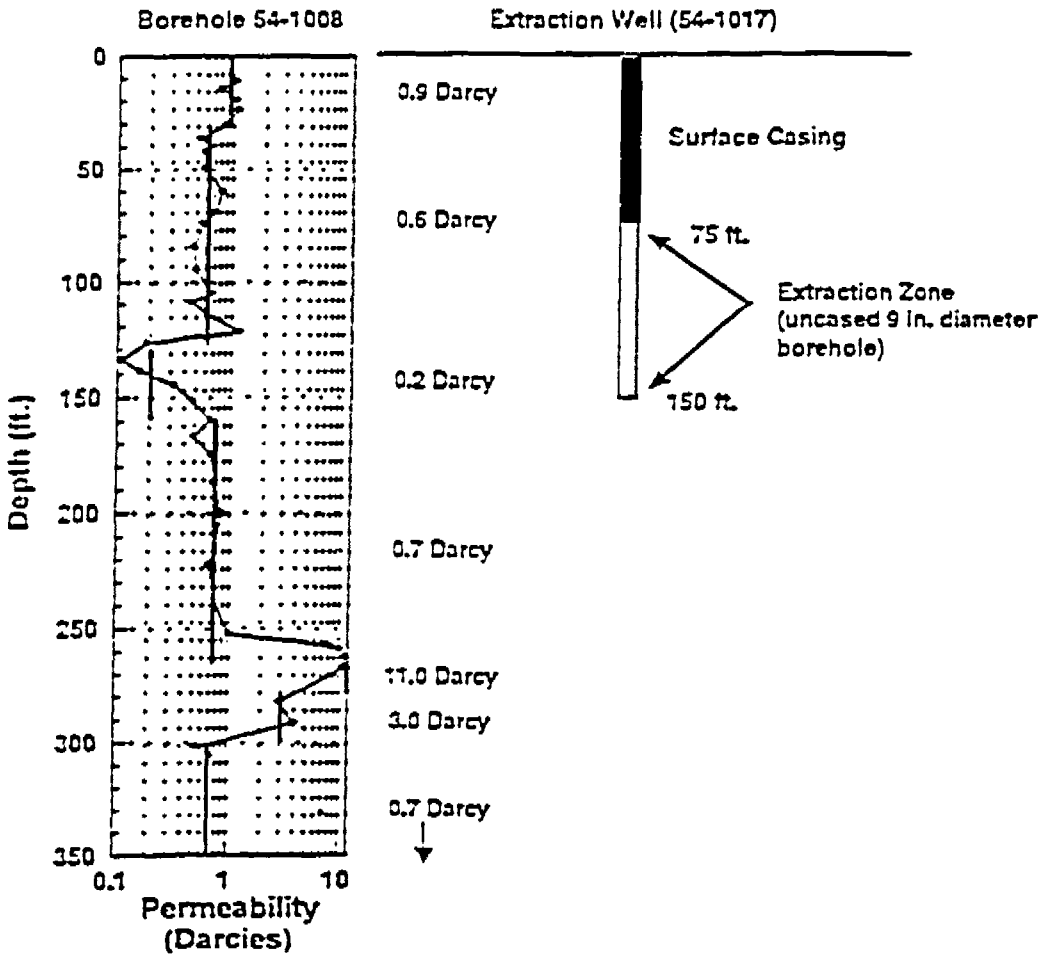

Figure 5-1. In-situ measured air permeability in borehole 54-1018, extraction well configuration, and permeability distribution used in AIR3D model.

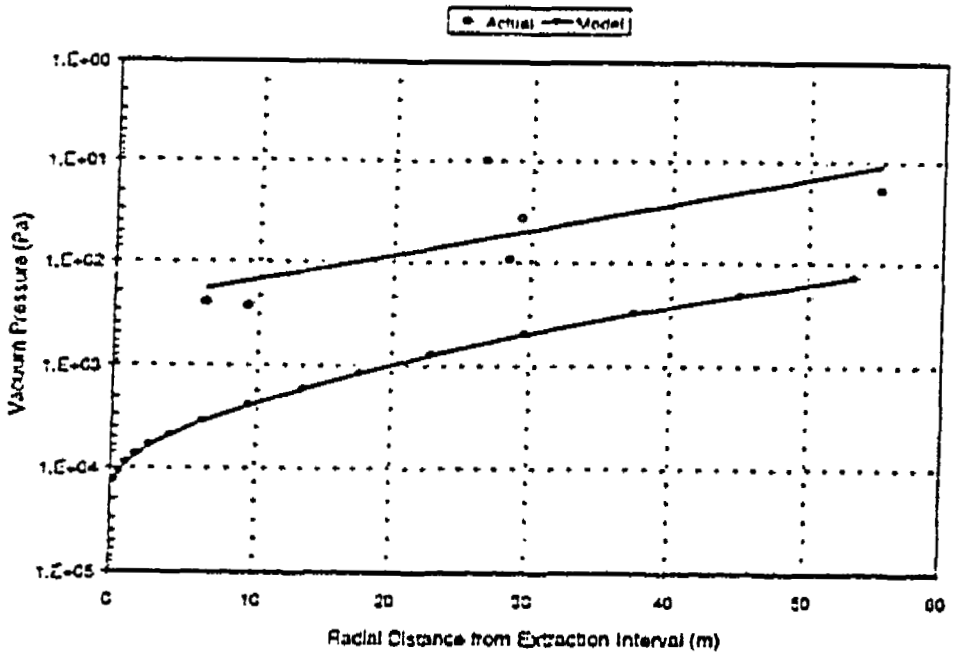

Figure 5-2. Modeled and measured vacuum pressure profiles at steady state conditions during the vapor extraction test.

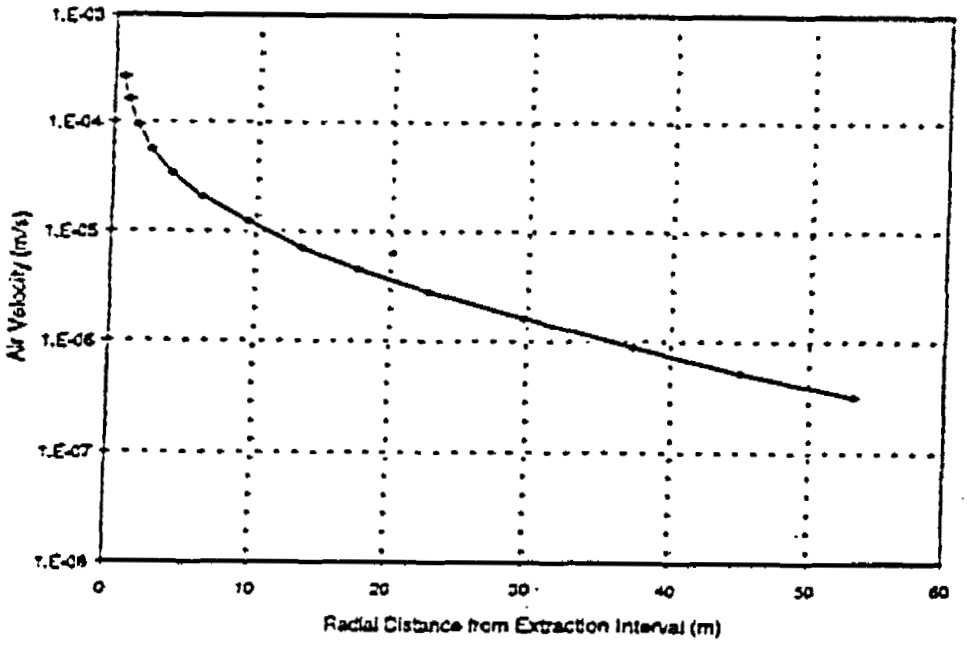

Figure 5-3. Modeled radial (positive toward the well) soil gas velocity profile at steady state conditions during the extraction measurement.

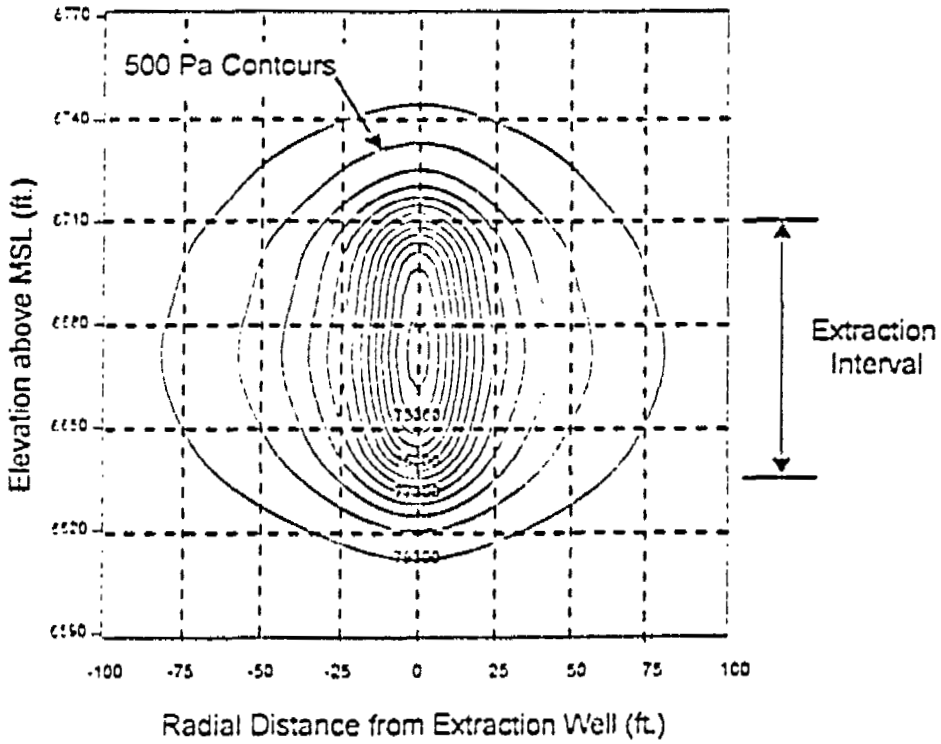

Figure 5-4. AIR3D modeled pressure distribution about the extraction zone. Contours are in 500 Pa increments. Ground surface is at 6785 ft. elevation.

5.2.1 Determination of Steady State

The assumptions in the analytical expression for one-dimensional compressible radial flow require the system to reach steady state. The vapor-phase pressure distribution can then be used to approximate R_I.

The time the system took to reach steady state was determined by plotting the difference in pressure over time between two locations at equal depths within the colonnade but at different radii from the extraction well. Steady state is reached when the pressure difference stabilizes. Figure 5-5 shows a plot of the pressure difference between pressure monitoring locations within the colonnade in wells 54-1018 and 54-2024. As shown in the figure, the pressure differential between the two points before and after the test fluctuated around zero. The climb to a steady state vacuum began immediately once the well-head vacuum was applied. The system was determined from the figure to be well into steady state five days after the test was initiated on day 262. On this basis the average

steady state parameters needed for the analytical equations were calculated from day 268 to day 296.

The test air flow rate was recorded and logged in standard cubic feet per minute (scfm). This was converted to an actual downhole flow rate using the combined gas law method presented in Equation (5-1).

$$Q_f = Q_s (P_s / P_f)(T_f / T_s) \qquad \text{(Eq. 5-1)}$$

Q_s = standard air flow rate at wellhead (26.2 scfm)
P_f = P_{atm}(absolute atmospheric pressure (62091 Pa))
P_s = standard atmospheric pressure (101325 Pa)
T_f = average steady state downhole temperature (284.6 K)
T_s = standard temperature (293 K)
Q_f = final average steady state downhole flow rate (41.5 cfm)

The final steady state downhole flow rate was calculated to be 0.0196 m^3/s (41.5 cfm).

5.2.2 Estimation of the Radius of Influence (R_I) and Near Field Permeability

In order to estimate R_I, a semilog plot of the steady state subsurface vacuum pressure data as a function of distance from the extraction well within the colonnade was prepared and a best-fit line was drawn through the points (Figure 5-6). R_I was then identified as the distance from the extraction well where the vacuum pressure reaches zero (Johnson et. al., 1992). Using this approach R_I was determined to be approximately 140 ft.

The one-dimensional steady-state radial flow expression relating the downhole flow rate (Q) and the radial distance from the extraction well (R) to the permeability (k) of the tuff is presented in Equation (5-2).

where

k_w = permeability of tuff to air flow (m^2)
Q = downhole vapor extraction flowrate (m^3/s)
μ = viscosity of air @ 11.6°C (Pa s)
H = thickness of vapor flow test interval (m)
P_A = pressure at inner radius (Pa)
R_A = Inner Radius (m)
P_B = pressure at outer radius (Pa)
R_B = Outer Radius (m)

Equation (5-2) was used to estimate the near-field permeability around the extraction well, for comparison with the permeabilities determined with small-scale packer tests in the extraction well and in monitoring well 54-101S (SEA-175). Well 54-101S is 6.1 m (20 ft) from the extraction well and was used to define

the approximate outer boundary of the near-field. At radial distance greater than 6.1 m (far-field), the field results indicated that gas velocities can be better predicted assuming linear rather than radial flow.

The vapor flow interval (H) for the test was considered to extend from the top of the extraction well to the bottom of the colonnade and was equal to 17.1 m. The higher liquid saturation near the bottom of the colonnade was found in the packer tests to reduce the air permeability of the lower part of the test interval. The lack of significant air flow into the test well below this unit was confirmed by plume concentration data (Figure 5-7) showing little change in concentration during the test below this depth.

$$k_v = Q\,\mu / [H \pi P_A \{[1-(P_B/P_A)^2]/\ln(R_A/R_B)\}] \qquad \text{(Eq. 5-2)}$$

The downhole, steady state vapor extraction flow rate (Q_f)was previously determined to be 0.0196 m^3/s. The viscosity of air (μ) at 11.6°C (downhole temperature in extraction well) is 1.79×10^{-5} Pa s. The atmospheric pressure $(P)_{atm}$, averaged over the time period of the test was calculated to be 79621 Pa. The average applied well-head vacuum was 18340 Pa. The average absolute pressure in the well bore ($P_A = P_{atm}$- Applied Well-head Vacuum) was calculated to be 61281 Pa. The radius of the well (R_A) was 0.127 m and the near field radius (R_B) was 6.1 m. The average steady state pressure (P_B) in the colonnade at well 54-1018 was 79340 Pa based on monitoring data taken during the steady state period of the test. Applying these parameters to Equation (2) yielded an average near field tuff permeability of 0.61 darcy (6.1×10^{-13} m^2).

Comparison of the calculated near field permeability to the result of the packer tests in the same region yielded close results. The average near field permeability within the test interval above the bottom of the colonnade was estimated by the packer tests to be 0.6 darcy (SEA-175). The close comparison between the permeability calculated from the large-scale extraction test and that determined from the small scale packer tests indicated that the packer tests provided accurate measurements within radial distances of at least 6 m from the well. On this basis, the permeabilities measured by packer tests in wells farther from the extraction well were used to predict vapor velocities at greater distances from the extraction well.

5.2.3 Calculation of Vapor Velocity

Pressure draw down in a homogeneous medium is expected to follow a smooth exponential decay with the largest gradient within the first few meters from the extraction well. At the closest monitoring well in this test (R_B= 6.1 m) the maximum vacuum pressure in the colonnade was 703 Pa, about 4% of the induced vacuum. This is a much larger gradient than expected for a

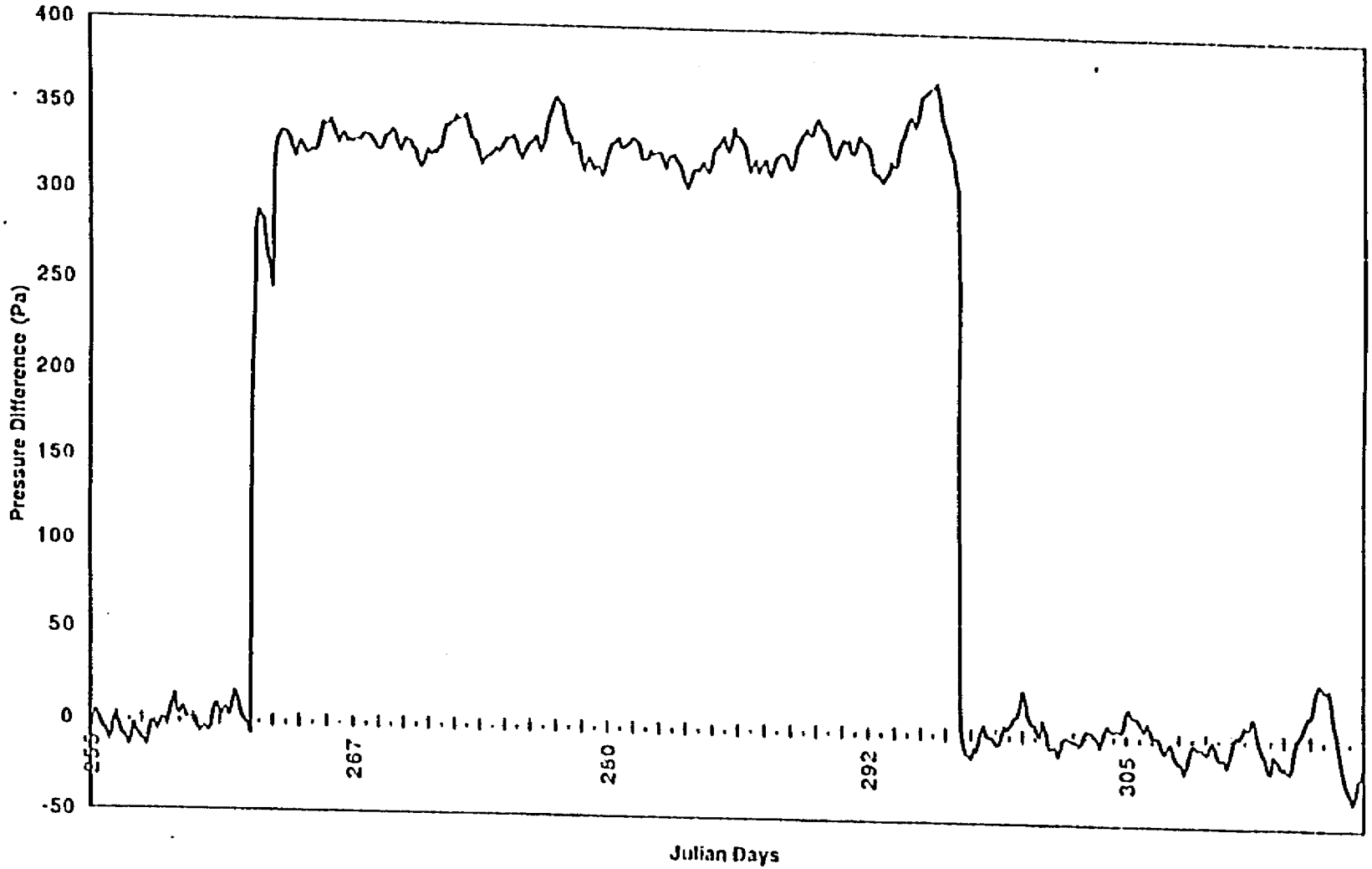

Figure 5-5. Method for Determining Steady-State Test Period.

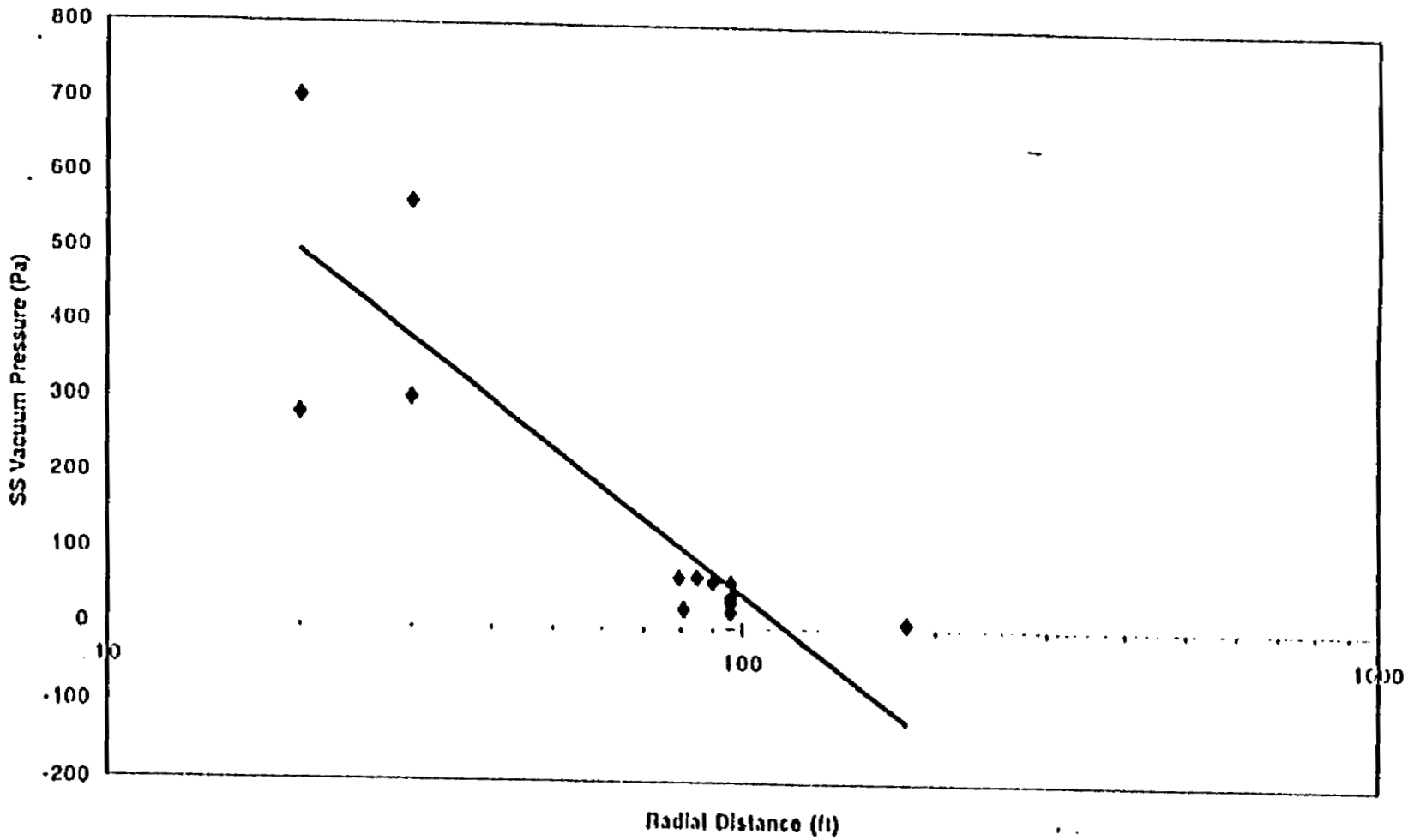

Figure 5-6. Method for Determining Radius of Influence

homogeneous medium and suggests that the permeability is lower near the extraction well than in the far field, causing a disproportionate amount of the pressure drop to occur in the near field and a rapid transition from radial to nonradial flow beyond about 6 m from the extraction well.

$V_{vapor} = k/\mu\phi * (\Delta P)$ (Eq. 5-3)
ϕ = effective porosity
$\Delta P = (P_A - P_B) / (R_B - R_A)$

The effective porosity was estimated from the average porosity of the colonnade (~0.493) and the maximum natural moisture content within this zone (~0.1) (see Table 2-1 of this report). Assuming moisture content restricts vapor flow, the average porosity of the colonnade was reduced by 0.1 to estimate an effective porosity (ϕ) of 0.4. The average far field permeability (k) was estimated to be 3 darcies (3×10^{-12} m^2) based on packer tests results from wells 54-1003 and 54-1004, both of which had average permeabilities of about 1.5 darcies within the test interval and from well 54-1006 which had an average permeability of 0.6 darcies in the test interval (SEA-020). The average velocity was calculated using the average pressures in the colonnade in wells 54-1003 and 54-1018 at radial distances of 29.6 m and 6.1 m, respectively. Well 54-1003 was near the outer boundary defined by the radius of influence (R_I) of the test. The average steady state vacuum at Well 54-1003 was 38 Pa, and the average steady state vacuum at well 54-1018 was 281 Pa. Using these values in Equation (3), the predicted vapor velocity (V_{vapor}) was estimated to be 0.4 m/day.

5.2.4 Calculation of Contaminant Plume Velocity

The contaminant velocity induced by the extraction test was estimated based on the rate of movement of the 40 ppm and 60 ppm TCA plume concentration contours toward the extraction well over a 20 day period (Figure 5-7). The 40 ppm contour moved an average of 35 ft, from radial distances of 85 ft to 50 ft, over the twenty day time period. The 60 ppm contour also moved an average of 35 ft, from radial distances of 55 ft to 20 ft, over the twenty day time period. This came to an average plume velocity of 0.5 m/day.

5.3 DISCUSSION OF MODELING RESULTS

The close agreement between both numerical and analytical modeling results suggests that plume movement toward an extraction well at MDA L can be adequately predicted for purposes of extraction system design and plume remediation. The numerical modeling results were based on the extraction flow rate and material properties obtained from field measurements independent of the extraction test. The predicted gas flow and velocity toward the extraction

well compared favorably with the field measured values. The analytical modeling results supported the packer test permeability measurements and numerical modeling, and also demonstrated that assumptions of unretarded porous medium Darcy flow can be successfully applied to air flow within the Bandelier tuff at MDA L.

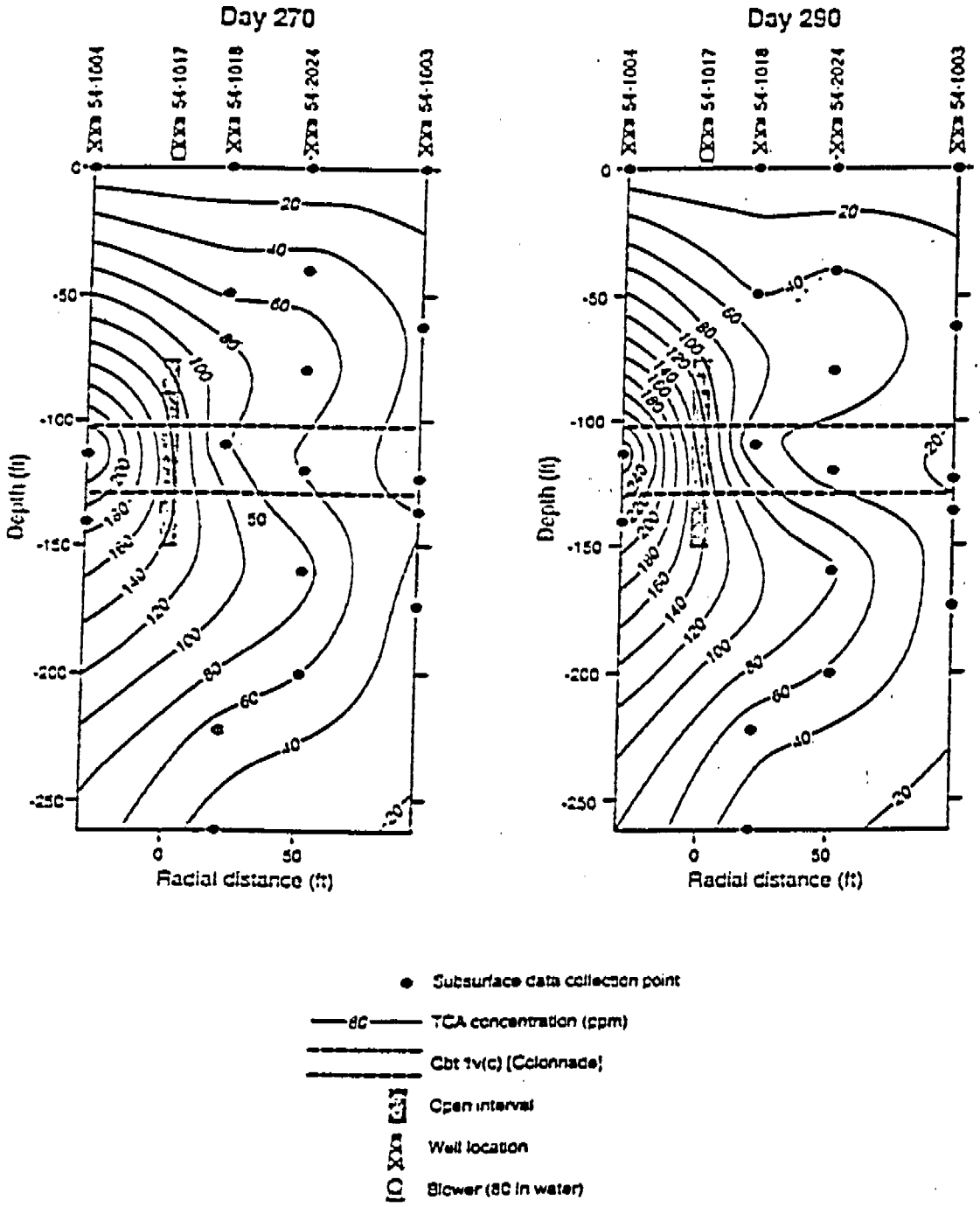

Figure 5-7. TCA concentration contours on Julian day 270 and 290.

6.0 CONCLUSIONS AND RECOMMENDATIONS

Based on the data obtained from the PVET, and the interpretations derived therefrom, the following conclusions are presented:

- the active extraction was successful in pulling VOCs toward the extraction well through the host units and subunits of the Bandelier Tuff;
- based on induced subsurface vacuum pressure at steady state, the radius of influence of the PVET was approximately 140 ft;
- air velocities of the plume within the colonnade averaged around 0.5 m/day;
- downgradient from and within the radius of influence of the extraction well, the active extraction caused a reduction in TCA concentrations;
- upgradient from and within the radius of influence of the extraction well, the active extraction caused an increase in TCA concentrations;
- the PVET effect on TCA concentrations and negative pressure propagation were different in various subunits of the Bandelier Tuff;
- the greatest change in TCA concentrations, and air flow caused by the PVET, occurred in subunit 1v(c) (colonnade) of the Tshirege Member of the Bandelier Tuff;
- subunit 1v(c) demonstrates geohydrologic characteristics which are conducive to enhanced air flow, including, induration supporting fractures, fine grain size enhancing porosity, and overall higher permeability to air flow than the units above and below it.

7.0 REFERENCES

LANL (Los Alamos National Laboratory), May 1992, "RFI Work Plan for OU 1148" LANL Report No. LA-UR-92-855 (LANL 1992)

Pilot Vapor Extraction Test Study Plan (PESP) for the Organic Vapor Plume at MDA L, Appendix A of the "RFI Work Plan for Operable Unit 1148" (LANL, 1992, 0788)

Active Pilot Vapor Extraction Test Final Report , ERM Program Management Co., September 1997 (ERM 1997)

Passive Air Flow Tests at Wells 54-1001 and 54-1017, September 1997, SEA-SF-TR-97-172 (SEA -172, 1997)

Thermocouple Psychrometer Stability Test at Los Alamos TA-54, Borehole 54-1018. September 1997, SEA-SF-TP-96-130, (SEA-130, 1997)

Monitoring of Pore Gas Pressures and Chemical Constituents at Wells 54-1015 and 54-1016 During 1995 and 1996. September 1997, SEA-SF-TP-97-170 (SEA-170, 1997)

Brief Tests of Passively Vented Boreholes at TA-54, MDA H, MDA J, and at TA-50, MDA C During 1995 and 1996. September 1997, SEA-SF-TP-97-171 (SEA-171, 1997)

Evaluation of the Tracter Gas Injection/Monitoring System Used with the Tonto Air rotary Drill Rig in TA-54, Los Alamos National Laboratory, Septembr 1997, SEA-SF-TP-(Draft) (SEA-Draft, 1997)

Data Report: Open Borehole Anemometry and In-Situ Gas Permeability Measurements in Boreholes 54-1001 Through 54-1006, Los Alamos Technical Area 54, December 1994, SEA-SF-TR-94-020 (SEA-020, 1994)

Joss, C.J. and A.L. Baehr, AIR3D: An Adaptation of the Groundwater Flow Code MODFLOW to Simulate Airflow in the Unsaturated Zone, U.S. Geologic Survey Open File Report, April 1994, Publication No. 4594 (Joss, et al. 1994)

Data Report for Permeability Measurements in Boreholes 54-1017 and 54-1018, Los Alamos National Laboratory TA-54, Area G , September 1997,SEA-SF-TR-97-175 (SEA-175).

Johnson, P.C., Ettinger, R.A., Some Considerations for the Design of In-Situ Vapor Extraction Systems: Radius of Influence -vs- Zone of remediation,

8.0 CONTRIBUTORS

The following people contributed significant portions of the text of this report, provided technical direction, or participated in the review and preparation of this report:

Veraun Chipman, SEA
Sandra Dalvit-Dunn, SEA
William Lowry, SEA
Jon Marin, ERM
Neva Mason, SEA
Donald Neeper, ERM/SEA
James Santo, ERM
John Smith, ERM
Charles Wilson, ERM

The preparers acknowledge the contribution of the following people in the conceptual development, planning and conduct of the work reported herein:

Robert Gilkeson, LANL
Steve Limback, LANL
Vince Trujillo, LANL
Keith Woloshun, LANL

APPENDIX A

RFI WORK PLAN
OPERABLE UNIT 1148

APPENDIX A

PILOT EXTRACTION STUDY PLAN
FOR THE ORGANIC VAPOR PLUME AT MDA L

Table of Contents

1.0 INTRODUCTION A-1
1.1 Background A-2
1.2 Environmental Setting A-2

2.0 CURRENT UNDERSTANDING OF THE ORGANIC VAPOR PLUME A-7
2.1 Analysis of Gas Samples A-7
2.2 Analysis of Core Samples A-26

3.0 CORRECTIVE ACTION SELECTION CRITERIA A-26
3.1 Space Restrictions A-26
3.2 Physical Setting A-30
3.3 Contaminant Characteristics A-30
3.4 Summary of Corrective Action Selection Criteria A-31

4.0 PILOT EXTRACTION STUDY A-31
4.1 Pilot Extraction Study Design A-31
4.2 Additional Data Gathering A-33
4.2.1 New Boreholes and Sampling A-33
4.2.2 Subsurface Air Flow Studies A-38
4.3 Preliminary Design Criteria A-39
4.3.1 Extraction Wells A-39
4.3.2 Piping A-39
4.3.3 Emissions Control System A-39
4.4 Pilot Tests to Evaluate Active Extraction A-40
4.4.1 Pilot Tests in the Perimeter Area A-40
4.4.2 Pilot Tests in the Source Area A-41

5.0 INSTALLATION OF THE ACTIVE EXTRACTION SYSTEM A-41

6.0 SCHEDULE A-42

REFERENCES A-43

ATTACHMENT 1: Schedule of Core Samples From Angle Boreholes A-44

ATTACHMENT 2: Schedule of Core Samples From Deep Vertical Boreholes A-51

APPENDIX A

PILOT EXTRACTION STUDY PLAN FOR THE ORGANIC VAPOR PLUME AT MDA L

1.0 INTRODUCTION

This Appendix to the RFI Work Plan of Operable Unit 1148 presents the pilot extraction study plan (PESP) to remediate the organic vapor plume emanating from inactive subsurface disposal units at material disposal area (MDA) L (SWMU 54-006).

The purpose of the pilot study is to investigate:

a) retraction of the horizontal boundary of the plume to the vicinity of the security fence at MDA L;
b) retraction of the bottom of the plume to the depth of the basalt layer (if indeed the plume has spread to lower depths); and
c) a means for preventing any future regrowth of the plume away from the subsurface sources.

This plan describes data that are required concerning:

a) natural mechanisms responsible for the generation of the plume, in order to evaluate the engineered application of natural mechanisms to prevent future regrowth of the plume;
b) characteristics of the plume that are necessary to design the corrective action; and
c) characteristics of the subsurface geology that are necessary to design the corrective action.

The field investigations for this study are integrated with field investigations for the RFI to the extent practicable. For example, drill holes will gather data for this study and the RFI. The same drill holes will be used as vapor extraction wells, vapor monitor wells, or air injection wells during pilot extraction of the plume. Some of the drill holes might be used in the future as part of an engineered system that uses passive mechanisms to prevent future regrowth of the plume after it has been retracted by forced venting.

This plan identifies data and outlines pilot tests that are required for design of a full scale vapor extraction system. If the investigations and tests are successful, a full scale vapor extraction system will be designed and implemented. (If the investigations and tests are not successful, a new revised plan will be submitted to EPA.) The objective of this system will be to retract the vapor plume to the vicinity of the disposal shafts that are the evident source of the plume. Even if the extraction process removed all available volatile materials from the disposal shafts, a buried container might in principal rupture at some time in the future, thereby becoming a new source of volatile contaminants. Therefore, after extraction, subsequent regrowth of the plume from any present or future sources in the shafts will be prevented by installation of physical barriers or by continued venting of the region near the

disposal shafts. Data obtained during the investigations described in this plan may enable design of a passive venting system for long-term control of the source region. A plan for the long-term control, with supporting data, will be submitted to EPA before the control is installed.

1.1. Background

MDA L is a 2.58 acre site within TA-54 that was historically used as a disposal site for hazardous chemicals. Land disposal occurred from the late 1950's to 1985. The MDA is currently used for RCRA-permitted chemical waste storage and treatment, and for mixed waste storage under interim status authority. The location of the MDA is shown in Figure A-1. Historical records indicate that solvents were disposed in one pit (Pit A), and 34 disposal shafts. Three impoundments were also used for waste disposal at the MDA. However, there is no information that solvents were disposed in the impoundments. The location of inactive, subsurface disposal units within MDA L are shown in Figure A-2.

Pit A measures 200 ft long, 12 ft wide, and 12 ft deep. Disposal shafts at MDA L range from 3 ft to 8 ft in diameter and 60 ft to 65 ft in depth. The 28 disposal shafts in the eastern part of the MDA (shafts 1-28) were active from February, 1973 to December, 1985. The six disposal shafts in the western part of the MDA (shafts 29-34) were active from December, 1983 to April, 1985. (See Table 5.3-2 in the work plan for dates of use and capacity of the individual disposal units.) Additional information on the history of waste disposal at MDA L is presented in Sec 5.3.1 of the work plan.

1.2 Environmental Setting

The general environmental setting at TA-54 including MDA L is presented in Chapter 3 of the work plan. Specific attributes of the environmental setting that are important to the migration of the OVP are discussed here. MDA L is located on flat land on top of a narrow finger mesa (Mesita del Buey) at an elevation of approximately 6800 ft. The mesa is approximately 400 ft wide at the MDA and is bounded on the north by Canada del Buey and on the south by Pajarito Canyon. The canyon bottoms are approximately 120 feet below the top of the mesa.

The geologic setting of Mesita del Buey is described in Chapter 3 of the work plan and is briefly reviewed here with regard to the setting at MDA L. A geologic section along the axis of the mesa is shown in Figure A-3. Several layers of tuff, formed by volcanic ash flows, extend from the surface to a depth of 200 or 300 ft. The tuff is underlain by basalts with inter-layered conglomerates. As shown in Figure A-3 the volcanic tuff section varies in thickness because of the irregular surface of the basalt. The tuff and a thick section of the basalt are unsaturated. The top of the main aquifer is estimated to be at a depth of 850 feet below the MDA. Surge beds within Unit 2 of the Tshirege member (see Figure A-3) may provide a preferential pathway for lateral migration of contaminants. Refer to Section 3.5.2.3 off the work plan for more information on the surge beds. There is no information on characteristics of the basaltic rock below the MDA. Vertical joints and fractures are common in the basalt at outcrops in the Rio Grande Valley. There is no information to indicate whether the basalt forms a barrier to vertical migration of volatile contaminants.

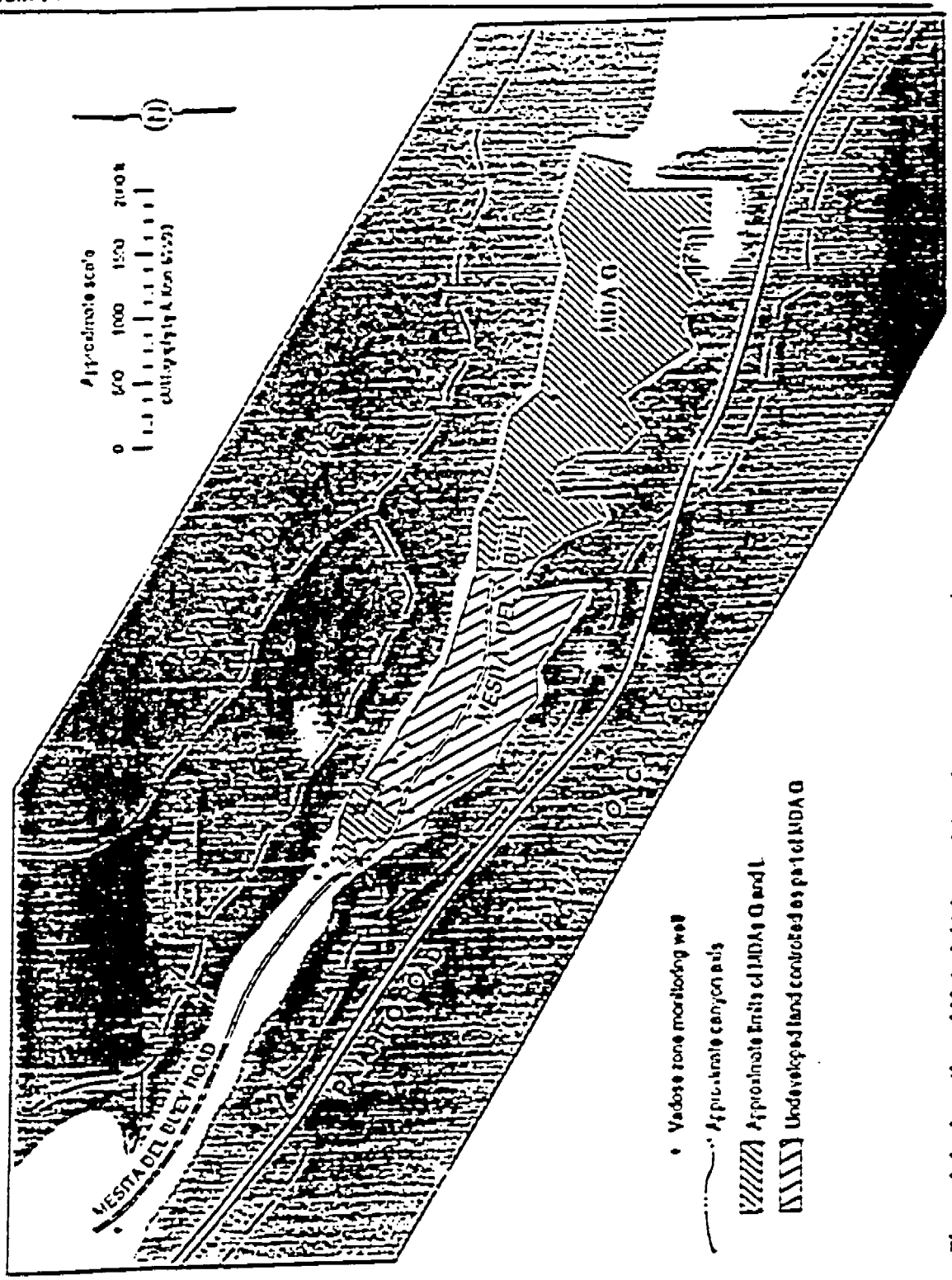

Figure A-1. Location of Material Disposal Areas L, G

Most fractures within the tuff are nearly vertical, generally exhibit spacing intervals between 3 feet and 6 feet, and are believed to be an important pathway for lateral and vertical migration of vapor phase contaminants. A field study of fractures in the walls of a new disposal pit in MDA G was performed in the past year. The pit is 45 feet deep. One objective of this study was to provide information for the optimal angle and direction of drill holes at MDA L to intercept the most fractures at depths greater than 30 feet below the mesa.

Interception of fractures is expected to improve the performance of vapor extraction wells. Fractures in the pit at depths greater than 30 feet display a dominant east-west direction. The preferential dip direction is to the north. For 120 measurements, the median value of the dip angle is 84 degrees from horizontal. The mean value of the dip angle is 75 degrees from horizontal.

In 1985 and 1986, a variety of tests were conducted to evaluate physical characteristics of the unsaturated volcanic tuff beneath MDA L. The tests included instrumentation of boreholes with thermocouple psychrometers, thermistors, and pressure gages (transducers); air injection and vacuum tests in boreholes using packers to isolate test intervals; and laboratory tests on core samples. Complete test results can be found in the IT Corporation report (1987, 0327) and the Kearl et al Report (Citation of Bendix GJ44 1986,0135). A summary of the test results is presented here:

- Porosity of the volcanic tuff is high with average values near 50%.
- Air permeability varies between 10^{-8} and 10^{-7} cm^2 with the highest values measured in fractured zones. The measurements were from packer tests performed in boreholes with air injection.
- Intrinsic permeability (Klinkenberg tests on core samples) varies between 1.5×10^{-8} and 2.5×10^{-8} cm^2.
- Water potential varies from -1 bar near the surface to as low as -15 bars below 30 foot depth. The measured variation is erratic, possibly a result of stability problems with the psychrometers that were used.
- Water content (gravimetric measurement) is usually in the range of 2%–4% (by volume), except at some fractures, or within the more highly welded portion of Unit 1b, or at some contact surfaces, where the content may reach 10% or 20%.
- Temperature is in the range 9-10°C, and is nearly independent of depth, below 30 ft depth. The data indicates a (peak-to-peak) temperature variation of approximately 2°C at all sensors below 30 feet during the month of data acquisition centered on November 1, 1985. However, one cannot tell if this is a diurnal swing, a monotonic seasonal drift or variation correlated with some other phenomenon.

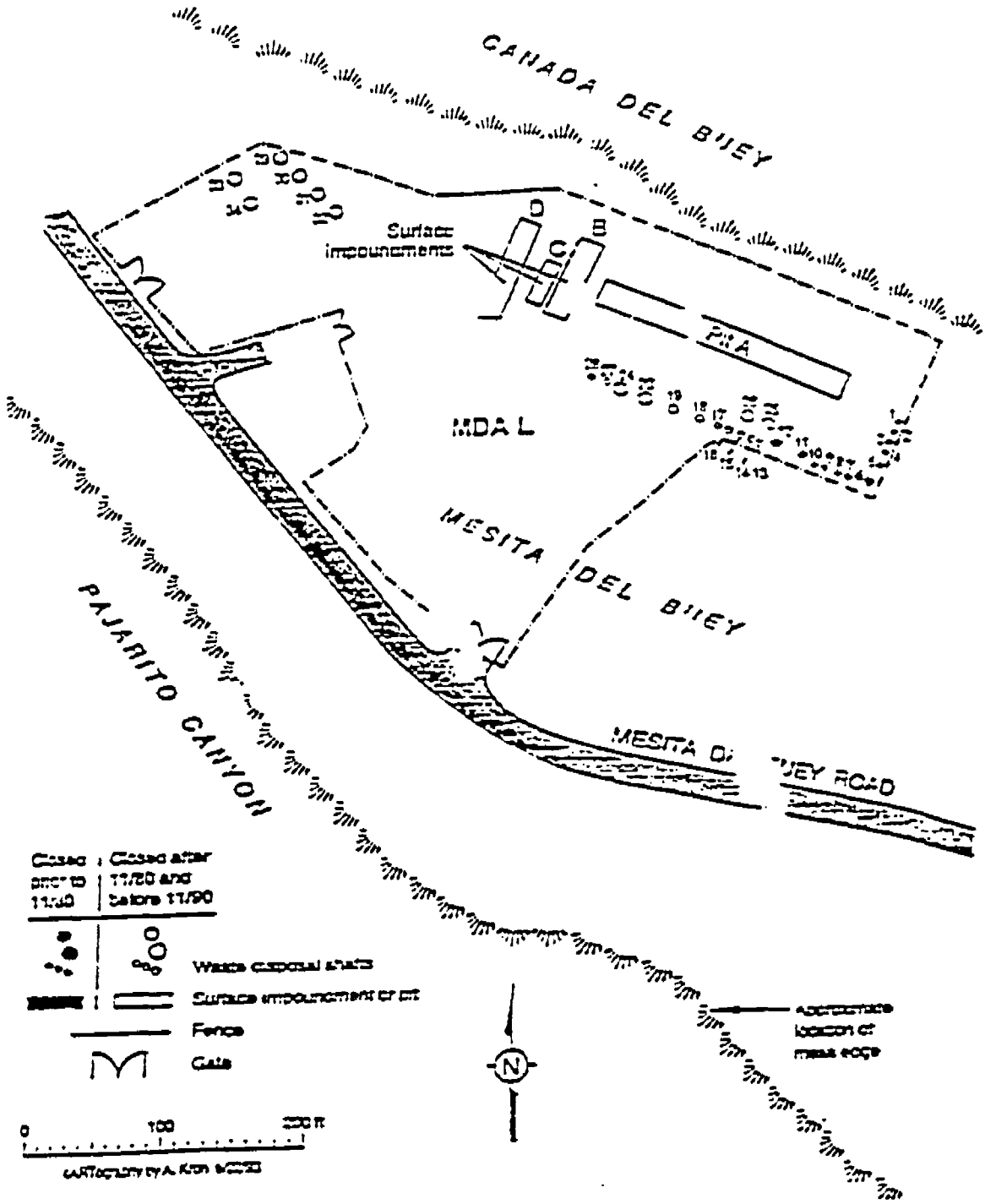

Figure A-2. Location map of inactive pits, shafts, and impoundments (SWMU 54-005) at MDA L

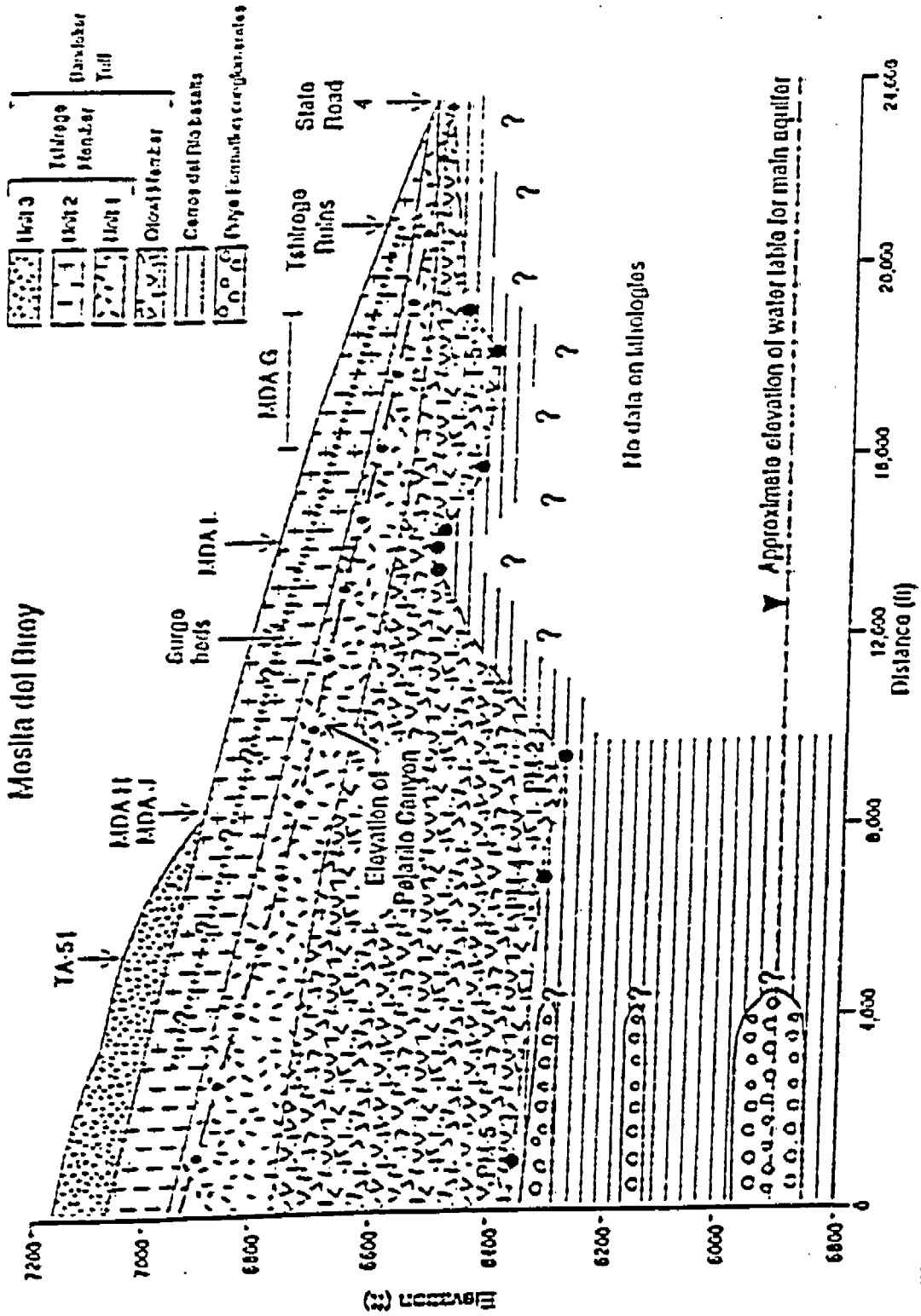

Figure A-3. Profile of Mesita del Buey showing top of mesa, elevation of floor of Pajarito Canyon, and subsurface geologic units and elevation of water table in main aquifer.

- Pressure was measured at the surface and at various depths by transducers. However, review of instrument specifications reveals that the transducers all measured absolute pressure, and were insufficiently sensitive to resolve either typical atmospheric fluctuations or the resulting damped fluctuations at depth.

- Moisture characteristics were measured on core samples over the range of 0 to -15 bars potential. At -15 bars, the volumetric moisture of various samples varied between 0.1% and 10%.

A subsurface plume of vapor is usually considered to spread by diffusion. However, vapor can be dispersed by natural subsurface air flow. Cyclic variations in barometric pressure may cause subsurface air flow in the mesa. The depth in the mesa to which flow is affected by atmospheric pressure change is not known. Rock dilatation due to cyclic gravitational forces may also force air flow in the mesa, probably to great depths. Diurnal and seasonal temperature differences between the rock within the mesa and that of the surrounding atmosphere may affect air flow within the mesa. Wind pressure against the walls of the mesa may also affect air flow within the mesa. Understanding the influence of the natural mechanisms on subsurface air flow is important to evaluating whether an engineered passive system can be used for long term control of the organic vapor plume. Measurements will be made in monitor wells and at land surface to evaluate these mechanisms.

2.0 CURRENT UNDERSTANDING OF THE ORGANIC VAPOR PLUME

2.1 Analysis of Gas Samples

The vapor plume is monitored by a network of 19 multiport monitor wells that are located within and surrounding MDA L. The monitor well locations are shown on Figure A-4. The date of well installation, the construction design, and the depth intervals for sampling ports in each monitor well are listed in Table A-1. Gas samples are collected quarterly. Analytical data are available from June 1988 to the present. Gas samples are analyzed for the compounds listed in Table A-2. The field procedure for collecting gas samples is to first extract a calculated volume of pore gas at each port to purge gas present within the well tubing. Next, 1.2 liters of air was drawn through a cartridge that contained a charcoal sorbent. In the laboratory, carbon disulfide is used to extract VOCs from the cartridge. Analysis is performed with a gas chromatograph/mass spectrometer (GC/MS). The analytical results are reported as micrograms of contaminant per 1.2 L of air. In order to convert this value to ppmv, the temperature and pressure of the extracted air must be known. These data are not available. Therefore, the analytical results are reported in this pilot extraction study plan as $\mu gm/1.2L$, which is approximately equal to parts per million (mass). An improved sampling and analytical procedure is being developed.

The principal vapor phase contaminants listed in descending order of concentration are 1,1,1-trichloroethane (TCA), trichloroethene (TCE), carbon tetrachloride, chloroform, tetrachloroethene (PCE), toluene, and benzene. Other contaminants that have been detected at much lower concentrations include chlorobenzene, xylenes, and 1,2,4-trimethylbenzene.

TCA is the contaminant with the highest concentration and greatest lateral and vertical extent in the plume. The measured concentrations of TCA are almost an order of magnitude greater than values measured for TCE, the contaminant of second highest concentration.

Figures A-5 and A-6 present TCA vapor concentrations measured in samples from ports in monitor wells No. 12 and No. 14 from 1988 to 1992. Well No. 12 is located in the western cluster of disposal shafts and well No. 14 is colocated with disposal shafts in the eastern part of the MDA (see Figure A-4 for monitor well locations). The figures show that TCA concentrations have greatly declined over time. This decline is also observed in the TCA data from monitor well Nos. 15 and 16. Figures A-7, A-8 and A-9 present TCA vapor concentrations measured in samples from ports in monitor well Nos. 1, 2, and 25. Well No.1 is located immediately west of MDA L, well No. 2 is located immediately south of the eastern disposal shafts, and well No. 25 is located 116 feet east of the MDA. The data are erratic. However, the following general trends are evident. Contaminants are now present in all monitor ports. The highest TCA concentrations in well No. 1 were measured in March 1992 and have sharply declined for samples collected in June, 1992 and September, 1992. TCA concentrations in well No.2 show a great reduction from 1988 to 1992. The highest TCA concentrations in well No. 25 occurred in 1990 and have declined from 1990 to 1992.

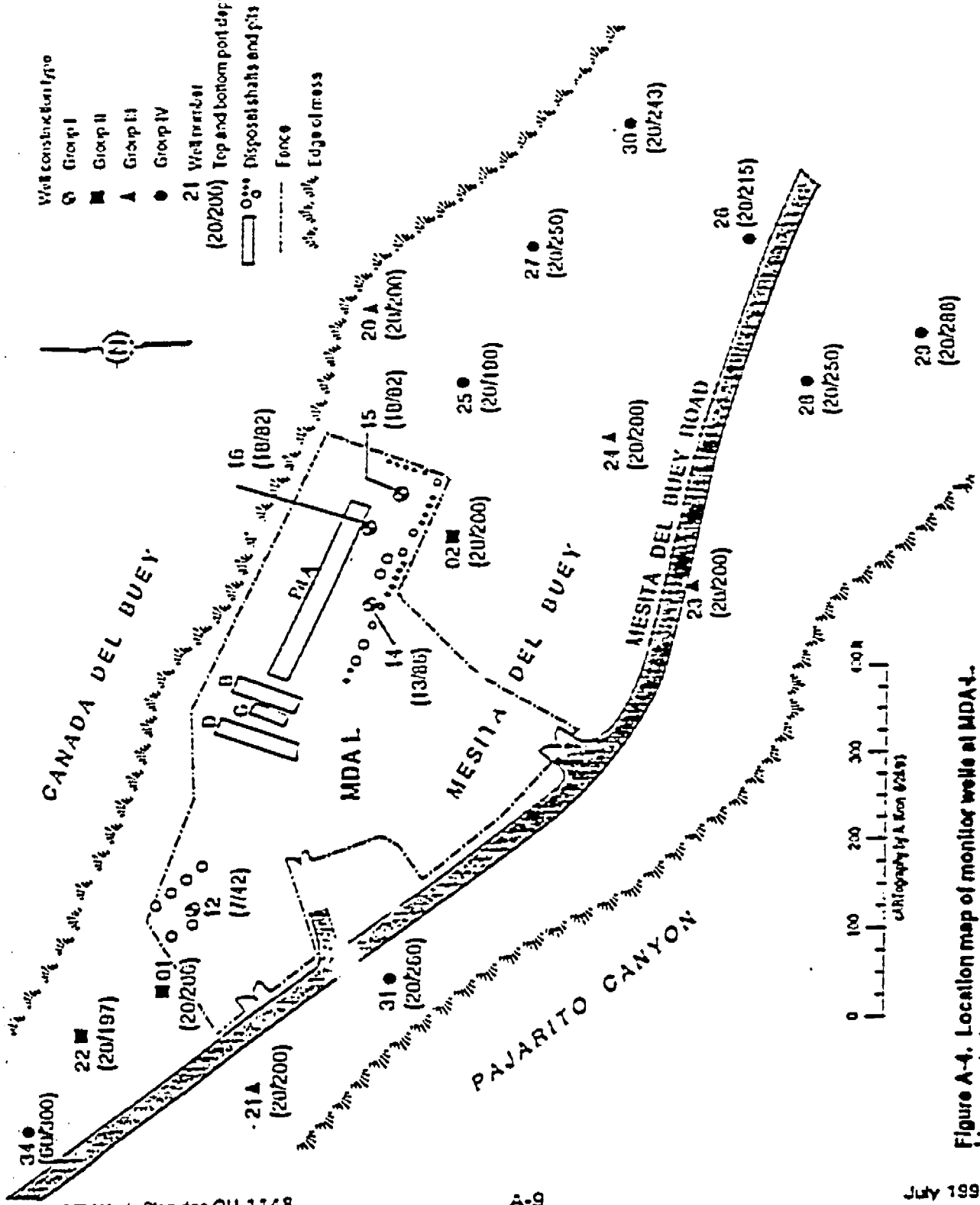

Figure A-4. Location map of monitor wells at MDAL.

TABLE A-1

INSTALLATION INFORMATION ON MONITOR WELLS AT MDA L

WELL[a] NUMBER	INSTALLATION DATE	CONSTRUCTION METHOD[b]	SAMPLE PORT DEPTH (FEET FROM SURFACE)
12	Summer 1985	1	7,27,42
14	Summer 1985	1	13,31,46,86
15	Summer 1985	1	18,31,82
16	Summer 1985	1	7,18,31,82,102
01	Summer 1986	2	20,40,60,80,100,130,140,160,180,200
02	Summer 1986	2	20,40,60,80,100,120,140,160,180,200
20	Summer 1986	3	20,40,60,80,100,130,140,160,180,200
21	Summer 1986	3	20,40,60,80,100,120,140,160,180,200
22	Summer 1986	2	20,40,60,80,100,120,140,160,180,197
23	Summer 1986	3	20,40,60,80,100,120,140,160,180,200
24	Summer 1986	3	20,40,60,80,100,120,140,160,180,200
25	Summer 1988	4	20,60,100,160,190
26	Summer 1988	4	20,60,100,160,200,215
27	Summer 1988	4	20,60,100,160,200,220,250
28	Summer 1988	4	20,60,100,160,200,220,250
29	Summer 1988	4	20,60,100,160,200,220,260,288
30	Summer 1988	4	20,60,100,160,200,220,243
31	Summer 1988	4	20,60,100,160,200,220,260
34	Summer 1988	4	60,100,160,200,220,260,300

(a) Well locations are shown on Figure A-4

(b) Group 1 wells are constructed with welded sample ports on a continuous galvanized steel pipe. Sample tubes run inside the pipe from each sample port to the surface. The annulus space for each sample interval is filled with a 5 ft thick graded sand pack with bentonite seals above and below the sand pack. The annulus space between sample intervals is filled with a bentonite/gravel mixture. Group 1 wells are the only wells constructed with the continuous pipe in the borehole.

Group 2, 3, and 4 wells have individual sampling tubes running from sample zones to the surface.

- In Group 2 wells individual sample zones consist of 5 ft thick graded sand packs with upper and lower bentonite seals that are 1-3 ft thick. The borehole is filled with crushed tuff between sample intervals.

- In Group 3 wells, individual sample intervals are 20 ft thick and are filled with crushed tuff. Thin (1 ft) bentonite seals separate each interval.

- In Group 4 wells sample ports were separated by a distance of 20 ft and the borehole was back-filled with clean sand. No bentonite layers were used to isolate individual sample zones.

TABLE A-2

ANALYTES FOR QUARTERLY GAS SAMPLES COLLECTED
IN CHA" "OAL CARTRIDGES FROM MONITOR WELLS AT MDA L

ANALYTE	CAS#
Ethylbenzene	100414
Bromobenzene	108861
Toluene	108883
Chlorobenzene	108907
Tetrachloroethene	127184
Mix-xylenes	1330207
Carbon Tetrachloride	56235
Chloroform	67663
Benzene	71432
1,1,1-Trichloroethane	71556
Trichloroethene	79016
o-Xylene	95476
1,2,4-Trimethylben[illegible]ne	95636

Note: Samples are taken by passing a known volu[illegible]e of gas phase sample through a sample cartridge that contains charcoal as a sorbe[illegible]. Sample constituents are extracted from the cartridge with carbon disulfide. Analysis is by GC/MS.

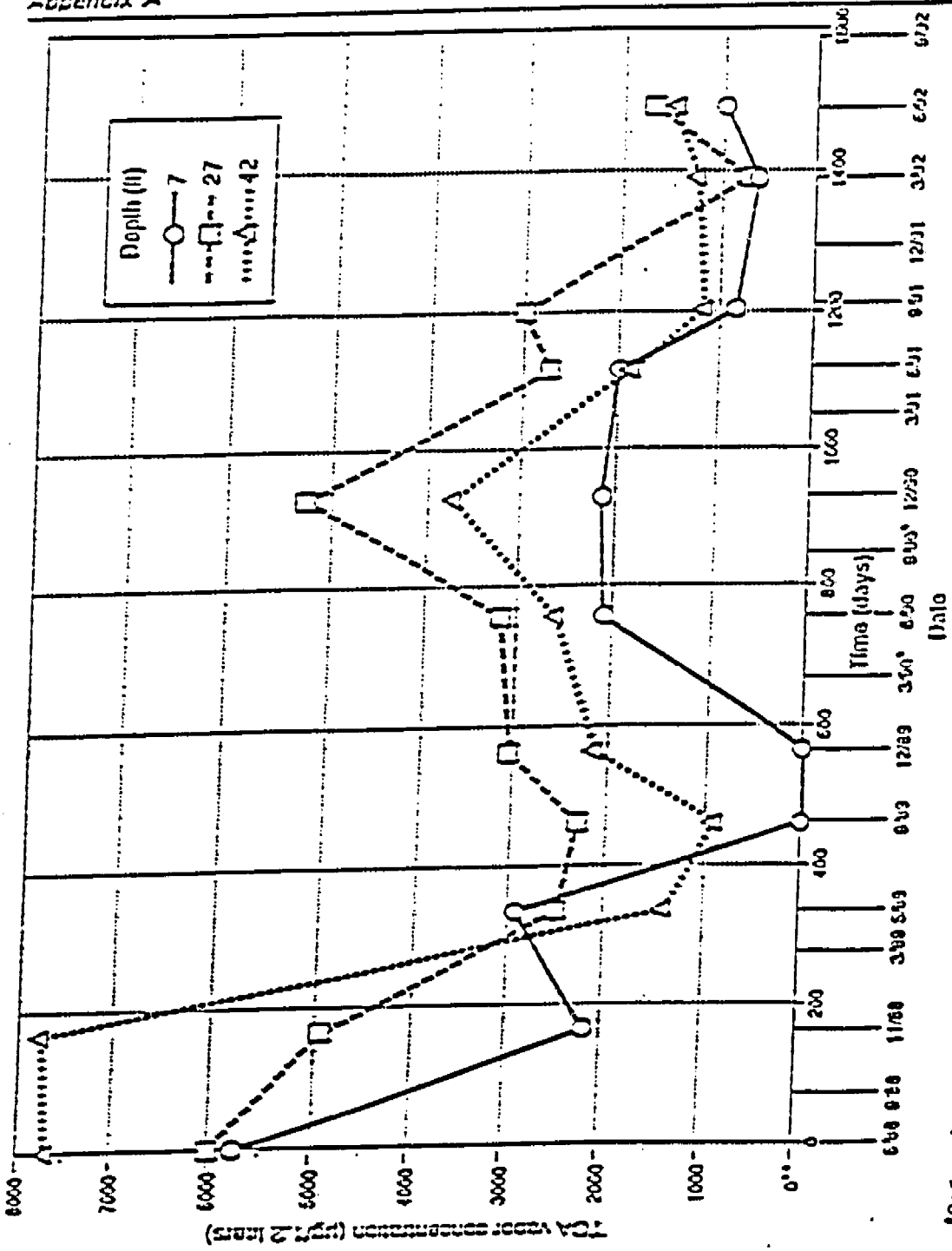

Figure A-5. Time-series TCA vapor concentration in gas samples from ports in Well 812.

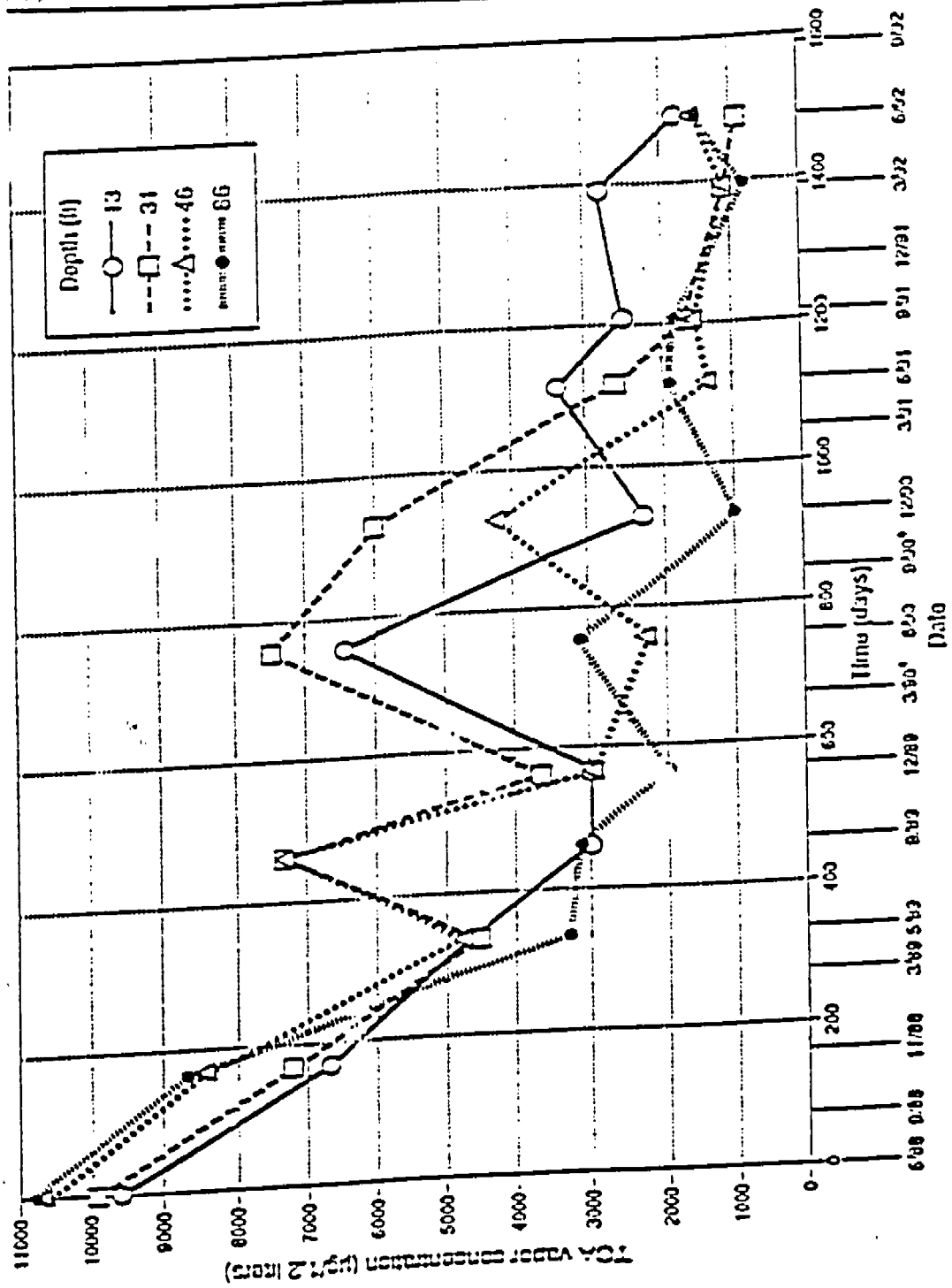

*On these dates measured values in all samples were spurious.

Figure A-8. Time-series TCA vapor concentration in gas samples from ports in Well 614.

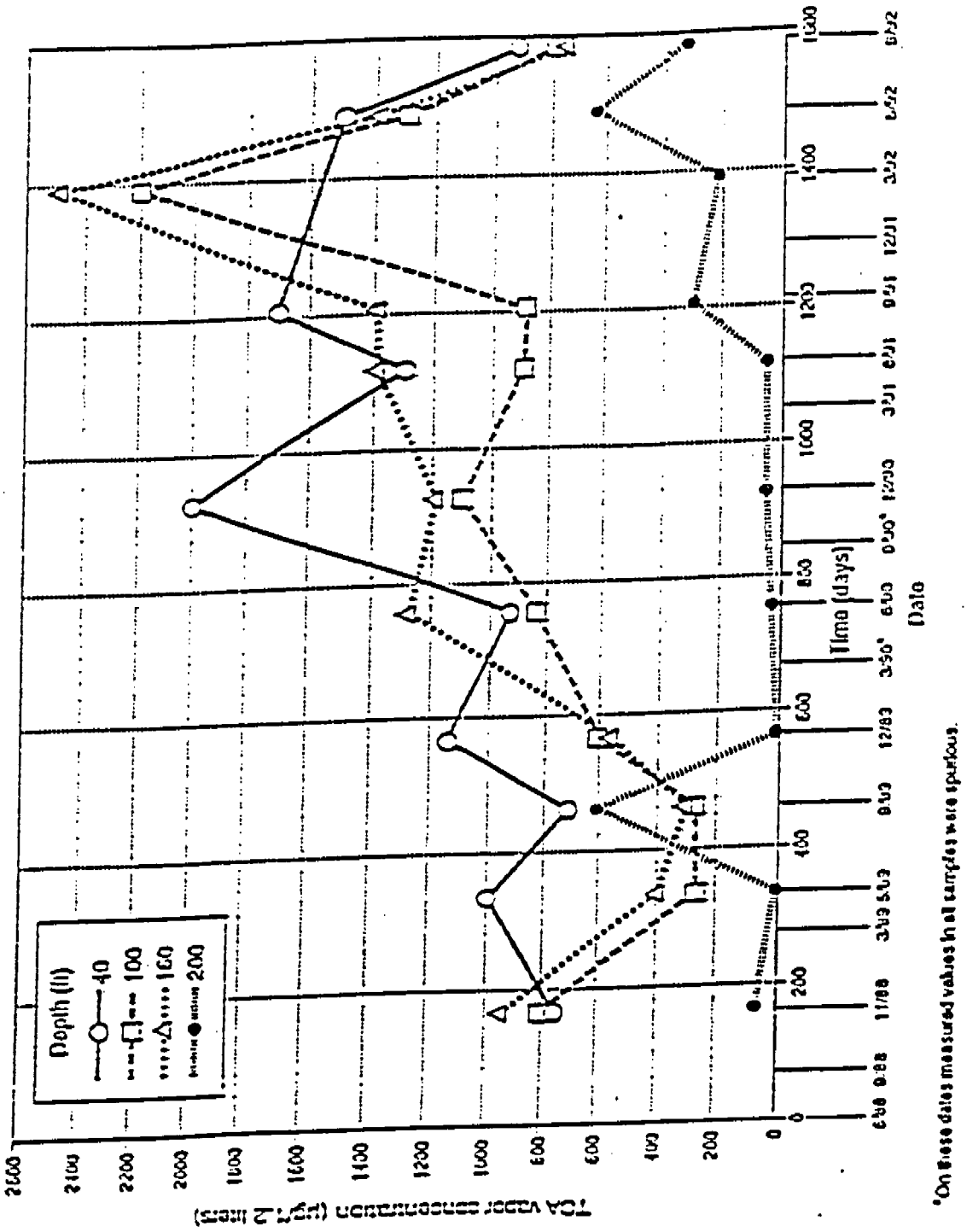

*On these dates measured values in all samples were spurious.

Figure A-7. Time-series TCA vapor concentration in samples from selected ports in Well E1.

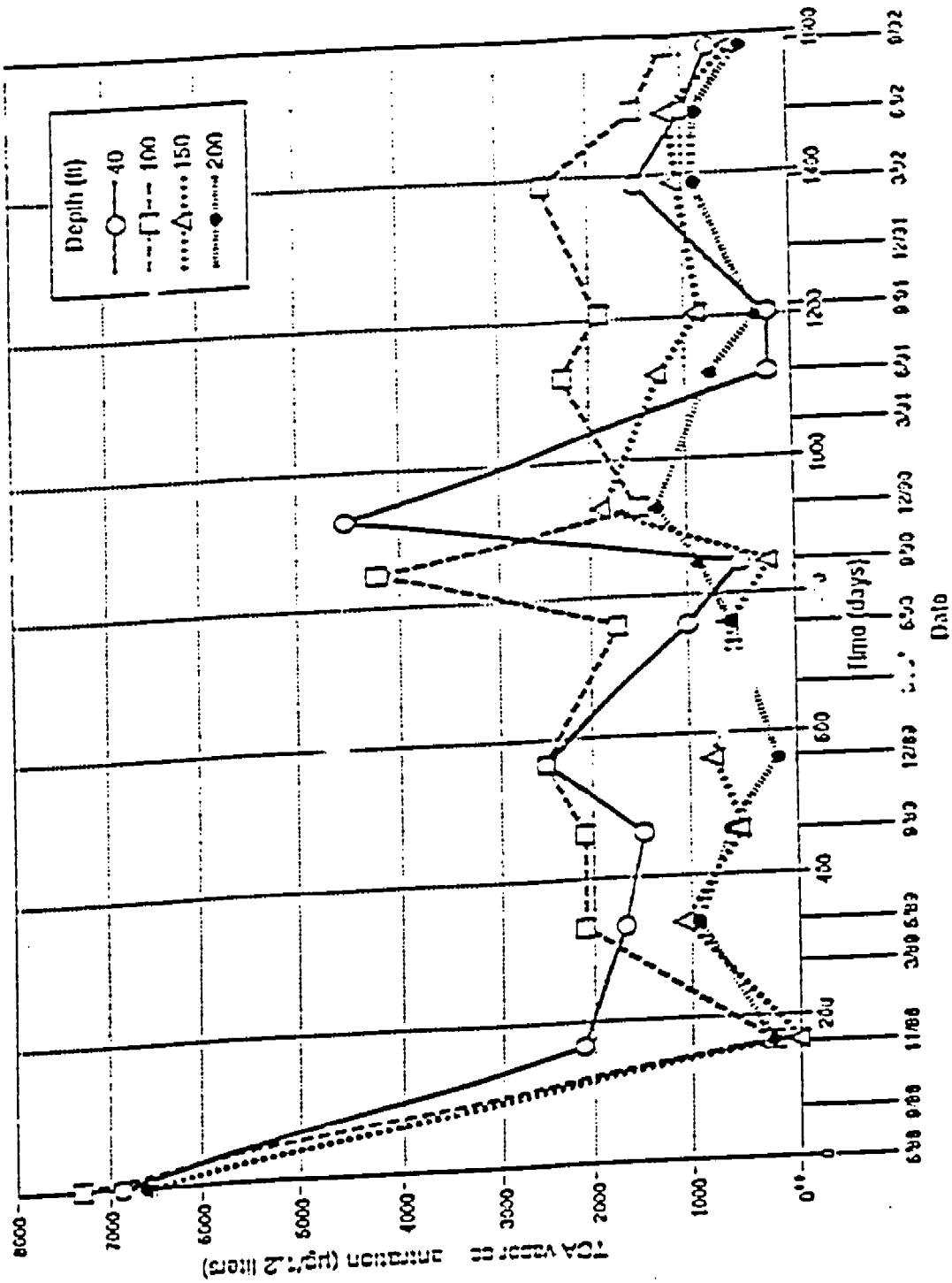

*On this date measured values in all samples were spurious.
**Zero values indicate contaminant was not detected in the sample.

Figure A-8. Time-series TCA vapor concentration in gas samples from selected ports in Well 82.

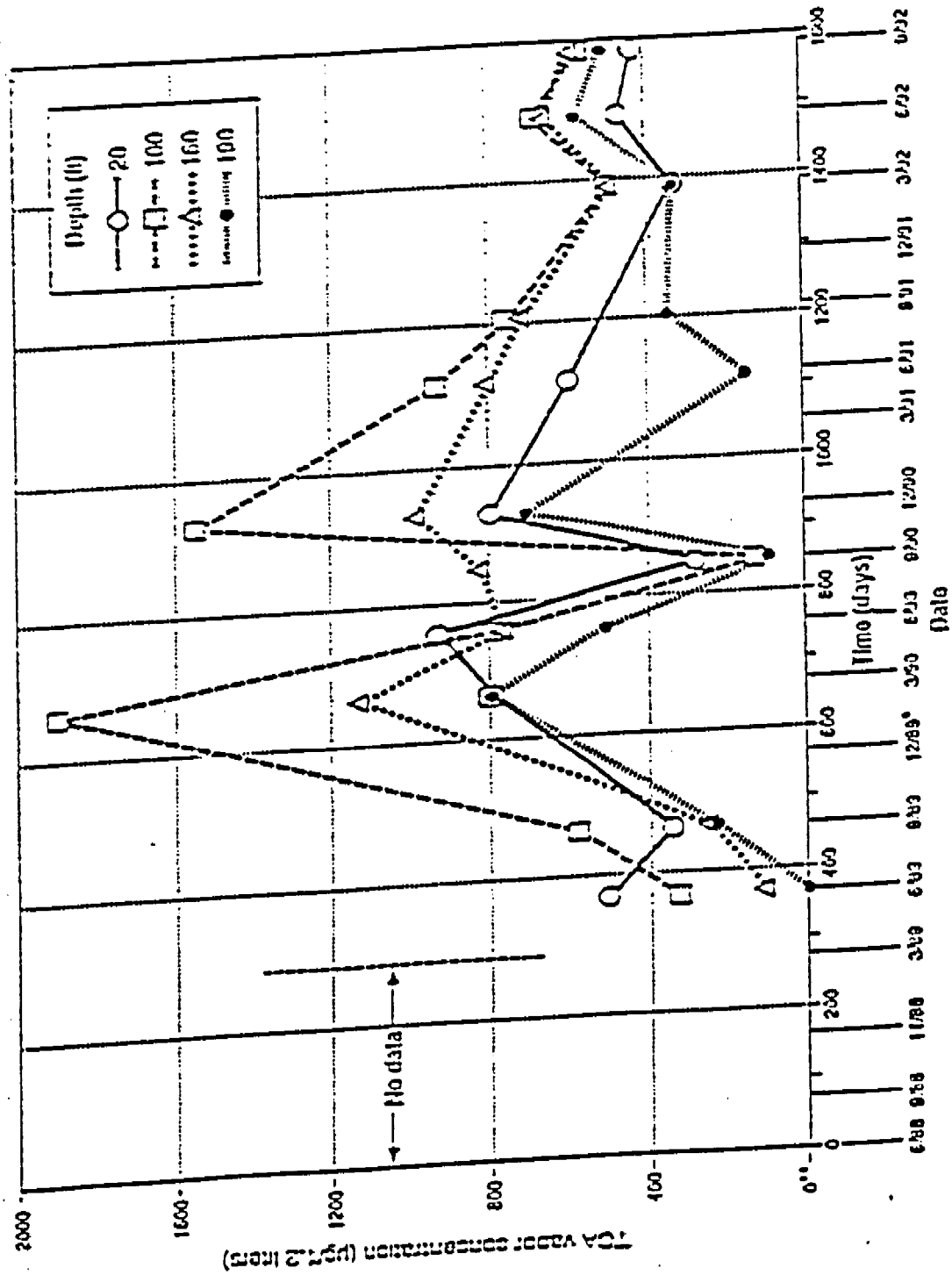

*On this date measured values in all samples were spurious.

**Zero value indicates TCA was not detected in the sample.

Figure A-9. Time-series TCA vapor concentration in gas samples from selected ports in Well 825.

Figures A-10 and A-11 present the maximum TCA and TCE concentrations measured in gas samples collected from the network of monitor wells for the first three quarterly sampling events in 1992. The figures show the maximum measured values at various depths in each monitor well. The highest TCA values (greater than 4,000 ppm (mass)) occur near disposal shafts in the eastern part of MDA L. The maximum value measured near the western cluster of disposal shafts was 3400 ppm (mass) at a depth of 130 ft in well No. 1. TCE values greater than 1000 ppm (mass) were measured in both the western and eastern parts of the MDA. Figures A-12 and A-13 are contour maps of the distribution of TCA and TCE therein based on the data reported in Figures A-10 and A-11. The highest TCA and TCE values occur within MDA L near the disposal shafts and Pit A.

TCA and TCE have never been detected in samples from well No. 34, indicating the plume has migrated northwest of the MDA a distance of less than 225 feet. Monitor well Nos. 29,26, and 30 are distributed across the mesa and bound the extent of the plume southeast of the MDA. Low values of TCA (generally less than 10 ppm (mass) are sporadically detected in samples from these wells, where as TCE has never been detected. TCA has migrated approximately 450 feet southeast of disposal shafts in the eastern part of the MDA.

Figures A-14 and A-15 present vertical profiles for VOCs measured in gas samples from well No. 24 in September, 1991 and September 1992. TCA and TCE were detected at all ports, with the highest concentrations in the depth interval between 60 feet to 160 feet. TCA and TCE concentrations exhibit little change from 1991 to 1992. Chloroform, PCE, and carbon tetrachloride were present at low concentrations in the September 1991 samples but were not detected in the September 1992 samples.

In summary, the data indicate that vapor phase concentrations of TCA have declined markedly over time at monitor wells located within or near MDA L, and that TCA (in vapor phase) is continuing to slowly move outward from the MDA. The vertical extent of the plume is not known. The monitor wells located within the MDA do not have sampling ports at depths greater than 86 feet. Figures A-7, A-8, and A-9 show that TCA has consistently been present at a depth of 200 feet. The TCA plume has migrated a distance of approximately 450 ft east of the MDA. Migration of the plume a similar distance vertically below the MDA is possible. probable?

The plots in Figures A-5 to A-9 show that the concentration of TCA at any particular sampling port varies erratically from one quarter to another, sometimes with variation of 50-100%. The data may represent actual variation of the pore gas concentration, caused by natural ventilation of the mesa. However, the variation might also be an artifact of either the sampling method or the analytical process. Therefore, higher quality data are required to evaluate natural air flow in the subsurface and to evaluate the effectiveness of pilot tests to extract the vapor. To meet this need, a revised system for sampling and analyzing pore gas is being developed. The revised system will provide more accuracy, and will detect the larger list of contaminants presented in Table A-3. In addition, data on the subsurface pressures and flows will be gathered so that pore gas concentrations can be correlated with barometric and tidal effects.

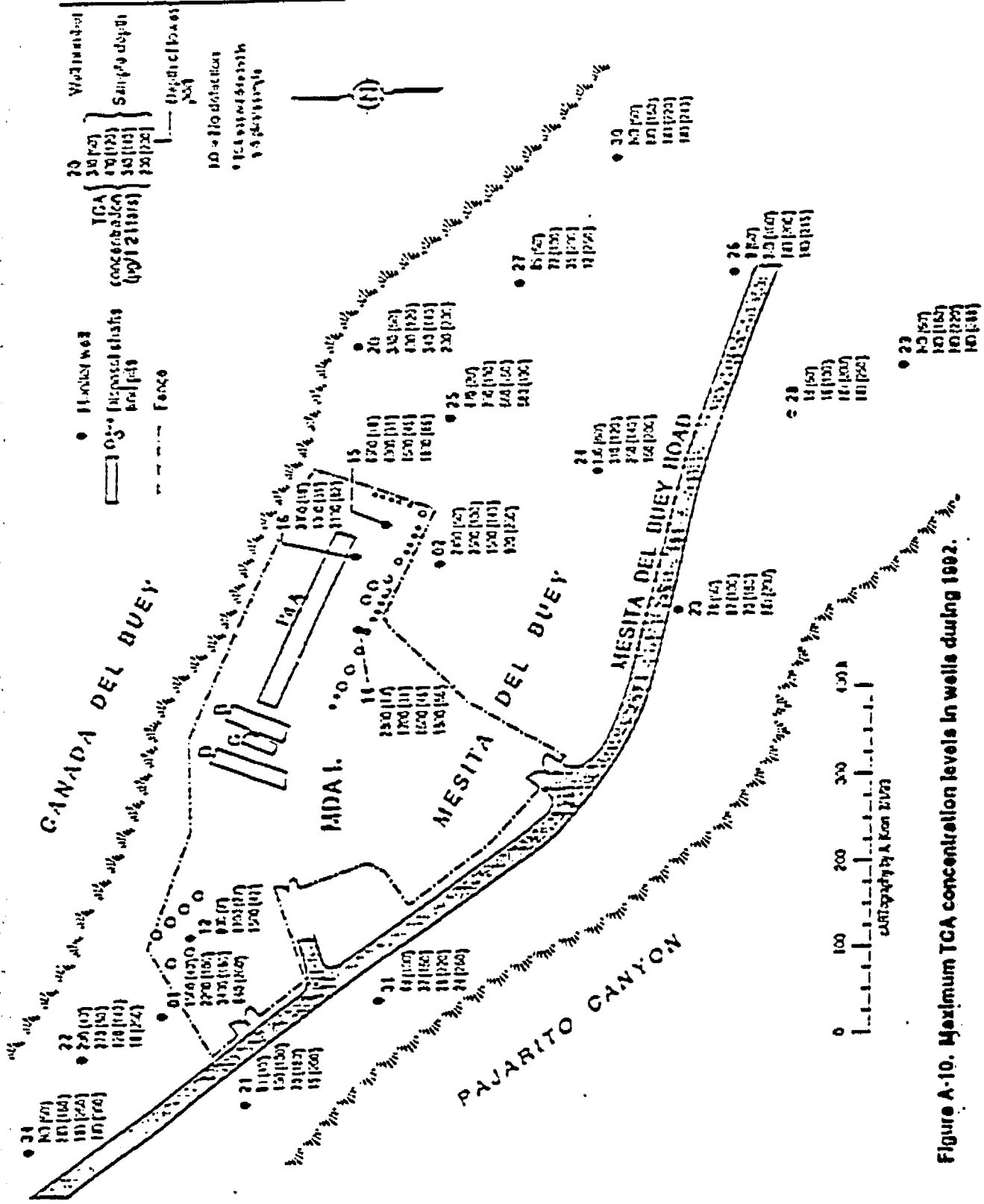

Figure A-10. Maximum TCA concentration levels in wells during 1992.

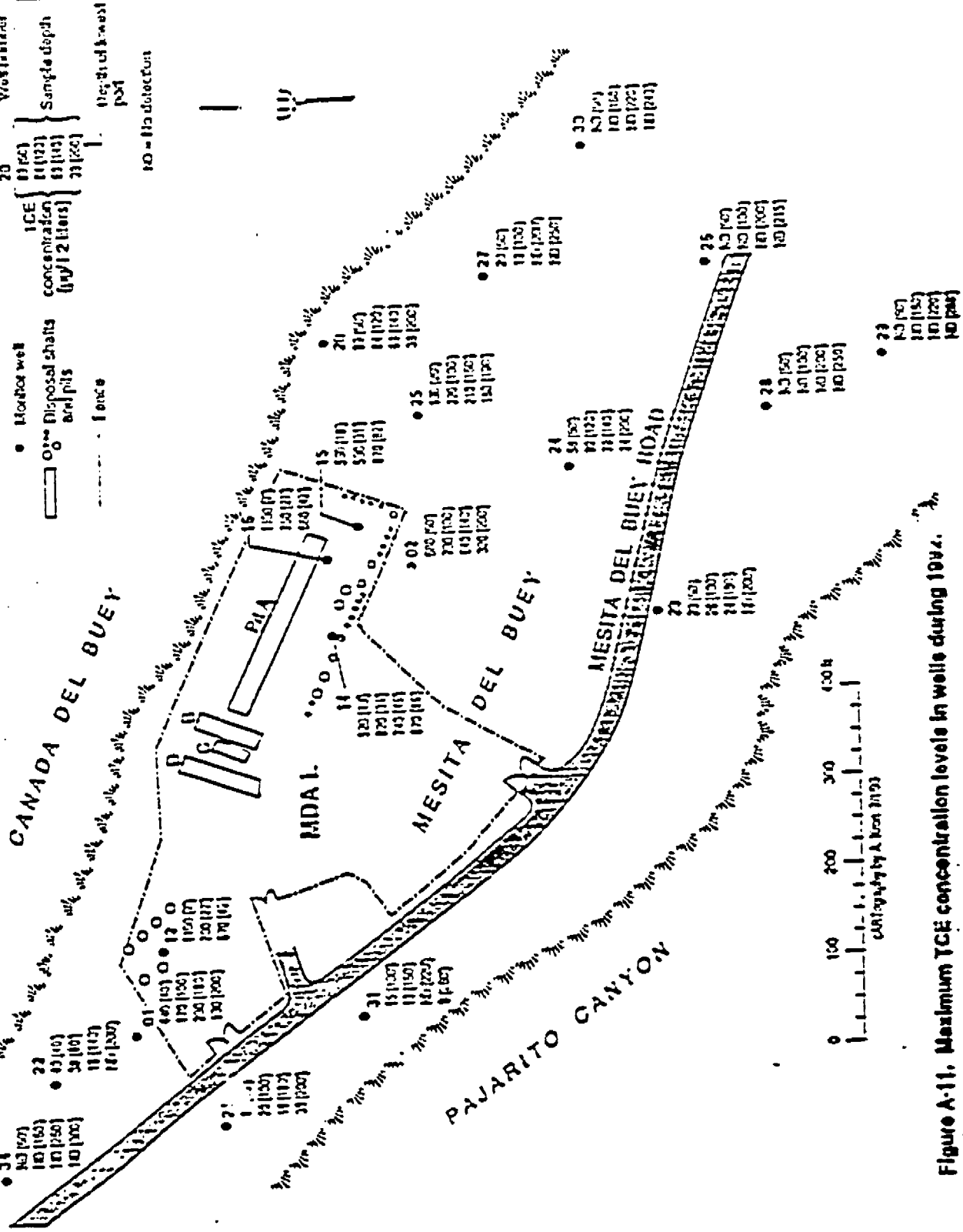

Figure A-11. Maximum TCE concentration levels in wells during 1992.

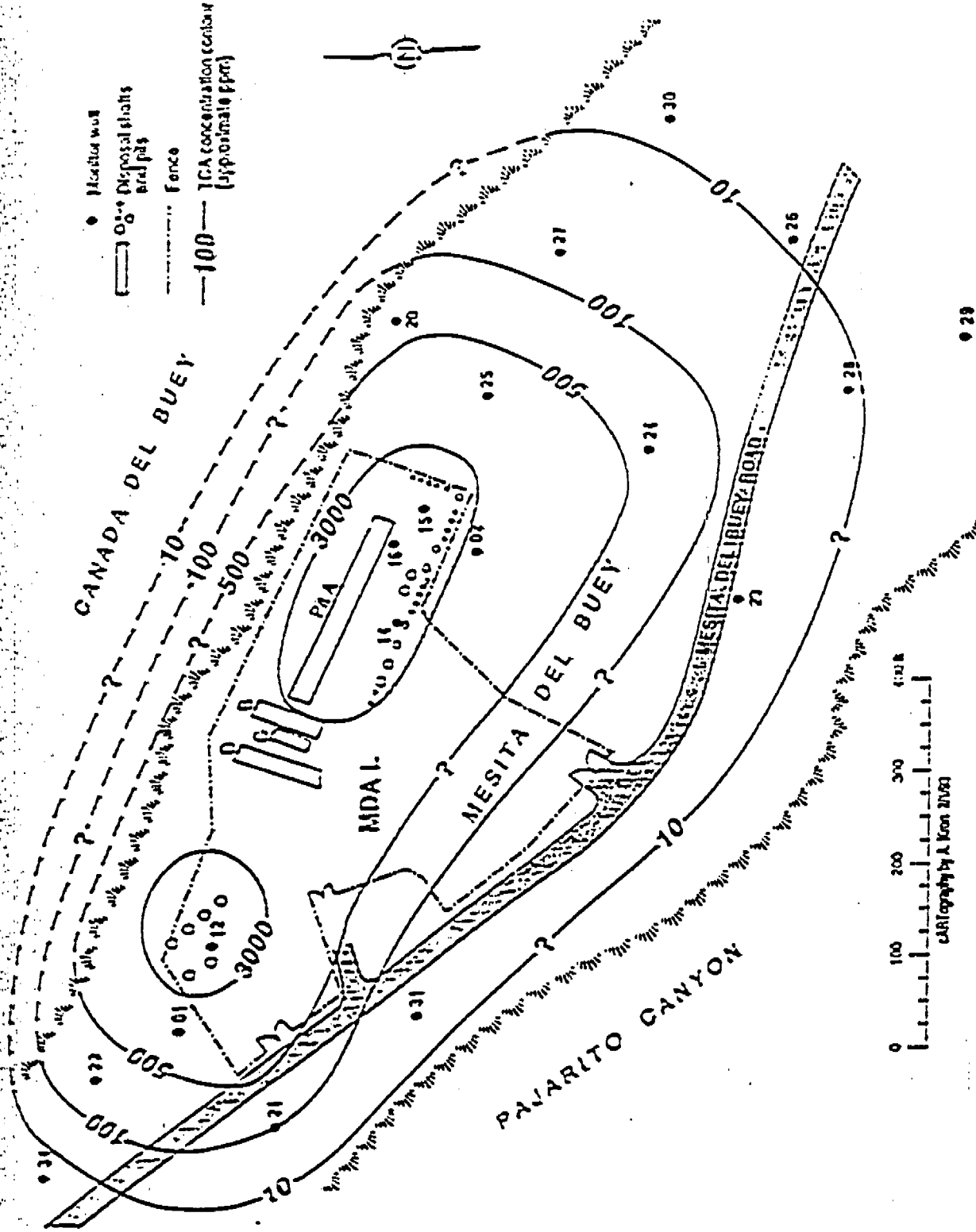

Figure A-12. Distribution of the TCA plume in 1992.

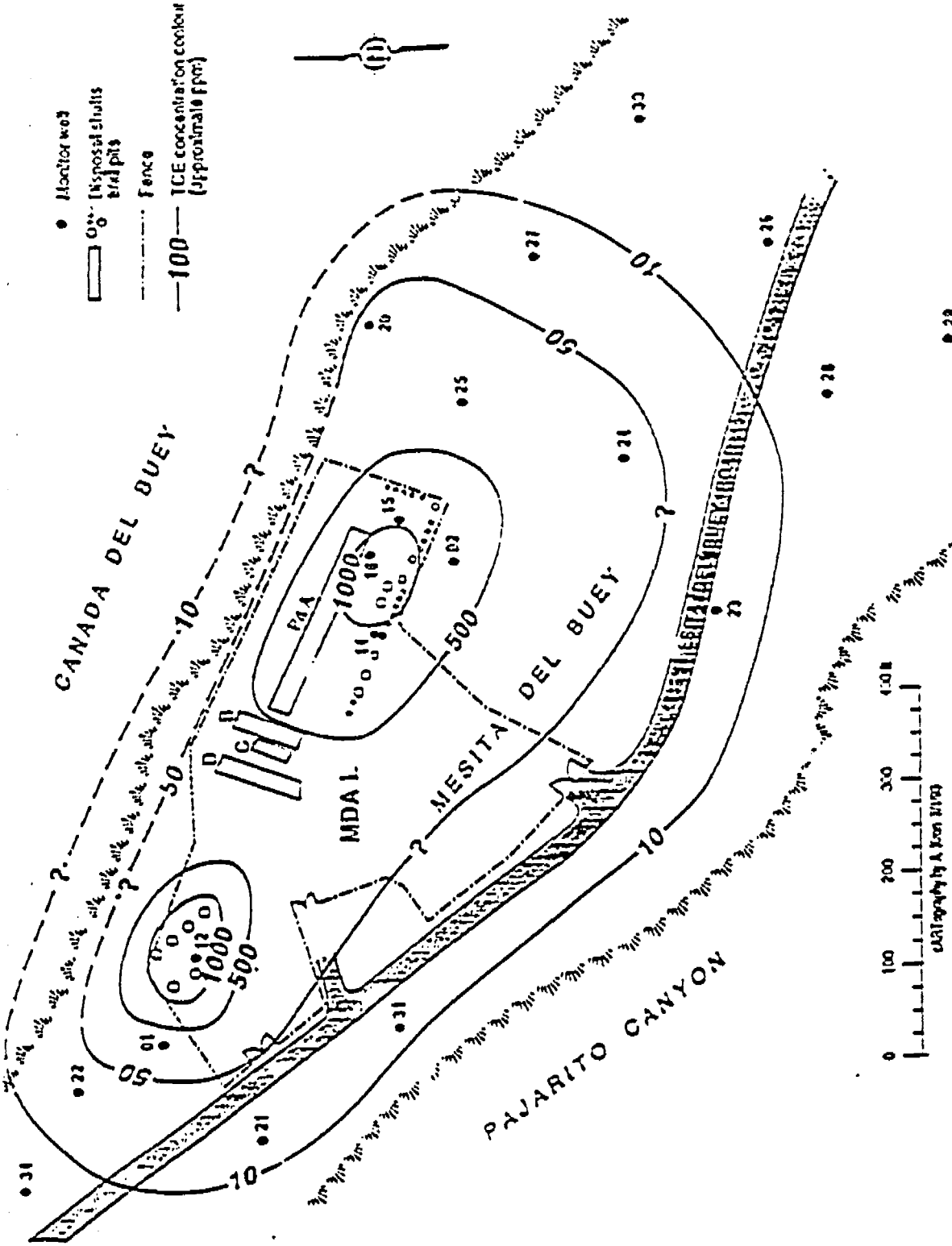

Figure A-13. Distribution of the TCE plume in 1992.

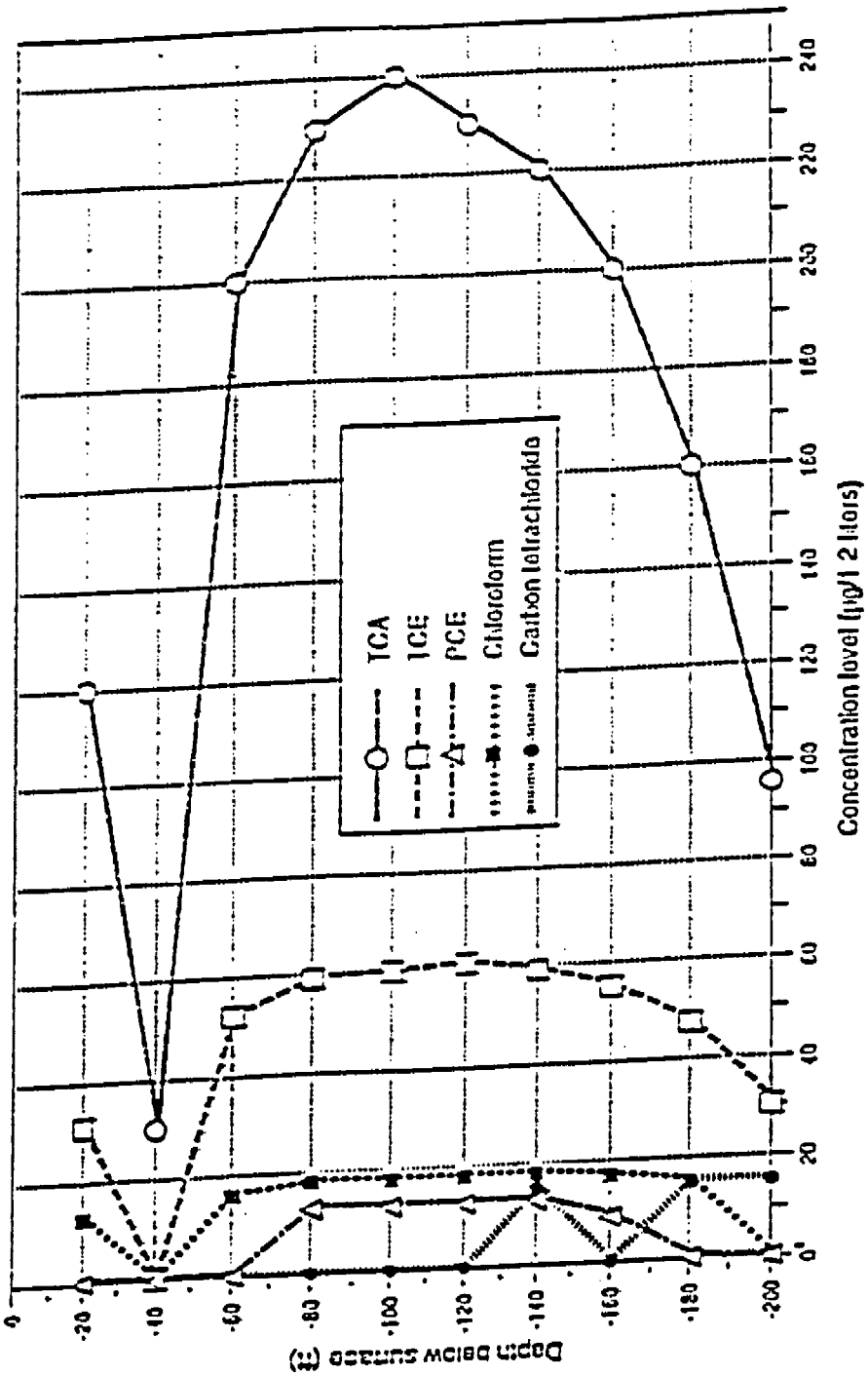

*Zero values indicate the contaminant was not detected in the sample.

Figure A-14. VOC distribution at Well #24 for 9/91 sampling period.

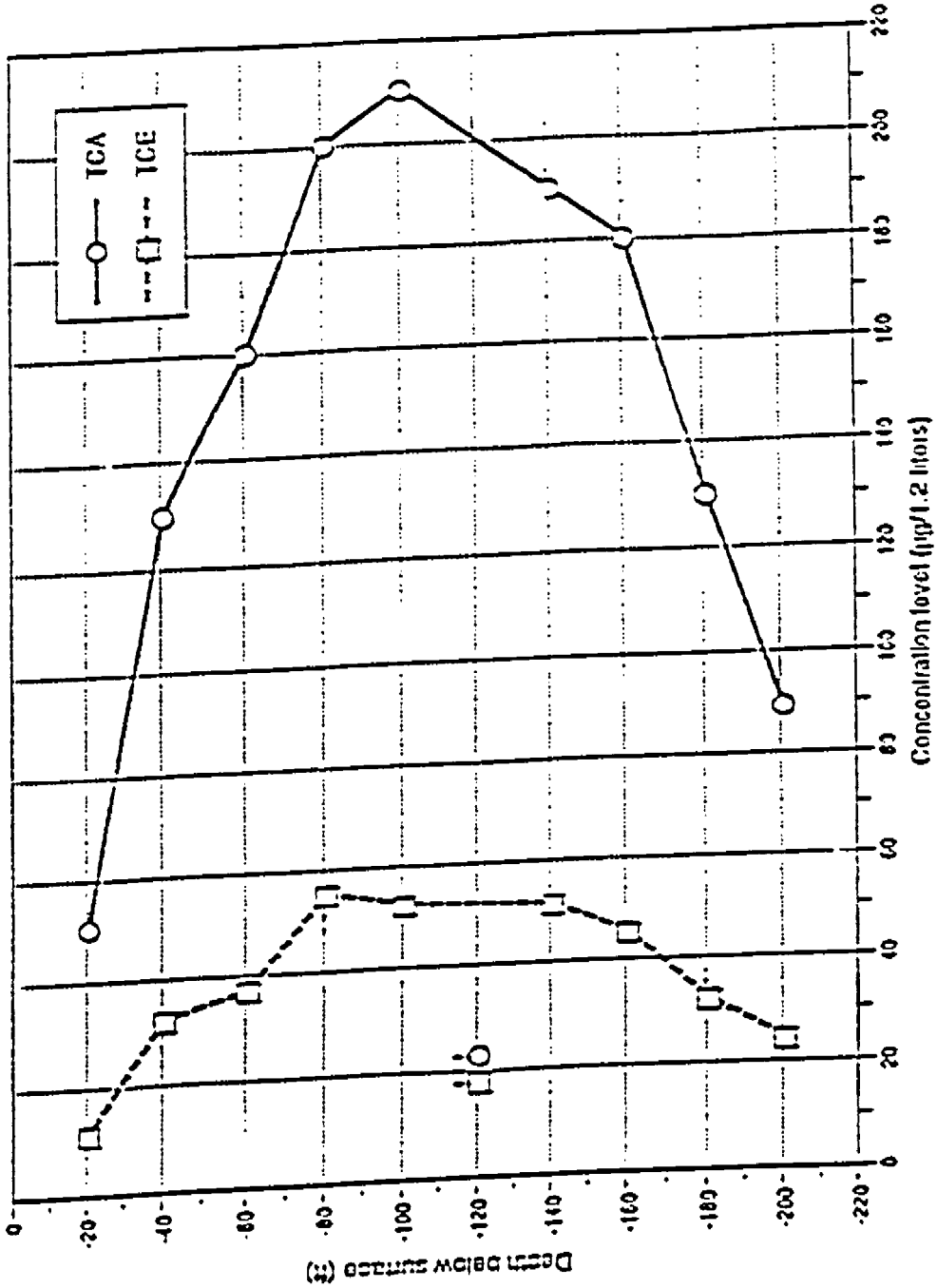

*These values are interpreted as spurious.

Figure A-15. TCA and TCE concentrations at Well 824 for 9/92 sampling period.

TABLE A-3

ANALYTES FOR GAS SAMPLES COLLECTED IN CARTRIDGES CONTAINING CARBON RESIN (revised pore gas monitoring methods)

GROUP[a]	COMPOUND	CAS#
A	Trichlorofluoromethane	75694
A	Chloroethane	75003
A	Chloromethane	74873
A	Dichlorodifluoromethane	75718
A	Vinyl Chloride	75014
A	Bromomethane	74839
B	2,2-Dichloropropane	594207
B	Dibromomethane	74953
B	1,1,1-Trichloroethane	71556
B	1,2-Dichloroethane	107062
B	Chloroform	67663
B	c-1,2-Dichloroethene	156592
B	1,3-Dichloropropene(cis and trans)	10061015
B	1,2-Dichloropropane	78875
B	1,1-Dichloropropene	563586
B	Carbon Disulfide	75150
B	Tetrachloroethene	127184
B	Trichloroethene	79016
B	Trichlorotrifluoroethane	76131
B	1,3-Dichloropropane	142289
B	t-1,2-dichloroethene	156605
B	1,1-Dichloroethene	75343
B	Bromochloromethane	74975
B	1,1-Dichloroethene	75354
B	1,1,2,2-Tetrachloroethane	79345
B	Carbon Tetrachloride	56235
B	1,1,2-Trichloroethane	79005
B	Methylene Chloride	75092
B	1,1,1,2-Tetrachloroethane	630206
B	Bromodichloromethane	75274
B	Chlorodibromomethane	124481
B	t-1,3-Dichloropropene	10061026
C	2-Hexanone	591786
C	Acetone	67641
C	2-Butanone	78933
C	4-Methyl-2-pentanone	108101

TABLE A-3 (Continued)

GROUP[a]	COMPOUND	CAS#
D	Bromobenzene	108861
D	Bromoform	75252
D	Chlorobenzene	108907
D	Ethylbenzene	100414
D	1,3,5-Trimethylbenzene	108678
D	Toluene	108883
D	m-Xylene	1330207
D	Benzene	71432
D	1,3-Dichlorobenzene (M)	541731
D	n-Propylbenzene	103651
D	o-Xylene	1330207
D	1,2,4-Trimethylbenzene	95636
D	Styrene	100425
D	1,4-Dichlorobenzene (P)	106467
D	1,2-Dichlorobenzene (O)	95501
D	p-Xylene	1330207
E	1,4-Difluorobenzene	
E	Chlorobenzene-d5	
F	Toluene-d8	
F	4-Bromofluorobenzene	

(a) Group: Used to sort compounds for the convenience in standards preparation. Group "E" are internal standards and group "F" are surrogates.

Note: Samples tubes (glass, 5mm ID X 9cm length) contain 150mg each of 20/40 carbotrap c. 20/40 carbotrap b. 60/80 carbosieve SIII (custom from Supelco, Inc.)

Samples are taken by passing a known volume of gas phase sample through a sample tube containing the adsorbent material(s) listed above. Organic sample constituents are absorbed into the adsorbent. While passing an inert gas through the tube, the tube is heated this desorbs the organic sample constituents off the adsorbent. The inert gas stream is directed to the head of a GC column, where the gas stream is split 1:50. Analysis by GC/MS then proceeds.

2.2 Analysis of Core Samples for Organic Contaminants

Cores from drill holes 14, 15, 16, and 18 were analyzed for the 43 organic compounds listed in Table A-4. This list includes nine of the twelve compounds detected in gas samples obtained from monitoring ports that were subsequently installed in the holes. Of the nine compounds analyzed both in the cores and in the pore gas, only toluene was detected in the cores--and it was detected at a concentration of 12 mg/kg. The analytical results for the core samples are presented in Table A-5. It is somewhat surprising that neither TCA nor TCE were detected in any of the core samples, although these compounds show the largest concentrations of all analytes of the pore gas.

In addition to toluene, priority pollutants detected in the core samples include methylene chloride and 1, 2-dichloroethane. The pore gas samples have not been analyzed for these constituents. The contaminant that occurred at the highest concentration in the core was acetone, which has not been an analyte in the quarterly gas sampling. However, the revised system for pore gas monitoring will include analyses for methylene chloride, 1, 2-dichloroethane, and acetone.

methyl + acetone are common laboratory contaminants

3.0 CORRECTIVE ACTION SELECTION CRITERIA

For the purposes of the pilot study, the site is considered to extend along the crest of Mesita del Buey and includes MDA L and the entire area over which the contiguous contaminant plume can be detected. The selected corrective action must conform to the particular constraints imposed by the setting of the site. These constraints include the following:

- minimal interference with active waste treatment and storage facilities at MDA L and the disposal facilities at MDA G;
- the space restrictions imposed by the site's position along the crest of a narrow ridge;
- the physical setting of the site, including lithology and permeability characteristics;
- natural forces (barometric pressure, earth-tides, wind, and temperature conditions) that may induce air flow within the mesa; and
- the characteristics of the contaminants in the plume.

3.1 Space Restrictions

The site is situated along the crest of a narrow mesa; the width of which ranges from 300 to 500 ft. The depth of the contaminant plume is in excess of 200 feet and may

TABLE A-4

ORGANIC COMPOUNDS ANALYZED
IN CORES FROM DRILL HOLES[1]

PRIORITY POLLUTANTS	DETECTION LIMIT (µg/kg)[2]
Acrolein	100
Acrylonitrile	100
Benzene	5
Bromoform	5
Carbon tetrachloride	5
Chlorobenzene	5
Chlorodibromomethane	5
Chloroethane	10
2-Chloroethylvinyl ether	5
Chloroform	5
Dichlorobromomethane	5
1,1-Dichloroethane	5
1,2-Dichloroethane	5
1,1-Dichloroethene	5
1,2-Dichloropropane	5
1,3-Dichloropropylene	5
Ethylbenzene	5
Methylbromide	10
Methylchloride	10
Methylene chloride	10
1,1,2,2-Tetrachloroethane	5
Tetrachloroethene	5
Toluene	5
1,2-trans-Dichloroethene	5
1,1,1-Trichloroethane	5
1,1,2-Trichloroethane	5
Trichloroethene	5
Vinyl chloride	10

NON-PRIORITY POLLUTANTS

Acetone	Dimethoxymethane	Propanol
1,4-Dioxane	Ethanol	1-Butanol
Acetonitrile	Propanol	Tetramethylpentanone
Tetrahydrofuran	Methyl-2-Propanol	Chlorodifluoromethane
2-Butanone	4-Methyl-2-Pentanone	Bisoxymethane

(1) Data from IT Corporation 1987, 0327.
(2) Analysis by Gas Chromatography/Mass Spectrometry

ORGANIC COMPOUND ANALYTICAL RESULTS FOR DRILL HOLE CORES AUGUST 1985[1]

DRILL HOLE NUMBER	DEPTH INTERVAL (FT)	VOLATILE ORGANIC COMPOUND	CONCENTRATION (µg/kg)
LLC-85-14	38-39	Acetone	190[e]
		Acetonitrile	27[e]
		Tetrahydrofuran	67[BJ]
	48-49	Acetone	670[e]
		2-Butanone	100[e]
		4-Methyl-2-Pentanone	110[e]
		Acetonitrile	1,100[e]
		Tetrahydrofuran	620[BJ]
		Dimethoxymethane	25[BJ]
		Unknown (oxygenated HC)	10[BJ][c]
		Unknown (oxygenated HC)	7[BJ]
LLC-85-15	18-19	Methylene Chloride	17
		Toluene	12
		Acetone	4,300[e]
		2-Butanone	470[e]
		4-Methyl-2-Pentanone	140[e]
		Ethanol	5[BJ]
		2-Propanol	6[BJ]
		Tetrahydrofuran	210[BJ]
		2-Methyl-2-Propanol	11[BJ]
	38-39	Acetone	300[e]
		2-Butanone	170[e]
		4-Methyl-2-Pentanone	420[e]
		Ethanol	170[e]
		Bisoxymethane	270[BJ]
		Propanol	270[BJ]
		Propanol (Isomer)	150[BJ]
		2-Methyl-2-Propanol	77[BJ]
		1,4-Dioxane	200[BJ]
		1-Butanol	280[BJ]

VOLATILE ORGANIC ANALYTICAL RESULTS FOR DRILL HOLE CORES AUGUST 1985[1]

DRILL HOLE NUMBER	DEPTH INTERVAL (FT)	VOLATILE ORGANIC COMPOUND	CONCENTRATION (µg/kg)
LLC-85-16	5.5-7.0	1,2-Dichloroethane	19
		Methylene Chloride	30
		Acetone	110[a]
		4-Methyl-2-Pentanone	27[a]
		2-Propanol	6[a]
		1-Butanol	17[b]
		Fluorinated Aliphatic	6[b]
		Tetramethylpentanone	7[b]
	17-19	Methylene Chloride	18
		Acetone	82[b]
	97-99	Methylene Chloride	15
		Acetone	110[a]
		4-Methyl-2-Pentanone	5[a]
		Chlorodifluoromethane	10[b]
LLC-85-18[d]	18-19	Methylene Chloride	17
		Acetone	130[a]
		Chlorodifluoromethane	12[b]
		Unknown Hydrocarbon	20[b]
		Ethanol	190[b]
		C_6-Hydrocarbon	9[b]
	78-79	Acetone	70[a]
		2-Butanone	55[a]
		Unknown Hydrocarbon	9[b]

(1) Data from IT Corporation 1987, 0327
Analytes not shown were below detection limits.
(a) Concentration determined from analysis of analytical standard.
(b) Concentration estimated using total ionization peak area relative to the internal standard.
(c) Best computer match is [2,2'Methylene bis (oxy)] bis propane.
(d) Drill hole LLC 85-18 was located at the southwestern corner of pit A. The drill hole was not completed as a monitor well for pore gas samples.

be as great as 500 feet. The site occupies approximately 10 acres and includes the source(s) of the plume at inactive waste disposal units located within MDA L, presently operating treatment and storage units at MDA L, support facilities for disposal operations at MDA G, and land that will be occupied by future expansion of MDA G.

The space and usage constraints of the site targeted for corrective action preclude the mass excavation of wastes, soils, and bedrock as a remedial measure. Excavation of the buried organic wastes within the source area is also not considered as an option because of the high cost and increased risk of exposure of personnel. In addition, the vapor plume is located below the maximum depth of cost-effective excavation. *Ex situ* methods are, therefore, precluded, and only *in situ* methods will be considered.

3.2 Physical Setting

The plume is within the Bandelier Tuff, which comprises the mesa upon which the site is located. The air permeability of the tuff matrix is moderate, in the range of 10^{-8} to 10^{-7} cm^2. The rate of vapor migration may be increased by the permeability interconnected fractures and the horizontal surge bed deposits. Several of the stratigraphic units within the Bandelier Tuff exhibit regularly spaced vertical cooling fractures. Fractures are better developed in welded tuff than in nonwelded tuff.

The lateral interconnection of fractures may vary within tuff units, and the vertical interconnection may be interrupted at boundaries between tuff units by differences in fracture systems in the different units. In addition, laterally extensive surge bed deposits may be present. The deposits are especially prominent between units 2a and 2b, at a depth that is penetrated by the disposal shafts. The migration of the vapor may follow lateral movement along the surge beds, combined with both lateral and vertical movement along fractures. In preparing for the remediation, we will investigate the air flow in the fractures and surge beds. If these are dominant pathways for vapor migration, the corrective action method must access them.

The tuff matrix may hinder any attempt to remove or contain the plume. The tuff contains a large amount of poorly connected pore space and may have high sorptive capacity. It is reasonable to assume that organic constituents may have been sorbed onto the matrix. This sorption could have occurred from the vapor phase, and possibly from the liquid phase in the vicinity of the source of the organics. The corrective action might, therefore, be required to remedy both the organic vapors contained within fractures and joints, and the slower desorption from the matrix.

3.3 Contaminant Characteristics

Available data indicates that the plume consists predominantly of TCA, as well as TCE, carbon tetrachloride, chloroform, and tetrachloroethene (PCE). Other detected constituents present at lower concentrations, or detected less consistently include toluene, xylenes, and 1,2,4-trimethylbenzene. TCA, TCE, carbon tetrachloride, chloroform, and PCE have similar major physical and chemical characteristics (See Table A-6). They have relatively high vapor

pressures, low solubilities in water, and relatively high Henry's Law coefficients, indicating strong partitioning into the vapor phase. All have specific gravities in excess of 1 in the pure liquid phase, and atively low viscosities. In addition, a saturated mixture of air and any of the constituents apor phase considerably more dense than air alone. Dry air saturated with TCA, for example, is approximately 1.5 times more dense than dry air with no TCA (Schwille 1988, 0750). Due to their low viscosity and high specific gravity, the primary constituents migrate readily in the liquid phase through both water-filled and air-filled fracture systems. The density of the vapor evaporated from a liquid encourages downward migration of the vapor plume through interconnected fractures. The fact that the contaminants have migrated extensively in the vapor phase indicates that the corrective action must be capable of removing vapor phase constituents.

The persistence of chlorinated constituents in the subsurface for long periods of time indicates that an active method will be required to retract the vapor plume. In addition, the inactive pit and disposal shafts will continue to be a source of vapor phase chlorinated hydrocarbons in the future, which will require an engineered system to prevent regrowth of the plume.

3.4 Summary of Corrective Action Criteria

The following information was used to select the technology for remediation of the organic vapor plume at MDA L:

- Technologies requiring excavation of the contaminated soil and rock are not feasible due to the depth of contamination, volume of contaminated material, and the operations being performed at MDAs L and G.
- The technology must be able to remove and treat vapor phase contaminants from pore space and fractures at depths exceeding 200 ft.
- The technology must remove and treat contaminant vapors as they are desorbed from the rock matrix over time and as they are released from the source area in the future.
- Bioremediation technologies are not feasible because of the high persistence of the chlorinated solvents and the potential production of vinyl chloride.
- The technology should serve as part of the long term stabilization of the MDA to prevent regrowth of the plume in the future.

4.0 PILOT EXTRACTION STUDY

4.1 Pilot Extraction Study Design

Vapor extraction is selected as the preferred technology for the corrective action. In vapor extraction, a vacuum pump draws vapors from boreholes to an emission treatment system.

TABLE A-6
PHYSICAL PROPERTIES AND ACTION LEVELS FOR VOLATILE ORGANIC COMPOUNDS DETECTED IN SOIL GAS SAMPLES AT MDA L AND THEIR BREAKDOWN PRODUCTS

COMPOUND (1)	CAS ID NUMBER (2)	VAPOR PRESSURE (mm @ 20°C) (2)	VAPOR DENSITY (g/L @ 25°C) (2)	HENRY'S LAW CONSTANT (atm m3/mol) (2)	SOLUBILITY IN WATER (mg/L @ 25°C) (2)	PEL (Air) (mg/m3) (2)	SUBPART S ACTION LEVEL (air) (mg/m3) (3)	SUBPART S ACTION LEVEL (soil) (mg/kg) (3)
Benzene	71-43-2	76	3.19	005	1,780	~30	NL	NL
Carbon tetrachloride (a)	56-23-5	90	6.29	.030	800	10 ppm	.03	5
Chlorobenzene	108-90-7	9	4.60	.0036	500	~350	20	2,000
Chloroethane	75-00-3	1,011	2.76 kg/m3 @ 20°C	.0111	5,740	~2,600	NL	NL
Chloroform (a)	67-66-3	160	4.88	.003	8,200	~240	.04	100
Chloromethane	74-87-3	3,789	2.06	.00882	7,250	~205	NL	NL
1,1 Dichloroethane	75-34-3	182.1	4.04	.0043	5,500	~400	NL	NL
1,2 Dichloroethane (a)	107-06-2	64	4.04	.00091	8,690	50 ppm	.04	8
1,1 Dichloroethene (a)	75-35-4	495	3.96	021	400	~20	03	10
Trans-1,2 Dichloroethene	156-60-5	265	3.96	.00074	600	NL	NL	NL
Ethylbenzene	100-41-4	7.08	4.34	.0066	152	~435	NL	8,000
Methylene Chloride (a)	75-09-2	348.9	3.47	.0020	20,000	500 ppm	.3	90
Tetrachloroethene (a)	127-18-4	14	6.78	015	150	100 ppm	1	10
Toluene	108-88-3	22	3.77	.0067	515	~375	7,000	20,000
1,1,1 Trichloroethane	71-55-6	100	5.45	.018	1,360	~1,900	1,000	7,000
Trichloroethene (a)	79-01-6	57.8	5.37	.009	1,100	~270	NL	60
Vinyl chloride	75-01-4	2,580	2.55	2.78	1,100 @ 25°C	1 ppm	NL	NL
o-Xylene	95-47-6	6.6 @ 25°C	4.34	.005	152	~435	1,000 (b)	200,000 (b)

FOOTNOTES:
a. Listed as carcinogen in Appendix A, Proposed Subpart S, 40 CFR, Part 264.
b. Reference for mixed xylenes.
NL. Not Listed

REFERENCES:

1. Flotard, R.D., M.T. Homshen, J.S. Wolff and J.M. Moore. 1986. Volatile Organic Analytical Methods Performance and Quality Control in Remedial Site Investigation: Hazardous and Industrial Solid Waste Testing, Fifth Volume ASTM STP 925.
2. "Groundwater Chemicals Desk Reference", John H. Montgomery and Linda M. Welkom, Lewis Publishers, Chelsea Michigan, 1990.
3. Appendix A, Proposed Subpart S, Part 264, 40 CFR, in "Federal Register 55", 30798, July 27, 1990.

Figure A-16 presents a schematic diagram of a typical system. EPA guidance (EPA 1991, 0707) indicates that vapor extraction is a feasible corrective action for a site with intrinsic permeability greater than 10^{-10} cm^2 with contaminants having vapor pressure greater than 0.5 torr. Both of these conditions are met for the plume at MDA L. In addition, vapor extraction meets the criteria discussed in the previous section by requiring only minimal excavation and space so that it will not interfere with ongoing operations at MDAs L and G and by being able to remove vapor phase contaminants from depths greater than 200 ft.

Vapor extraction has the capability to:

- withdraw vapor phase constituents from pore space and fractures;
- enhance the evaporation of constituents from the pure liquid or aqueous phase, if present, and subsequently remove them as a vapor phase; and
- control the further migration of vapors within the subsurface.

4.2 Additional Data Gathering

4.2.1 New Boreholes and Sampling

Additional data on the tuff matrix and the vapor plume are needed for design of a vapor extraction system. Boreholes that will provide samples for the RFI Work Plan will also provide the information needed to design and implement the corrective action. Six angle boreholes to the top of the basalt and three deep vertical boreholes into the basalt will be installed in the plume to further characterize the plume and the site geologic properties.

The six angle boreholes will be 8 inches in diameter to provide good efficiency as extraction wells. Steel casing with 8-inch inside diameter will be installed in the upper 30 feet of the borehole and will be grouted to prevent short circuiting of airflow from the surface near the borehole. The angle boreholes will intercept the near-vertical fractures, and will be drilled to the top of the Chino Mesa Basalt (estimated to be at a depth of 220 feet to 300 feet). The angle borehole locations are shown on Figure A-17. The boreholes are located to provide data on the plume and the subsurface environment. The angle boreholes will reveal the lithology of a cross-section of the mesa, and will be completed so that they can monitor the vapor extraction process or serve as active extraction wells or injection wells in the future. Information to be gathered from the six angle boreholes includes the following:

- Continuous core will be collected for description of lithology and fractures.
- Geotechnical tests performed on core samples include
  - Saturated hydraulic conductivity;
  - Moisture content, bulk density, and porosity;
  - Moisture characteristic curve with data in the dry range extending to approximately 2% moisture by weight, or drier if possible;
  - Specific gravity (particle density)

KEMRON ENVIRONMENTAL SERVICES
TEST RESULTS BY SAMPLE

Test Code: LAS270 Lab No: 01A Collected: 07/26/95
Sample Description: 0508-95-0008/02 Category: SOIL
Test Description: Semivolatile Compounds Method: 8270

Analyst: MDC Extracted: 07/27/95 File #: LA03056
Instrument: HPMS_3 Injected: 08/01/95 Factor: 33 Units: ug/kg Verified: SDT

CAS#	COMPOUND	RESULT	DETECTION LIMIT
50-32-8	Benzo(a)pyrene	ND	170
193-39-5	Indeno(1,2,3-cd)pyrene	ND	170
53-70-3	Dibenzo(a,h)anthracene	ND	170
191-24-2	Benzo(g,h,i)perylene	ND	170
62-53-3	Aniline	ND	170
62-75-9	N-Nitrosodimethylamine	ND	170

LIBRARY SEARCH COMPOUNDS:

CAS#	COMPOUND	RESULT
108-60-1	2,2'-Oxybis(1-Chloropropane)	NF

SURROGATES:

2-Fluorophenol	66 % Recovery	(25% - 121%)
2-Fluorobiphenyl	44 % Recovery	(30% - 115%)
Phenol-d6	54 % Recovery	(24% - 113%)
2,4,6-Tribromophenol	71 % Recovery	(19% - 122%)
Nitrobenzene-d5	40 % Recovery	(23% - 120%)
p-Terphenyl-d14	85 % Recovery	(18% - 137%)

NOTES AND DEFINITIONS FOR THIS SAMPLE
ND = NOT DETECTED AT OR ABOVE THE METHOD DETECTION LIMIT (MDL)
NA = NOT ANALYZED
DL = DILUTED OUT
NF = NOT FOUND

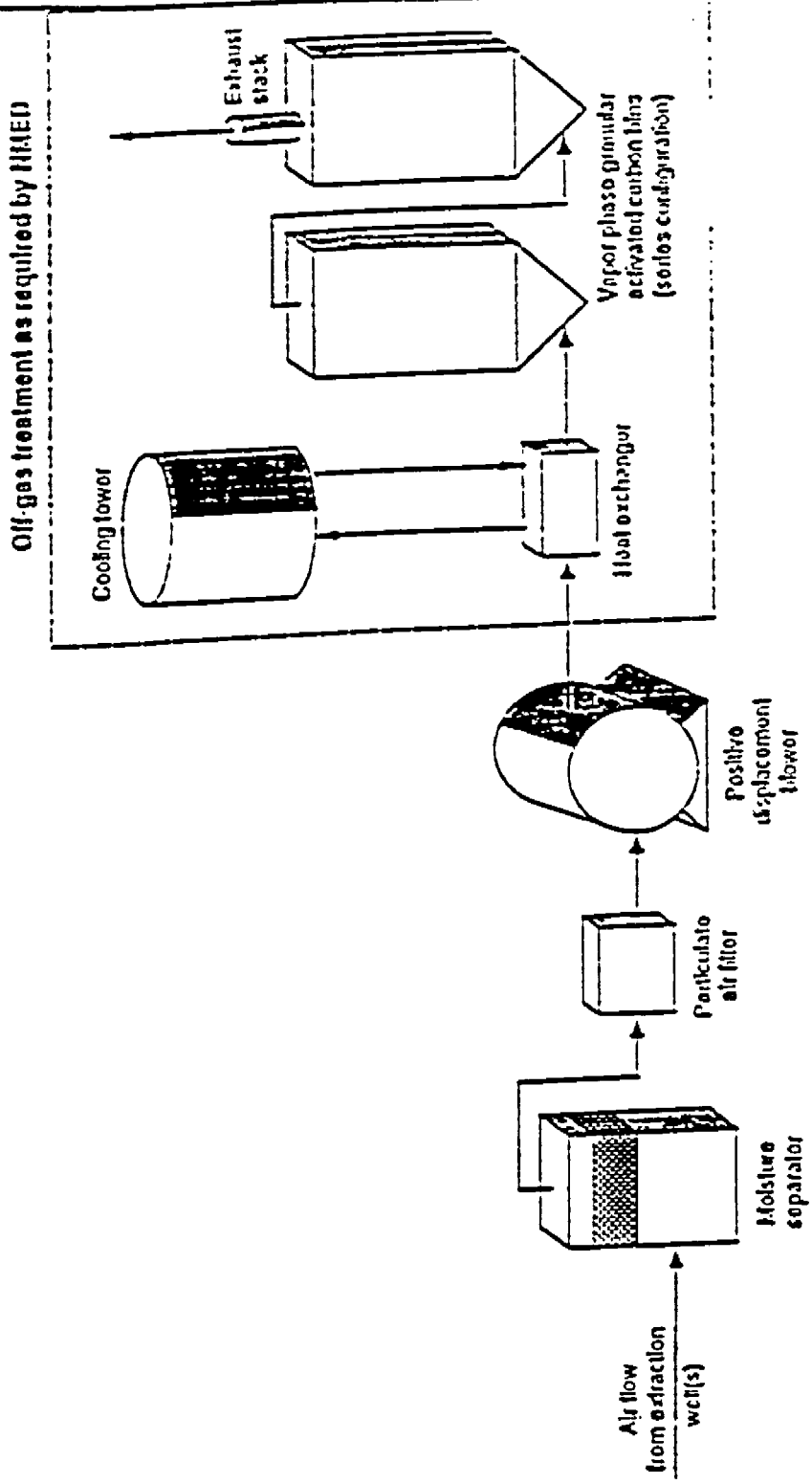

Figure A-18. Conceptual design of vapor extraction unit.

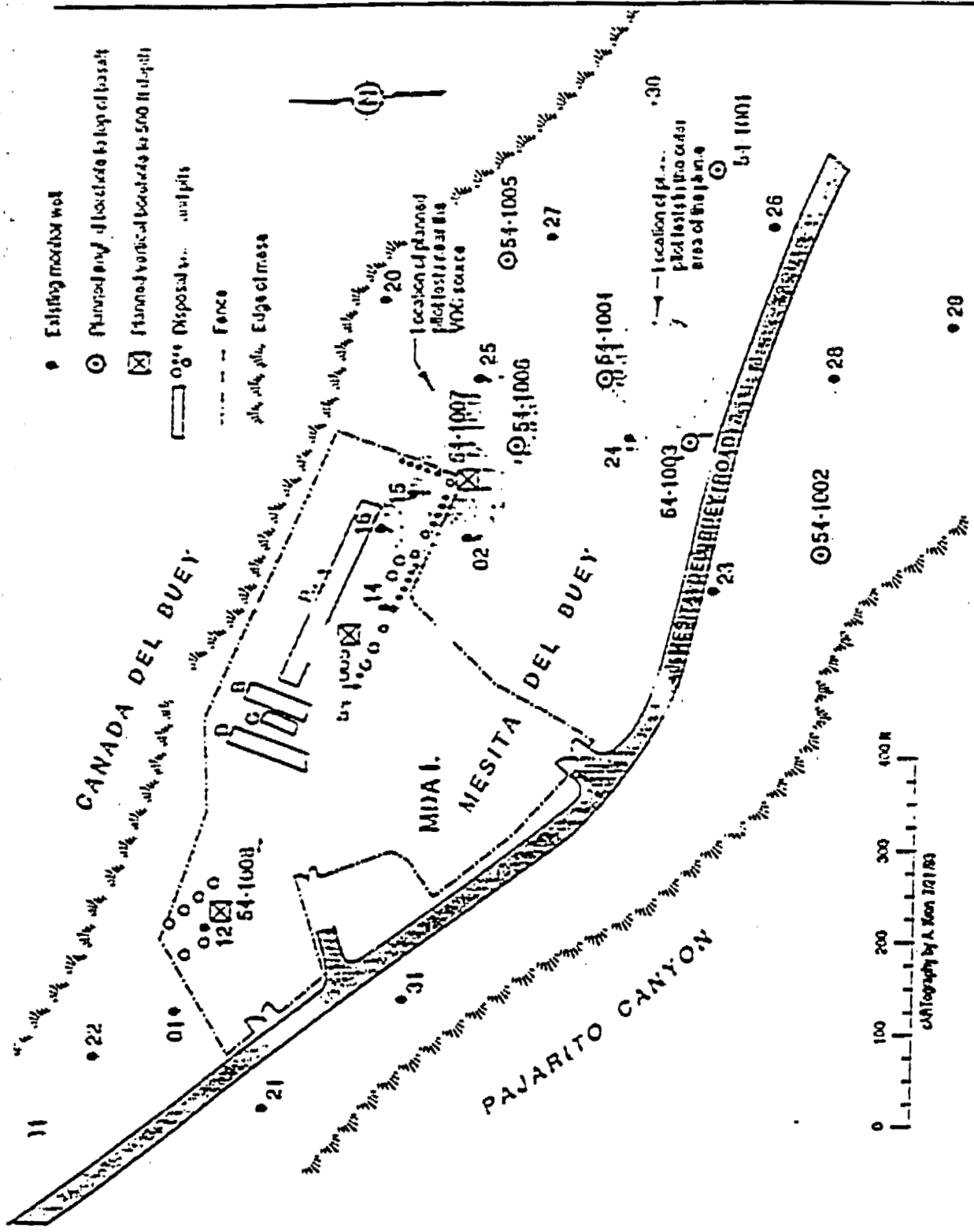

Figure A-17. Location map of planned boreholes and pilot tests in the Voluntary Corrective Action Plan.

- Specific surface (BET method); and
- Air permeability.

- Caliper logs and borehole video logs will be performed in the open boreholes to identify fracture zones and fracture orientations.

- A borehole deviation log will be performed on the open boreholes to determine the trajectory of the angle holes.

- Air flow profiles will be gathered in at least one open borehole to identify zones of relatively higher and lower air permeability.

- Packer tests will be performed in at least one open borehole to determine the air permeability in selected zones.

Cores from the six angle boreholes will be analyzed for moisture and VOCs according to the schedule presented in Attachment 1 to this Appendix. Because of the large distance between these boreholes and the sources, these cores will not be analyzed for non-volatile contaminants.

Five of the angle boreholes (well ID No.s 54-1002 to 54-1006 on Figure A-17 will be instrumented with SEAMIST™ flexible liner monitoring systems (or equivalent) to provide the following measurements at selected locations in each borehole at 12 depth intervals:

- temperature,
- matric potential,
- pressure, and
- VOC concentrations in pore gas

One of the angle boreholes (54-1001) will be used for open hole measurements of air flow as a function of changes in atmospheric pressure and/or gravitational tides. This borehole is located at the perimeter of the plume where TCA concentrations are very low. A liner will subsequently be used to seal this borehole. Data from the existing monitor wells and the six angle holes will be used to assess natural air flow within the tuff (to the top of the basalt) that is in response to atmospheric pressure changes, wind, seasonal temperature variation, and gravitational tides.

The sampling and core logging will reveal variations in subsurface geology along the axis of the mesa and transverse to the mesa. The in-situ measurements will reveal the natural breathing of the mesa in response to barometric and tidal variations, and the effect of these variations on vapor concentrations. In turn, this knowledge will enable better design of an active vapor extraction system to retract the plume, and may enable the design of a passive ventilation system for long-term control of the vapor sources. Data on the hydrogeologic properties will be applied in future modeling of transport. (Additional drilling and sampling for the RFI, but not needed for this study, is described in the body of the RFI Work Plan.)

The three deep vertical boreholes near disposal units at MDA L (well ID No.s 54-1007 to 54-1009 on Figure A-17 will assess the vertical extent of contamination below the MDA as part of the RFI for MDA L. The basalt section of the boreholes will be instrumented with SEAMIST™ liner systems or equivalent to characterize air flow deep in the mesa and to monitor the vertical extent of the organic vapor plume. The [illegible]0 foot depth for these boreholes was determined from the fact that the plume has migrated approximately this distance laterally from the disposal units. The boreholes stop at a distance of 350 to 400 feet above the top of the water table to alleviate concerns that a deep borehole to the aquifer would be a potential pathway for contaminants. The boreholes will be drilled with Odex® technology that installs steel casing during drilling to prevent migration of contaminants along the borehole during or after drilling. After drilling, a polymer casing will be installed within the steel outer casing, and the intervening annular space will be grouted from a tremie while the outer casing is withdrawn. This will leave a secure, gas-tight completion from the surface to the top of the dense basalt, below which flexible or fixed casings may be used. When the deep boreholes are no longer needed, the holes will be drilled to remove the polymer casing and plugged with grout to eliminate a potential pathway for future vertical migration of contaminants.

Information to be gathered from the three 500-foot-deep vertical holes includes the following:

- Continuous core will be collected for description of lithology and fractures.
- Geotechnical tests performed on core samples include
  - Saturated hydraulic conductivity
  - Moisture content, bulk density, and porosity;
  - Moisture characteristic curve with data in the dry range extending to approximately 2% moisture by weight, or drier if possible;
  - Specific gravity (particle density)
  - Specific surface (BET method); and
  - Air permeability.
- Caliper logs and borehole video logs will be performed in the open boreholes to identify fracture zones and fracture orientations.
- A borehole deviation log will be performed on the open boreholes to determine the path of the vertical holes.
- Air flow profiles will be gathered in an open borehole to identify zones of relatively higher and lower air permeability.
- Packer tests will be performed in an open borehole to determine the air permeability in selected intervals.
- As part of the RFI, core samples will be analyzed for volatiles, semi-volatiles, metals, cyanide, pesticides, herbicides, PCB's, tritium, gamma spectrometry, gross alpha, and gross beta. Analytes and analytical methods are described in the work plan. Attachment 2 to this appendix presents the depth interval for analyses on core.

- As part of the RFI, gas samples will be collected from each 20 foot depth interval during drilling. The samples will be collected on carbon resin and analyzed for the compounds listed in Table A-3. Attachment 2 to this appendix presents the schedule for collection of gas samples at each borehole.

4.2.2 Subsurface Air Flow Studies

Investigation of barometric effects. It is now known that an oscillatory flow of air (as contrasted with a steady flow, or no flow) in a porous medium can dramatically increase the effective rate of diffusion of a contaminant vapor. The barometric pressure at Los Alamos displays cycles with 12-hour, 24-hour, 2-day, and 5-day periods. These cycles may produce oscillatory air flow (so-called "barometric pumping") within the tuff, which may in turn accelerate the spread of the organic vapor plume. In estimating any future dispersion of the plume, it is therefore important to know the magnitude, and the influence, of the natural periodic subsurface flow. Also, vapor extraction to remedy the plume should be conducted so as to work with, rather than against, natural dispersion.

The subsurface pressure will be measured as a function of time at ports in several of the existing monitor wells, and in at least one of the new angle boreholes. By comparison of the Fourier components of the surface pressures with the Fourier components of the subsurface barometric pressure, one can determine the logarithmic decrease of oscillatory pressure amplitude with depth, which is theoretically a function of frequency, permeability, and porosity. Irregular behavior of the penetration depth may reveal whether fractures in the tuff provide barometric ventilation, and therefore whether the fractures will also influence applied vapor extraction. Because many of the fractures are filled with clay, it is not obvious whether the fractures have greater or less permeability than the tuff matrix.

Concurrent with the subsurface pressure measurements, a continuous-reading instrument will be used to monitor changes in the concentration of one or more of the volatile contaminants in the pore gas as a function of time. The existing monitor wells have been sampled quarterly for several years. As shown in Figure A-5 through A-9, measured concentrations of VOCs show a large scatter. It is possible that the scatter is due to barometric pumping. Continuous measurement of pressure and VOC concentration may reveal the extent to which barometric pumping causes short-term variations in VOC concentration. The techniques developed for subsurface pressure and VOC monitoring will be applied during vapor extraction pilot tests to measure the distribution of vacuum and short-term changes in pore gas concentration. These techniques will also be used as diagnostics if forced oscillatory flow is deliberately applied to circumvent diffusion limitation during pilot or full-scale extraction.

Long-term remediation. It is expected that application of conventional soil vapor extraction technology, possibly enhanced by forced oscillatory flow, will retract the VOC plume to the vicinity of the disposal shafts at Area L. However, applied vapor extraction is unlikely to remedy the sources within the shafts because much of the waste was buried in containers that may still be sealed. In principle, a container could rupture at any time in the future, thereby permitting a new release of volatile materials from a shaft. The subsurface air flow studies may enable design of a passive ventilation system operated by barometric oscillations. The system would be intended to intercept and extract any future volatile emissions from the

shafts. Such a system would prevent future re-growth of the plume without electric power, rotating machinery, or extensive maintenance.

4.3 Preliminary Design Criteria

The following sections provide information on the vapor extraction system (VES) that will be designed to retract the plume at MDA L. The current design parameters are based on present knowledge of site and plume conditions and the documented experience with VES at other sites. Pilot tests will be conducted near one or more of the six angle boreholes in the low contaminated area to evaluate the initial design parameters and to develop a final VES design. Tentative locations for the pilot tests are shown on Figure A-17.

4.3.1 Extraction Wells

Wells utilized for vapor extraction may be vertical or angled. As discussed in Section 1.2, the fracture systems within which the vapor plume is presumably migrating appear to have an orientation which is predominantly vertical and near-vertical. Angle and/or horizontal wells may therefore encounter a larger number of fractures than vertical wells, with a correspondingly higher removal efficiency. However, such wells would be both more difficult and more costly to install than vertical wells. The information obtained from the six angle boreholes for site characterization will be used to determine the best design for vapor extraction wells.

4.3.2 Piping

All well heads of a final VES will include the following accessories:

- Flow rate indicator;
- pressure gauge;
- a sample port; and
- a valve to admit atmospheric air.

Gracing and sumps will collect condensed moisture. A knockout device and particulate filter will be installed on the suction side of the vacuum pump. This will remove entrained liquid and remove particles that might damage the pump.

4.3.3 Emissions Control System

The New Mexico Environment Department may require an emissions control system to reduce contaminant concentrations in the effluent airstream of a pilot test and/or the full-scale operation. Treatment options include thermal oxidation, catalytic oxidation, condensation, carbon absorption, and incineration. Of these options, thermal oxidation and incineration provide incomplete destruction of chlorinated hydrocarbons. Condensation would require

sophisticated cooling and heat exchange systems to achieve greater than 90 percent contaminant removal, especially because adiabatic compression increases the temperature of the extracted air.

If treatment is required, carbon absorption will be used during the initial pilot tests because it is a proven technology that is cost effective for short-duration tests at low concentrations. Because the purpose of the pilot test is to evaluate the effects of different pumping rates and flow schemes on contaminant movement in the subsurface, adjustment of a catalytic oxidation system is impractical. Carbon absorption units are easily changed when breakthrough occurs. The actual carbon usage rate and contaminant flux determined from the pilot test will be used to evaluate the cost effectiveness of carbon absorption versus catalytic oxidation for emissions control if it is required during full-scale operation.

4.4 Pilot Tests to Evaluate Active Extraction

Pilot tests to provide information for the design of the full-scale VES at MDA L will be conducted at two locations: first in the perimeter region of the plume where total concentrations are low; and second, near the source area where total concentrations are high and more contaminants are present.

4.4.1 Pilot Tests in the Perimeter Area

The pilot tests of the VES in the vicinity of the angle boreholes, near the perimeter of the plume, will be conducted in two steps:

- performance of a stepped extraction test from a single extraction well; and if diffusion limitation occurs
- performance of a test using two or more wells which will oscillate between extraction, passive venting, and injection.

The data gained from the pilot tests will be used to assess flow, radius of influence, and contaminant removal rate from extraction intervals of various depths. If data from the initial pilot tests on contaminant removal rates are inconclusive, additional tests will be conducted closer to the sources of vapor.

Based on the additional data described in Section 4.2, the location of the initial pilot test will be determined. This well will be located in the middle of the mesa in the perimeter area where VOC concentrations are low (Figure A-17). The pilot extraction well will be approximately 25 feet from one of the instrumented angle boreholes.

The initial pilot tests will provide information on the vacuum required to achieve a specific flow rate, radius of influence, whether diffusion limitation occurs, and contaminant concentrations in extracted air. The information will be used to design a second pilot system employing two or more wells and time-varying flows.

The second pilot system will use two or more extraction wells. The wells will be alternated between extraction, passive venting, and injection. The oscillatory flow scheme will be designed to prevent dead air zones and to improve contaminant extraction rates under diffusion limited conditions.

4.4.2 Pilot Tests in the Source Area

One or more pilot tests will be conducted in the region of higher contamination, near the source. Test(s) in this region are necessary because the presence of additional VOCs with different properties may affect the extraction efficiency.

5.0 INSTALLATION OF THE ACTIVE EXTRACTION SYSTEM

The extraction wells installed for the pilot tests will be the first wells in the active system to extract the plume. Additional wells will be added in a phased approach based on performance. When practicable, existing monitor wells will be converted to serve as extraction wells. The schedule for characterization, pilot tests, and installation of the full-scale volatile extraction system is presented in Table A-7.

6.0 SCHEDULE

TABLE A-7

SCHEDULE FOR IMPLEMENTATION OF PESP *

Activity	Completion Date
Install instrumented angle and vertical boreholes for geologic characterization, plume characterization, and air flow measurements	November 30, 1993
Measure natural airflow in instrumented boreholes	September 1994
Design and install single well extraction test in outer area of plume	September 1994
Perform single well extraction test in outer area of plume	December 1994
Design and install multiple well extraction test in outer area of plume	May 1995
Perform multiple well extraction test and analyze data	June 1995
Design volatile extraction system for outer area of plume	March 1996
Complete installation of volatile extraction system in outer area of plume	February 1997
Start operation of volatile extraction system in outer area of plume	March 1997
Design and perform extraction test(s) near volatile sources and analyze data	March 1997
Design volatile extraction system for volatile source area	September 1997
Install volatile extraction system for volatile source area	December 1998
Place full scale volatile extraction system in operation	January 1999

* Contingent upon funding

REFERENCES

Appendix A, Proposed Subpart S, Part 264, 40 C R, In "F eral Register 55", 30798, July 27, 1990.

EPA (U.S. Environmental Protection Agency), September 1991. "Guide for Conducting Treatability Studies under CERCLA: Soil Vapor Extraction, Interim Guidance," EPA 5402-91/019A, Washington, D.C. (EPA 1991, 0707)

Flotard, R.D., M.T. Homsnen, J.S. Wolff and J.M. Moore. 1986. Volatile Organic Analytical Methods Performance and Quality Control in Remedial Site Investigation: Hazardous and Industrial Solid Waste Testing, Fifth Volume ASTM STP 925.

IT Corporation 1987. "Hydrogeologic Assessment of Technical Area 54, Areas G and L, Los Alamos National laboratory," Project No. 301017.02, Los Alamos, New Mexico. (IT Corporation 1987, 0327)

Kearl, P.M., J.J. Dexter, and M. Kautsky, March 1986. "Vadose Zone Characterization of Technical Area 54, Waste Disposal Areas G and L, Los Alamos National Laboratory, New Mexico. Report 3: Preliminary Assess ent of : a Hydrologic System. "Bendix Field Engineering Corporation Report GJ44, Grand Junction, Colorado. (Kearl et al. 1986, 0135)

Montgomery, J.H. and L.M. Welkam 1990. "Groundwater Chemicals Desk Reference," Lewis Publishers Inc., Chelsea, Michigan. (Montgomery and Welkam 1990, 0749)

Schwille, F. 1988. "Dense Chlorinated Solvents in Porous and Fractured Media," Lewis Publishers, Inc., Chelsea, Michigan. (Schwille 1988, 0750)

ATTACHMENT 1

:HEDULE OF CORE SAMPLES FROM ANGLE BOREHOLES

location id	sample no	sample depth	voa	moisture	semi-voa	metal	pesticide	herbicide	pcb	cn	tritium	gross alpha	gross beta	gamma spec
:1001	1	5	x	x										
	2	10	x	x										
	3	15	x	x										
	4	20x	x	x										
	5	25	x	x										
	6	30	x	x										
	7	35	x	x										
	8	40x	x	x										
	9	45	x	x										
	10	50	x	x										
	11	55	x	x										
	12	60x	x	x										
	13	65	x	x										
	14	70	x	x										
	15	75	x	x										
	16	80x	x	x										
	17	85	x	x										
	18	90	x	x										
	19	95	x	x										
	20	100x	x	x										
	21	105	x	x										
	22	110	x	x										
	23	115	x	x										
	24	120x	x	x										
	25	125	x	x										
	26	130	x	x										
	27	135	x	x										
	28	140x	x	x										
	29	145	x	x										
	30	150	x	x										
	31	155	x	x										
	32	160x	x	x										
	33	165	x	x										
	34	170	x	x										
	35	175	x	x										
	36	180x	x	x										
	37	185	x	x										
	38	190	x	x										
	39	195	x	x										
	40	200x	x	x										
	41	205	x	x										
	42	210	x	x										

SCHEDULE OF CORE SAMPLES FROM ANGLE BOREHOLES

	43	215	x											
	44	220x	x											
	45	225	x											
	46	230	x											
	47	235	x											
	48	240x	x											
	49	245	x											
	50	250	x											
	51	255	x											
	52	260x	x											
	53	dup x	x											
	54	blind x												
	55	method x												
	56	field x												
54-1002	57	5	x											
	58	10	x											
	59	15	x											
	60	20x	x											
	61	25	x											
	62	30	x											
	63	35	x											
	64	40x	x											
	65	45	x											
	66	50	x											
	67	55	x											
	68	60x	x											
	69	65	x											
	70	70	x											
	71	75	x											
	72	80x	x											
	73	85	x											
	74	90	x											
	75	95	x											
	76	100x	x											
	77	105	x											
	78	110	x											
	79	115	x											
	80	120x	x											
	81	125	x											
	82	130	x											
	83	135	x											
	84	140x	x											
	85	145	x											
	86	150	x											
	87	155	x											
	88	160x	x											
	89	165	x											
	90	170	x											
	91	175	x											
	92	180x	x											

CHEDULE OF CORE SAMPLES FROM ANGLE BOREHOLES

	93	185	x	
	94	190	x	
	95	195	x	
	96	200	x	x
	97	205	x	
	98	210	x	
	99	215	x	
	100	220	x	x
	101	225	x	
	102	230	x	
	103	235	x	
	104	240	x	x
	105	245	x	
	106	250	x	
	107	255	x	
	108	260	x	x
-1003	109	5	x	
	110	10	x	
	111	15	x	
	112	20	x	x
	113	25	x	
	114	30	x	
	115	35	x	
	116	40	x	x
	117	45	x	
	118	50	x	
	119	55	x	
	120	60	x	x
	121	65	x	
	122	70	x	
	123	75	x	
	124	80	x	x
	125	85	x	
	126	90	x	
	127	95	x	
	128	100	x	x
	129	105	x	
	130	110	x	
	131	115	x	
	132	120	x	x
	133	dup	x	x
	134	blind	x	
	135	method	x	
	136	field	x	
	137	125	x	
	138	130	x	
	139	135	x	
	140	140	x	x
	141	145	x	
	142	150	x	

SCHEDULE OF CORE SAMPLES FROM ANGLE BOREHOLES

	1443	155	x											
	1444	160	x	x										
	1445	165	x											
	1446	170	x											
	1447	175	x											
	1448	180	x	x										
	1449	185	x											
	1450	190	x											
	1451	195	x											
	1452	200	x	x										
	1453	205	x											
	1454	210	x											
	1455	215	x											
	1456	220	x	x										
	1457	225	x	x										
	1458	230	x	x										
	1459	235	x											
	1460	240	x	x										
	1461	245	x											
	1462	250	x											
	1463	255	x											
	1464	260	x	x										
4-1004	1465	5	x											
	1466	10	x											
	1467	15	x											
	1468	20	x	x										
	1469	25	x											
	1470	30	x											
	1471	35	x											
	1472	40	x	x										
	1473	45	x											
	1474	50	x											
	1475	55	x											
	1476	60	x	x										
	1477	65	x											
	1478	70	x											
	1479	75	x											
	1480	80	x	x										
	1481	85	x											
	1482	90	x											
	1483	95	x											
	1484	100	x	x										
	1485	105	x											
	1486	110	x											
	1487	115	x											
	1488	120	x	x										
	1489	125	x											
	1490	130	x											
	1491	135	x											
	1492	140	x	x										

SCHEDULE OF CORE SAMPLES FROM ANGLE BOREHOLES

	193	145	x											
	194	150	x											
	195	155	x											
	196	160	x	x										
	197	165	x											
	198	170	x											
	199	175	x											
	200	180	x	x										
	201	185	x											
	202	190	x											
	203	195	x											
	204	200	x	x										
	205	205	x											
	206	210	x											
	207	215	x											
	208	220	x	x										
	209	225	x											
	210	230	x											
	211	235	x											
	212	240	x	x										
	213	cub	x	x										
	214	blind	x											
	215	method	x											
	216	field	x											
	217	245	x											
	218	250	x											
	219	255	x											
	220	260	x	x										
54-1005	221	5	x											
	222	10	x											
	223	15	x											
	224	20	x	x										
	225	25	x											
	226	30	x											
	227	35	x											
	228	40	x	x										
	229	45	x											
	230	50	x											
	231	55	x											
	232	60	x	x										
	233	65	x											
	234	70	x											
	235	75	x											
	236	80	x	x										
	237	85	x											
	238	90	x											
	239	95	x											
	240	100	x	x										
	241	105	x											
	242	110	x											

HEDULE OF CORE SAMPLES FROM ANGLE BOREHOLES

	2431	115	x											
	2441	120x	x											
	2451	125	x											
	2461	130	x											
	2471	135	x											
	2481	140x	x											
	2491	145	x											
	2501	150	x											
	2511	155	x											
	2521	160x	x											
	2531	165	x											
	2541	170	x											
	2551	175	x											
	2561	180x	x											
	2571	185	x											
	2581	190	x											
	2591	195	x											
	2601	200x	x											
	2611	205	x											
	2621	210	x											
	2631	215	x											
	2641	220x	x											
	2651	225	x											
	2661	230	x											
	2671	235	x											
	2681	240x	x											
	2691	245	x											
	2701	250	x											
	2711	255	x											
	2721	260x	x											
	2731	dua x	x											
	2741	blind x												
	2751	metric x												
	2761	field x												
2-CCS	2771	5	x											
	2781	10	x											
	2791	15	x											
	2801	20x	x											
	2811	25	x											
	2821	30	x											
	2831	35	x											
	2841	40	x											
	2851	45	x											
	2861	50	x											
	2871	55	x											
	2881	60	x											
	2891	65	x											
	2901	70	x											
	2911	75	x											
	2921	80x	x											

CHEDULE OF CORE SAMPLES FROM ANGLE BOREHOLES

293	85	x											
294	90	x											
295	95	x											
296	100	x	x										
297	105	x											
298	110	x											
299	115	x											
300	120	x	x										
301	125	x											
302	130	x											
303	135	x											
304	140	x	x										
305	145	x											
306	150	x											
307	155	x											
308	160	x	x										
309	165	x											
310	170	x											
311	175	x											
312	180	x	x										
313	185	x											
314	190	x											
315	195	x											
316	200	x	x										
317	205	x											
318	210	x											
319	215	x											
320	220	x	x										
321	225	x											
322	230	x											
323	235	x											
324	240	x	x										
325	245	x											
326	250	x											
327	255	x											
328	260	x	x										
329	dup	x	x										
330	blind	x											
331	method	x											
332	field	x											
333			98	376	0	0	0	0	0	0	0	0	0	0

ATTACHMENT 2

SCHEDULE OF GAS AND CORE SAMPLES
FROM DEEP VERTICAL BOREHOLES

location id	sample no	sample depth	moisture	gas-voa	voa core	metals	cn	semi voas	pesticide	herbicide	PCB's	gamma spec	tritium	gross alpha	gross beta
54-1007	11	51x													
	21	101x		x	x	x	x	x	x	x	x	x	x	x	
	31	151x													
	41	201x		x	x	x	x	x	x	x	x	x	x	x	
	51	251x													
	61	301x		x	x	x	x	x	x	x	x	x	x	x	
	71	351x													
	81	401x		x	x	x	x	x	x	x	x	x	x	x	
	91	451x													
	101	501x		x	x	x	x	x	x	x	x	x	x	x	
	111	551x													
	121	601x	x	x	x	x	x	x	x	x	x	x	x	x	
	131	651x													
	141	701x		x	x	x	x		x	x	x	x	x	x	
	151	751x													
	161	801x	x	x	x	x	x		x	x	x	x	x	x	
	171	851x													
	181	901x													
	191	951x													
	201	1001x	x	x	x	x	x	x	x	x	x	x	x	x	
	211	1051x													
	221	1101x													
	231	1151x													
	241	1201x	x	x	x	x	x	x	x	x	x	x	x	x	
	251	1251x													
	261	1301x													
	271	1351x													
	281	1401x	x	x	x	x	x	x	x	x	x	x	x	x	
	291	1451x													
	301	1501x													
	311	1551x													
	321	1601x	x	x	x	x	x	x	x	x	x	x	x	x	
	331	1651x													
	341	1701x													
	351	1751x													
	361	301x	x	x	x	x	x	x	x		x		x	x	
	371	1851x													
	381	1901x													
	391	1951x													
	401	2001x	x	x	x	x	x	x	x	x	x	x	x	x	

41	205	x												
42	210	x												
43	215	x												
44	220	x	x											
45	225	x												
46	230	x												
47	235	x												
48	240	x	x	x										
49	245	x												
50	250	x												
51	255	x												
52	260	x	x											
53	265	x												
54	270	x												
55	275	x												
56	280	x	x	x										
57	285	x												
58	290	x												
59	295	x												
60	300	x	x	x	x	x	x	x	x	x	x	x	x	x
61	305	x												
62	310	x												
63	315	x												
64	320	x	x											
65	325	x												
66	330	x												
67	335	x												
68	340	x	x											
69	345	x												
70	350	x												
71	355	x												
72	360	x	x	x										
73	365	x												
74	370	x												
75	375	x												
76	380	x	x											
77	385	x												
78	390	x												
79	395	x												
80	400	x	x	x	x	x	x	x	x	x	x	x	x	x
81	dup		x											
82	field		x											
83	method		x											
84	blind		x											
85	405	x												
86	410	x												
87	415	x												
88	420	x	x											
89	425	x												

	90	430	x													
	91	435	x													
	92	440	x	x	x											
	93	dup			x											
	94	field			x											
	95	method														
	96	blind														
	97	445	x													
	98	450	x													
	99	455	x													
	100	460	x	x												
	101	465	x													
	102	470	x													
	103	475	x													
	104	480	x	x	x											
	105	485	x													
	106	490	x													
	107	495	x													
	108	500	x		x	x	x			x	x	x	x	x	x	
	109	dup				x	x		x	x	x	x	x	x	x	
	110	field				x	x	x	x	x	x	x	x	x	x	
	111	method				x	x	x	x	x	x	x	x	x	x	
	112	blind				x	x	x	x	x	x	x	x	x	x	
			100	29	26	27	27	27	27	27	27	27	27	27	27	
location id	sample no	sample type	moisture	gas-voa	[illegible]	metals	cn	semi voas	pesticide	herbicide	PCB's	gamma spec	tritium	gross alpha	gross beta	
54-1008	1	5	x													
	2	10	x		x	x	x	x		x	x	x	x	x	x	
	3	15	x													
	4	20	x	x	x	x	x	x	x	x	x	x	x	x	x	
	5	25	x													
	6	30	x		x	x	x	x	x	x	x	x	x	x	x	
	7	35	x													
	8	40	x	x	x	x	x	x	x	x	x	x	x	x	x	
	9	45	x													
	10	50	x		x	x	x	x	x	x	x	x	x	x	x	
	11	55	x													
	12	60	x	x	x	x	x	x	x	x	x	x	x	x	x	
	13	65	x													
	14	70	x		x	x	x		x	x	x	x		x	x	
	15	75	x													
	16	80	x	x	x	x	x		x	x	x	x	x	x	x	
	17	85	x													
	18	90	x													
	19	95	x													

20	100	x	x	x	x	x	x	x	x	x	x	x	x	x
21	105	x												
22	110	x												
23	115	x												
24	120	x	x	x	x	x	x	x	x	x	x	x	x	x
25	125	x												
26	130	x												
27	135	x												
28	140	x	x	x	x	x	x	x	x	x	x	x	x	x
29	145	x												
30	150	x												
31	155	x												
32	160	x	x	x	x	x	x	x	x	x	x	x	x	x
33	165	x												
34	170	x												
35	175	x												
36	180	x	x	x	x	x	x	x	x	x	x	x	x	x
37	185	x												
38	190	x												
39	195	x												
40	200	x	x	x	x	x	x	x	x	x	x	x	x	x
41	205	x												
42	210	x												
43	215	x												
44	220	x	x											
45	225	x												
46	230	x												
47	235	x												
48	240	x	x	x										
49	dup			x										
50	field			x										
51	method			x										
52	blind			x										
53	245	x												
54	250	x												
55	255	x												
56	260	x	x											
57	265	x												
58	270	x												
59	275	x												
60	280	x	x	x										
61	dup		x											
62	field		x											
63	method		x											
64	blind		x											
65	285	x												
66	290	x												
67	295	x												
68	300	x	x	x	x	x	x	x	x	x	x	x	x	x

69	305	x												
70	310	x												
71	315	x												
72	320	x	x											
73	325	x												
74	330	x												
75	335	x												
76	340	x	x											
77	345	x												
78	350	x												
79	355	x												
80	360	x	x	x										
81	365	x												
82	370	x												
83	375	x												
84	380	x	x											
85	385	x												
86	390	x												
87	395	x												
88	400	x	x	x	x	x	x	x	x	x	x	x	x	x
89	405	x												
90	410	x												
91	415	x												
92	420	x	x											
93	425	x												
94	430	x												
95	435	x												
96	440	x	x	x										
97	445	x												
98	450	x												
99	455	x												
100	460	x	x											
101	465	x												
102	470	x												
103	475	x												
104	480	x	x	x										
105	485	x												
106	490	x												
107	495	x												
108	500	x	x	x	x	x	x	x	x	x	x	x	x	x
109	dup			x	x	x	x	x	x	x	x	x	x	x
110	field			x	x	x	x	x	x	x	x	x	x	x
111	method			x	x	x	x	x	x	x	x	x	x	x
112	blind			x	x	x		x	x	x	x	x	x	x
113		00	25	6	21	31	2	21	21	21	21	21	21	21

APPENDIX B

FINAL REPORT:
PILOT SCALE VAPOR EXTRACTION SYSTEM DESIGN FOR OU-1148

Sandra Dalvit Dunn
William Lowry
David Cremer
Eric Cramer

Science and Engineering Associates
3205 Richards Lane, Suite A
Santa Fe, New Mexico 87505

(505) 424-6955
(505) 424-6956 Fax

For:
ERM Program Management Company
Los Alamos, NM

Original Publication Date: March 14, 1995
Revision Date: October 10, 1997

SEA-SF-94-039

Science & Engineering Associates, Inc.

TABLE OF CONTENTS

Section		Page
1	INTRODUCTION AND SUMMARY	1
2	AIR FLOW PREDICTIONS	3
	A. CASING LENGTH ANALYSIS	3
	B. EXTRACTION INTERVAL	8
	C. TRANSIENT RESPONSE	16
	D. BOUNDARY CONDITION CHECK	16
3	EXTRACTION AND MONITOR WELL LAYOUT	23
4	REGULATORY ISSUES ASSOCIATED WITH VAPOR EXTRACTION SYSTEMS AT TA-54	33
5	PILOT VAPOR EXTRACTION SYSTEM	35
APPENDIX		
	AN OVERVIEW OF AIR3D	A-1

LIST OF FIGURES

Figure		Page
1	Schematic of the model used in casing length calculations	4
2	Steady-state pressure contours through a cross-section of the mesa	5
3	Mass balance breakout of replacement air for extraction test	7
4	Gross vertical flow through the medium for the baseline and the 100 ft. casing length runs	9
5	Velocity shadow plots for (A) the 100 ft. casing length and (B) the baseline runs	10
6	VOC distribution at Well #24 for 9/91 sampling period	11
7	Contaminant plume measured in LLC-86-25 during the third quarter of 1994	12
8	Comparison of the calculated steady-state pressure response at several depths for the 50 and 100 ft extraction interval cases	14
9	Steady-state pressure contours through a cross-section of the mesa (A) 50 ft. casing, 50 ft. extraction interval, and (B) 50 ft. casing, 100 ft. extraction interval	15
10	Series of pressure contours through a cross-section of the mesa with time for the recommended case; (A) after 0.85 hours, (B) after 5.26 hours, (C) after 10.86 hours, and (D) at steady state conditions	17
11	Comparison of the calculated pressure response at several time steps for the recommended case	18
12	Calculated pressure histories at 137.5 ft. bgs (in the center of the extraction region) for the recommended case of a 75 ft. casing and a 75 ft. extraction interval; (A) shows histories for points away from mesa edge, (B) shows histories for points toward mesa edge. Calculated responses differ only for points greater than 75 ft. from the well	19
13	Schematic of the geometric model initially used	20
14	Steady state pressure contours through a cross-section of the mesa for a 50 ft. casing length, 100 ft. extraction interval case with a point no flow boundary at the bottom surface	21
15	Steady state pressure contours through a cross-section of the mesa for a 50 ft. casing length, 100 ft. extraction interval case with a low flow layer between 325 and 350 ft. bgs	21
16	Steady state pressure contours through a cross-section of the mesa for the baseline case of a 50 ft. casing and 100 ft. extraction interval	21
17	Comparison of steady-state pressure response at 87.5 bgs (in the extraction interval) for all three cases checking the bottom boundary conditions	22
18	Series of pressure contours through a cross-section of the mesa with time for the homogeneous, increased permeability case (k=6D); (A) after 0.85 hours, (B) after 5.26 hours, (C) after 10.86 hours, and (D) at steady state condition	24
19	Series of pressure contours through a cross-section of the mesa with time for the non-homogeneous case; (A) after 0.85 hours, (B) after 5.26 hours, (C) after 10.86 hours, and (D) at steady state conditions	25

LIST OF FIGURES

Figure		Page
20	Comparison of the calculated pressure response at several time steps for (A) the homogeneous case of k=6D and (B) the non-homogeneous case	26
21	Calculated pressure histories at 137.5 bgs (in the center of the extraction region) for the homogeneous case of k=6D	27
22	Calculated pressure histories at 137.5 bgs (in the center of the extraction region) for the non-homogeneous case	28
23	Proposed layout of the new extraction and monitoring well if they are drilled at a 25° angle to vertical	31
24	Proposed layout of the new extraction and monitoring well if they were drilled vertically	32
25	Pilot vapor extraction system hardware	36

LIST OF TABLES

Table		Page
1	Mass balance summary for casing length calculations	6
2	Mass balance summary for extraction interval calculations	13
3	Mass balance summary for the extraction well location calculations	29

SECTION I
INTRODUCTION AND SUMMARY

The objective of the pilot extraction test is to evaluate the large scale airflow characteristics of the mesa, such that an effective extraction system design can be developed for the vapor phase plume of volatile organic contaminants (VOCs) that are emanating from the inactive chemical waste disposal site at Area L. In 1994, both small and large scale in-situ, as well as laboratory airflow measurements were performed on the tuff in Area G, within the region of the VOC plume, to characterize the airflow tendencies in the mesa. During this period several long term measurements have also been conducted to evaluate the barometric pumping characteristics of the mesa.

The pilot extraction test will apply a moderate extraction vacuum to a vertical well located in Area G, within the region of the plume. The test will use existing monitoring wells, consisting of older standard vapor point monitoring installations installed in the late 1980s, and more recently installed SEAMIST™ vapor monitoring systems in the wells drilled in late 1993. One additional monitoring well will also be drilled and a multipoint SEAMIST™ system installed specifically to monitor the airflow characteristics very near the extraction well.

The major issues to be treated in the design of the pilot vapor extraction system include the following:

- Where should the uncased region of the extraction well be placed to maximize the effectiveness of the vapor extraction system given the field and laboratory measured gas permeability characteristics, the mesa geometry, and the contaminant distribution known from adjacent monitoring wells?
- Given the planned vacuum to be applied to the uncased region of the extraction well, what will the radius of influence of the extraction well be as a function of time?
- To what depth should the surface casing be extended to maximize the replenishment of soil gas from regions horizontally adjacent to and below the extraction zone, and minimize the replenishment of air from the surface of the mesa?
- Given the airflow characteristics of the tuff, the geometry of the mesa, and anticipated borehole configurations, what will the total flow characteristics of the extraction well be for a specified extraction vacuum?
- What is the anticipated range and magnitude of the resulting pressure perturbations in the tuff so that the monitoring well and SEAMIST™ port locations can be specified for a new monitor well?

The analysis was conducted using AIR3D, a finite difference 3-dimensional program capable of both steady-state and transient simulations of airflow through porous unsaturated media. The significant results of this analysis are summarized as follows:

1. The lateral movement of the pressure field will be fairly rapid. For a homogeneous medium of 1.5D permeability, it will take only 8 days for a steady state condition to be reached. The majority (99%) of the calculated pressure decrease in the region of influence will be reached after only 30 hours of extraction. For a 6D permeability medium, these times are reduced to 80 hours and 8 hours, respectively. A measurable pressure response (1 in. w.c.) will be seen to a radial distance of approximately 120 ft. from the extraction well.
2. Given the estimated permeability of the medium (approximately 1.5 Darcies) and a draw-down vacuum of approximately 50 inches water column (a 1.8 psi vacuum), the resulting airflow rate for a 100 ft. extraction interval will be approximately 54 standard ft^3/min (230 lbs/hr).
3. The length of the surface casing should be chosen such that it maximizes contaminated gas removal The deeper the casing the lower the percentage of replacement air comes from the mesa surface, and the greater the region of influence becomes.
4. The extraction interval is recommended at a total length of 75 ft., centered on the peak concentration region of the plume. This will optimize the airflow with respect to the concentration profiles such that the air is drawn from the regions with the highest contaminant concentrations.
5. The proposed extraction well is located among the existing SEAMIST™ monitoring wells such that it can maximize the use of existing vapor sampling points and extract from a region that is central to a north/south array of monitoring wells. It is located south of borehole 54-1004 and allows use of the monitoring points in wells 54-1004, 54-1006, 54-1003, and the older monitoring wells, 86-24 and 86-25.
6. The new monitoring well will be drilled approximately 20 ft. east of the extraction well. This location will provide lateral pressure measurements at spacings of 20, 30, 40, 90, and 100 ft. from the well. The monitoring well should extend below the extraction well (ideally to at least 300 ft.) to provide a measurement of the vertical distribution of the pressure field. Points are to be located on the extraction well in regions of interest with potentially high permeability and at uniform spacings throughout the borehole.

This report also documents the design of the pilot extraction system hardware and instrumentation, which was presented to Los Alamos and ERM in September of 1994, as well as air emissions permitting issues.

SECTION 2
AIR FLOW PREDICTIONS

A numerical model was used to optimize the design and location of the pilot extraction well by looking at three distinct issues. First, numerous steady state calculations were performed to determine the affect of the casing length on the origin of replacement air. Second, several calculations were performed to determine the effect of the extraction zone interval on well flow characteristics. And finally, a transient calculation was performed to help anticipate the region of influence of the extraction process as a function of time. The code used in the modeling effort was AIR3D, a three-dimensional model for air flow in the unsaturated zone. Appendix A gives a brief overview of the code, and Section 2D describes conditional checks performed on the model.

A. CASING LENGTH ANALYSIS

Four separate calculations were performed to determine the effect of casing length on the nature of the overall flow field. The baseline case (Figure 1) included a 50 ft. casing with an extraction region extending from the bottom of the casing to a depth of 150 ft. The extraction well was given a 50-inch water column drawdown (approximately 1.8 psi) and was modeled as a 0.524 ft. square (giving it the equivalent surface area of an 8-inch diameter well). The grid used in the modeling was 1040 ft. wide by 1040 ft. long by 500 ft. high. The mesa was modeled as a block 100 ft. high by 600 ft. wide. The well was placed 170 ft. from one edge of the mesa. This distance was chosen based on the locations of the existing monitoring wells. An air block was simulated on either side and above the mesa by assigning the zones a very high permeability and porosity (10,000 Darcies and 95 percent, respectively). A homogeneous medium with a permeability of 1.5 Darcies was used for the remainder of the model. Constant pressure boundaries (an atmospheric pressure of 11.2 psi was used, which is appropriate for the TA-54 elevation) were assigned to all surfaces of the model. Three variations to the baseline case were run. In each, only the casing length was altered. Lengths of 25, 75, and 100 ft. were compared to the baseline case of 50 ft.

Figure 2 shows the calculated steady-state pressure contours for a cross section of the mesa through the well for the minimum and maximum casing depths. Table 1 provides a mass balance summary for each model surface. Figure 3 shows this information in the form of a bar chart. In general,

- as casing length increases, flow through mesa surface decreases, flow from the valley floor increases, and flow from the medium increases;
- flow from the mesa sides increases as casing length increases until the casing length approaches the height of the mesa (100 ft.);

- increasing the casing length below the mesa causes a decrease in flow from the mesa sides; and
- the amount of air extracted from the well decreases as casing depth increases, but with the very low permeability of the medium, this decrease is negligible.

Boundary conditions:

- lateral boundaries = constant pressure (11.2 psi)
- bottom boundary = constant pressure (11.2 psi)
- surficial layer -> k = 10,000D (air)

Well (centered along length of grid, 170' from one edge of mesa):

- 0.524" square (equivalent surface area to an 8" diameter well)
- casing depths vary from 25' to 100' in 25' increments
- extraction zone length constant at 100', starting at the bottom of the casing
- well pressure = 9.4 psi (equivalent to a 50" w.c. drawdown)

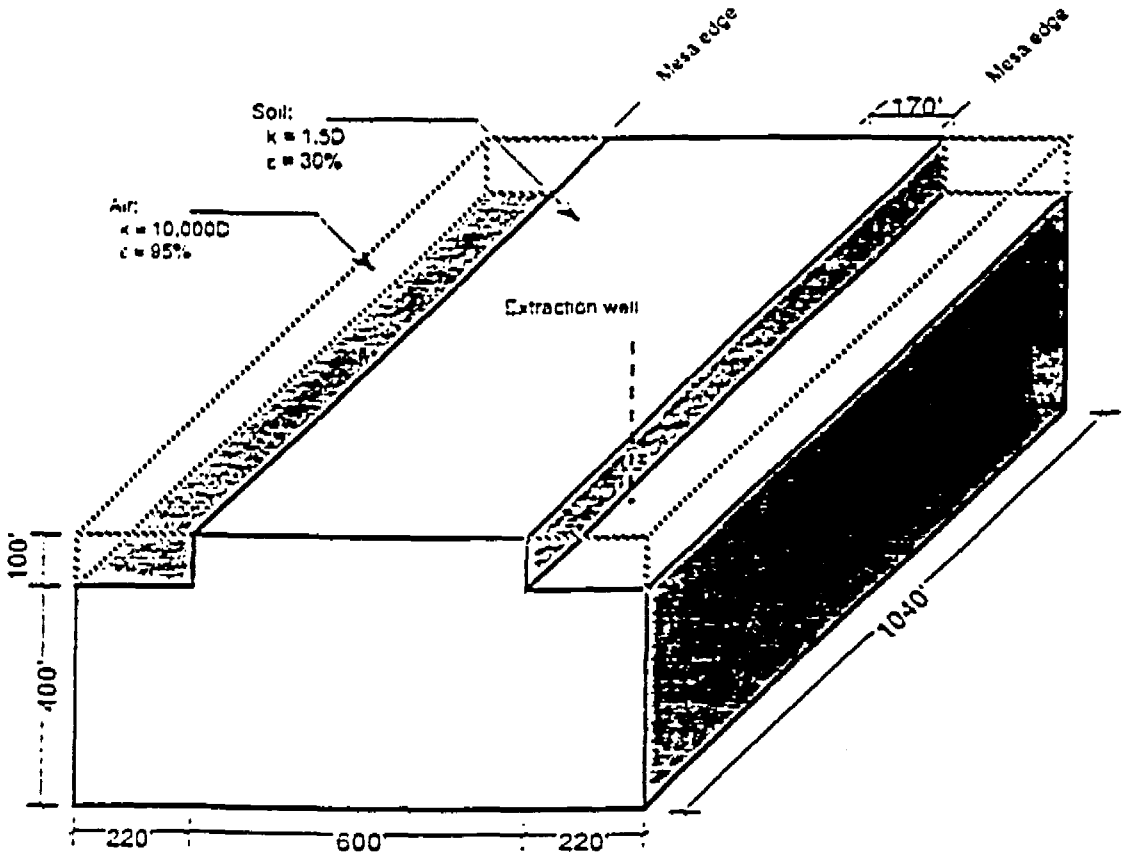

Figure 1. Schematic of the geometric model used in casing length calculations.

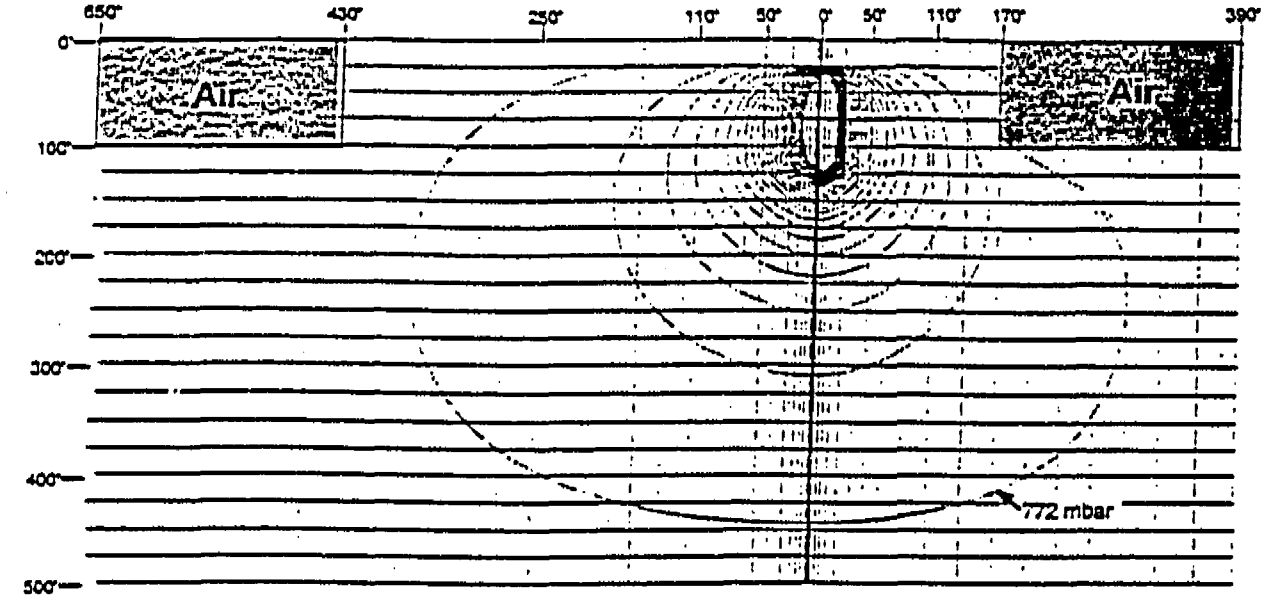

(A)

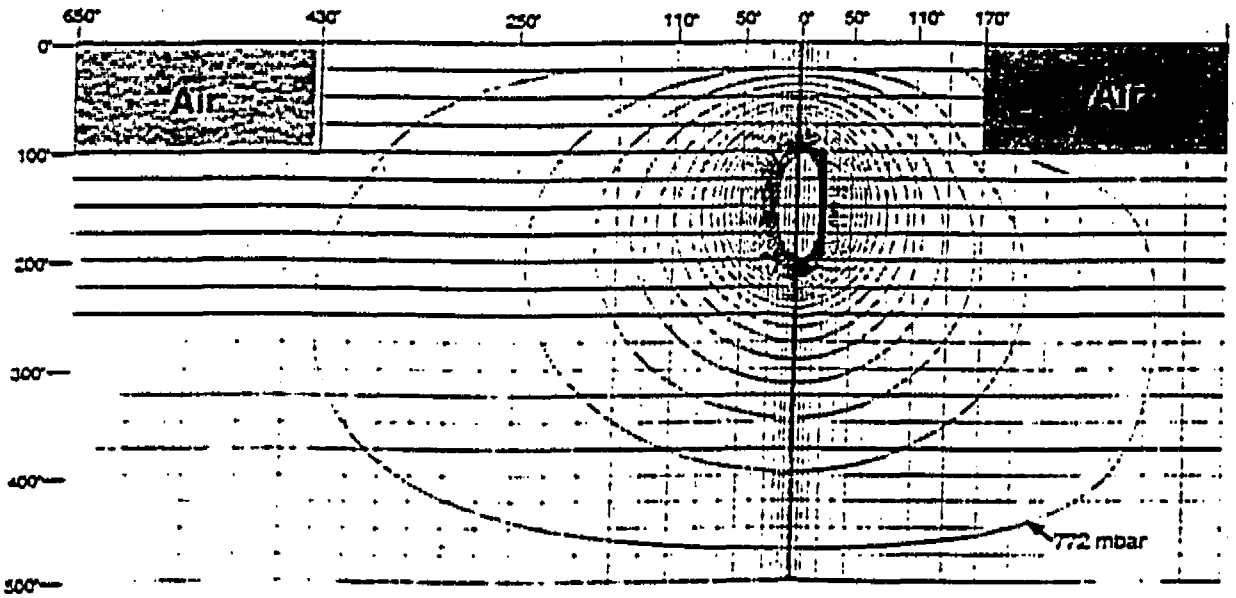

(B)

Contours:
Minimum level shown = 740mbar
Maximum level shown = 772mbar
Interval = 1mbar

Figure 2. Steady-state pressure contours through a cross-section of the mesa. (a) 25 ft. casing, 100 ft. extraction interval, (b) 100 ft. casing, 100 ft. extraction interval.

Table 1. Mass balance summary for casing length calculations.				
Mass balance summary	25' Casing length 100' extr. interval % of vented air contributed by surface	50' Casing length 100' extr. interval % of vented air contributed by surface	75' Casing length 100' extr. interval % of vented air contributed by surface	100' Casing length 100' extr. interval % of vented air contributed by surface
Flow thru mesa surface (A)	75.8%	65.8%	58.5%	51.5%
Flow thru mesa side, far (B)	0.4%	0.5%	0.6%	0.7%
Flow thru valley surface, far (C)	0.0%	0.7%	0.9%	1.0%
Flow thru soil, side below mesa, far (D)	0.4%	0.5%	0.7%	0.8%
Flow thru mesa side, near (E)	4.6%	6.8%	6.3%	6.3%
Flow thru valley surface, near (F)	4.4%	5.8%	7.1%	8.0%
Flow thru soil, side below mesa, near (G)	2.1%	2.9%	3.7%	4.5%
Flow thru soil, E/W sides, total (H)	3.6%	4.8%	6.0%	6.9%
Flow thru soil, bottom (I)	8.7%	12.2%	16.2%	20.2%
Flow from well (lb/hr)	239.39 (53.20 SCFM)	233.21 (51.82 SCFM)	230.51 (51.22 SCFM)	229.02 (50.89 SCFM)

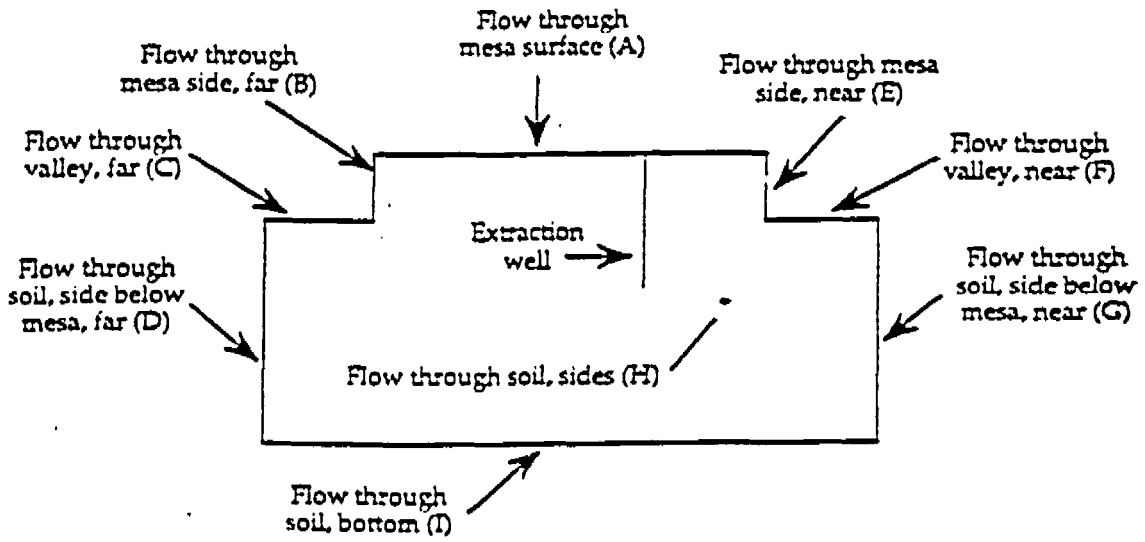

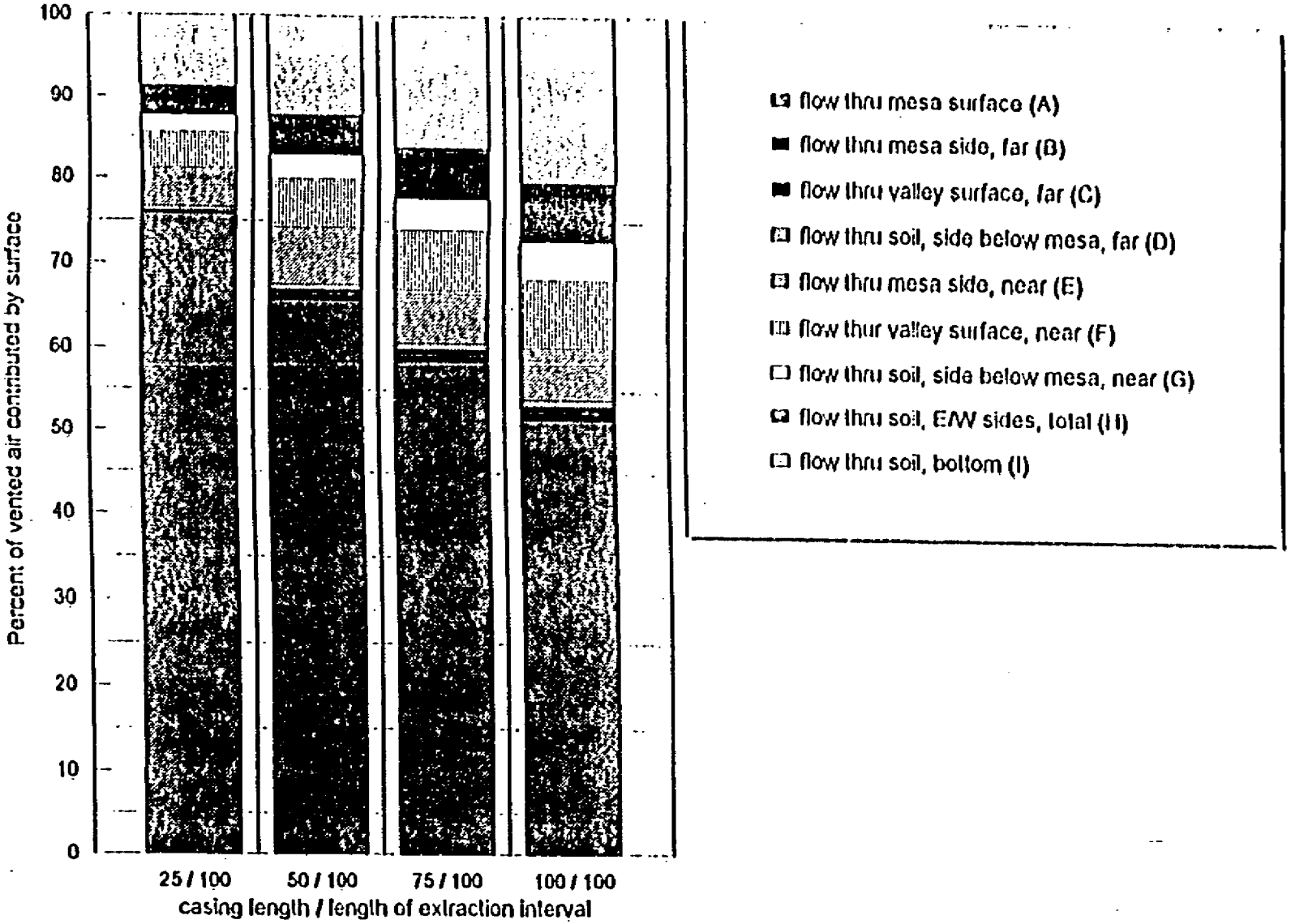

Figure 3. Mass balance breakout of replacement air for extraction test.

Figure 4 plots the net vertical flow through the soil of each 25 ft. layer for the baseline (50 ft.) and 100 ft. casing length runs. For the baseline case, the greatest amount of vertical flow comes from the mesa surface and the uppermost portion (top 50 ft.) of the mesa sides. Flow from the lower 50 ft. of the mesa sides and from the valley floor is vertically downward and lateral toward the extraction region (witnessed by the slope of the curve). Flow in the bottom 25 ft. layer of the extraction region decreases rapidly with depth and is predominantly upward. Comparing the curve from the 100 ft. casing length run shows the greatest vertical flow comes from the valley floor rather than the mesa surface, and that vertical flow reversal occurs in the center rather than the bottom of the extraction region. Thus as casing depth increases, the amount of clean make-up air (air from the mesa surface which will not contribute to site remediation) decreases, but a larger volume of contaminants (from the surface to a region in the extraction interval) will be drawn deeper into the medium. Figure 5 graphically depicts regions of flow velocities for the same cases. Flow regions between .001, .011, .108, and 1.08 lb/hr (at 60°F and 11.2 psi these equate to .019, .19, 1.87, and 18.71 ft^3/hr) are shown. The deeper casing influences a larger region of the medium. In both cases, a region of higher velocity is created from the base of the mesa toward the extraction region.

Contaminant profiles shown in the RFI Work Plan for Operable Unit 1148 (July 1993) suggest the contaminant plume extends from very near the surface of the mesa to at least 200 ft. below ground surface (bgs) near the proposed site. The maximum concentration levels of the plume are approximately 100 ft. bgs. Measurements taken more recently (third quarter of 1994) confirm this distribution. Figure 6, from the RFI Work Plan, shows the volatile organic contaminant distribution at well #24 for the 9/91 sampling period. Figure 7 plots the more recently acquired data from hole #25, which is also nearby. Given this contaminant distribution, the modeled effect of the casing length on the origin of replacement air, and the calculated flow patterns, a casing depth of 75 ft. would allow the extraction interval to start near the highest concentration of the contaminant plume. This maximizes the contamination extracted while minimizing the amount of replacement air from the mesa surface and the amount of contamination above the extraction zone which will be drawn deeper into the soil toward the extraction region.

B. EXTRACTION INTERVAL

The length of the extraction zone will affect both the amount of flow from the extraction well and the direction of the flow. The model used was identical to that used in determining the affects of casing length, described above. Two problems were run, the baseline case having a 50 ft. casing length and a 100 ft. extraction zone and a comparison case having a 50 ft. casing length and a 50 ft. extraction interval. In both cases the drawdown pressure of the well was held constant at 50 inches w.c.

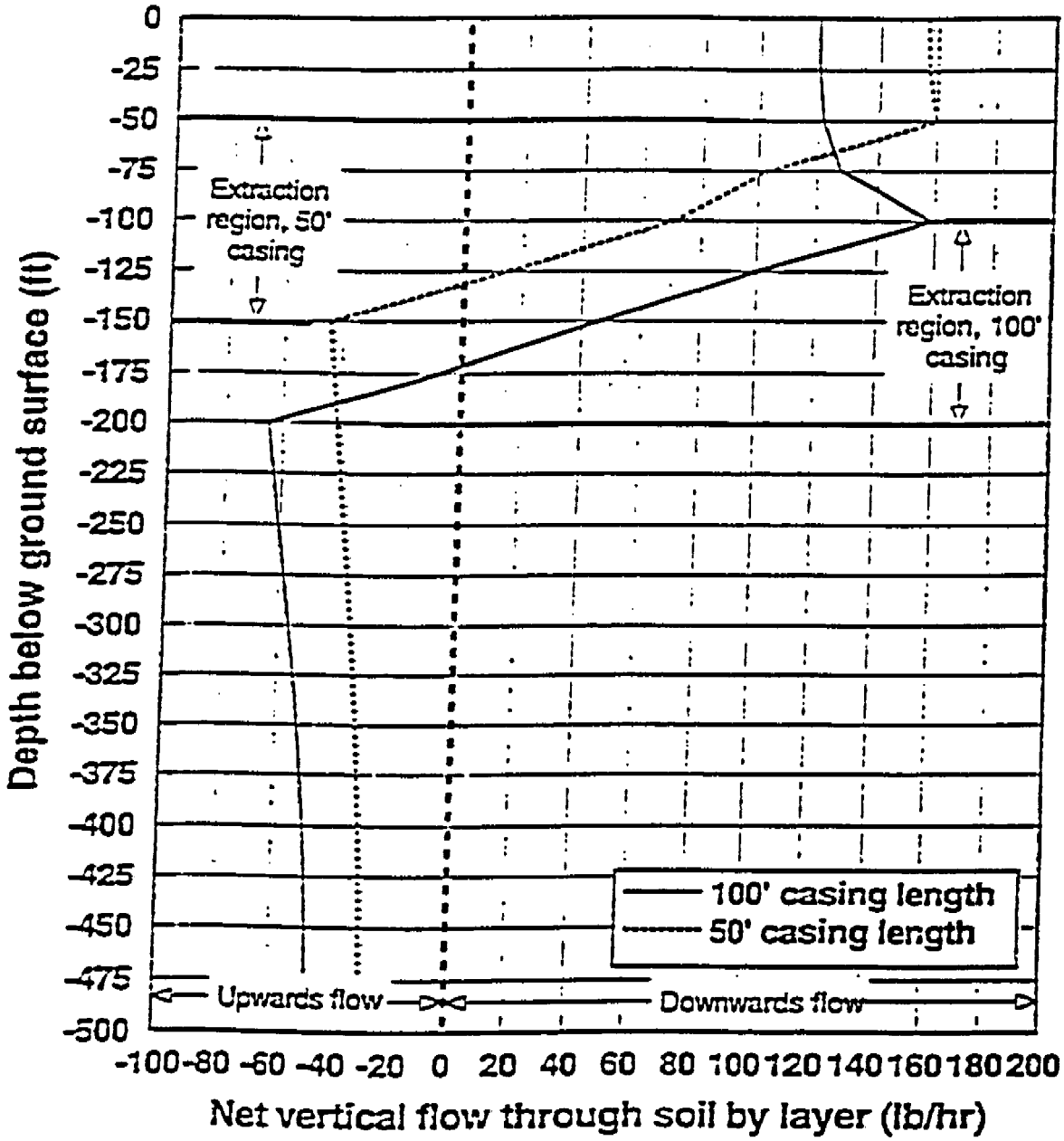

Figure 4. Net vertical flow through the medium for the baseline (50 ft) and the 100 ft. casing length runs.

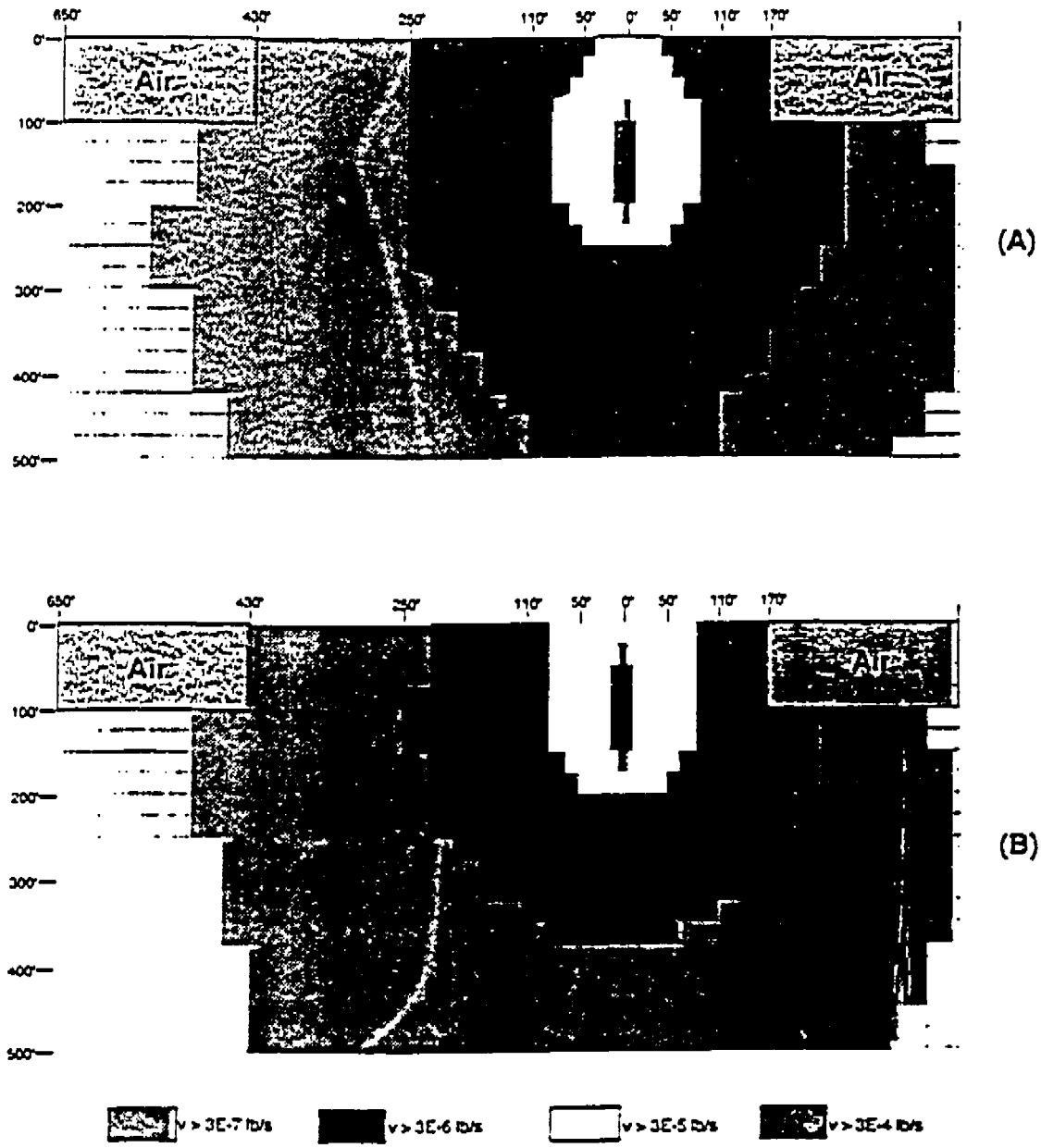

Figure 5. Velocity shadow plots for (A) the 100 ft. casing length and (B) the baseline runs.

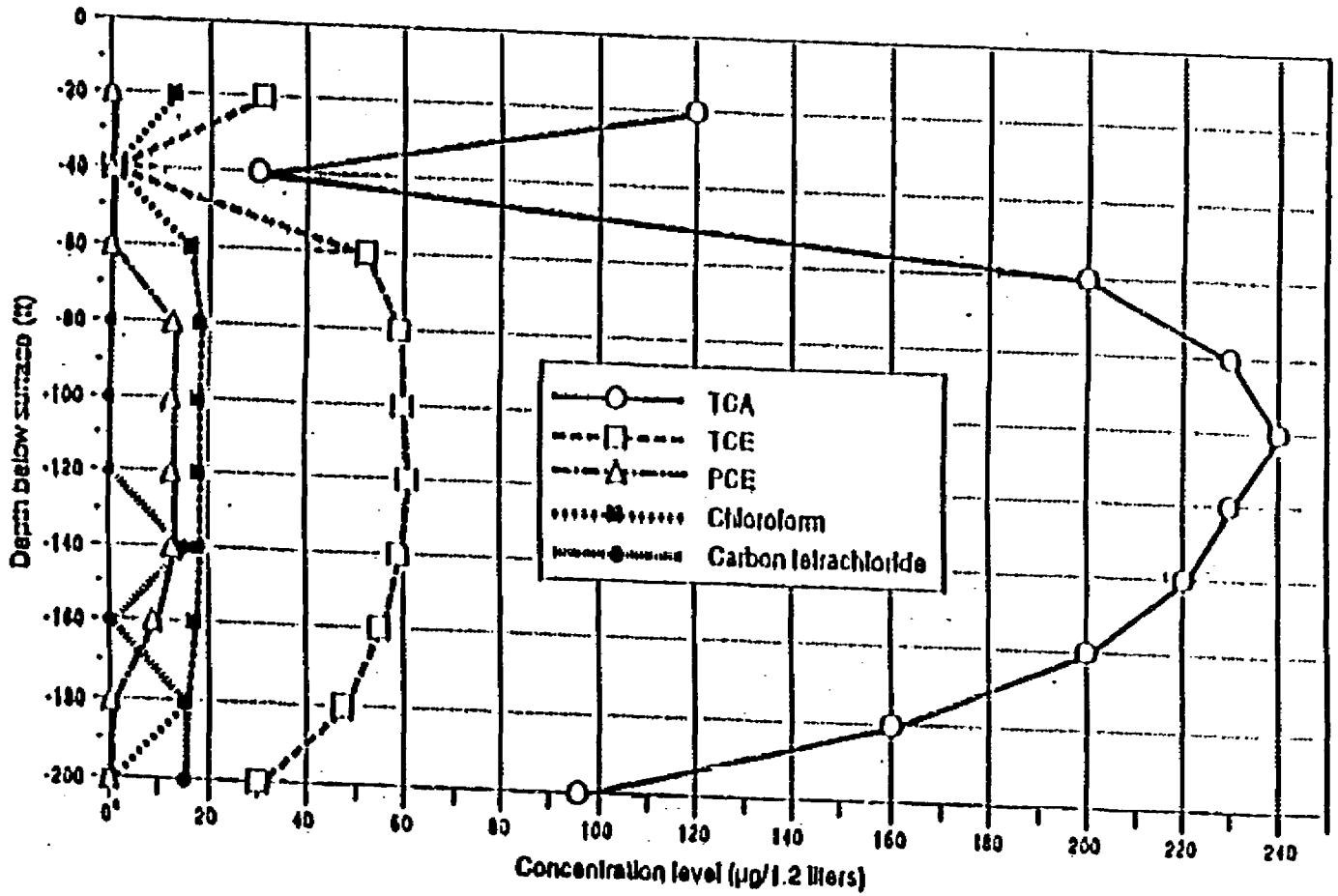

*Zero values indicate the contaminant was not detected in the sample.

Figure 6. VOC distribution at Well #24 for 9/91 sampling period.

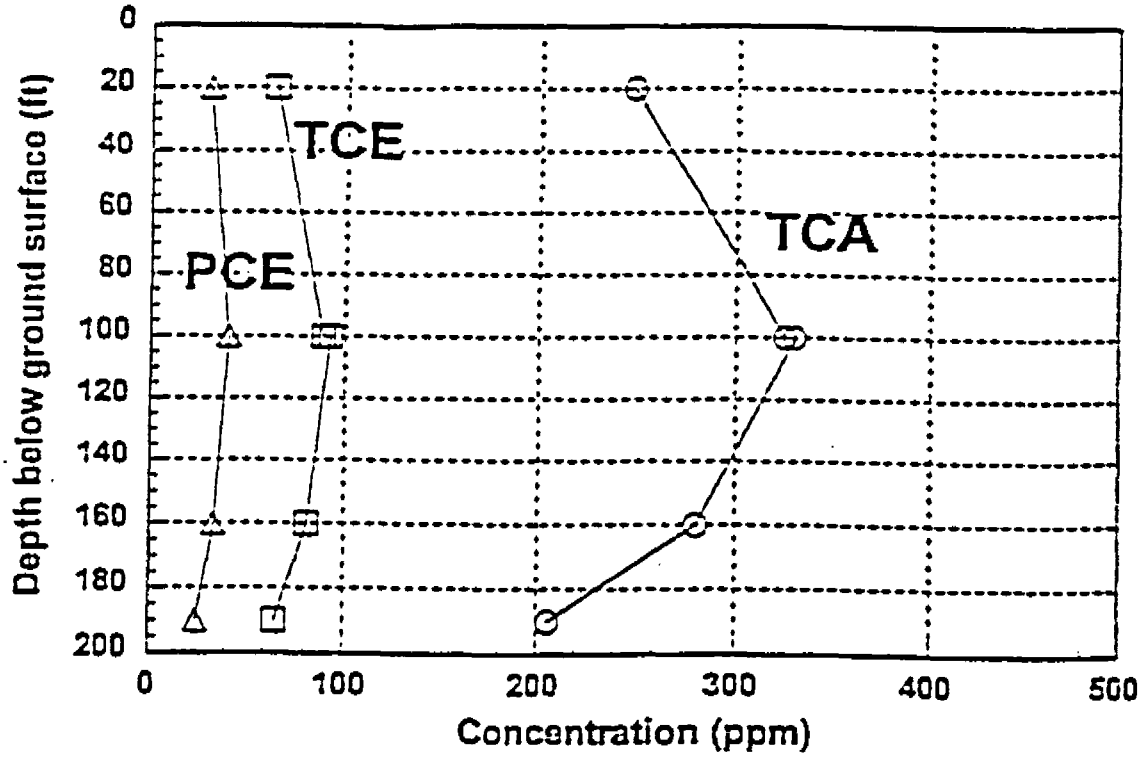

Figure 7. Contaminant plume measured in LLC-86-25 during the third quarter of 1994.

Results from the analysis show that the shorter zone gives slightly more flow from each layer (the shorter the extraction interval, the more closely a spherical flow field is approached). Doubling the length of the extraction zone causes the average flow from the well in each 25 ft. layer to drop from 63.4 to 58.3 lb/hr, a decrease of 8.1 percent. Additionally, the percentage of the replacement air from each source showed significant shifts. For the shorter extraction interval, a larger percentage of the replacement air comes from the mesa surface (75.0 percent versus 65.8 percent). Flow contributed by the valley floor and mesa sides remains essentially the same, while a smaller percentage of the flow is contributed by the remainder of the soil boundaries. Table 2 gives a breakdown of the origin of replacement air and air flow from the wells for the two cases.

Although there was a decrease in the flow by layer for the longer zone, it actually showed a larger area of influence from the extraction process. Figure 8 plots pressure versus distance from the extraction well for each of the two test cases at two depths (in the extraction interval (87.5 bgs) and at depth (187.5 bgs). As seen from the figure, very little area is influenced by the extraction at depth. Consequently, to remediate the contaminants at 200 ft. bgs with the currently proposed well drawdown of 50 inches w.c., either the extraction interval must extend to very near that depth or the extraction time must be sufficiently long for contaminants to be drawn up to the extraction region. The figure also shows

Table 2. Mass balance summary for extraction interval calculations.		
Mass balance summary	50' Casing length 100' extr. interval % of vented air contributed by surface	50' Casing length 50' extr. interval % of vented air contributed by surface
Flow thru mesa surface (A)	65.8%	75.0%
Flow thru mesa side, far (B)	0.5%	0.4%
Flow thru valley surface, far (C)	0.7%	0.5%
Flow thru soil, side below mesa, far (D)	0.5%	0.4%
Flow thru mesa side, near (E)	6.8%	5.0%
Flow thru valley surface, near (F)	5.8%	4.5%
Flow thru soil, side below mesa, near (G)	2.9%	1.8%
Flow thru soil, N/S sides, total (H)	4.8%	3.7%
Flow thru soil, bottom (I)	12.2%	8.7%
Flow from well (lb/hr)	233.21	126.88
Flow from first 25' interval of the extraction zone	61.26	63.70
Flow from second 25' interval of the extraction zone	56.33	63.18
Flow from third 25' interval of the extraction zone	55.88	
Flow from fourth 25' interval of the extraction zone	59.73	
AVERAGE (lb/hr)	58.30 (12.96 SCFM)	63.44 (14.10 SCFM)

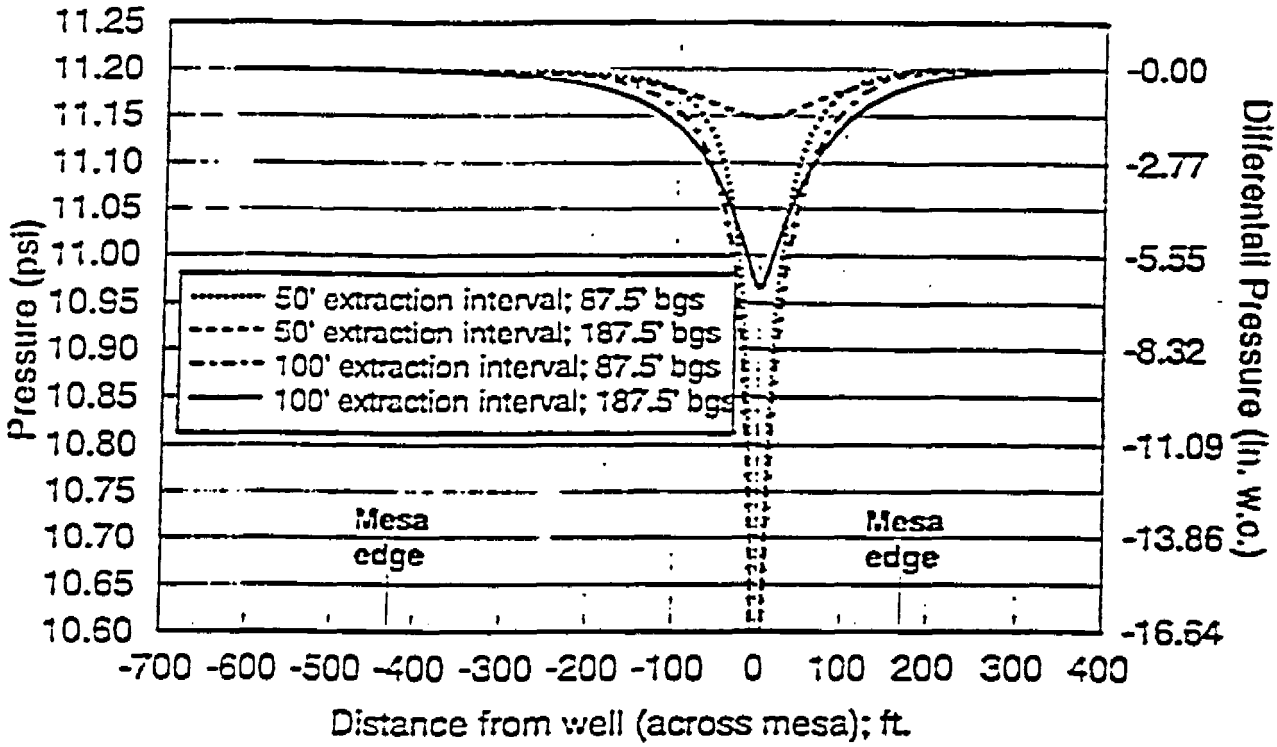

Figure 8. Comparison of the calculated steady-state pressure response at several depths for the 50 and 100 ft extraction interval cases.

that the mesa edge closest to the well (170 ft.) has little effect on the calculated pressure response. Figure 9 shows the pressure contours for cross-sections across the mesa through the well for the two cases.

Using the fan curve for the pump chosen for the test (Section 5), the proposed 50-inch w.c. draw-down (at 60°F and 11.2 psi), and the calculated maximum extraction rate per 25 ft. of extraction zone length of 1200 cubic feet per hour, the maximum length of the extraction zone treated by the selected blower will be approximately 140 ft. (i.e., the blower has sufficient capacity to support this test). Again referring to the contaminant profiles from wells near the proposed location of the extraction experiment (Figures 6 and 7), and assuming a casing length of 75 ft., an extraction interval of 125 ft. would allow air to be extracted over the depth of the measured contaminant plume. Or, a shorter extraction length of 75 ft. would draw a smaller total volume of air but with a higher concentration of contaminants per volume, letting the replacement air draw contaminants above the casing (75 ft. bgs) down to the extraction zone and contaminants below the extraction interval (150 ft. bgs) up to the extraction zone. Due to the relatively short test period (6 months) the 75 ft. extraction length is recommended.

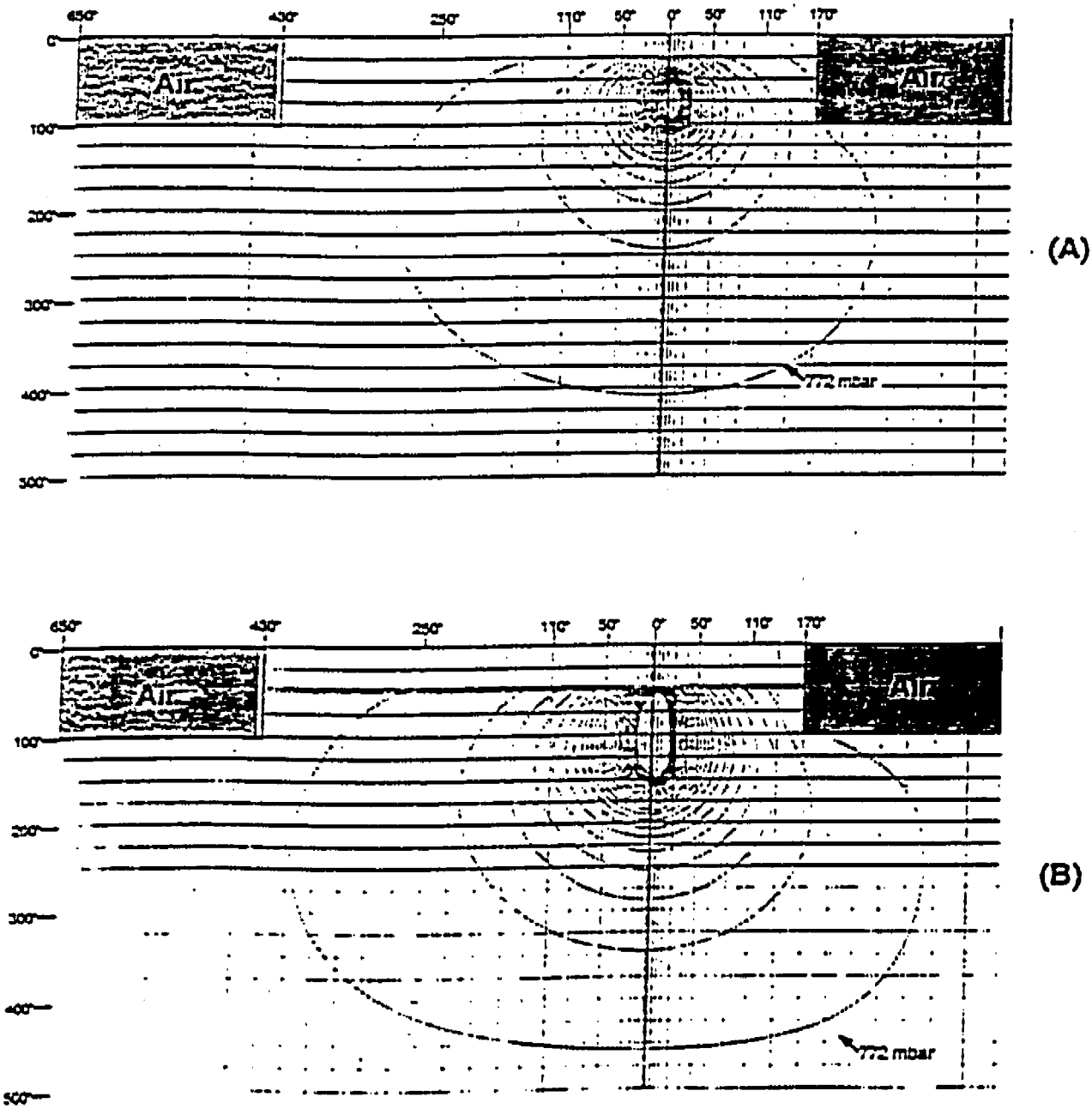

Figure 9. Steady-state pressure contours through a cross-section of the mesa (A) 50 ft. casing, 50 ft. extraction interval, and (B) 50 ft. casing, 100 ft. extraction interval.

C. TRANSIENT RESPONSE

A transient analysis was performed on the recommended case (75 ft. casing depth with the extraction interval extending from the bottom of the casing to a total depth of 150 ft. bgs) to determine the region of influence of the extraction process as a function of time. The analysis was run to 2000 hours as the low average permeability of the medium (1.5 Darcies) would impede flow. Steady state conditions were reached after less than 200 hours of extraction, with over 99 percent of the calculated pressure response at any given distance from the well occurring within the first 30 hours of extraction. Pressure contours for various times are shown in Figure 10. Figure 11 plots pressure profiles versus distance from the extraction well for several extraction times for a region in the extraction interval. Figure 12 plots pressure histories for numerous distances from the extraction well at a depth of 137.5 ft. bgs (the center of the extraction region). Figure 12(A) shows values calculated for distances between the well and the southern mesa edge. Figure 12(B) shows values calculated for points between the well and the northern mesa edge. Pressure histories for points within a 75-ft radius of the well showed no differences, e.g. the mesa edge did not affect the calculated pressure histories near the well, even with the well located only 170 ft from the northern mesa edge. A measurable pressure differential (1 inch w.c.) was calculated to distances up to 125 ft from the extraction well. Pressure changes less than 1 inch w.c. will be difficult to differentiate from variations due to barometric pressure oscillations.

D. BOUNDARY CONDITION CHECK

The general model set-up used for initial validation calculations is shown in Figure 13. The extraction well was given a 50-inch water column drawdown and was modeled as a 0.524 ft. square (giving it the equivalent area of an 8-inch diameter well). It was located in the center of a 600-ft. wide by 600 ft. long by 500 ft. high grid. The mesa was modeled as a block 300 ft. wide by 600 ft. long by 100 ft. high. An air block was simulated on either side and above the mesa by assigning the zones a very high permeability and porosity (10,000 Darcies and 95 percent, respectively). A homogeneous medium with a permeability of 1.5 Darcies and porosity of 30 percent was used for the remainder of the model. Constant pressure boundaries were assigned to all surfaces of the model.

As with all model simulations, the parameters chosen in the model set-up can adversely affect the results. In particular, boundary conditions and locations, and cell dimensions are often suspect. Each of these parameters was tested; results were compared against the baseline case.

The location and conditions used for the side boundaries reflect the actual geometry and physical characteristics of the mesa. The surface boundary of air was modeled using a permeability of 10,000 Darcies. Higher and lower permeability values were tested (1,000 and 100,000 Darcies). No

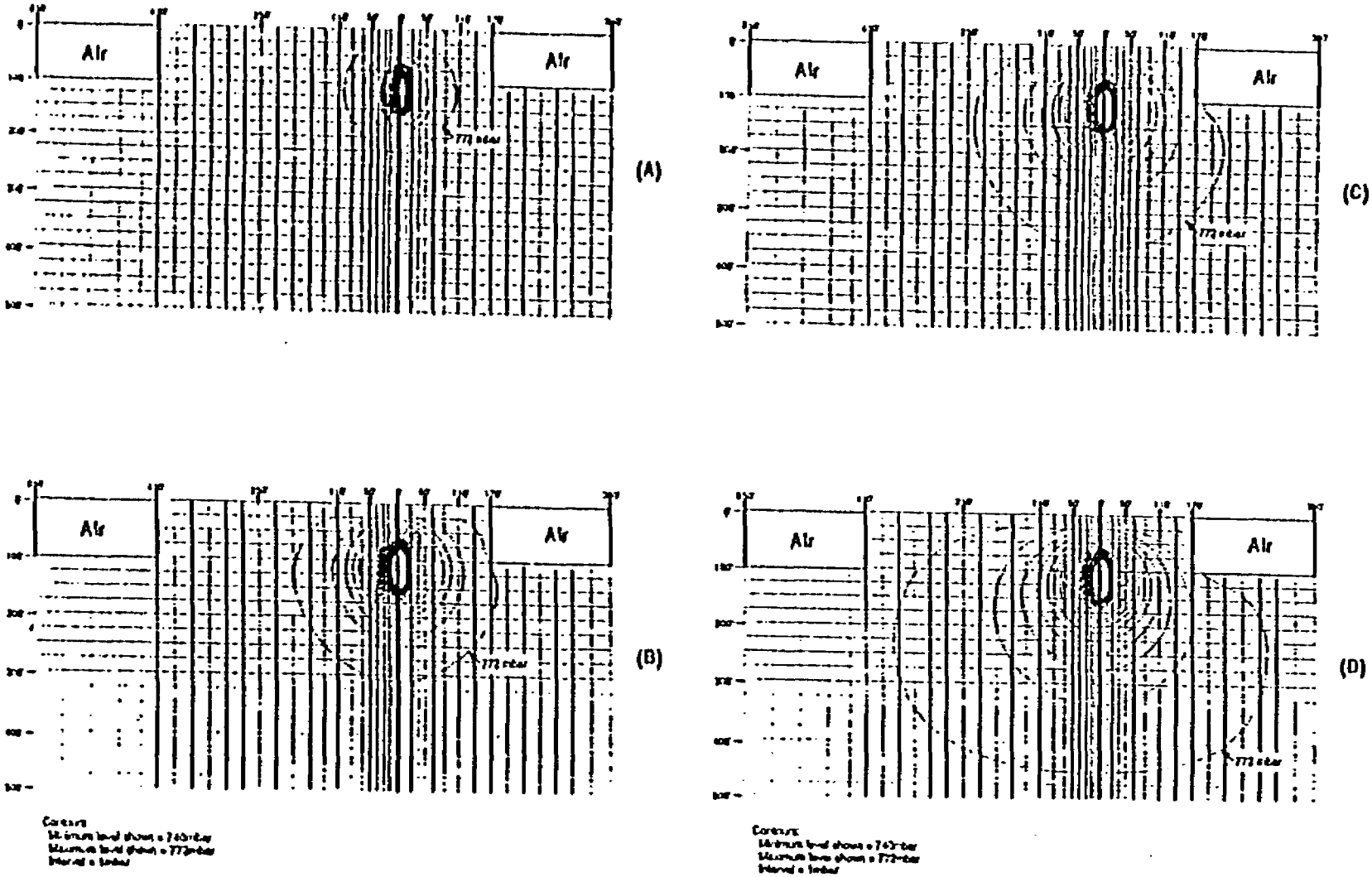

Figure 10. Series of pressure contours through a cross-section of the mesa with time for the recommended case; (A) after 0.85 hours, (B) after 5.26 hours, (C) after 10.86 hours, and (D) at steady state conditions.

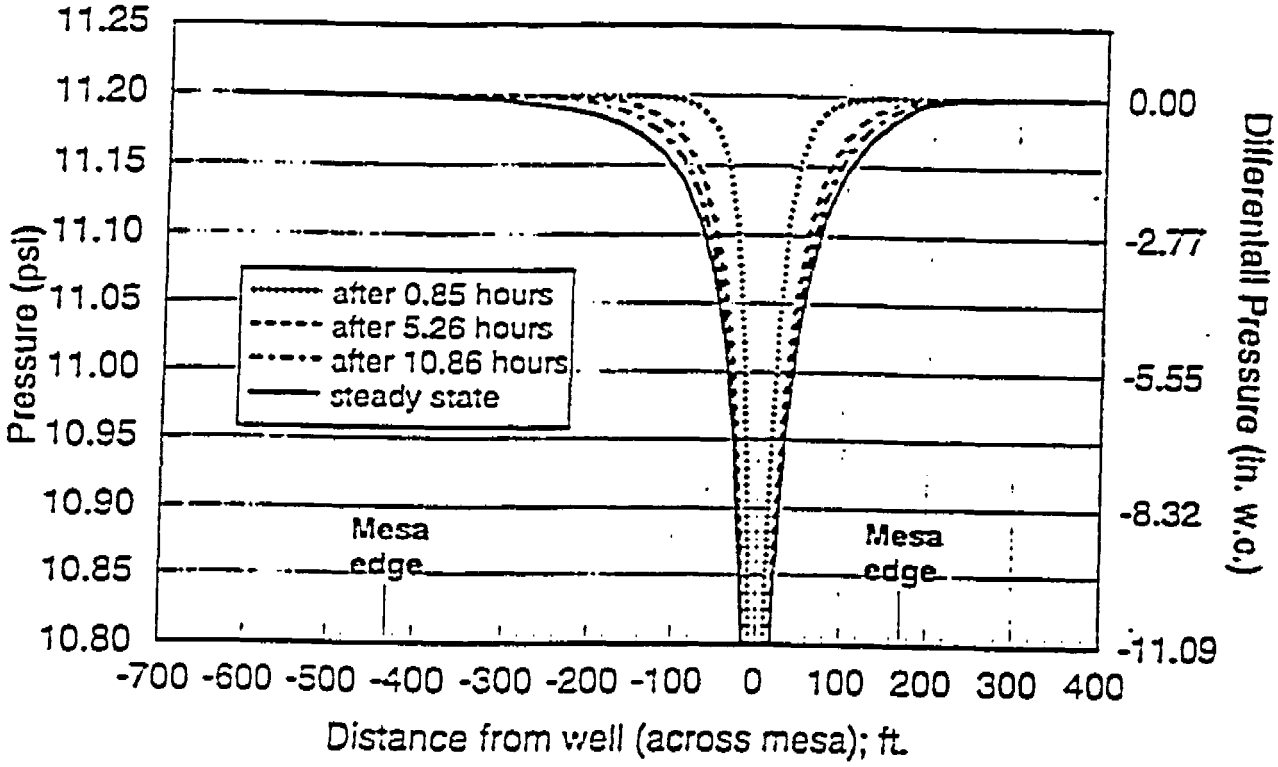

Figure 11. Comparison of the calculated pressure response at several time steps for the recommended case.

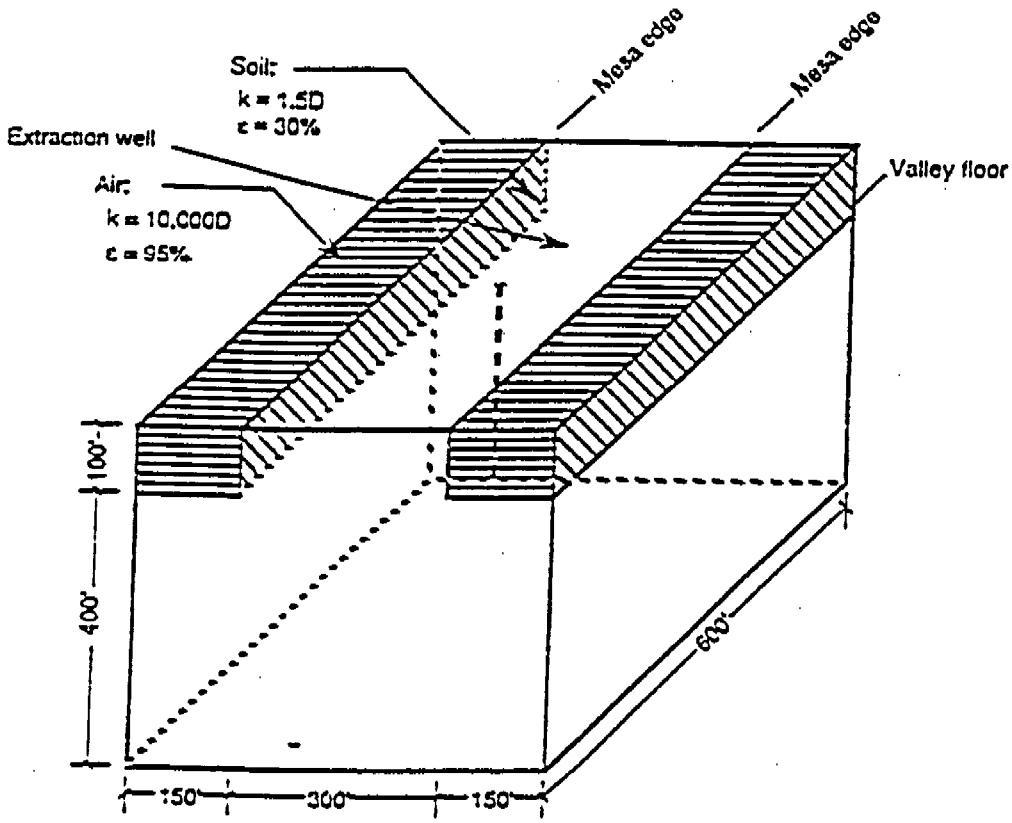

Figure 13. Schematic of the geometric model initially used.

change was noted in code results. The bottom boundary condition chosen is arguably the least likely to model reality. The geology and soil characteristics below 300 ft. are not known as well as they are from the surface to 300 ft. A basalt layer begins near the 300 ft. depth, and permeability in this region could be very different than the values measured in the existing monitoring wells. Even if the permeability doesn't change significantly at the tuff/basalt interface, it could easily change at some greater depth. Two simulations were performed to test the affect of changing the bottom boundary. In the first case, the boundary condition was changed from constant pressure to no-flow. In the second, a very low permeability (k = 0.01D) region was added between 325 and 350 ft. bgs, simulating a region of low permeability but also checking how the location of the bottom boundary affected the results. Figures 14 through 16 show the calculated cross-sectional pressure contours for the cases. Figure 17 plots the pressure versus distance curves for all three cases. While pressure contours at the mesh boundaries are noticeably different, the results near the extraction interval show no change from the baseline case. Resultant flow rates were virtually identical.

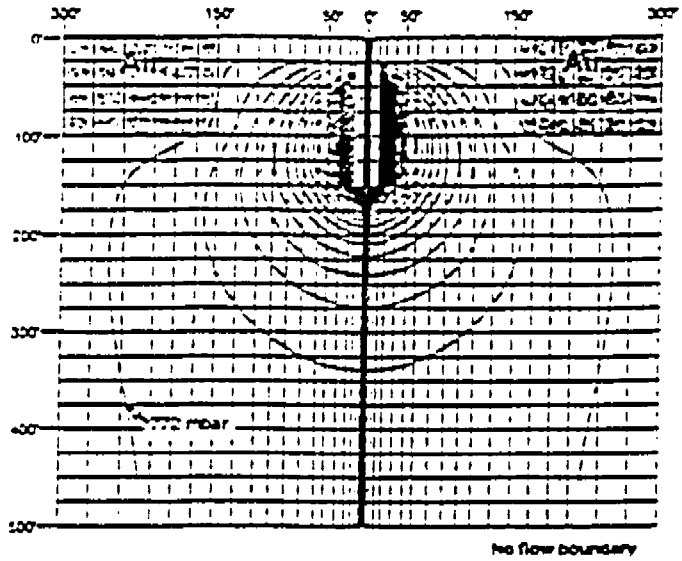

Figure 14. Steady state pressure contours through a cross-section of the mesa for a 50 ft. casing length, 100 ft. extraction interval case with a no flow boundary at the bottom surface.

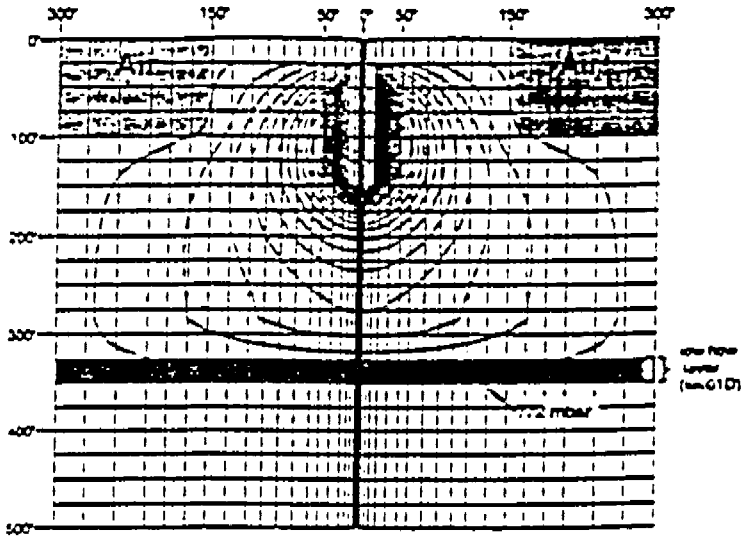

Figure 15. Steady state pressure contours through a cross-section of the mesa for a 50 ft. casing length, 100 ft. extraction interval case with a low flow layer between 325 and 350 ft. bgs.

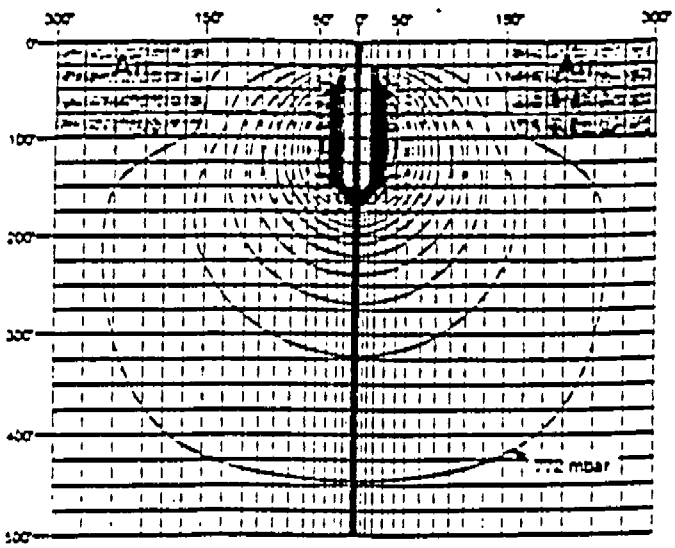

Figure 16. Steady state pressure contours through a cross-section of the mesa for the baseline case of a 50 ft. casing and 100 ft. extraction interval.

Contours:
Minimum level shown = 740mbar
Maximum level shown = 772mbar
Interval = 1mbar

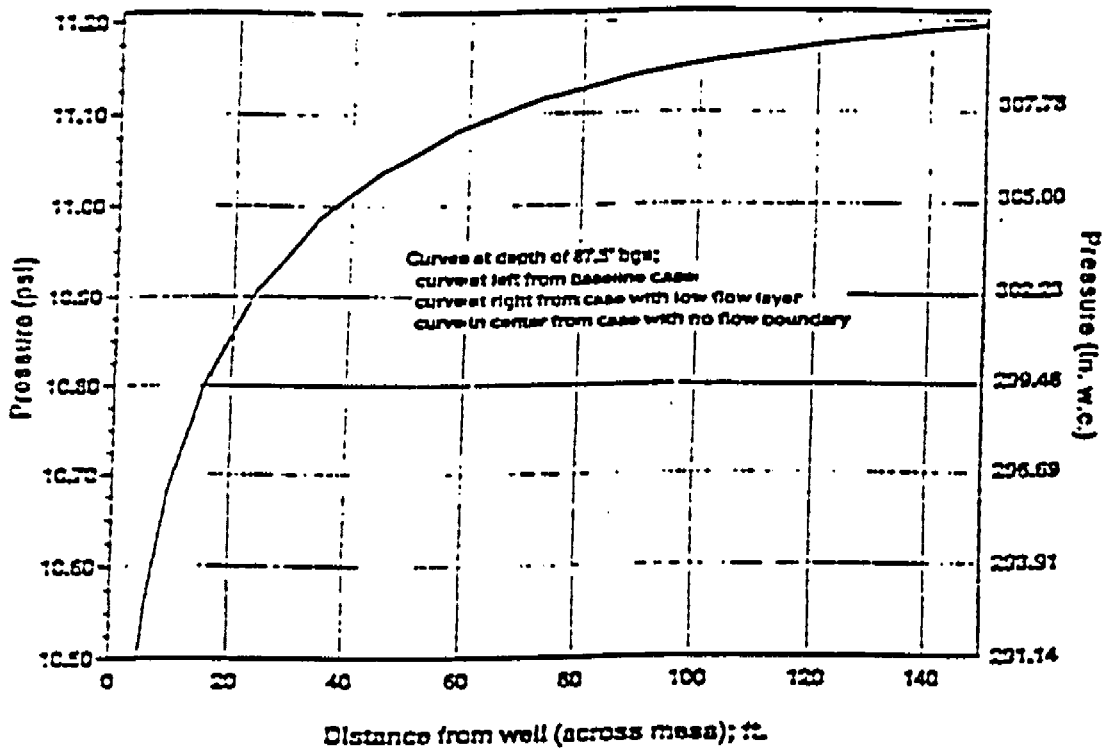

Figure 17. Comparison of steady-state pressure response at 87.5 bgs (in the extraction interval) for all three cases checking the bottom boundary conditions. Curves are identical on this scale, indicating that the bottom boundary condition of the mesh was not violated.

Finally, all dimensions were checked to assure the zoning did not affect results. Adjacent cells in the x-y plane were limited to a 50 percent increase in the baseline model. A test case restricting this increase to 20 percent was run. Results were the same for both runs.

Extensive checks were also performed to validate the code. Checks were performed against analytical models, a two-dimensional cylindrical model, and a University of Wisconsin two-dimensional heat flow code.

SECTION 3
EXTRACTION AND MONITOR WELL LAYOUT

Section 2.C discussed how the proposed extraction well (75-ft. casing, 75-extraction interval) would influence the surrounding medium with time given a homogeneous, 1.5D permeability, 30 percent porosity medium.

Previous field experience at the site has shown that slanting a well may substantially increase fracture flow in the medium. To help determine how this characteristic might affect the region of influence of the extraction well, two additional transient cases were run. In the first case, the permeability of the soil was increased from 1.5D to 6D.* (all else remaining the same as the baseline proposed extraction geometry). In the second case, a non-homogeneous medium was modeled where the bulk of the grid was given a permeability of 1.5D, with the extraction region (75 to 150 bgs) having a permeability of 6D. Figures 18 and 19 show cross-sections of pressure contours at several different times for the cases. Figure 20 shows the calculated pressure versus distance from the well for 137.5 ft. bgs (the center of the extraction region) for each case. Figures 21 and 22 depict pressure histories for numerous radial distances from the extraction well at this same depth (137.5 ft. bgs). Table 3 gives a mass balance summary for each of the comparison cases and the baseline recommended case.

Increasing the permeability affects how quickly the region of influence changes. In the lower permeability case, steady state conditions were reached after slightly less than 200 hours of extraction, with over 99 percent of all pressure changes occurring within the first 30 hours of extraction. In the higher permeability case, steady-state conditions are reached after approximately 80 hours of extraction, with 99 percent of all pressure changes occurring after only 8 hours of extraction.

In the non-homogeneous case, the region influenced by the extraction is increased from 120 ft. to over 150 ft., with a 2.1 inch w.c. drawdown being seen at 147.5 ft from the well. In this case, the mesa edge is marked on the resultant pressure profiles.

---

* The original permeability of 1.50D was chosen as a medium value measured in monitoring wells numbers 54-1003 and 54-1004. The 6D value was chosen as a conservative median measured in borehole 54-1006 (a slant well) for the proposed extraction region. Permeability data was taken from the 1994 SEA in-situ measurements.

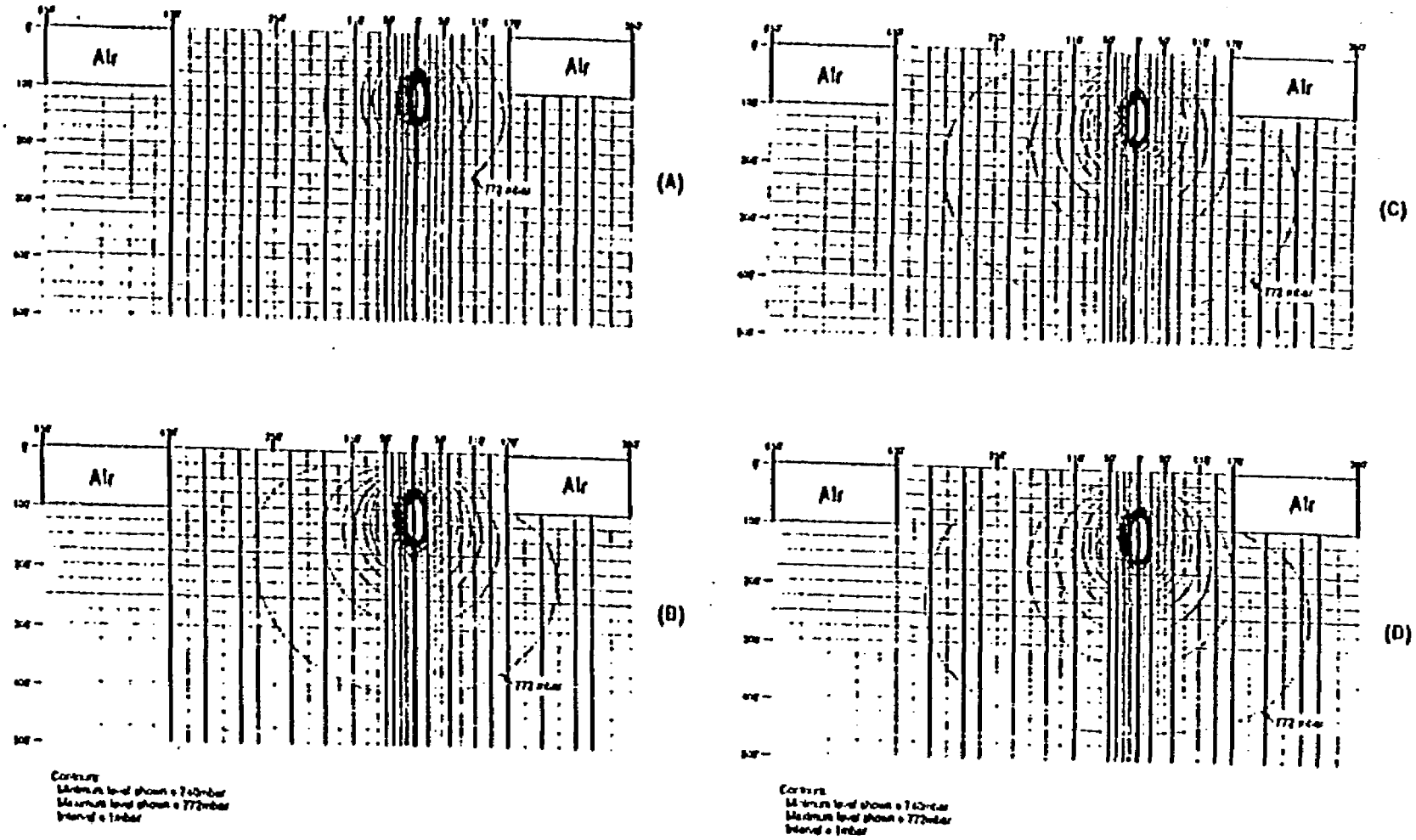

Figure 18. Series of pressure contours through a cross-section of the mesa with time for the homogeneous, increased permeability case (k=6D); (A) after 0.85 hours, (B) after 5.26 hours, (C) after 10.86 hours, and (D) at steady state condition.

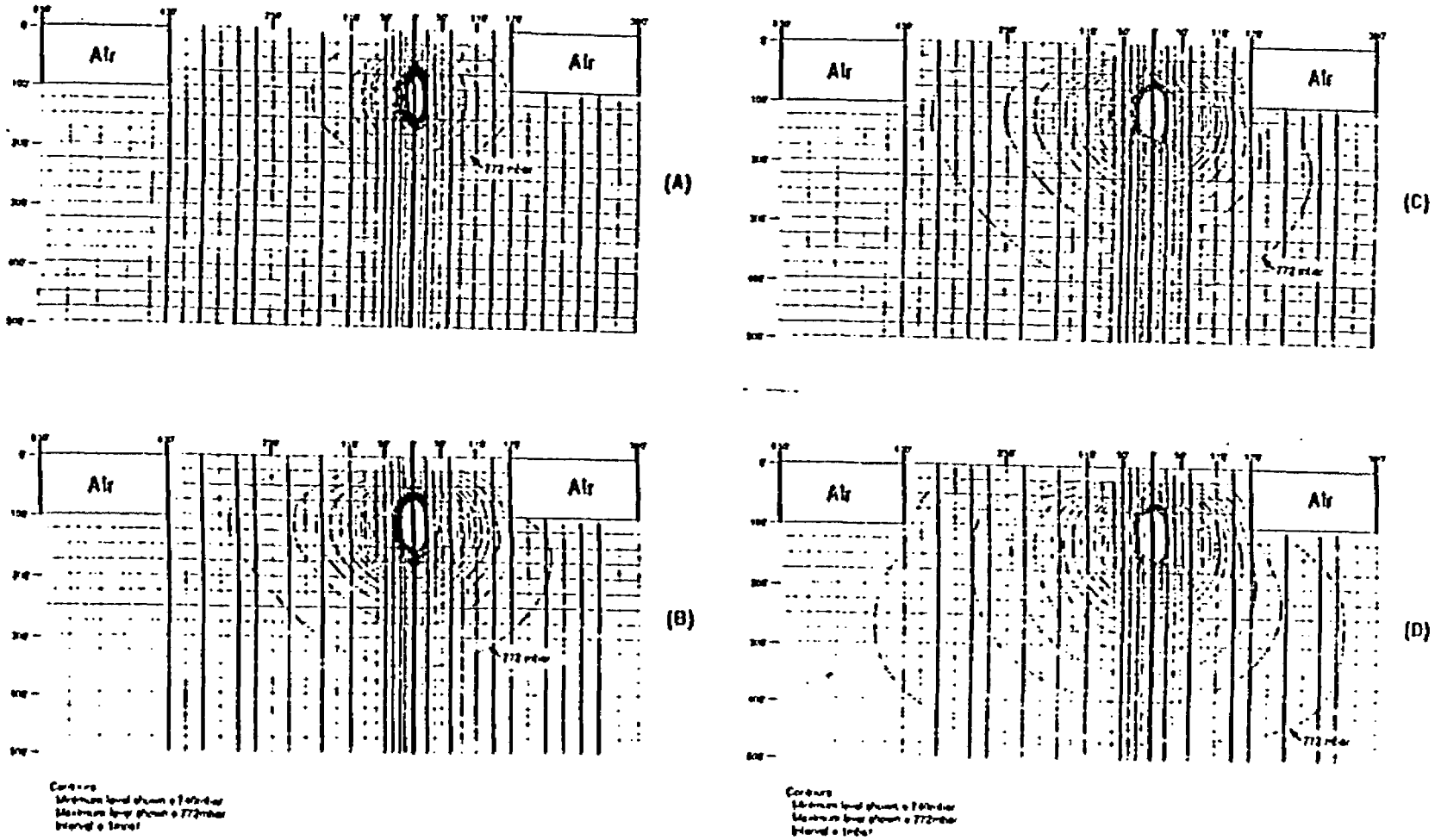

Figure 19. Series of pressure contours through a cross-section of the mesa with time for the non-homogenous case; (A) after 0.85 hours, (B) after 5.26 hours, (C) after 10.86 hours, and (D) at steady state conditions.

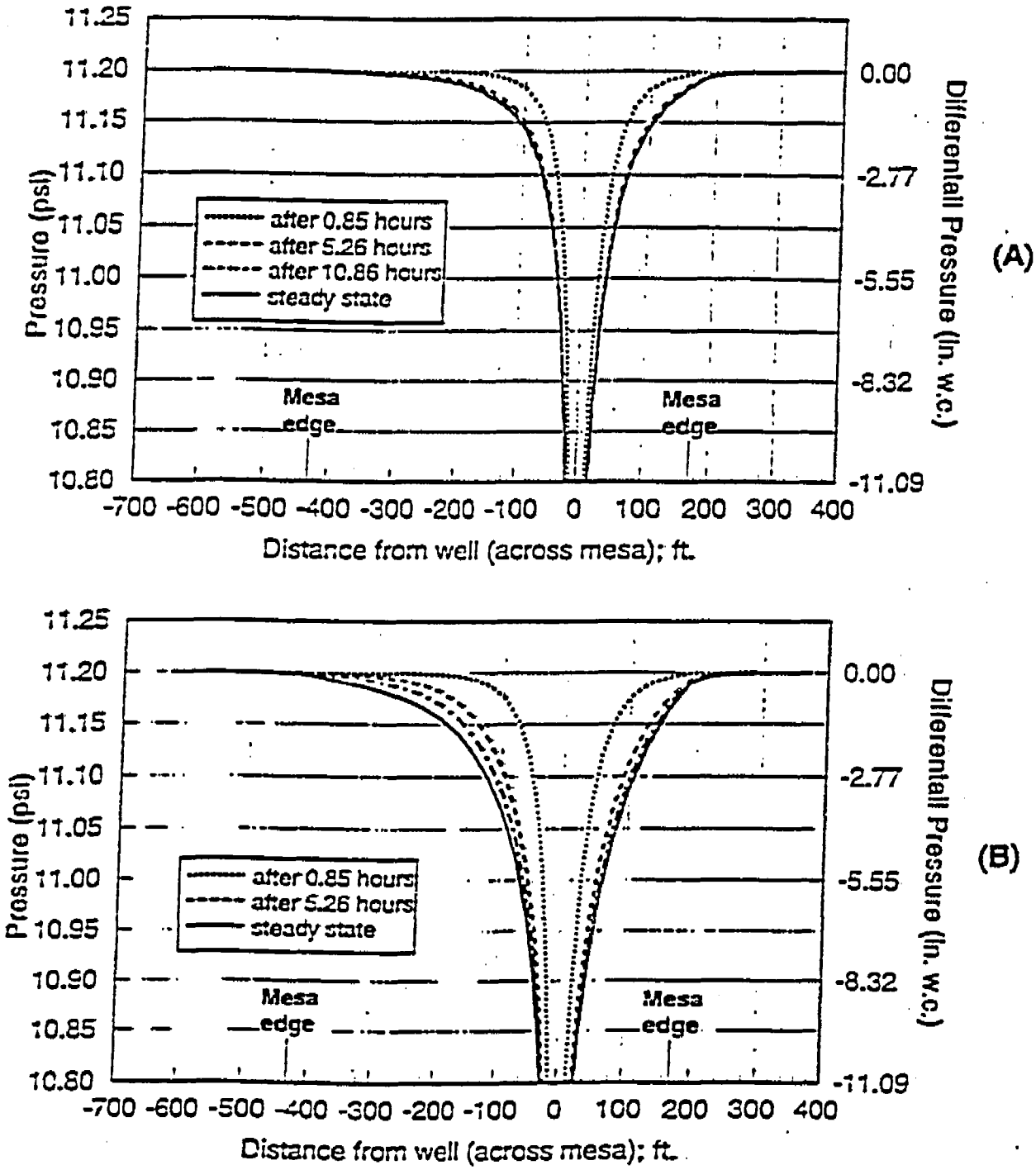

Figure 20. Comparison of the calculated pressure response at several time steps for (A) the homogeneous case of k=6D and (B) the non-homogeneous case.

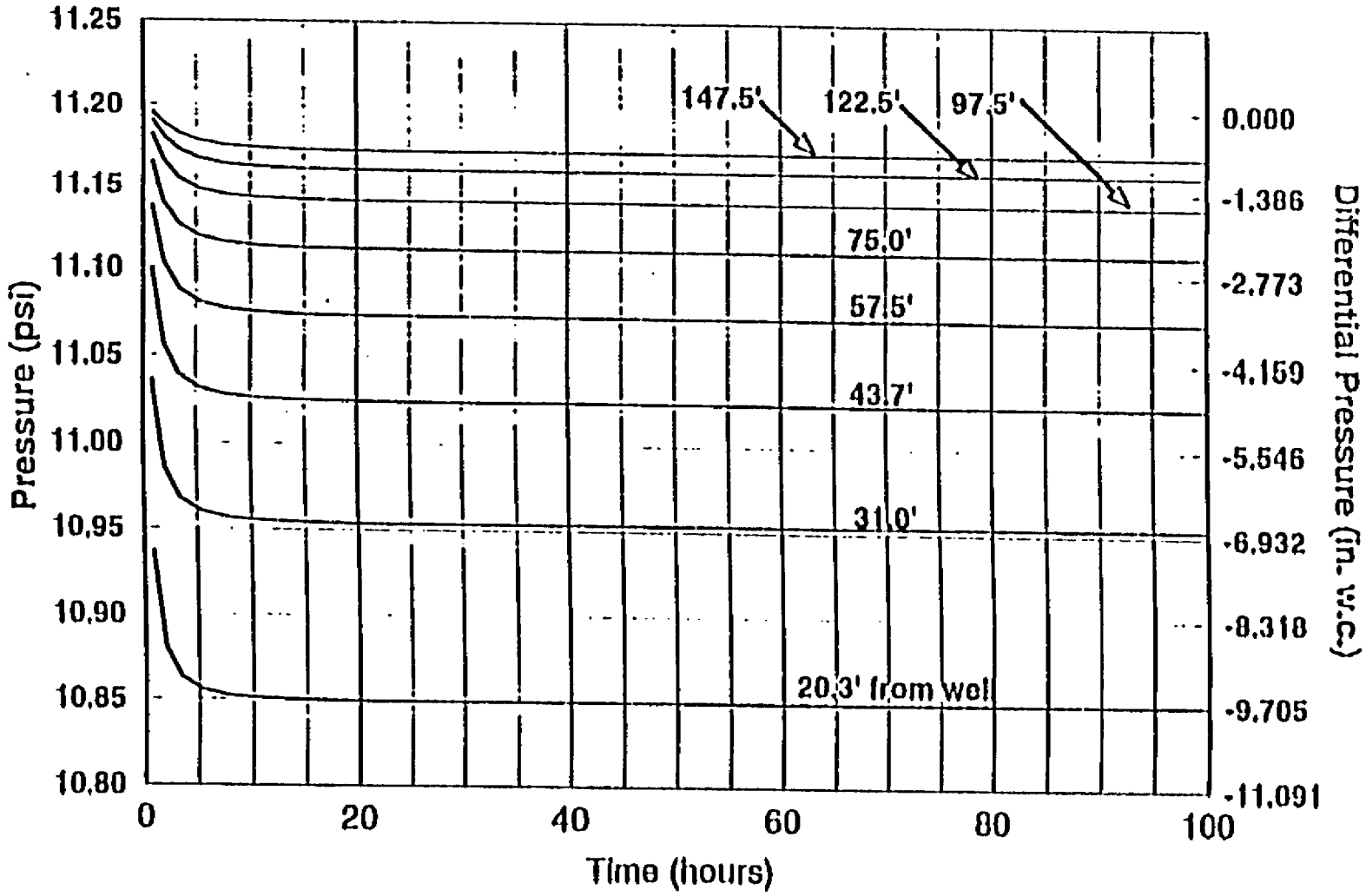

Figure 21. Calculated pressure histori. s at 137.5 bgs (in the center of the extraction region) for the homogeneous case of k=6D.

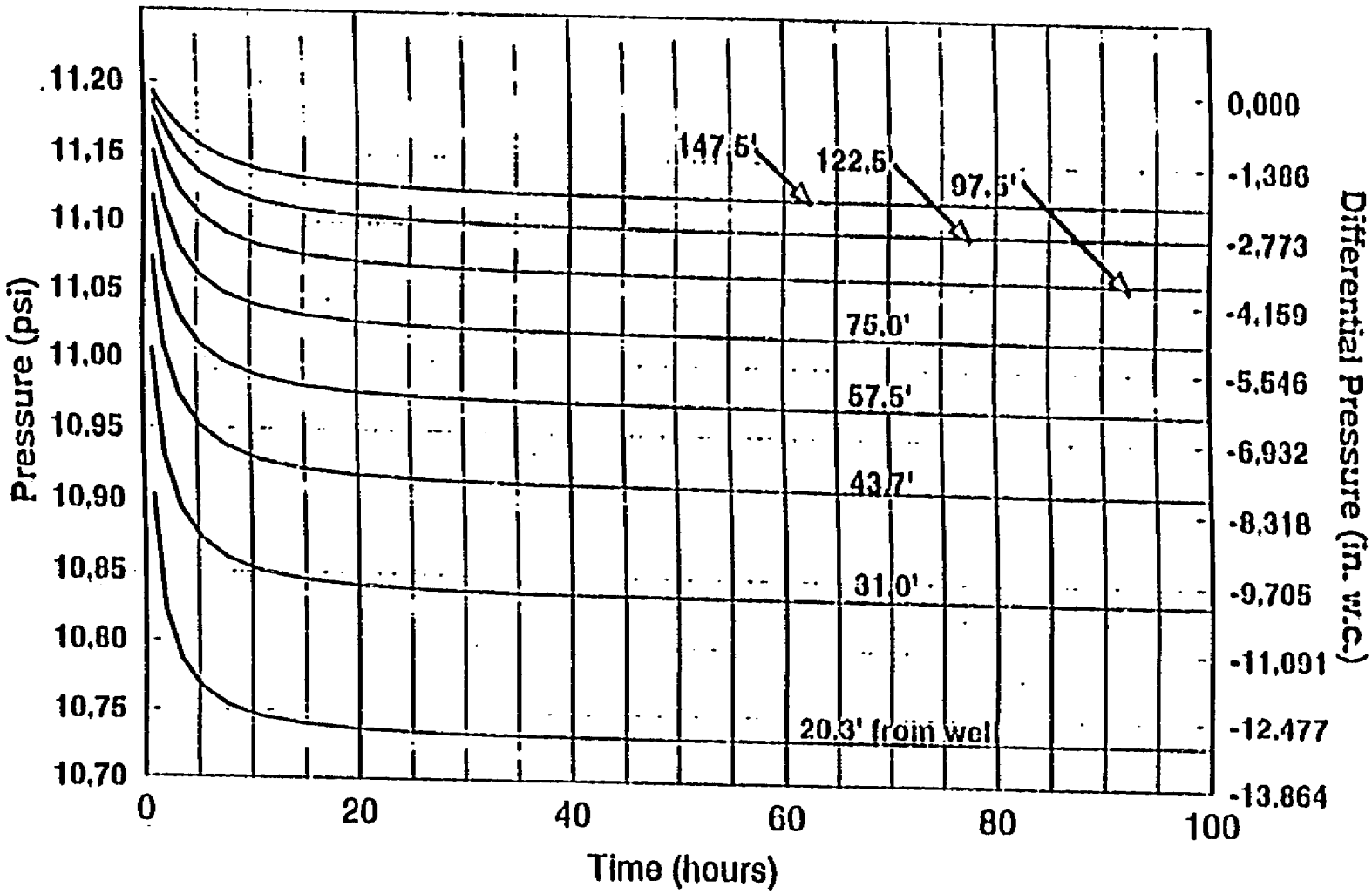

Figure 22. Calculated pressure histories at 137.5 bgs (in the center of the extraction region) for the non-homogeneous case.

Table 3. Mass balance summary for the extraction well location calculations.			
Mass balance summary	75' casing length 75' extr. interval homo. medium, k=1.5D % of vented air	75' casing length 75' extr. interval homo. medium, k=6D % of vented air	75' casing length 75' extr. interval non-homo. medium % of vented air
Flow thru mesa surface (A)	62.5%	62.1%	50.5%
Flow thru mesa side, far (B)	0.6%	0.6%	2.0%
Flow thru valley surface, far (C)	0.2%	0.8%	2.0%
Flow thru soil, side below mesa, far (D)	0.6%	0.6%	0.5%
Flow thru mesa side, near (E)	6.2%	6.2%	13.1%
Flow thru valley surface, near (F)	6.6%	6.6%	12.5%
Flow thru soil, side below mesa, near (G)	3.4%	3.3%	1.8%
Flow thru soil, N/S sides, total (H)	5.5%	5.5%	8.5%
Flow thru soil, bottom (I)	14.3%	14.2%	9.1%
Flow from well (lb/hr)	179.06 (39.8 SCFM)	716.26 (159.2 SCFM)	636.72 (141.5 SCFM)

Thus, depending on how the well is drilled and the resulting medium characteristics, a measurable pressure response should be seen to at least 120 ft. from the well. It would be most beneficial if the extraction region could be located in a central area to the existing monitoring wells. If the monitor well is drilled at a 25 degree angle from vertical to the south to maximize air flow, it will be parallel to wells 54-1001, 54-1002 and 54-1006. If it is drilled to the proposed depth of 150 ft. bgs with the well head due east of 54-1006, the center of extraction region would be approximately 40 ft. from the vertical borehole 54-1004, 80 ft. from boreholes 86-24 and 86-25, and 40 ft. from the slant borehole 54-1006. None of the other existing wells would be close enough to see a significant pressure response from the extraction unless there is some geologic characteristic (layers of higher permeability, fractures, etc.). Location of the new monitoring well would depend on whether the well was drilled vertically or at an angle. If it is vertical, it could be placed halfway between the center of the extraction interval of the extraction well and borehole #54-1004 (due west of 54-1004). This would allow it to measure the near field pressure response, approximately 20 ft. from the extraction well. If it is angled, it could be placed between the extraction well and 54-1006, again placing it approximately 20 ft. from the extraction well. Figure 23 shows a plan view of the site, with projections of the pertinent slant wells. Radial distances of 20, 40, 60, 80, and 100 ft. from the mid-point of the extraction region are shown.

While drilling the well at an angle will maximize air flow (and thus contaminant removal), it will also make it more difficult to interpret/model results from the field test. If the extraction well is drilled vertically, it could be located 30 ft. south of 54-1004. This would place it in line along a N/S array of wells which include 86-25, 54-1004, 86-24, and 54-1003 giving monitoring points at distances of 102, 30, 41, and 88 ft. respectively. Monitoring ports in the slant well 54-1006 would also be within the anticipated region of influence. Ports in the extraction plane would be approximately 80 ft. from the extraction well. None of the other existing wells would be close enough to see a significant pressure response. The new monitor well would be used to measure the near field pressure response (20 ft from the extraction well). If it is located east of the monitoring well it could also be used to help determine non-homogeneous characteristics of the medium. Figure 24 shows a plan view of this proposed layout. Radial distances of 20, 40, 60, 80, and 100 ft. from the extraction region are shown. Because the vertical installation would both move the extraction well further from the highly contaminated area of the mesa and allow for a more straightforward interpretation of the field test results, it is this scenario which is recommended.

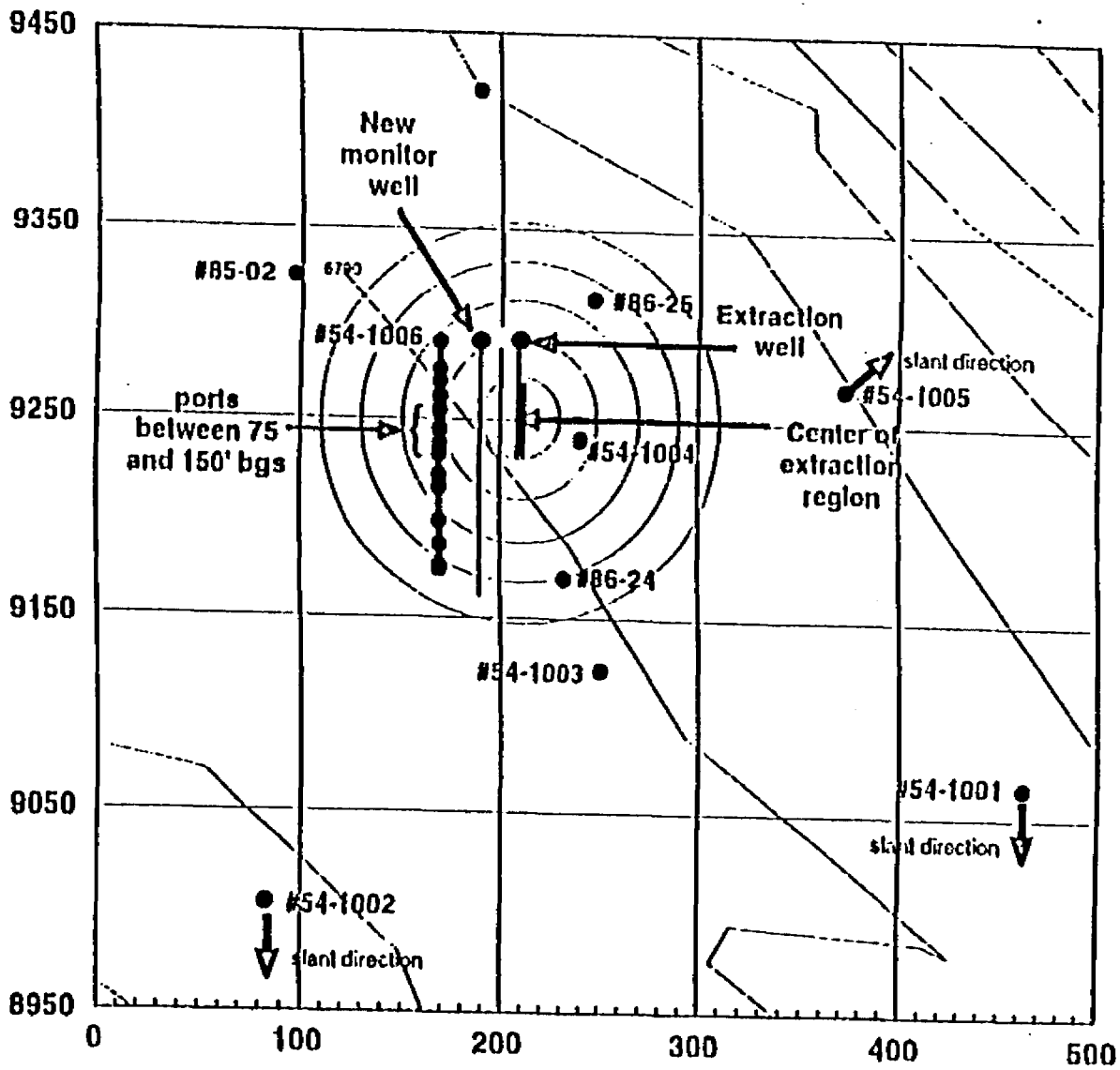

Figure 23. Proposed layout of the new extraction and monitoring well if they are drilled at a 25° angle to vertical. Radial contours shown are 20, 40, 60, and 100 ft. from the center of the extraction region.

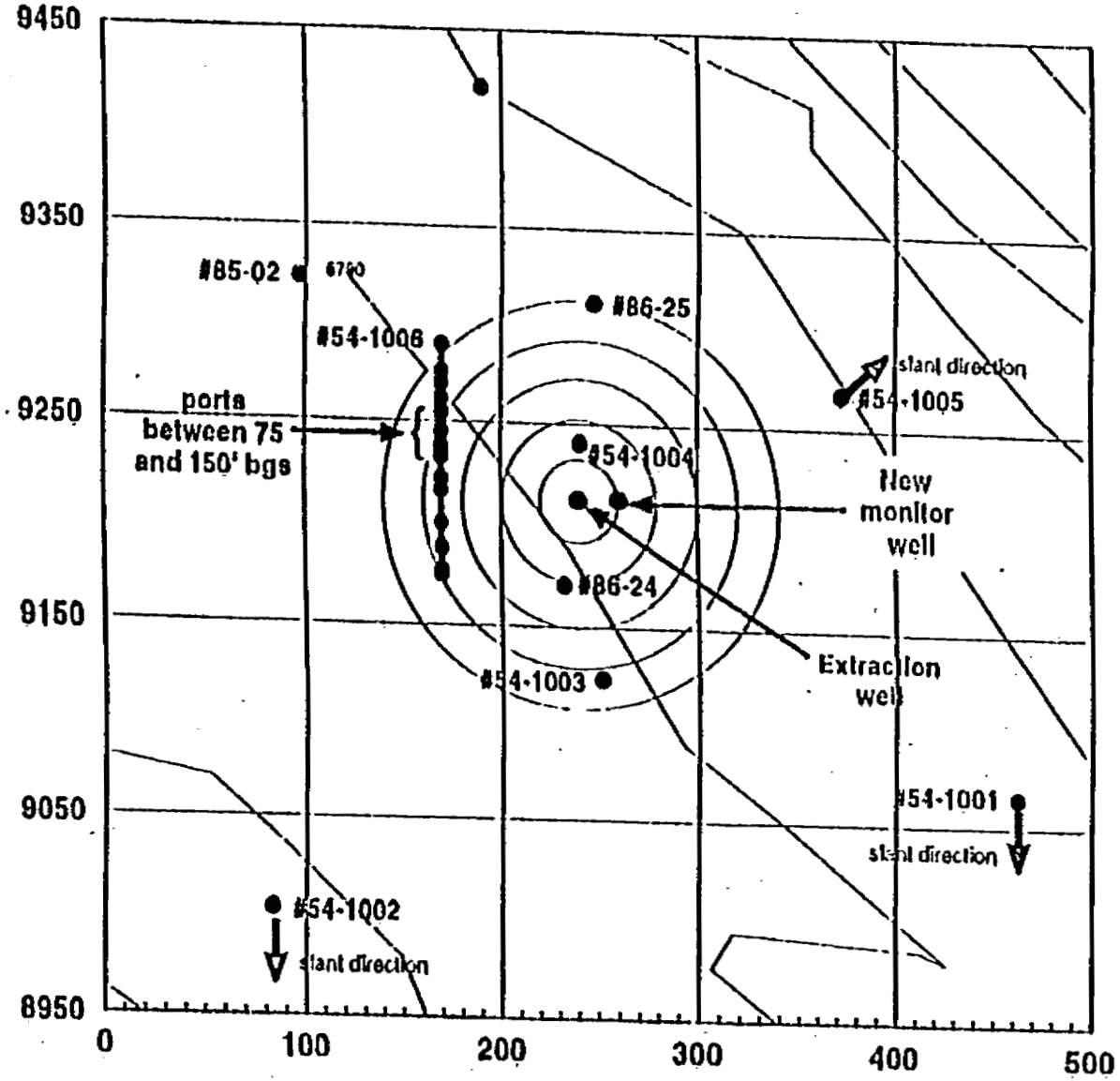

Figure 24. Proposed layout of the new extraction and monitoring well if they are drilled vertically. Radial contours shown are 20, 40, 60, 80, and 100 ft. from the extraction well.

SECTION 4

REGULATORY ISSUES ASSOCIATED WITH VAPOR EXTRACTION SYSTEMS AT TA-54

Air Emissions

The following is a summary of pertinent information found on air emission standards. Most of the standards are an outgrowth or expansion of the Clean Air Act Amendment which was signed into law by President George Bush in 1990. Portions of the act are still evolving as they are phased in. The purpose of the act was to establish national air quality standards and to enforce those standards through operating permits. The operating permit is administered on the state level, where each state submits a permit program to the EPA for approval. New Mexico submitted its permit program on November 15, 1993. On May 19, 1994 the EPA proposed interim program approval (59 FR 26158).

The operating permit program for New Mexico is administered by the State Environment Department, Air Quality Bureau under Air Quality Control Regulation 702 - Permits (EIB/AQCR 702). Part Two of the regulation states in paragraph A.1.a.(i) that permits must be obtained by

> "Any person constructing a stationary source which has a potential emission rate greater than 10 pounds per hour or 25 tons per year of any regulated air contaminant for which there is a National or New Mexico Ambient Air Quality Standard."

However, a more stringent section is Part Three: Permits for Toxic Air Pollutant Emissions. In this section it states that

> "a permit must be obtained from the division by any person prior to the construction or modification of a new source which has total potential emissions of toxic air pollutant into the ambient air that exceed the emission level in pounds per hour specified in Appendix A..."

A key phrase to note from both of these passages is "potential emission," which means that all analysis must be done on a worst case basis, not the expected operating conditions.

Emissions from the TA-54 extraction system will not need a permit based on the following analysis. The most prominent contaminant found with the TA-54 monitoring wells is 1,1,1 trichloroethane (TCA) which is found at concentrations almost an order of magnitude higher than the next most prominent contaminant. The maximum level of TCA found during 1992 (at the monitoring well closest to the location that will be used for the extraction well) was approximately 700 ppm (mass). The New Mexico regulation does not list 1,1,1 TCA, but rather 1,1,2 TCA. It is conservative to use the emission rate for the latter compound, however, since the rate is based on exposure limits and 1,1,2 TCA has a much lower limit. Specifically, the time weighted average TLVs listed by the ACGIH for 1,1,1 TCA and 1,1,2 TCA are

350 ppm and 10 ppm respectively. Therefore, using the emission rate of 1,1,2 TCA leaves over an order of magnitude safety factor. The maximum anticipated flow rate that can be achieved with the extraction system blower is 150 cfm. If this value is combined with the 700 ppm maximum measured 1,1,1 TCA concentration, then the maximum obtainable flow 1,1,1 of TCA will be 0.48 lbs/hr. This is 84% less than the New Mexico standard of 3 lbs/hr for 1,1,2 TCA.

SECTION 5
PILOT VAPOR EXTRACTION SYSTEM

The following summary is intended to clarify the mechanical design of the pilot vapor extraction system. The following information summarizes the technical approach based on an engineering estimate of an anticipated maximum flow rate of 150 CFM and a maximum vacuum pressure in the borehole of 50 inches water column. A schematic of the mechanical components of the system is shown in Figure 25.

A regenerative blower will provide the necessary vacuum and flow conditions. The maximum air flow and vacuum specifications require that a 5 hp blower be used. The blower selected for this application is a 208 volt 3-phase unit capable of 203 CFM and a maximum vacuum pressure of 88 inches of water. A minimum flow is required to cool the motor and is rated at 25 percent of the no load condition of the blower. In order to ensure that this flow condition is met, a vacuum relief valve will be installed at the inlet to the blower. This relief valve is preset at the pressure setting corresponding to the minimum required flow specification for that particular blower. This also relates to the maximum allowable vacuum in the borehole. The inlet port on the blower is also fitted with an in-line filter rated at 10 microns. The maximum pressure drop across the filter is 2 inches of water at 203 CFM. A low point water collection port will also be located at the inlet to minimize condensate from entering the blower. The exhaust side of the blower will have a tee to allow for the integration of the gas treatment system. A ball valve located on the upstream side of this interface will allow for flow control to the gas treatment system. An additional ball valve will be located on the exhaust port to allow for flow control to the gas treatment system The other side of the tee will be fitted with an additional ball valve for flow control to the gas treatment system and also allow for the exhaust air from the blower to vent to the atmosphere through a vertically mounted 10 ft. PVC pipe.

Located on the inlet side of the blower upstream from the vacuum relief valve is a manually actuated plastic butterfly valve. This allows for control of the volumetric flow which in turn varies the pressure in the borehole. There are several option available for future configurations of this valve. The valve could simply be configured with an electric actuator that is capable of two position movement (e.g. fully open, and X percent closed). The other option is to have fully adjustable flow control with the use of an electric actuator and positioner/controller. This would allow a variable process signal from the 21X datalogger to place the valve in any position for full range of motion. The cost of the valve alone is on the order of $200 and can be retrofitted in the future to accommodate the options mentioned above. For the two position actuator the estimated cost is $700 and the fully operable electrically actuated valve is approximately $1500.

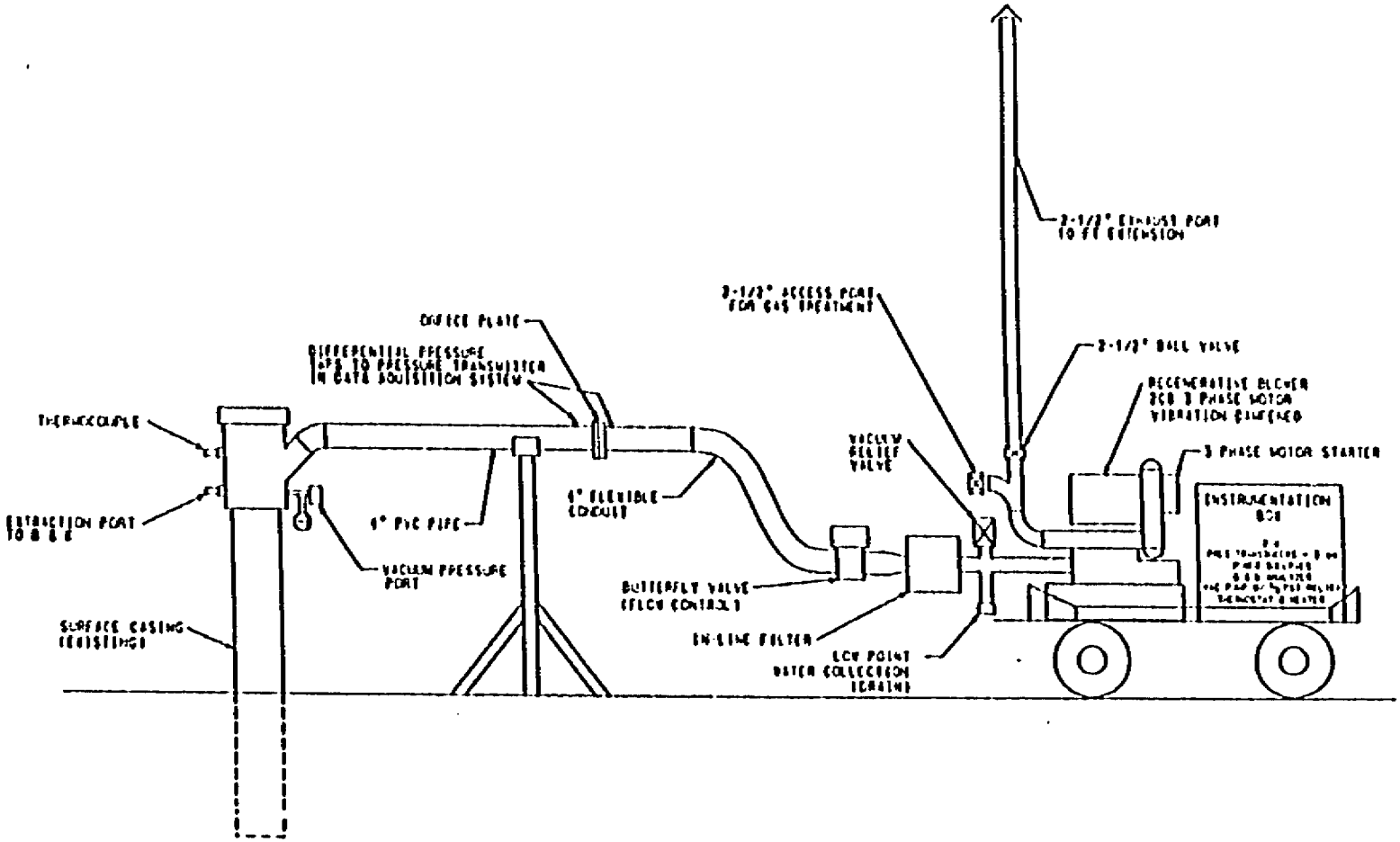

Figure 25. Pilot vapor extraction system hardware.

The mass flow measurement is made with the use of differential pressure measurement across an orifice plate. The orifice size is 2.555 inches and is placed in a 4-inch PVC pipe. Based on the orifice size, straight pipe sections a minimum of 12 pipe diameters upstream and 4 diameters downstream are required for accuracy. At maximum anticipated flow conditions, the pressure drop across the orifice is calculated to be approximately 3 inches water column. This pressure is measured with a differential pressure transducer located in the instrumentation box. The output from the transducer is then input to the 21X datalogger upon which a calibration curve is used to correlate transducer output to flow rate.

The borehole vacuum pressure is measured with a pressure transducer that is housed inside the instrumentation box. The vacuum transducer selected covers a pressure range of -5 to 0 psig. The output of the transducer is sent to the 21X datalogger and scaled to indicate inches of water column vacuum. A 1/4 -inch diameter tube connects the transducer to the vacuum pressure port located in the fitting just above the surface casing. The vacuum pressure port is also fitted with a removable vacuum gage for visual indication of borehole pressure. A barometric pressure transducer will also be located in the instrumentation box.

A thermocouple located at the well head will provide extraction air temperature. The thermocouple is a standard type K thermocouple and is wired directly to the 21X datalogger in the instrumentation box. The Brüel & Kjær gas analyzer can also be housed in the instrumentation box. Gas samples for the Brüel & Kjær are drawn through a sampling tube via a vacuum pump, from an extraction port located at the well head.

The instrumentation box internal temperature will be monitored and controlled with an industrial thermostat and heater to ensure that the internal temperature does not drop below freezing. The internal temperature will be recorded with the 21X datalogger so that correlations can be made with the data to both the instrumentation temperature and the air stream temperature. The instrumentation box will house the following hardware:

- 21X - Data logger
- Barometric pressure transducer
- Well pressure vacuum transducer
- Orifice plate differential pressure transducer
- 24V power supply for transducers
- Vacuum pump for gas sampling

Thermostat and heat lamp

Brüel & Kjær gas analyzer

Thermocouple - internal temperature

The regenerative blower and the instrumentation box will be mounted on a small portable wagon truck approximately 48" X 24" X 14". The total weight of the trailer with the hardware is estimated at less than 350 pounds.

The power requirement for the regenerative blower is 208-230 Volt 3-phase with full load amperage at 13-12 respectively. A 30 amp service breaker is considered sufficient. In addition the system also requires two separate 115 VAC instrumentation power circuits.

APPENDIX A: AN OVERVIEW OF AIR3D

AIR3D is a three-dimensional model for air flow in the unsaturated zone. It uses the popular MODFLOW (McDonald and Harbaugh 1988) code, originally designed to simulate saturated ground-water flow systems, for the majority of the computations. AIR3D adapts MODFLOW to simulate air flow in the unsaturated zone by altering the variables used in the ground-water flow equation to represent air flow. In doing this, the following simplifying assumptions were used to arrive at a linear air flow equation:

- Darcy's Law is valid for air flow;
- Elevation component of pneumatic head is neglected;
- Isothermal conditions are assumed;
- Ideal gas law is assumed as model for compressibility;
- Klinkenberg effect is neglected;
- Water movement and consolidation are neglected, therefore porosity is constant with respect to time;

The consequences of the above assumptions were examined (Baehr and Hult[1]). It was concluded that they gave a good working model for environmental applications. The development, function, and operation or AIR3D as well as the model testing and comparisons to analytical solutions are well documented by Joss and Baehr[2].

---

[1] Baehr, A. L. and M. F. Hult, "Evaluation of Unsaturated-one Air Permeability through Pneumatic Tests", Water Resources Research 27(10), 26505-2617, 1991.

[2] Joss, C. J. and A. L. Baehr, "AIR3D: An Adaptation of the Groundwater Flow Code MODFLOW to Simulate Airflow in the Unsaturated Zone," U.S. Geological Survey Open File Report, Publication expected 1994.

ER Document Signature Form Read/Write Access Person Making Entry is PPC/172228/Norris, Josephine V. (Created on 12/21/2000)

Home | Update | Delete | Reset | Bottom

Document Catalog Number ER2000-0738 (Please prefix the name of all electronic versions of this document with this number.)

* Required Field

*Document Title / Subject	Pilot Vapor Extract Test at TA-54, MDA L, October 1997. LA-UR-00-6024
PRSs	None
Associated Document Catalog Number(s)	None
*Author	Hopkins, John K 667-9551 johnhopkins@lanl.gov
*Author Organization	Material Disposal Areas
Document Team	Norris, Vivian Word 665-5221 vivianm@lanl.gov
*Document Type	Letter Former OU N/A
Date Due 12/21/2000	Date Final Complete 12/21/2000 Date Sent to DOE
Date Sent to NMED	Date Sent to RPF (Paper & Electronic)
Received Per RPF	RPF ER ID Number
CT No	LA-UR Number
Performance	
AA Deliverable ☐	Certification Required ☐ Force Peer Review ☐
Distribution TO:	
Distribution FROM:	
Distribution COPY:	
Distribution THRU:	

Attachment Notes	
Status/Comments	

Reviewer Signatures: (By signing, the reviewer indicates that he/she reviewed and approves the document.)

Reviewer (Print reviewer's name under title)	Signature	Date
Word Processor VIVIAN NORRIS	Vivian Norris	12/21/00
Proof Reader ELISHA VIGIL	Elisha Vigil	12-21-00
Author N/A	N/A	
Team Leader N/A	N/A	
Focus Area Leader/Designee JOHN HOPKINS	[illegible]	12/21/00
ER Program Manager JULIE CANEPA	[illegible]	12/21/00
DOE/LAAO Program Manager N/A	N/A	
Distributed By VIVIAN NORRIS	Vivian Norris	12/21/00

Document Catalog Number ER2000-0738

Top

Environmental Restoration RPF Record Return Form

Part I (to be completed by RPF personnel)

The attached record (or records package) was reviewed and determined to be incomplete for processing.

Author's name John K. Hopkins Date of record 12-21-00

Organization _____ Mail stop _____

Date returned to author 2-20-01 Return to RPF by 3-20-01

ER document catalog number ER 2000-0738 Symbol number _____

✓ 1. Incomplete—ER Project Document Signature Form (if required), electronic file (if required), pages, attachments, or enclosures are missing.

_____ 2. Not properly authorized (required signatures or initials are missing).

_____ 3. Incomplete records listing for records package. Information is not properly identified.

_____ 4. Document quality is poor; does not provide adequate image. If this is the "best available copy," please return the document to the RPF.
Please initial _____ and date _____ here.

✓ 5. Other: no electronic version of enclosure found in ER RPFIN Box.

Part II (to be completed by the author/originator)

Please take appropriate corrective action and return ~~the~~ this record *and this form* to the ER Records Processing Facility (RPF), MS M707.

Note: This record (or records package) must be returned within 30 working days.

Comments (Optional) An electronic copy is not available. The contractor no longer works for LANL.

QP-4.3

Los Alamos
Environmental Restoration Project